The Identification of Desirable Parameters for Aluminium Cutting Using Various Cutting Fluids and Limited Volume Lubrication

B.E.Meister

UNIVERSITEIT VAN PRETORIA
UNIVERSITY OF PRETORIA
YUNIBESITHI YA PRETORIA

The Identification of Desirable Parameters for Aluminium Cutting Using Various Cutting Fluids and Limited Volume Lubrication

by

B.E.Meister

A dissertation submitted in partial fulfillment
of the requirements for the degree

Master of Engineering

in the

Faculty Engineering, Built Environment and Information Technology

University of Pretoria

October 2002

The Identification of Desirable Parameters for Aluminium Cutting using Various Cutting Fluids

Author: Bernhard Meister
Mentor: Prof. P.L. de Vaal
Department: Chemical Engineering
University of Pretoria
Degree: Master of Engineering

Synopsis:

Standard equipment to determine friction and wear properties of lubricants cannot be used to determine the performance of cutting fluids. In addition, a technique was required that would enable characterisation of cutting fluids applied in limited volumes.

To address these requirements, a standard shaper was instrumented and served as a test bench for the evaluation of cutting fluid performance.

The parameters that were measured in the tests were assigned weights and were used to rank the cutting fluids that were tested. The most important parameters when comparing the different cutting fluids are:

- 1) the smooth fraction on the underside of the chip - this is related to the distance that can be cut until the built-up edge forms.
- 2) the distance cut to formation of the built-up edge.
- 3) the chip shape, specifically the chip radius.
- 4) the distance cut to first break.
- 5) the ease of chip flow.
- 6) the temperature at the quarter way mark at 52mm length of cut.
- 7) the temperature at which the built-up edge forms.

Results obtained, making use of a variety of cutting fluids, indicated that the methodology that had been developed to evaluate performance of cutting fluids enabled ranking of the cutting fluids according to their performance with respect to the above-mentioned parameters.

The performance ranking methodolgy developed can be adapted, depending on the application, resulting in a useful technique with direct practical possibilities.

Keywords
Cutting fluids, limited volume lubrication, metal cutting, performance testing.

Die Identifisering van Wenslike Parameters vir die Sny van Aluminium by die Gebruik van Verskillende Sny-olies

Outeur: Bernhard Meister
Studieleier: Prof. P.L. de Vaal
Departement: Chemiese Ingenieurswese
Universiteit van Pretoria
Graad: Magister in Ingenieurswese

Sinopsis:

Standaard toerusting om die wrywing- en slytasie-eienskappe van smeerolies te bepaal kan nie gebruik word om die werkverrigting van sny-olies te bepaal nie. Bykomend was dit ook nodig om 'n tegniek te ontwikkel om die karakterisering van sny-olies wat in beperkte volume smering gebruik word, moontlik te maak.

Om hierdie bykomende tegniek te ontwikkel is 'n standaard sterkarmskaaf geinstrumenteer. Die skaaf is gebruik as 'n toetsbank vir die evaluering van die werkverrigting van 'n verteenwoordigende reeks sny-olies.

Daar is gewigte toegeken aan die parameters wat in die sny-proses gemeet is, wat toe gebruik is om die sny-olies te rangskik volgens hulle werkverrigtingsvermoë. Die belangrikste parameters ter sprake was:

- 1) die gladde fraksie aan die onderkant van die spaander - 'n direkte verwantskap tussen die fraksie en die afstand wat gesny kan word tot waar die opgeboude rif vorm, is waargeneem.
- 2) die afstand wat gesny word tot waar die opgeboude rif vorm.
- 3) die spaander vorm, spesifiek die spaanderradius.
- 4) die afstand wat gesny word tot waar die spaander die eerste keer breek.
- 5) die gemak waarmee die spaander vorm.
- 6) die temperatuur by die kwartpadmerk (52 mm) van die snit.
- 7) die temperatuur waarby die opgeboude rif vorm.

Die resultate wat behaal is, vir 'n verskeidenheid van sny-olies, het aangetoon dat die metode wat ontwikkel is om die werkverrigting van die sny-olies te evalueer, dit moontlik maak om die sny-olies volgens hulle werkverrigting te rangskik.

Die rangskikkingsmetode volgens werkverrigting kan aangepas word, afhangende van watter gewigte aan die parameters toegeken word. Die gevolg is 'n bruikbare tegniek met direkte praktiese toepassing.

Sleutelwoorde
Sny-olies, beperkte volume smering, metaal-snyprosesse, werkverrigtingstoetse

Acknowledgements

The author expresses thanks and gratitude to:

The Triune God for the talents, good health and insight He bestowed on me so that this project could be performed.

Mr. J.W.Bornman for his time and patience in showing and explaining how to perform micro-hardness tests and how to etch and make micrographs. Thank you also for the use of the equipment.

Professor P.L. de Vaal for the many hours spent in his office for discussing planning of the project and for listening to the discussion of results obtained in the project, and also for motivation and for the proof reading of the manuscript.

Professor G.T. van Rooyen for a valuable discussion on metal cutting

Mr. E. du Plessis from Producut Lubrication Technologies (Pty.) Ltd. for sponsoring the project

My colleague Carl Sandrock, and my friends:
Senta, William, and Ralf for all the questions they asked and all the patient listening that they did.

Table of contents

Nomenclature List

Symbol	Description	Units of measurement
C	heat capacity	kJ/kg.K
	constant in Taylor equation	m/min.
F	cutting force	N
J	mechanical equivalent of heat	kJ
k	shear flow stress	N/m^2
l	length	mm
M	mass	g
n	gradient of slope log-log plot of Taylor equation	m/min^2
	constant in chip temperature equation	J
Q	work rate	W
R	rate of metal removal	cm^3/min
	overall performance ranking	
T	temperature	°C
	tool life	min
t_1	depth of cut	mm
t_2	mean chip thickness	mm
v	cutting speed / velociy	m/min
W	work	J
w	width of cut	mm

Greek

α	rake face angle	°
β	clearance angle	°
γ	chip shear strain	dimensionless length per length
ν	cutting speed	m/s
ρ	density	g/cm^3
Ø or Φ	shear plane angle.	°
ω	parameter	

Subscripts

c	chip, cutting
f	feed
i	the i-th parameter
r	rake face
s	shear plane

Definitions:

BUE - built-up edge, it is a greatly strain hardened lump of work-piece material that has welded to the rake face of the tool

LVL – limited volume lubrication

Peening - surface hardening technique
Swarf - metal debris/chips from the cutting process

1.Introduction

In metal cutting as in any business undertaking, the focus lies on performing the work at hand as cost efficiently as possible. A further factor that must be kept in mind is the environmental impact that cutting fluids have. Environmental issues play an ever-increasing role in decisions affecting process development and applications of technology. Limited volume lubrication for metal cutting is able to aptly address both issues.

Very little lubricant is used and this greatly reduces the probability for skin contact by human operators, makes chip recovery easier than when conventional flood lubrication is used and decreases the possibility that the cutting fluid will tarnish the finished work-piece surface, while disposal and maintenance of used cutting fluid are not an issue. Limited volume lubrication is applied as a jet of fine mist and as a result the fine droplets have more kinetic energy than an adhered layer of conventional flood applied lubricant and thereby can displace the adhered layer on the metal surface more rapidly, providing a fresh layer of cutting fluid. Conductive and convective cooling of the cutting process are enhanced thereby.

In this study aluminium was cut using a shaper, a tungsten carbide tool and limited volume lubrication. A shaper is representative of an intermittent cutting process. All cutting process parameters were kept constant, except for the chemical composition of the cutting fluid that was used.

The aim of the investigation was to determine the effect that different cutting fluid chemistries have on intermittent cutting using limited volume lubrication as this has significant benefits to offer both in terms of cutting performance and in terms of environmental issues. The ultimate goal of the project was to develop a practical in-house test and to establish a methodology to identify and measure the parameters that should be measured in order to quantify the performance of cutting fluids used in limited volume lubrication.

To evaluate the various cutting fluids a variety of cutting process parameters were measured using a computer and relevant instrumentation. These included:

- the average tool/work-piece interface temperature, measured by means of a thermocouple that is formed by the dissimilar metals of the tool bit and the work-piece itself,
  - the temperature at which the built-up edge forms
  - the temperature at the one quarter mark of the length of cut
  - determination of the distance cut until formation of the built-up edge
- the cutting force by means of a strain gauge on the tool bit,

as well as several physical measurements of the chips formed in each cut, namely:

- the averages of the smooth distance on the underside of the chip,
- the chip thickness ratio,
- the length to first break,
- the chip shear strain,

- the shear plane angle,
- the chip hardness profile in the non built-up edge region of the cut,
- the approximate flow-zone thickness up against the rake face of the tool,
- the ease of metal deformation
- the chip shape (the chip radius in particular)
- and the surface finish on the work-piece.

When a built-up edge is not present, as is the case when higher cutting speeds are used, the welded zone should be smaller for a cutting fluid that has superior anti-weld properties and consequently the cutting force and the cutting temperature should be lower than for a cutting fluid that has lesser anti-weld properties. Better anti-weld properties should allow improved tool life and reduced operating costs as well as decrease the down-time as toolbits will have to be changed less often. At lower speeds the length that is cut prior to formation of the built-up edge in combination with the temperature at which the built-up edge forms should also give an indication of the anti-weld properties of the cutting fluid. A cutting fluid of superior anti-weld properties should show a longer smooth fraction on the underside of the chip and possibly a longer length cut to first break of the chip. If a cutting fluid is able to facilitate ease of chip flow then the chip should undergo less strain hardening despite possibly incurrring a high strain, i.e. the chip should be softer for the same amount of metal deformation than for a cutting fluid that does not facilitate ease of chip flow so well. If a cutting fluid can produce a chip that is softer than for other cutting fluids for the same cutting conditions then that cutting fluid can possibly increase the tool life. The cutting force and temperature should serve well to establish which measurements and physical characteristics of the chip produce the best reflection of the success of the cutting process.

The intent is also to use the shaper as a bench test for the evaluation of cutting fluids for metal cutting other than aluminium. To determine the success of the laboratory bench test and how well the predictions from the acquired data correlate with practice requires data from industrial applications.

It is envisaged that from research it might become possible to establish a guideline of parameters that should preferably be looked at in the laboratory for the development of cutting fluids before they are tested industrially. In the past and even now, cutting fluids are chosen and developed by trial and error. This involves a vast amount of empirical testing. The physical and chemical characteristics of lubricants and coolants may be changed and tests may be performed to determine which characteristics are desirable for a specific machining operation. Results obtained in laboratory tests sometimes do not correlate well with practice. The question is: how can laboratory tests be performed so as to achieve results that will correlate well with practice?

In this work the theoretical subject matter is divided into six parts. An overview of metal cutting is presented first. A comprehensive background is given with respect to the mechanical aspects of metal cutting, so as to provide the necessary background for meaningful interpretation of the experimental results, and for future developments. Without this background the experimental planning and interpretation of results would

not be possible. Thereafter issues pertaining to the chip, such as how and where it forms and the flow patterns of the metal deformation that may be observed in the chip after it has been etched are presented. The parameters that are important to measure and how they can be measured during metal cutting are discussed next. They are cutting force and temperature. The emphasis of this study is on the cutting fluids, hence they are the parameter that changes from one test to the next and more attention is paid to the cutting fluids and their effects than to the metallurgy involved in metal cutting. The reduction of metal to metal affinity is important because this becomes manifest as anti-weld capability leading to reduced cutting temperatures and reduced tool wear when cutting with different cutting fluids. In chapter 6 the machinability of aluminium is discussed. Then the experimental apparatus and experiments conducted are described. This is followed by the results and the discussion of the results obtained, after which some conclusions and recommendations are made.

2. Metal cutting

Terminology

In order to understand the role that cutting fluids play in metal cutting an overview of metal cutting is necessary. Metal cutting cannot be performed by means of an ordinary knife. Metals and alloys are too hard, so that no known tool materials are strong enough to withstand the stresses which they impose on very fine cutting edges i.e edges that have a very fine included angle like a knife for example. If both faces forming the tool edge act to force the two newly formed surfaces apart very high stresses are imposed, much heat is generated, and both the tool and the work surfaces are damaged. These considerations make it necessary for a metal-cutting tool to take the form of a large-angled wedge, which is driven asymmetrically into the work material, to remove a thin layer from a thicker body. (See figure 2.1)

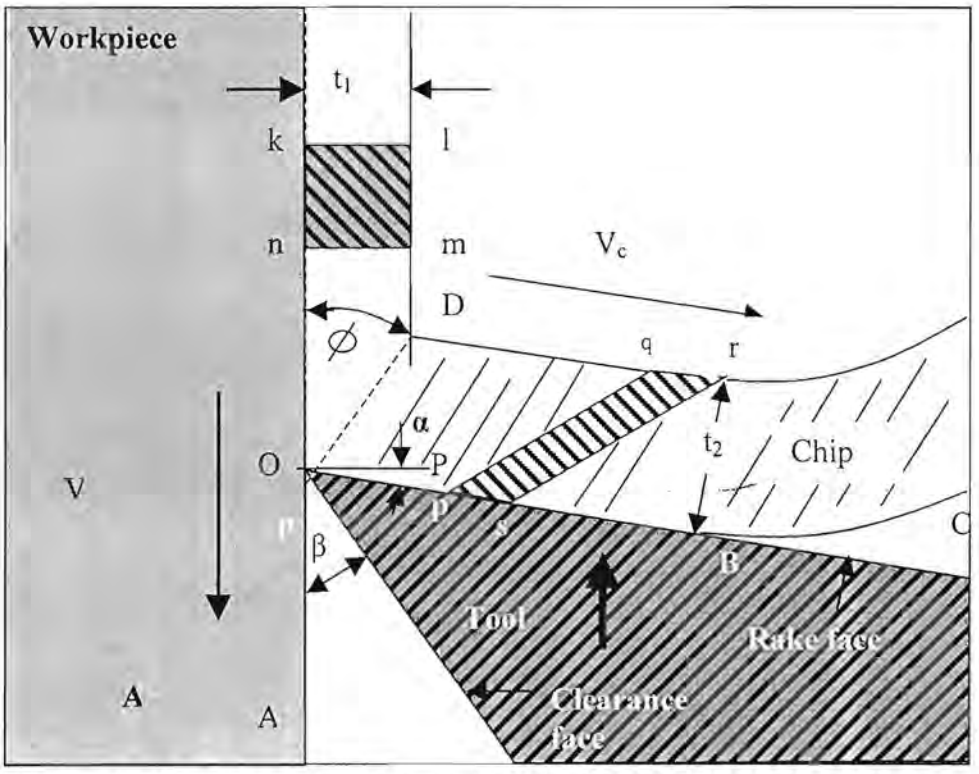

Figure 2.1 Metal cutting diagram for the tool and the work-piece (Trent,1977)

The layer must be thin to enable the tool and the work to withstand the imposed stress. There exists a range of how thin the tool can be to still have sufficient rigidity and mechanical strength to withstand the imposed stress and how thick without causing extreme chip deformation, work hardening and increased operating costs. A clearance angle β must be formed on the tool to ensure that the clearance face does not make contact with the newly formed work surface, because this will lead to increased friction and undesired surface defects like scratches. If the heat build up in this region becomes too intense a tertiary welded or contact zone will develop leading to more shear and yet

more heat and rapid catastrophic tool failure may result due to overheating. These are features of all metal cutting operations and provide common ground from which to commence an analysis of machining.

In figure 2.1 the angle α between the rake face and the line OP is called the rake angle. The chip must flow over the rake face. The cutting edge is formed by the intersection of the clearance face, or flank, with the rake face. The rake angle is measured relative to the line OP and if the rake face lies below this line it is referred to as a positive rake angle. The rake face is inclined at an angle to the axis of the work material and this angle can be adjusted to achieve optimum performance for a particular tool material, work material and cutting conditions. This refers to the rake angle.

Positive rake angles (α) may be up to 30° but the greater robustness of tools with smaller rake angles leads in many cases to the use of zero or negative rake angle. (See figure 2.2)

Metal Cutting Operations and Terminology

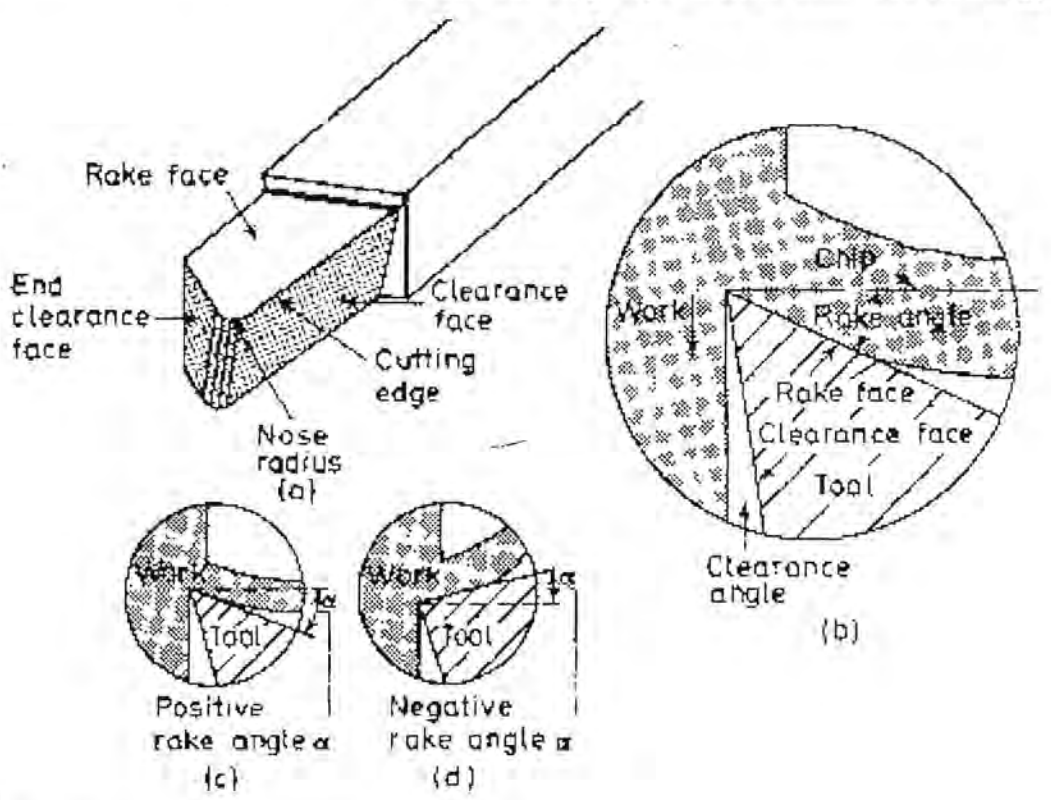

Figure 2.2 Cutting tool terminology.
(Trent, 1977)

The tool terminates in an end clearance face (see figure 2.2(a)) which also is inclined at an angle as to avoid rubbing against the freshly cut surface. The nose of the tool is at the intersection of all three faces and may be sharp, but more frequently there is a nose radius between the two clearance faces.

For the shaper that was used in this study the tool looks somewhat different (see figure 2.3).
The different parameters that play a role in metal cutting, are (Boston, 1952)

- the material of construction of the cutting tool
- the hardness of the cutting tool
- the red hardness or hot hardness of the cutting tool
- the temperature at which the tool operates
- the depth of cut
- the feedrate of the workpiece

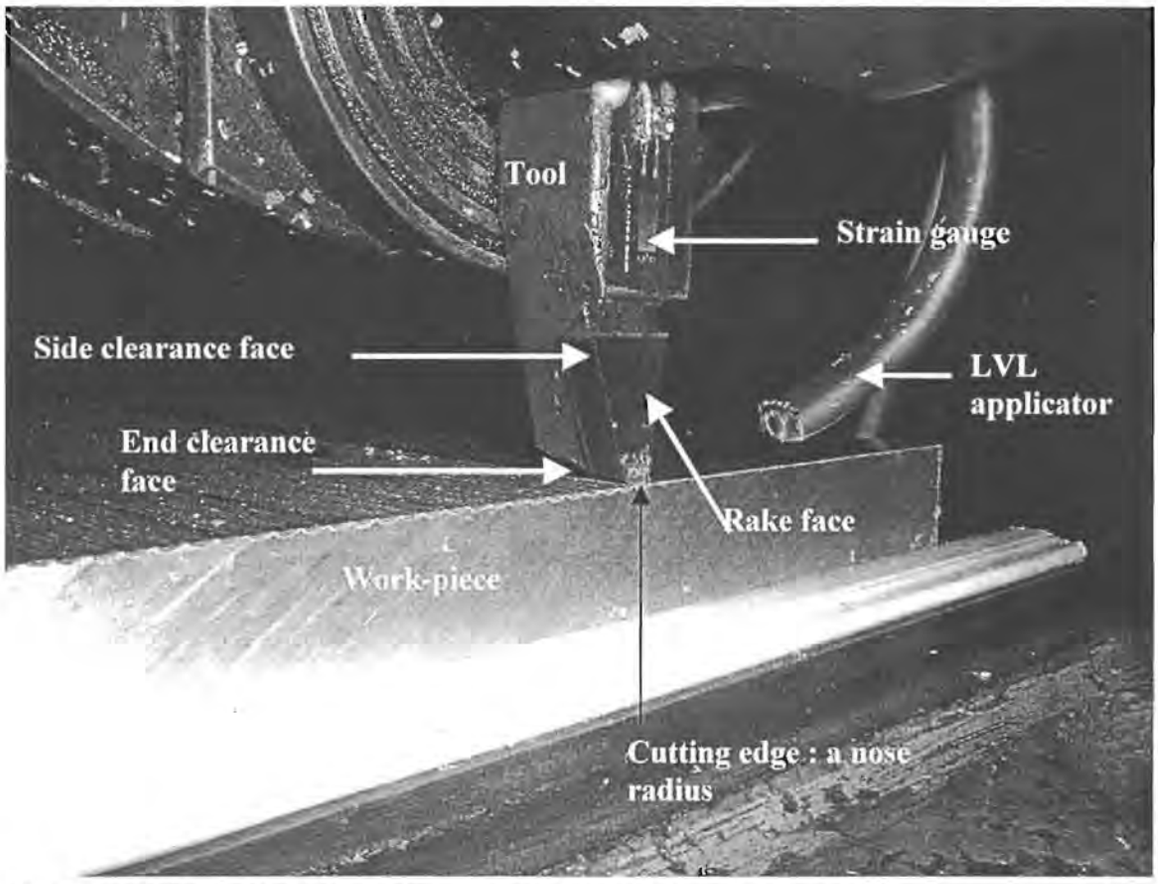

Figure 2.3 View of the tungsten carbide cutting tool in the shaper

- the cutting speed
- the volumetric rate of metal removal
- the structure of the metal being cut
- the stiffness of the metal being cut
- the toughness of the metal being cut
- the hardness of the metal being cut
- the toughness of the tool and the shank material
- the stiffness of the tool and the shank material
- the hardness of the tool material

- the heat capacity and the conductivity of the tool material
- the treatment of the tool during preparation of the tool. The treatment can involve peening and different heat treatments.
- the geometry of the cutting tool, and that includes a keen cutting edge. Hand ground tools will never have the same geometry from one time of sharpening to the next. This would result in non-repeatability of results during testing
- the cutting fluid used and its properties (to be discussed later)
- the atmosphere in which the metal cutting occurs. (Bartz, 1996)
- the type of machine used for the cutting process

According to de Chiffre and Belluco (de Chiffre & Belluco, 2002) the performance ranking of cutting fluids is not independent of the type of machine tool used, nor is it independent of the type of work material that is used. The hypothesis was investigated that one will get the same performance ranking for the different metal working fluids that were used regardless of which machining test is used, when the fluids are of the same type. For water-based fluids they used on austenitic stainless steel the hypothesis was mostly true, but the ranking did change depending on the test for the straight oils. This difference was even more pronounced for other work materials. Esters and vegetable oils performed best in all the tests in both the water-based and the straight oil group. The tests that were used were turning, drilling, reaming and tapping.

The type of machine that is used can be one for continuous cutting or one for intermittent cutting. With continuous cutting a steady state temperature is attainable provided that no built-up edge is present. With intermittent cutting the temperature at the tool tip continuously fluctuates. If this fluctuation becomes excessive, large thermal stresses are imposed on the tool tip that can contribute to comb crack formation which may lead to accelerated tool wear.

In machining cutting fluid may be considered an accessory that is frequently applied in order to increase production rate, improve surface quality, reduce costs and consequently increase profit. This is true in most applications but it can also cause problems in a few cases. Machining with ceramic tools, particularly alumina-based ceramics, with inadequate fracture toughness, may not tolerate the application of cutting fluid. The heated zone in the tool promoted by the cutting action will experience thermal shocks in the presence of cutting fluid which often leads to severe cracks or even fracture of the entire tool edge.
Cutting fluid can also be detrimental to intermittent cutting operation, such as milling, where comb cracking is the major tool failure mode. This failure mode can be enhanced by fluctuation of the cutting temperature, heating in the active period of cut and cooling in the idle period during revolution of the milling cutter. This temperature fluctuation causes stress variation on the tool due to a steep temperature gradient, leading to the formation of cracks usually perpendicular to the cutting edge, and culminating in the formation of comb cracks. Application of cutting fluid under this situation will further increase the temperature fluctuation due to its cooling ability during the idle period, thus increasing the stress variation and consequently accelerating the process of comb crack formation. (Vieira, Machado and Ezugwu, 2001)

Depth of cut is always measured in the direction in which there is no motion. The feed direction and the cutting direction both experience motion.

It is difficult to appreciate the action of many types of tool without actually observing or, preferably using them. **The performance of cutting tools is very dependent on their precise shape.** In most cases there are critical features or dimensions which must be accurately formed for efficient cutting. These may be the clearance angles, the nose radius and its blending into the faces, or the sharpness of the cutting edge. The importance of precision in tool making, whether in the tool room of the user, or in the factory of the toolmaker, cannot be over-emphasised.

Most of the practical work that was performed for this investigation was done on a shaper. (See figure 2.4) Shaping is one of the methods that can be used to produce flat surfaces, grooves or slots. In shaping, the tool has a reciprocating movement; the cutting takes place on the forward stroke along the full length of the surface that is generated. On the return stroke the cutting tool has to be lifted clear so as to prevent wear on the tool and damage to the work surface. The next stroke happens once the work-piece has moved on laterally horizontally or vertically by the set feed distance. The cutting times between interruptions are longer than in milling operations but shorter than in most turning operations.

A shaper was used rather than a saw blade or a saw tooth as a saw tooth would lack sufficient mechanical rigidity if it would protrude far enough from the tool holder so that a strain gauge can be mounted on its surface. The strain gauge is necessary for cutting force data collection. Also the geometry of a saw tooth would need to be adapted so that for a long open chip, the chip would not end up damaging the strain gauge due to clogging up the gullet. The gullet is the space between two consecutive saw blade teeth. The blade would also only be equipped with one strain gauge, as strain gauges on the following teeth of the blade would run a higher risk of becoming damaged. Multiple strain gauges would not necessarily result in more useful data capture for cutting fluid evaluation. A shaper can also produce grooves, as can a saw, thus operating the shaper in this way results in performing the same task and consequently the data that is captured should also be quite relevant for a sawing operation.

The shaper has a clapper box and this has a pivot (see figure 2.4). On the push stroke when the tool is cutting, the tool is held down into the cut. On the return stroke the tool pivots up and slides over the work-piece, so that the tool does not cut on the return stroke. The depth of cut is how deep the tool goes into the metal, and is determined by adjusting the position of the vertical slide.

The cutting tool that was used for the experimental work on the shaper is a tungsten carbide tool (see figure 2.3). In practical machining with a shaper the included angle of the tool rake face and the plane of machining varies between 60° and slightly more than 90°, so that the removed layer, the chip, is diverted through an angle of at least 60° as it moves away from the work, across the rake face of the tool. In this process, **the whole volume of metal is subjected to plastic deformation** and thus a large amount of energy

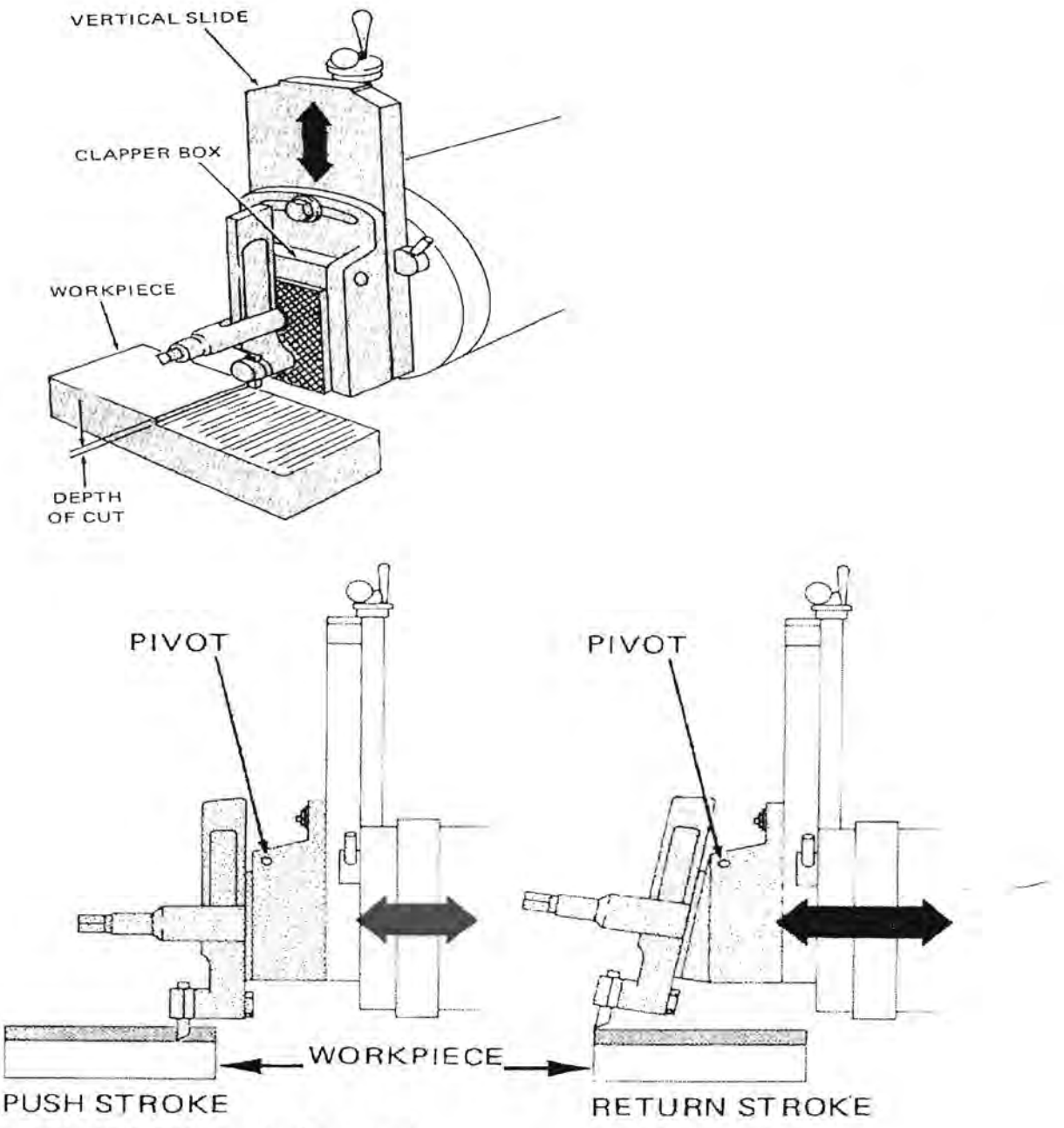

Figure 2.4 Schematic of a shaper
(Follette D.,1980)

is required to form the chip and to move it across the tool face. In the process, two new surfaces are formed, the new surface of the work-piece (OA in figure 2.1) and the under surface of the chip (BC). To form new surfaces requires energy, but in metal cutting this represents an insignificant amount of the energy for cutting as most energy goes into plastic deformation of the whole volume of metal when forming the chip. (Trent, 1977). The cutting force measurement by strain gauge includes only the force necessary to perform the cut and thus does not incorporate the force that the electric motor must

provide to drive the machine tool. Similarly, the energy for cutting does not include the energy needed to drive the machine tool.

That a large amount of energy is required to form the chip may be substantiated in another way. If one looks at a chip under a scanning electron microscope (SEM) (see figure 2.5) a large number of slip bands are evident on the rough chip surface. If each slip band is taken as a new surface that was produced then the total area of the surfaces produced in the chip far exceeds that of the surfaces at the underside of the chip and on the work-piece surface.

If one further takes into account that these surfaces are sheared across each other under conditions of seizure and/or high friction and that the chip is being moved and deformed to curl as it leaves the tool, then it is clear that most of the energy during cutting goes into forming the chip.

The main objective with machining is forming or shaping the work surface to the desired geometry. Based on this it may appear that most of the attention should be paid to the forming of new surfaces, but the main energy consumption takes place in the forming and

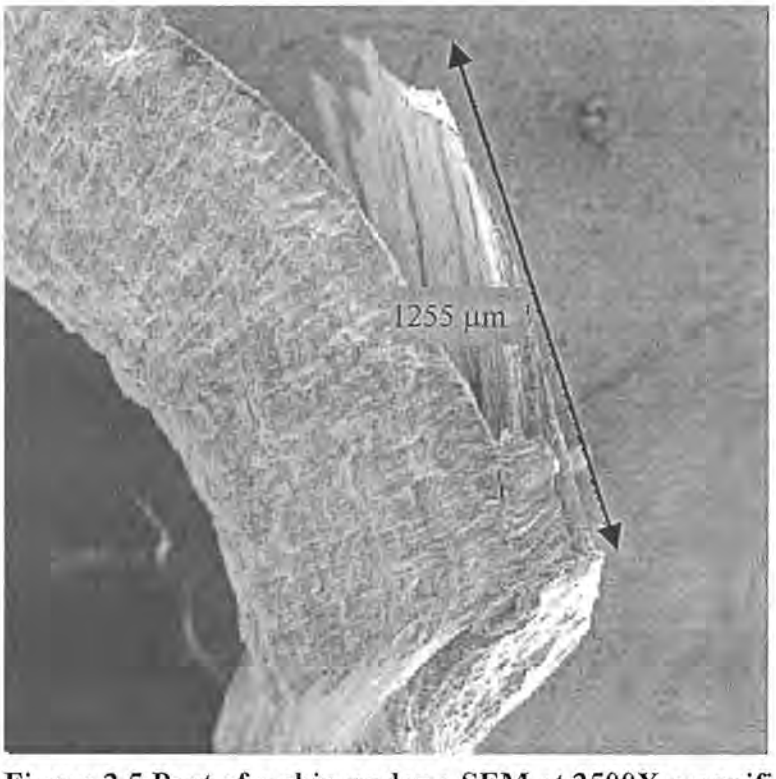

Figure 2.5 Part of a chip under a SEM at 2500X magnification

moving of the chip, therefore the main economic and practical problems concerned with rate of metal removal and tool performance, can be understood only by studying the work material as it is formed into the chip and moves over the tool. Even the condition of the machined surface itself can be understood only with knowledge of the process of chip formation.

The rate of metal removal may be determined by the following relationship:

$$R = v \cdot w \cdot t_1 \qquad \textbf{Eqn 2.1}$$

where
R is the rate of metal removal (cm^3/min)
v is the cutting speed (m/min)
w is the width of the cut and (mm)
t_1 is the depth of cut (mm)
The cutting speed and the feed rate or amount fed per cut are the two most important parameters which can be adjusted by the operator to achieve optimum cutting conditions.

The chip

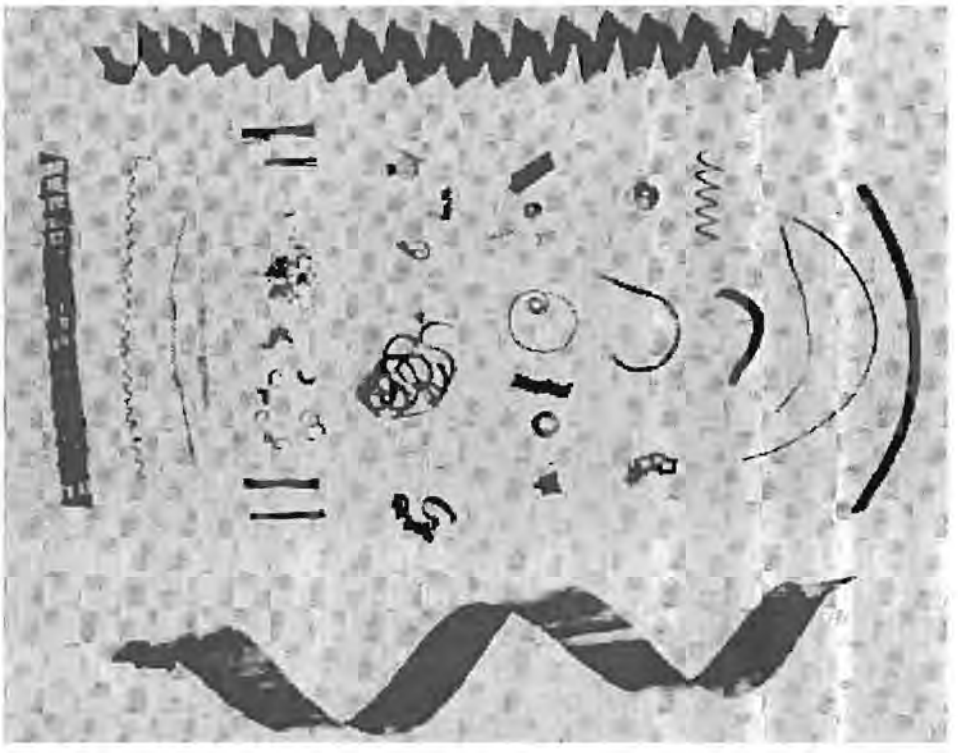

Figure 2.6 Chip shape an essential feature of metal cutting.

The chip is enormously variable in shape and size in industrial machining. Figure 2.6 shows some of the forms. The formation of all types of chips involves shearing of the work material in the region of a plane extending from the tool cutting edge to the position where the upper surface of the chip leaves the work surface (OD in figure 2.1). A very large amount of strain develops in this region in a very short time, and not all metals and alloys can withstand this strain without fracture. Grey cast iron chips, for example, are always fragmented, and the chips of more ductile materials may be produced as segments under unfavourable conditions of cutting. This discontinuous chip is one of the principal classes of chip form, and has the practical advantage that it is easily cleared from the cutting area. Under a majority of cutting conditions, however, ductile metals and alloys do not fracture on the shear plane and a continuous chip is produced. Continuous chips

may adopt many shapes – straight, tangled or different types of helix shapes. Often they have considerable strength, and controlling size and chip shape is one of the problems machinists and tool designers face.

Simple chips, i.e. those chips that have only two dimensions, are the easiest to measure and analyse. Chip shape depends on the tool geometry, the lubricant and the mode of lubrication that is used and on other parameters like the type of metal being cut, the feed rate, the cutting speed and the type of tool that is used. Continuous and discontinuous chips are not two sharply defined categories, and a transition between the two types can be observed.
The longitudinal shape of continuous chips can be modified by mechanical means, for example by grooves in the tool rake face, which curl the chip into a helix. **The longitudinal cross-section of the chips and their shape and thickness are of great importance in the analysis of metal cutting,** and need to be considered in some detail. For the purpose of analysing the cutting process chip formation in relation to basic principles of metal cutting should be studied. It is useful to start with the simplest cutting conditions, consistent with maintaining the essential features common to cutting operations. (Trent, 1977)

Techniques for the study of chip formation:

Firstly the conditions are simplified for the beginning stages of a laboratory investigation. These conditions are known as orthogonal cutting. In orthogonal cutting the tool edge is straight, it is normal to the direction of cutting, and also normal to the feed direction. In this study a shaper is used and this meets the requirements of orthogonal cutting. The cutting speed is the same at each point on the cutting tool. Depending on the cut and the tool that is used, the chip is free to move to both sides, or to one side, or to no side at all but only to the top. When a chip can move to no side at all, but to the top, it will be referred to as bi-directional restraint of chip flow. These chips are two-dimensional. The cutting is intermittent, as is also the case with a sawing operation and a milling operation.

The time of continuous machining on a shaper is short and speeds are limited. There are eight different speeds available on the shaper used for this study, and they range from about 5.7m/min to 90m./min. The study of the formation of chips is difficult because of the speed of the cutting operation in industrial machining and because of the small scale of the phenomena that are to be observed. The shaper in this case is better than a lathe because it meets orthogonal cutting conditions more closely than a lathe since on a lathe the cutting speed can change significantly from one point on the tool to another when a small radius work-piece is machined and the depth of cut is deep. Another reason for using the shaper is that it offers single cut motion, the cut is simple i.e. with bi-directional restraint of chip flow the cut is symmetrical and the feed force is balanced from either side which gives a resultant force of zero. The downward force is negligibly small in relation to the cutting force and the feed force (Trent, 1977, and Follette D, 1980) and therefore force analysis is the simplest possible for the metal cutting operation as it becomes one dimensional for all practical purposes. (See also figure 2.4 and figure 3.1).

In the past high-speed cine-photography at low magnification was used to reveal the changing external shape of the chip (Trent, 1977). Today this kind of work is done by means of a high speed digital video camera. A thousand frames per second or more are possible. Such a camera can be a very useful accessory. "The external shape can be misleading if used to reflect the cutting action at the centre of the chip." (Trent,1977) The outermost layer of the chip is much cooler than the innermost layer. This and that the external shape can be misleading is quite obvious when one studies the internal chip deformation from lateral cross sections after etching and from studying micro-hardness profiles through the chip.

No useful information about chip formation can be gained by studying the end of the cutting path after cutting has been stopped in the normal way by disengaging the feed and the drive to the work. (Trent, 1977). By stopping the cutting action suddenly, however, it is possible to retain many of the important details – to 'freeze' the action of cutting.

Chip shape:

Even with orthogonal cutting the chip shape is not strictly rectangular. For the case of performing the cutting operation with a shaper the chip is free to move as mentioned above. The chip flows in all the directions in which it is not constrained.

Figure 2.7 Cross section of an aluminium chip showing thick middle section and taper towards sides

Figure 2.8 Rough upper serrated edge of an aluminium chip from the shaper

The chip spread is smaller with harder alloys, but when a softer metal is cut using a small rake angle, chip spread of more than one and a half times the original depth of cut has been observed (Trent, 1977). Usually the chip is the thickest in the middle, tapering off somewhat towards the sides (see figure 2.7), but this depends on the constraints of the available volume into which it can flow.

The upper side of the chip is always rough, usually with minute corrugations or steps as is clear from figure 2.8. It is interesting, especially from figure 2.7, that the chip cross section is not perfectly round, but actually is a five sided shape. The reason for this probably is that the metal exposes its surfaces of lowest surface energy for maximum stability. (See appendix A) Compare this with the shape of the tool of figure 2.3 - the tool has a round cutting edge as it has a nose radius.

Even with a strong continuous chip periodic cracks are often seen, breaking up the outer edge into a series of segments. A complete description of chip form would be very complex, but, for purposes of analysis of stress and strain in cutting, many details can be ignored and a much-simplified model may be assumed. The making of these assumptions is justified in order to build up a valuable framework of theory, provided it is kept in mind that reality can be completely accounted for only by reintroducing the complexities, which were ignored in the first analysis.

An important simplification is to ignore both the irregular cross section of real chips and the chip spread, and to assume a rectangular cross section, whose width is the measured

mean width of the chip, and whose height is the measured mean thickness of the chip. With these assumptions, the formation of chips is considered in terms of the simplified diagram, figure 2.1, an idealised section normal to the cutting edge of a tool used in orthogonal cutting.

Chip formation

In practice, the mean chip thickness can be obtained by weighing the chip and measuring the length of a piece of chip. The mean chip thickness, t_2, is then

$$t_2 = 1000 \cdot M / \rho\, w\, l \qquad \text{Eqn. 2.2}$$

where t_2 = mean chip thickness (mm)
M = mass of the chip (g)
ρ = the density of the work material/chip material (assumed to be the same) (g/cm^3)
w = the width of the chip (mm)
and l = length of the piece of chip (mm)

The mean chip thickness is a most important parameter. In practice the chip is never thinner than the feed, which in orthogonal cutting, is equal to the undeformed chip thickness, t_1, (figure 2.1). Chip thickness is not constrained by the tooling, and, with many ductile metals, the chip may be as much as five times as thick as the feed, or even more.

The chip thickness ratio is defined as t_2 / t_1. The chip thickness ratio may also be obtained in another way, namely by marking the work piece with permanent marking ink at a known distance from the beginning of the cut. When the cut is completed, the chip is collected and the distance from the start of the chip to where the mark appears on the chip is measured. The ratio of the first length to the second length is the mean chip thickness ratio.
The chip thickness ratio t_2 / t_1 is geometrically related to the tool rake angle and the shear plane angle ϕ (figure 2.1), as will be shown below. (Trent, 1977).

The shear plane angle is the angle formed between the direction of movement of the work-piece OA (figure 2.1) and the shear plane represented by line OD, from the tool edge to the position where the chip leaves the work surface. For purposes of simple analysis the chip is assumed to form by shear along the shear plane. In fact the shearing action takes place in a zone close to this plane. The shear plane angle is determined from experimental values of t_1 and t_2 using the relationship

$$\cot \Phi = (t_2/t_1 - \sin \alpha\ ) / \cos \alpha \qquad \text{Eqn. 2.3}$$

And, where the rake angle, α, is zero

$$\cot \Phi = t_2/t_1$$

The chip moves away with a velocity v_c which is related to the cutting speed v and the chip thickness ratio

$$v_c = v \cdot t_1 / t_2 \qquad \text{Eqn. 2.4}$$

If the chip thickness ratio is high, the shear plane angle is small and the chip moves away slowly, while a large shear plane angle means a thin, high velocity chip.
As any volume of metal, e.g. *klmn* figure 2.1 passes through the shear zone, it is plastically deformed to a new shape *–pqrs*. The amount of plastic deformation (shear strain γ) has been shown to be related to the shear plane angle ϕ and the rake angle α by the equation (Hill, 1950)

$$\gamma = \cos \alpha / (\sin \Phi \cdot \cos (\Phi - \alpha)) \qquad \text{Eqn. 2.5}$$

See figure 2.9 for a graphical representation of strain vs. shear plane angle. The longer the contact-zone or welded zone the hotter is the flow-zone and consequently also the thicker. The metal is softer and thus deforms more easily and a higher chip strain and a smaller shear plane angle are observed. When the cutting speed is increased the welded-zone becomes smaller and the heat affected region although hotter is smaller and less strain in the chips is observed.

As the force analysis is really simple for cutting on a shaper and the cutting speed is kept constant in the experiments that were done the work done vs. strain attained by the chips would be an interesting quantity to display graphically. For the shaper the work is given by the sum of the work on the shear plane and on the rake face.

$$d/dt(W_r(t)) = Q_r(t) = F_c(t) \cdot v_c \qquad \text{Eqn. 2.6}$$

Where W_r is the work performed on the rake face (J)
t is time (s)
Q_r is the rate at which work is done (Watts)
F_c is the cutting force (N) and
v_c as previously is the chip velocity (m/s).

After integration it follows that

$$W_r(t) = \int F_c(t) \cdot v_c \, dt \qquad \text{Eqn. 2.7}$$

All necessary data is available for numerical integration from the experiments that were performed.

The work (W_s) done on the shear plane is given by

$$d/dt(W_s(t)) = F_s \cdot v_s \qquad \text{Eqn. 2.8}$$

Where F_s is the shear force and v_s is the strain rate on the shear plane.

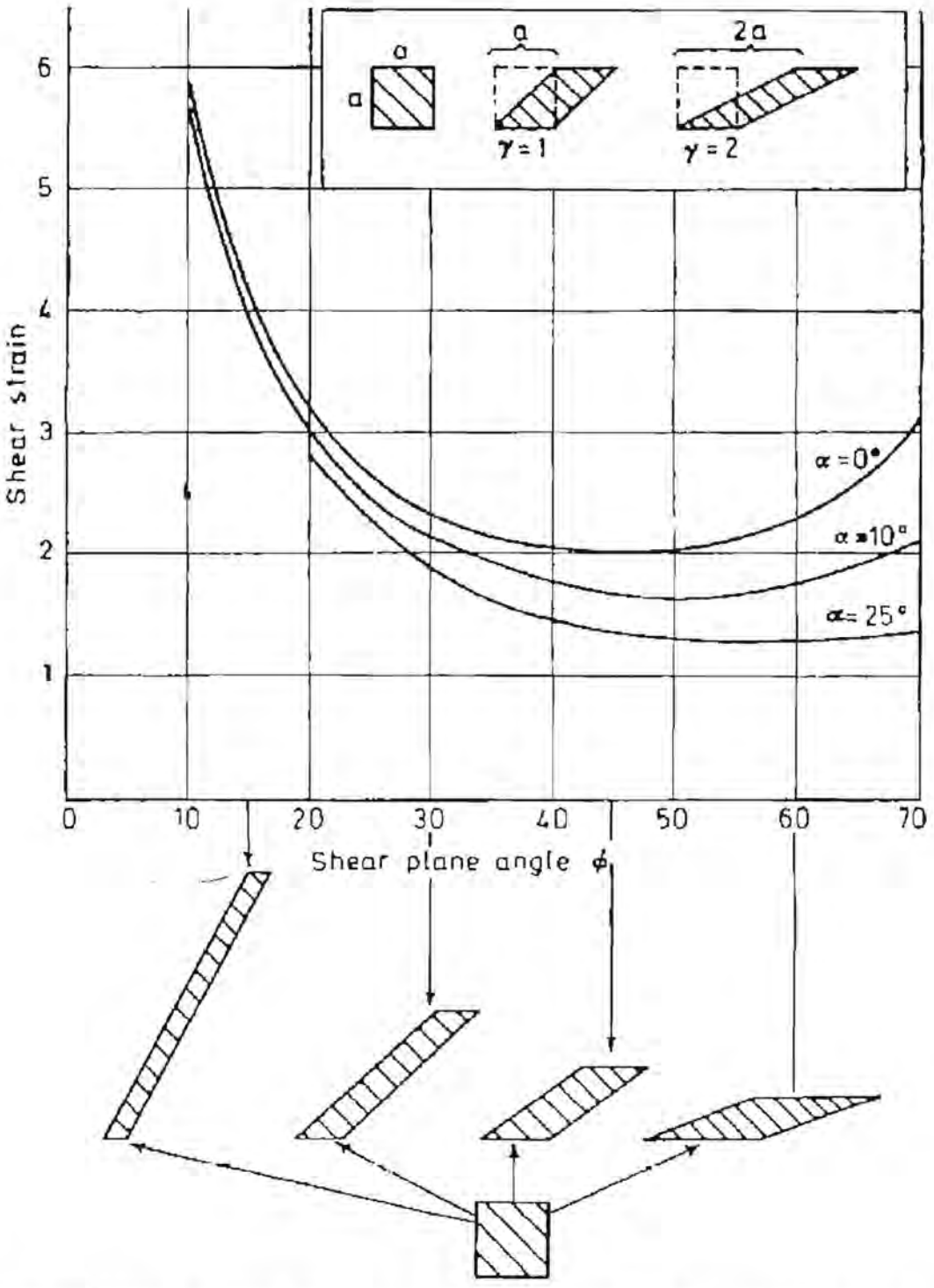

Figure 2.9 Strain on shear plane (γ) vs. shear angle (ϕ) for three values of rake angle (α) (Trent, 1977)

The shear force is given by

$$F_s = F_c \cdot \cos \Phi - F_f \cdot \sin \Phi \qquad \text{Eqn. 2.9}$$

(Trent,1977).
Since the Feed force F_f on the shaper is zero, the second term of equation 2.9 falls away.
The strain rate on the shear plane is given by

$$v_s = v / \cos \Phi \qquad \text{Eqn. 2.10}$$

and can easily be determined from figure 2.1 and work on the shear plane is thus:

$$W_s(t) = \int F_c(t) \cdot v \, dt \qquad \text{Eqn 2.11}$$

The total amount of work done in the cutting process is equal to the sum of the work done on the rake face and on the shear plane.

The graph of figure 2.9 shows the relationship between the shear strain in cutting and the shear plane angle for three values of the rake angle. For any rake angle there is a minimum strain when the mean chip thickness is equal to the feed ($t_2 = t_1$). For zero rake angle the minimum is at $\phi = 45°$. The change of shape of a unit cube after passing through the shear plane for different values of the shear plane angle is shown in the lower diagram of figure 2.9 for a tool with a zero rake angle. The minimum strain of the cube is apparent from the shape change. It is obvious that the more knife-like the cutting tool becomes i.e. the larger the rake angle becomes the less the chip is strained.

At zero rake angle the minimum shear strain is 2. Strain has units of length per length and therefore is dimensionless. The minimum strain becomes less as the rake angle is increased, and if the rake angle could be made very large; strain in the chip formation could become very small. In practice the optimum rake angle is determined by experience. Too large a rake angle weakens the tool and leads to fracture. Rake angles of greater than 30° are seldom used. In practice the tendency is towards a small rake angle because this way the tool can be made more robust. Harder but less tough tool materials can be used. Even under the best cutting conditions there is severe plastic deformation of the chip as it forms and this results in work hardening and structural change. It is not surprising that metals and alloys that lack ductility are sometimes fractured on the shear plane.

The Chip/Tool interface

The formation of the chip by the shearing action at the shear plane has attracted most of the attention in analyses of machining. It is equally important for the understanding of machinability and the performance of cutting tools to pay attention to the movement of the chip and of the work material across the faces and around the edges of the cutting tool. In most analyses this has been treated as a classical friction situation, in which 'friction forces' tend to restrain movement across the tool surface, and the forces have been considered in terms of a friction coefficient (μ) between the tool and the work materials. Detailed studies of the tool/work interface have shown that **this approach is**

inappropriate to most metal cutting conditions (Trent, 1977). Classical friction concepts do not apply.

According to classical friction principles the coefficient of friction (μ) is dependent only on (F) the force required to initiate sliding or to maintain sliding, and the normal force (N) at the interface at which sliding is taking place. The friction coefficient is defined as the ratio of the force(F) to the normal force (N). Put another way, the shear force (F) is proportional to the normal force (N). The friction coefficient is thus independent of the sliding area of the two surfaces. The proportionality results from the fact that real solid surfaces are never completely flat on a molecular scale, and therefore make contact only at the peaks of the asperites, while the valleys on the surfaces are separated by gaps. A profilometer can be used for measurement of the profiles of surfaces.

The frictional force is that force required to separate or shear apart the areas in actual contact at the asperity peaks. Under normal loading conditions for sliding, this real contact area is very small, often less than 0.1% of the apparent area of contact of the sliding surfaces. When the force acting normal to the surface is increased, the area of contact at the tops of the hills is increased in proportion to the load. The frictional force required to shear the contact areas, therefore also increases proportionately, so that the sliding force is directly proportional to the normal force. The above concepts are thus adequate for many engineering situations where stresses between the surfaces are small compared to the yield stress of the materials.

When the normal force is increased to such an extent that the real area of contact is a large proportion of the apparent contact area, it is no longer possible for the real contact area to increase proportionately to the load. In the extreme case, as with metal cutting, the two surfaces are in complete contact with each other and the real area of contact becomes independent of the normal force. Remember that in metal cutting due to metal shearing and friction there is enough heat build-up so that a welded-zone forms. (See also Hutchings 1992, but it must be pointed out that the load there is a static load and in metal cutting the load is dynamic, i.e. the load in metal cutting is applied where the two surfaces are in relative motion.) The force required to move one surface over the other becomes that necessary to shear or continue to shear the weaker of the two materials across the whole area. This force is almost independent of the normal force, but directly proportional to the apparent area of contact – a relationship that is directly opposed to that of classical friction concepts. This is evident for example when a built-up edge forms on the rake face of the tool or when a restricted contact tool is used then the apparent area of contact decreases and the cutting force decreases correspondingly. (see also figure 3.2)

It is therefore important to know what conditions exist at the interface between the tool and the work material during cutting. This is a very difficult region to investigate. Few significant observations can be made while cutting is in progress, and the conditions existing must be inferred from studies of the interface after cutting has stopped, and from measurements of stress, hardness profiles and temperature. The conclusions are deduced from studies mainly made by electron and optical microscopy (Trent, 1977), of the interface between work material and tool after use in a **wide** variety of cutting conditions.

Evidence comes from worn tools, quick-stop sections and from chips. In this study aluminium was cut and because it is soft relative to steel no worn tool resulted and the only evidence that was gathered came from measurements of cutting force and temperature during cutting and from the chips themselves.

The most important conclusion from the observations is that contact between tool and work surfaces is so nearly complete over a large part of the total area of the interface due to metal to metal welding, that sliding at the interface is impossible under most cutting conditions. (Trent,1977)

The evidence from optical electron microscopy demonstrates that the surfaces investigated (Trent,1977) are interlocked or seized to such a degree that sliding, as normally happens between surfaces with only the high spots in contact, is impossible. Some degree of metallurgical bonding is suggested by the frequently observed persistence of contact through all the stages of grinding, lapping and polishing of sections. There is however a considerable variation in the strength of bond generated, depending on the tool and the work materials and the cutting conditions.

In some cases the separation of the work material from the cutting tool occurs at the interface between the tool and the work material, but in other cases the break occurs in the chip itself. The chip undergoes ductile tensile fracture close to the interface, but not at the interface. This observation is from looking at cross-sections from quick-stop experiments. In quick-stop experiments the tool is explosively propelled away from the cutting position during cutting. (Trent,1977)

In the aluminium cutting that was done the separation occurred at the interface between the tool and the work-piece.

This kind of evidence demonstrates the mechanically interlocked and/or metallurgically bonded character of the tool-work interface as a normal feature of metal cutting. Under these conditions of cutting **movement of metal cannot be adequately described by the terms friction and sliding.**

They are inappropriate for two reasons:

- 1) there can be no relationship between the forces normal and parallel to the tool surface and
- 2) the force parallel to the tool surface is not independent of the total area of contact, but on the contrary, the area of contact between the tool and the work material is a very important parameter in metal cutting.

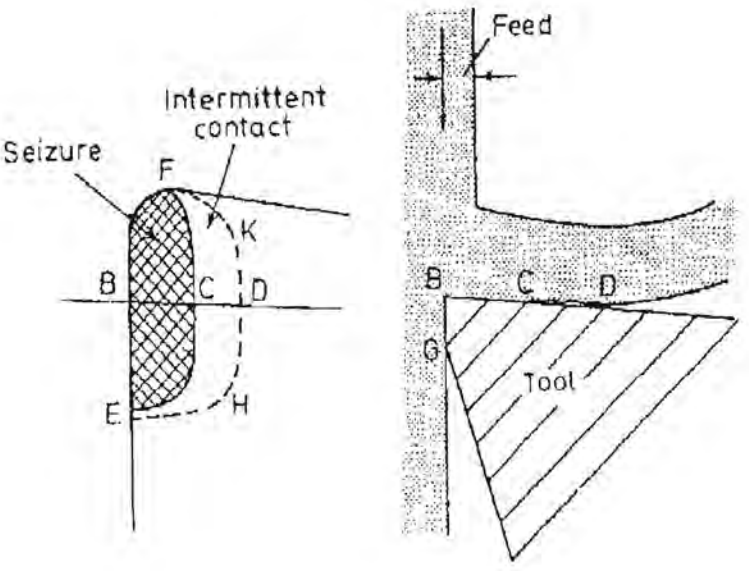

Figure 2.10 Areas of seizure on cutting tool

(Trent, 1977)

The size of this contact area or welded area directly influences the cutting forces and temperature. If it is bigger, metal is sheared for longer and a larger flow-zone, and consequently higher cutting forces and higher cutting temperatures are seen. The conditions at the work/tool interface are referred to as conditions of seizure as opposed to conditions of sliding. (Trent, 1977).

There is an enormous variety of cutting conditions that are encountered in practice. Mostly cutting takes place under conditions of seizure, but there are some situations where sliding does occur. This happens at very low cutting speeds of only a few cm/min and at these cutting speeds sliding is promoted by active lubricants. Low cutting speeds are common at the centre of a drill. Even under normal conditions of seizure it must be rare for the whole of the area of contact to be seized together. (figure 2.10)

The flank also undergoes wear. The flank is the underside of the cutting tool where the rake angle and the clearance angle apexes meet. BG represents the worn flank region and this counts as a secondary contact-zone in which more heat is generated and once the zone becomes large enough as flank wear progresses the tool overheats and tool failure is inevitable.

Chip Flow under conditions of seizure

Under sliding conditions relative movement of the surfaces can be considered to take place at the interface between the two bodies. Under seizure conditions this is not the case, because the force required to overcome the interlocking and bonding is normally higher than that required to shear the weaker of the two materials. The weaker material is thus sheared in a region of finite thickness which may lie adjacent to the interface or at some distance from it, depending on the stress system involved.

In sections through chips and in quick-stop sections, zones of intense shear near the interface are normally observed (see figure 2.11), except under conditions of sliding. This observation will partly be used for evaluation of cutting conditions on the experimental shaper set-up.

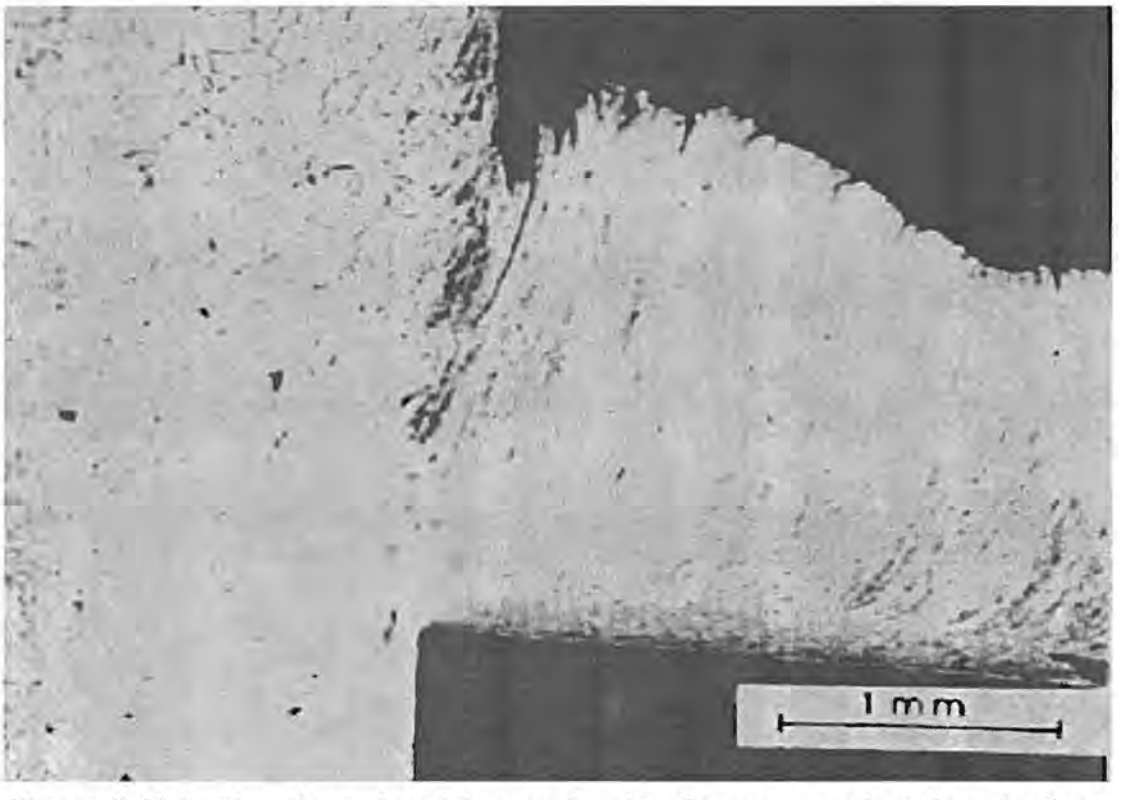

Figure 2.11 Section through quick-stop showing flow-zone against the rake face

(Trent, 1977)

The thickness of these zones is often of the order of 25 to 50 μm and strain/deformation within these regions is much more severe than on the shear plane, so that normal structural features of the metal or alloy being cut can be greatly altered or completely transformed. **It is in this region that the maximum temperature in the cutting process must be encountered.** The behaviour of the work material in these regions is in many ways like that of a very viscous liquid rather than that of a normal solid metal. Hence this region is referred to as the flow-zone. **The flow-zone blends in gradually with the rest**

of the chip meaning that there is no clear-cut distinction between the flow-zone and the chip or the work-piece. There is a flow pattern seen as a metal deformation pattern in the work material around the cutting edge and across the tool faces in the chip. The thickness and the pattern of the flow-zone is characteristic of the metal being cut and of the conditions during cutting. Different cutting fluids also affect the thickness of the flow-zone. The amount of strain and the degree of work hardening in the chip can vary greatly, depending on the material being cut, the tool geometry, and the cutting conditions, including whether a lubricant is used or not, and if a lubricant is used : the type of lubricant that is used. This is intended to be one of the focus areas of this study: i.e.:

i) what can and does the lubricant do for metal cutting and
ii) how can the chemistry involved contribute positively to the cutting process

The built-up edge (BUE)

The built-up edge is a condition of seizure that gives rise to one of the major types of chip formation. When cutting metal, hardened work material adheres around the cutting edge and along the rake face. It accumulates to displace the chip from immediate direct contact with the tool as shown in figure 2.12.

The built-up edge occurs frequently in industrial cutting and can be formed with either a continuous or a discontinuous chip as is the case with cutting steel and cast iron respectively.

The built up edge is not a separate body of metal during the cutting operation. It can be depicted as shown in figure 2.13 as the region that is shaded with a grey metal grain texture. It is welded to the tool surface. The maximum heat region is now somewhat removed from the tool surface as the flow-zone is in the chip very close to the interface between the built-up edge and the chip.

The built-up edge is between A and B and is continuous with the work material and the tool because there is seizure between the work material and the tool. The flow zone has been moved to the top of the built-up edge and is no longer on the tool surface. The new work surface is forming at A and the under surface of the chip is forming at B. The built-up edge is dynamic and is constructed of successive layers which are greatly hardened under extreme strain conditions. The size of the built-up edge cannot increase indefinitely. There comes a point when the shear stresses increase so much that part of the built-up edge is sheared off and carried away on the work surface or on the underside of the chip. In some cases the stress on the built-up edge becomes such that the whole build-up is sheared from the tool surface. After that the formation of a new built-up edge starts. The built-up edge is undesirable, because if it is sheared off and passes on the underside of the tool, it causes surface defects such as tears, smears and deposits on the worked material and it contributes to tool wear.

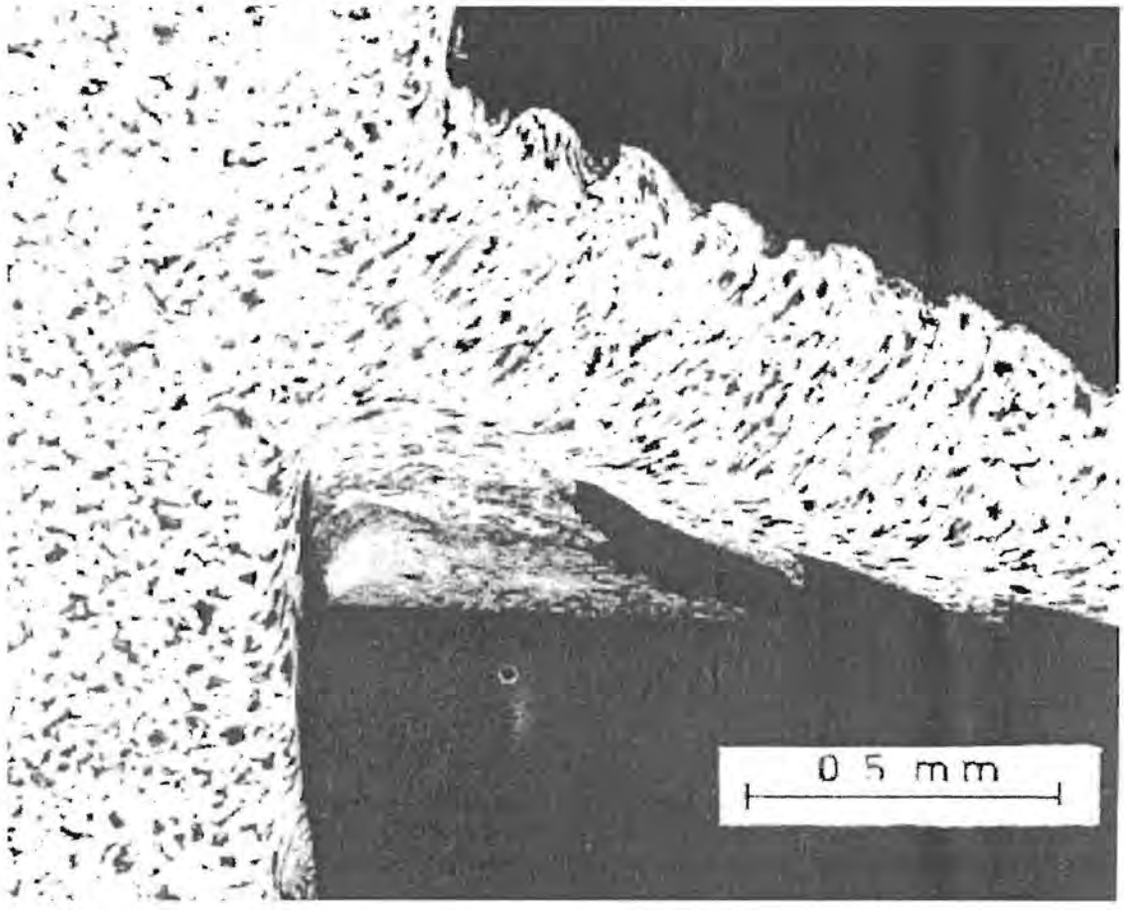

Figure 2.12 Section through quick-stop showing built-up-edge
(Trent, 1977)

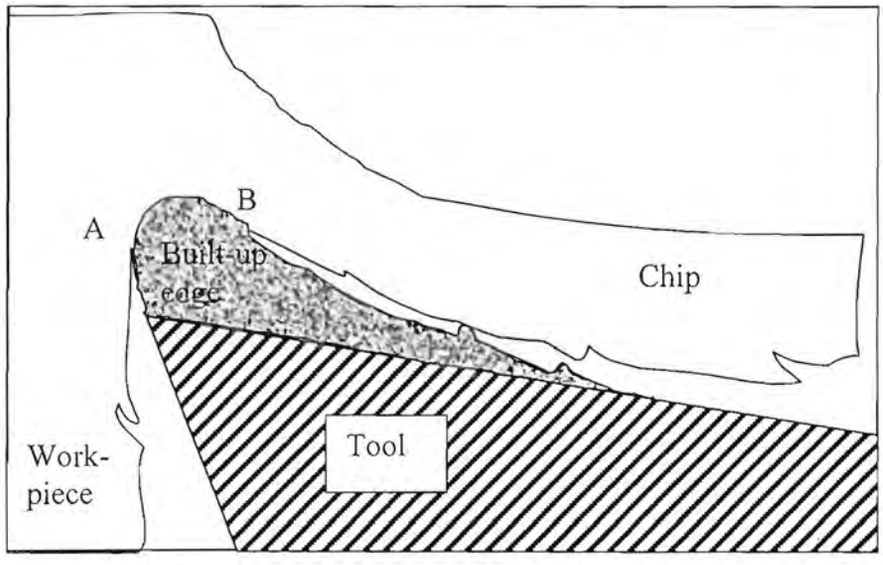

Figure 2.13 Shape of the built-up edge

(Trent, 1977; Follette, 1980)

There is no hard and fast line between the built-up edge and the flow zone. Compare figures 2.11 and 2.12. Seizure between tool and work material is a feature of both a built-up edge and a flow-zone and every shade of transitional form between the two can be observed. The built-up edge occurs in many shapes and sizes and it is not always possible to be certain whether it is present or not.

The built-up edge that is sometimes produced during metal cutting can be a major factor in influencing tool wear. At low cutting speeds, the built-up edge is more prevalent. A built-up edge can reduce tool life in one of at least three different ways. Firstly, when the built-up edge breaks away, it may take small fragments of the cutting edge with it. Secondly, the surface behind the built-up edge can experience severe wear in the form of a groove. Finally, since the tool material and the built-up edge material have different coefficients of thermal expansion, the heating - cooling cycle can produce cracks in the tool surface causing "flakes" of material to be removed. (Bartz, 1992)

The machined surface for analysis of the cutting process

Figures 2.11 and 2.12 demonstrated that the machined surfaces are formed by a process of fracture under shearing stresses. With ductile materials, both sides of a shear fracture are plastically strained, so that some degree of plastic strain is a feature of machined surfaces. The amount of strain and the depth below the machined surface to which it extends, can vary greatly , depending on the material being cut, the tool geometry, and the cutting conditions, including whether a lubricant is being used or not, and if a lubricant is used; the type of lubricant that is used.

The deformed layer on the cut surface can be seen as part of the flow pattern around the cutting edge which passes off with the work material, so that an understanding of the flow-pattern, and the factors which control it, is important in relation to the character of the machined surface. The presence or absence of seizure on those parts of the tool surface where the new work surface is generated can have a profound influence on the cutting process, as can the presence or absence of a built-up edge and whether the tool that is used is sharp or worn. The properties of the machined surface that are influenced are:

- the plastic deformation
- the hardness
- the roughness
- the precise geometry and
- the appearance.

3. Monitoring of the Cutting Process:

3.1 Parameters of the cutting process

A further factor to bear in mind when studying the cutting process is the cutting force. It is noted in the experimental work done that cutting forces are usually abnormally low when a built-up edge is present and that it is a phenomenon that occurs between two phased alloys but not with pure metals. The same was found by Trent. (Trent, 1977. The built-up edge changes the cutting conditions and therefore it should be avoided. The built-up edge acts like a restricted contact tool, effectively reducing the length of contact on the rake face (See figure 2.12). The cutting force is also lower for alloys than for pure metals over the whole cutting speed range, but is more pronouncedly so at low speeds than at high speeds. The reason for this is that alloys have a eutectic composition, that has a lower melting point than either of its constituent metals. (Rollason, 1973). That this is more pronouncedly so at low speeds is due to the melting of the pure metals being less complete as the cutting temperature in the flow-zone is lower. It is common experience, when cutting most metals and alloys, that the chip becomes thinner and the cutting force decreases when the cutting speed is increased. This is partly caused by a decrease in contact area and partly by a drop in shear strength in the flow zone as the temperature rises with increasing speed.

Tool speed or cutting speed is critical for tool life. The relationship between cutting speed and tool life may be plotted on a log-log graph from data and using the Taylor Equation (Follette, 1980; Trent, 1977; and Boston 1952) The Taylor equation in its simplest form is given by

$$v \cdot T^{n} = C \qquad \text{Eqn 3.1}$$

Where v is the cutting speed (m/min)
T is the tool life (min.)
C is a constant and is equal to the cutting speed on the log-log plot for a tool life of one minute. It is dependent on the conditions, the tool, the material, and the cutting fluid that is used.
n is the slope of the straight line on the log-log plot.

Tool life is also affected by fatigue. Mechanical fatigue, also caused by snap loading, and thermal fatigue are noteworthy contributors to tool failure, particularly in operations of an interrupted nature such as milling and shaping. The thermal fatigue is caused by the constant heating and cooling cycle in interrupted cutting. If the temperature difference between the hottest and coldest part of the cycle is too extreme minute cracks in the form of comb cracks start to develop in the tool surface.

Monitoring cutting force during metal cutting is also useful for determination of the state of wear of the tooling. Tools wear in several ways. In flank wear the flank below the side cutting edge is partly worn away by rubbing against the work-piece. The wedge of metal that is worn away leaves a land and the width of this land can be used to measure flank wear. In each case where a land forms, the area in the plane where shear occurs is

increased. The force needed to shear the work material on this plane is equal to the shear strength of the work material multiplied by the shear area, hence when this area increases the cutting force increases too, and by monitoring the cutting force it may be determined how far wear has progressed.

There is a minimum energy theory for the cutting of metals. The energy needed to do a cut is the work done on the shear plane and varies with the shear plane angle, and this curve therefore has the same shape as the curve for a tool with zero rake angle with a minimum at a shear plane angle of 45°. For a zero rake angle tool the minimum strain or metal deformation during cutting happens at a shear plane angle of 45°, (see figure 2.9). It is thus logical to have expected this because least deformation for a particular rake angle should correspond to least energy needed to perform the cut. (Trent, 1977).

The performance of tool dynamometers was greatly improved with the introduction of wire strain gauges, transducers or piezo-electric crystals as sensors to measure deflection to be able to calculate the cutting forces.

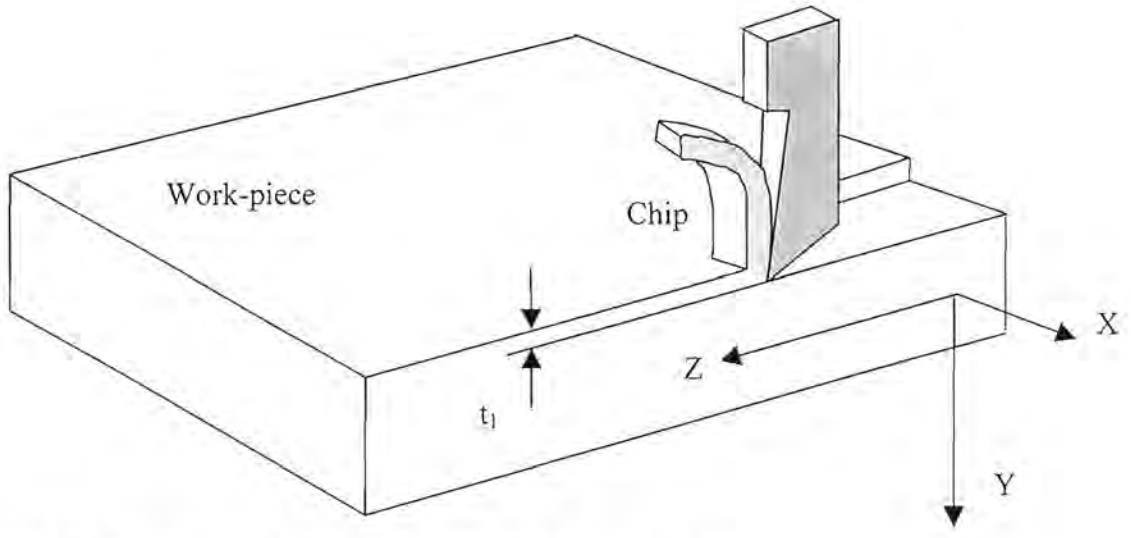

Figure 3.1 Schematic of the cutting process on the shaper

The cutting force F_c, is in the direction of the cut. That is in the Z direction on figure 3.1. It is usually the largest of the three force components and is referred to as the cutting force. The other force component is the feed force F_f and it acts in the direction parallel to the feed i.e., in the X-direction on figure 3.1. Lastly the normal force F_n, normal to the work-piece surface, that tries to push the tool out of the work-piece acting along the longitudinal axis of the tool, i.e. in the Y-direction on figure 3.1, is the smallest of all the components and is usually ignored and not even measured. It is referred to as the longitudinal force. t_1 indicates the depth of cut.

At low values of ϕ for the shear plane angle, the chip is thick, the area of the shear plane becomes larger, and, therefore the cutting force, F_c becomes larger. Therefore the

consequence of increasing either the shear yield strength at the rake face, or the contact area (length) is to raise the cutting force F_c.
As feed on the shaper takes place between cuts the feed force does not influence the cutting process, thus it is not monitored. The lateral force that would be classified as the feed force is balanced out in the experiments that were done as bi-directional restriction on chip flow was used. The contact area on the tool rake face in particular is seen to be a most important region, controlling the mechanics of cutting, and is a point of focus for research in metal cutting.

Pure metals are notoriously difficult to machine. The reason being that the cutting forces are high because the contact area on the rake face is very large and the shear plane angle is small and the very thick strong chips move away at slow speed.

The large contact area is probably associated with the high ductility of these pure metals. (Trent, 1977). One explanation for this is that the pure metals have a more regular crystal lattice structure with no interference from foreign metals or not the same metal atoms and that their atoms therefore can slide over each other more readily and therefore stay in contact with the cutting tool for longer. That the forces are due to the large contact area can be demonstrated by using a tool of restricted contact area as shown in figure 3.2.

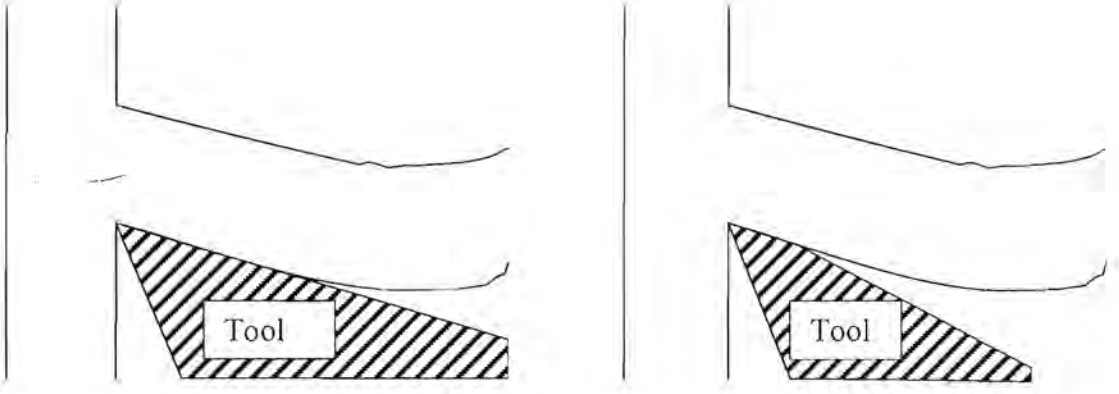

Figure 3.2 (a) Normal Tool; (b) tool with restricted contact on rake face

Results reported by Trent (Trent, 1977) show that the tool forces are much smaller (about half of those for the normal tool) for the tool of restricted contact. One possibility for experimental determination of contact lengths is to use tools of various restricted contact lengths and to see at which length the cutting force starts to decrease.

Reduction of the cutting forces by restricting the contact area on the rake face may be a useful technique in some conditions, but in many cases it is not practical because it weakens the tool. When the contact areas are small the chips that are produced are thin.

This then is another useful indication for a change in contact area. When only the cutting fluid and no other cutting parameter is changed and this observation is made then the contact area on the cutting tool may be determined from an etched micrograph and compared for the different cutting fluids. This would indicate that a cutting fluid has the ability to decrease the metal to metal affinity of the tool and the work-piece material.

It is common experience that when the cutting speed is increased when cutting most metals and alloys, that the tool forces decrease and the chips become thinner, but the temperature profile in the tool becomes higher i.e. the localised hot spots become hotter.

The decrease in tool forces is attributable to the decrease in shear strength in the flow-zone of the work material as it becomes hotter and also to the decrease in contact area upon increases in temperature, up to a point, thereafter upon further increases in temperature welding is promoted the contact area increases and when this becomes too intense the tool will fail catastrophically.

3.2 Heat in Metal cutting

The power consumed in cutting metal is mainly converted into heat in the flow-zone near the cutting edge of the tool, and many economic and technical problems are caused directly or indirectly by this heating action. The rate of metal removal that is attainable plays an important role in the economy of the cutting operation. There is however a limit to the rate, as too fast a metal removal rate will result in the tool life being shortened excessively. This is because the temperature of the tool at the contact-zone becomes too hot resulting in a decrease in its hardness and a corresponding increase in tool wear. When machining the softer metals and alloys tool life may not be the constraint, but rather the ability to handle large quantities of fast moving swarf.

It is important to understand the factors, which influence the generation of heat, the flow of heat and the temperature distribution in the tool and the work material near the tool edge. Determination of the temperatures and the temperature distribution in the vitally important region near the cutting edge is technically difficult. This region has fast dynamics, is very small and the conditions are harsh. To fit sensor equipment for temperature data acquisition in this region is not presently possible. Only methods such as micro-hardness tests and temperature dependent metal structure formations from which temperature and temperature distribution may roughly be inferred are used.

For an investigation into the chemistry of the lubricants used for the cutting process these temperatures also play a role because they influence the activation energy available for chemical reactions to occur.

Under most cutting conditions, the largest part of the work is done in forming the chip at the shear plane. In a simple model of action on the shear plane, the work material is heated instantaneously as it is sheared and all the heat is carried away by the chip. By this model, the temperature of the chip increases according to equation 3.2. (Trent, 1977).

$$T_C = n \cdot k \cdot \gamma / (J \cdot \rho \cdot C) \qquad \text{Eqn. 3.2}$$

where T_c = temperature increase in chip body (°C)
k = shear flow stress (N/m^2)
γ = shear strain dimensionless
J = mechanical equivalent of heat (kJ)
ρ = density (kg/m^3)
C = heat capacity (kJ/kg.°C)
$n \equiv$ constant (J)

A different equation to calculate chip temperature is given by Zorev & Shaw, 1966.This equation is very tedious to use and falls outside the scope of this investigation.

A reasonable estimate of the temperature that is reached within the chip body can be made in this way particularly at relatively high cutting speeds. The temperature of the chip can only affect the performance of the tool as long as it is in contact with the tool. After the chip breaks contact with the tool, the heat remains in the chip and is carried away with it out of the system. After the chip has become hot upon passing through the shear-zone it is not further deformed and heated as it passes over the rake face, and the time to pass over the rake face is very short. A cutting speed of 60 m/min. and a chip thickness ratio of two would give a chip speed of 30 m/min. For a contact length of 1mm on the rake face this equates to a time of 2 milliseconds as 30m/min is 500mm/s. This is a very short time and very little heat can be lost from the chip by any heat transfer mechanism. This is only based on the model and for this model the flow-zone has been ignored.

In reality heat may also be lost from the chip to the tool via conduction through the contact-zone or welded zone. This is so for very low cutting speeds. For speeds where the flow-zone just above the welded zone forms, the temperature in the flow-zone is higher than in the rest of the chip body. Heat then tends to flow into the chip body from underneath and no heat is lost from the chip into the tool by conduction. The chip temperature increases only very little because the flow-zone is very thin. Heat is also lost from the flow-zone into the tool.

The heat that is transferred to the work-piece from the shear plane can be partially accumulated in chips when more than one cut on or near the same place on the surface is made. For this reason the work-piece is often cooled so as to ensure dimensional accuracy. Part of the shear zone on the shear plane passes under the tool cutting edge and this leaves behind on the worked surface a heated and strained or deformed layer that has a very variable thickness. Any factors that contribute to a small shear plane angle increase the heat flow into the work-piece and the ductility of the work-piece. Alloying and any treatments to reduce the ductility of the work material or a larger shear plane angle, usually reduce the residual strain in the work-piece surface.

The heat generated at the tool/chip interface is of major importance in relation to tool performance. A reasonably good estimate of the amount of heat generated at the tool/chip interface can be made from the force and the chip thickness measurements. For a zero rake angle tool the heat generated, Q, is

$$Q = F_c \cdot v_c \qquad \text{Eqn.3.3}$$

Where F_c is the cutting force (N)
v_c is the chip velocity (m/s)

The temperature of the chip can be calculated with considerable accuracy, equation 3.2, because there is little error involved in assuming even distribution of strain rate across the shear plane, and neglecting heat losses during the short time interval involved. This simplification cannot be made for calculating temperatures in the flow-zone for three reasons:

1. Energy distribution in the flow-zone may be very non-uniform and the data from which to calculate it are unreliable because of the extremes of strain, strain-rate etc.
2. The thickness of the flow-zone, and the amounts of metal passing through are not accurately known.
3. The heat losses from the flow-zone may be large and difficult to calculate.

Many attempts have been made to calculate temperatures and temperature gradients on the rake face of the tool. The accuracy of these calculations is subject to considerable doubt. Although quantitative estimates of temperature by calculation are uncertain, it is helpful in understanding many aspects of tool life and machinability, to consider the general character of the flow-zone as a heat source. The material in the flow-zone is changing continuously since new material is continuously fed into the zone and it is sheared, deformed and compressed along all the way until it leaves the flow-zone.

Shearing and deformation heats the material significantly, and the temperature increase depends on the amount of work done on the quantity of metal passing through the flow-zone. The thickness of the flow-zone provides some measure of the latter; and the thinner the flow-zone the higher the temperature would be for the same amount of work done. The thickness varies considerably with the material being cut from more than 100 μm to less than 12 μm. It tends to be thicker at low speeds, but does not vary greatly with the feed. In general the flow-zone is very thin compared with the body of the chip – commonly of the order of 5% of the chip thickness. Since the work done at the tool rake face is frequently about 20% of the work done on the shear plane, much higher temperatures are found in the flow-zone than in the chip body, particularly at high cutting speeds.

The temperature in the flow-zone is also strongly influenced by heat loss by conduction because the heat is generated in a very thin layer of metal which has a large area of metallic contact both with the body of the chip and with the tool, i.e the area to volume ratio for this layer is very large. The maximum temperature in the flow-zone is way back

from the cutting edge and is reduced by heat loss by conduction into the chip. (see figure 3.3) After the chip leaves the tool surface, that part of the flow-zone which passes off on the under surface of the chip, cools very rapidly to the temperature of the chip body, because cooling by metallic conduction is very efficient. The increase in temperature of the chip is slight because of the relatively large volume of the chip body.

The conditions of heat loss from the flow-zone into the tool are different from those at the flow-zone/chip body interface because heat flows continuously into the same small volume of tool material. The bond at this interface is often completely metallic in character, and when this is true, as it often is, then the tool will effectively have the same temperature as the flow-zone material at the surface of contact. Under constant operating conditions a stable temperature gradient is built up in the tool as it acts as a heat sink into which heat flows from the flow-zone. The amount of heat lost from the flow-zone into the tool depends on the thermal conductivity of the tool, the tool shape, and any cooling method used to lower its temperature. The heat flowing into the tool from the flow-zone raises its temperature and this is the most important factor limiting the rate of metal removal when cutting the higher melting point metals.

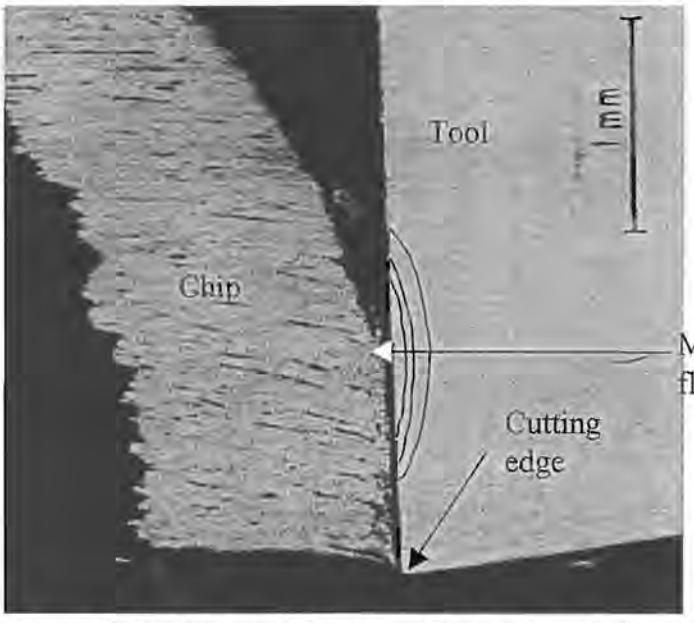

Figure 3.3 Maximum temperature region in flow-zone

(Adapted from Trent, 1977)

With aluminium and the other softer lower melting point materials the problem is to cope with large quantities of fast moving swarf. Managing chip shape here is therefore an important parameter. The temperatures reached in the flow-zone however do affect the surrounding material like the tool, the chip and the kind of lubricant, if used, and therefore for purposes of measuring lubricant performance in the cutting process it is important to be able to determine the temperatures and temperature profiles in response to the various lubricants used for metal cutting. The type of material used for the tool and

the type of material that constitutes the work-piece and the temperatures that are reached can all affect the chemistry of the lubricant that is used.

The tool clearance face needs to have a large enough clearance angle to prevent it from rubbing against the newly formed surface on the work material. A reasonable clearance angle is typically between 5° and 10 °. Making the clearance angle too big weakens the tool too much. With using a smaller clearance angle, 1° for example, there is a risk that a long contact path on the clearance face is established and this will be a third heat source, similar in character to the flow-zone on the rake face. Even with normal clearance angles, prolonged cutting results in 'flank wear', in which a new surface is generated on the tool more or less parallel to the cutting direction. A 'wear land' develops and the work material is often seized to it and when the wear land becomes long enough it becomes a serious heat source. Generation of high temperatures in this region is usually followed by immediate collapse of the tool.

3.3 Methods of tool temperature measurement

It is difficult to calculate temperatures and temperature gradients at or near the cutting edge, even for very simple cutting conditions. This indicates that it is important to be able to measure the temperatures, hence a few of the experimental methods used are now discussed.

Tool-work thermocouple

The tool/work-piece thermocouple method of tool temperature measurement makes use of the tool and the work material as the two elements of the thermocouple. The thermo-electric e.m.f. that is generated between the two dissimilar metals is typically of the order of millivolts. With standard thermocouples a 1°C-temperature change results in a few tens of microvolts change in the e.m.f. that is generated at the hot junction. The hot junction is the contact area at the cutting edge, while an electrical connection to a cold part of the tool forms the cold junction. The tool is electrically insulated from the machine tool; i.e. it is electrically floating. For the case of this investigation the machine tool is a shaper. Cutting is thus constant and intermittent. Care must be taken to avoid secondary electrical connections such as can happen when using tipped tools or when the chip curls back onto the tool as when using a chip breaker.

The e.m.f. can be measured and recorded during cutting. To convert the microvolt signal that is recorded to temperature it is necessary to calibrate the tool/work thermocouple against a standard thermocouple. Each different combination of tool and work material used must be calibrated separately.

This method of temperature determination is not so easy as it seems; it is subject to several sources of error. Somehow these errors must be eliminated or compensated for. Firstly the tool/work thermocouple does not consist of ideal thermocouple materials consequently the e.m.f. that is generated is low and the e.m.f. temperature response is far from linear. One may need to amplify the measured signal several hundred times for use

as a signal into a computer for data logging. With the amplification can be associated a significant amount of noise and this can cause difficulty in interpreting the observed signal. If the signal is not amplified and only measured and recorded with a sensitive millivoltmeter there may be noise that is camouflaged in the signal and thus one may not be aware of its presence. It is further doubtful that the thermo-e.m.f from a stationary couple, used in calibration, corresponds exactly to the thermo-e.m.f. during cutting conditions where the work material is severely strained. When calibration is done the conditions are static and during cutting, the conditions are dynamic. An experiment will show the effect that straining the tool/work-piece interface has on the e.m.f. that is generated.

Quite a large number of test results have been reported by other workers for different tool and work materials. (Trent, 1977; and Boston, 1952) All investigations show a large increase in temperature as the cutting speed is increased. The temperatures reached are dependent on the amount of material that passes through the flow-zone per time unit, i.e. on the amount of material being sheared per time unit. The dimensions of the flow-zone change with cutting speed. Temperatures of over 1000°C have been recorded. The reliability of the measured temperatures is in doubt because of the very steep gradients that exist at the tool/work interface. Figure 4.3 shows that these gradients are very steep. Under these conditions the measured e.m.f. may represent a mean or average value for the temperature, or possibly the lowest temperature at the interface. The use of thermocouples in the sub-surface of the rake face have the same problem, and they are further away from the flow-zone than the tool/chip interface is.

Another way of eliminating errors is to electrically insulate the aluminium work-piece in ceramic and then heat the work-piece. An RTD (resistance temperature device) is inserted into a hole very close to the tool/work-piece junction and the work piece is heated with a gas torch. As aluminium is a good conductor of heat, the RTD and the tool work-piece junction will be very close to the same temperature. Using a computer to log the temperature data corresponding to the e.m.f. as the work-piece is heated makes it possible to set up an nth order polynomial that relates the e.m.f. to temperature directly. (Considine, 1974; and Capgo, 2002).

Inserted thermocouples

To measure temperature and distribution of temperature in the tool has been the objective of many experimental studies. (Trent, 1977; Varadarajan, Philip & Ramamoorthy, 2001; and Kelly & Cotterell, 2001)
One simple but tedious method is to make a hole in the tool in the region where the temperature is to be measured, and to insert a thermocouple in a precisely determined place close to the cutting edge. For determining temperature distribution this process needs to be repeated many times in holes at different places so that temperature mapping can be done. The problem with this is twofold: 1) the tool is weakened by drilling the hole into it and 2) the temperature gradient in the tool is very steep. It is of the order of 300°C/mm and higher per positional change. (See figure 4.3) Now a thermocouple tip is

more than 1 mm in diameter, so the question is where exactly is it measuring the temperature? It is clear that this method will not be satisfactory to determine temperature distribution.
This method is probably as satisfactory in comparing tool temperatures when cutting different alloys as the tool/work thermocouple.

Other methods

Other methods involve:

i) measuring the radiation from the heated tool areas, but used to have the drawback that they only give an indication of the temperatures on the exposed surfaces. Nowadays remote sensors like single wavelength, dual wavelength and multi wavelength devices, which are non-contact devices, have special forms of filtration so that that they can read below the surface of a molten metal. (Brown, 2002) The problem however still remains one of exactly how deep below the surface and over what size of area is the measurement taken. Temperature gradients in metal cutting are extremely steep, as will be shown in chapter 4.

ii) An infra red laser type thermometer can also be used. This bounces an infrared ray on the surface where the temperature is to be measured, but also has the drawback that it can only measure the temperature on the exposed surfaces.

iii) The exposed surfaces can be photographed using film that is sensitive to infrared radiation. The heat image of the tool and the chip on the film is scanned using a micro-photometer, and from the intensity of the image the temperature gradient on the exposed surface may be plotted. For the rake surface the maximum temperature occurs at some distance back from the cutting edge, and the temperature is lower near the cutting edge itself.

iv) Yet another method is to use a PbS photo-resistor. By using tools with small holes in different positions and focussing the heat image through these holes onto the PbS photo-resistor, which is calibrated to measure temperature, a map of the temperature distribution on the rake face may be constructed. (Trent, 1977)

Structural changes in high speed steel (HSS) tools

The temperature gradients in three dimensions throughout the part of the tool near the cutting edge, are estimated by observing the structural changes in the metal of high speed steel tools under cutting conditions where the temperature is raised over 600 °C. This temperature and temperatures well in excess are reached when machining the high melting point metals and alloys at relatively high cutting speeds. Above 600°C HSS's are rapidly 'over-tempered' – the hardness after heating decreases and the structures pass through a series of changes which can be followed by micro-examination after polishing and etching. Polished sections are etched in Nital (a 2% solution of HNO_3 in alcohol) to reveal structural changes. The changes in tool steel can be followed by means of micro-hardness tests. There is a rapid decrease in hardness in those parts, which have been heated between 650 °C and 850 °C, and an increase in regions heated to temperatures above the transformation point, i.e. 900°C where the structure becomes austenitic and re-hardens when it cools very rapidly.

The above could come in useful for the performance evaluation of coolants and lubricants in as much that it could possibly help to verify the length of the contact/welded zone as the heat affected region should be smaller for a cutting fluid that is able to reduce the metal to metal affinity and able to enhance the Rebinder effect (Hutchings, 1992). The Rebinder effect is a chemo-mechanical effect that includes environmental factors that can influence plastic flow, by affecting the mobility of near-surface dislocations. Surface chemical reactions are greatly enhanced by friction. The Rebinder effect may be detected from micro-hardness measurements, (Hutchings, 1992) The softer the metal the more ductile/bendable it is. If the chip can thus curl easier then it will experience less work hardening and if it can curl sooner then a shorter welded-zone should result, which should result in cooler operating conditions or at least a smaller heat affected region.

4.Properties of Cutting Fluids

4.1 Functions of cutting fluids

Cutting fluids consist of those liquids and gases that are applied to the tool and the material being machined to facilitate the cutting operation. Vast quantities are used annually to accomplish a number of objectives. (Boston, 1952)

1) To prevent the tool from overheating, i.e. so that no temperature is reached where the tool's hardness and resistance to abrasion are reduced, thus decreasing the tool life.
2) To keep the work cool, preventing machining that results in inaccurate final dimensions.
3) To reduce power consumption, wear on the tool, and the generation of heat, by affecting the cutting process. This investigation wishes to establish a relationship between the surface chemistry of the lubricants involved and how they can accomplish reducing the contact length on the rake face of the tool where most of the heat during cutting is produced.
4) To provide a good surface finish on the work.
5) To aid in providing a satisfactory chip formation (related to contact length)
6) To wash away the chips/clear the swarf from the cutting area.
7) To prevent corrosion of the work, the tool and the machine.

The desirable properties of cutting fluids in general are (Boston, 1952)

1) High thermal conductivity for cooling
2) Good lubricating qualities
3) High flash point, should not entail a fire hazard
4) Must not produce a gummy or solid precipitate at ordinary working temperatures
5) Be stable against oxidation.
6) Must not promote corrosion or discoloration of the work material.
7) Must afford some corrosion protection to newly formed surfaces.
8) The components of the lubricant must not become rancid easily
9) No unpleasant odour must develop from continued use
10) Must not cause skin irritation or contamination
11) A viscosity that will permit free flow from the work and dripping from the chips.

4.2 Types of cutting fluids

Cutting fluids may be divided into four main categories (FVTC, 2000) :

i- straight or neat cutting oils
ii- water miscible or water-based fluids
iii- gases
iv- and paste or solid lubricants

The water-based fluids act mainly as coolants and the neat cutting oils act mainly as lubricants. There are many variants of both types. Fatty acids are often incorporated in the neat oils. Until recently both the emulsions or soluble oils as they are also called and the neat oils, contained chlorine and sulphur additives that improved lubrication under

extremely difficult conditions. Chlorine affects the skin detrimentally and its degradation products are often carcinogenic and sulphur is environmentally unacceptable. Consequently other lubrication improvers under difficult conditions are searched for. Ester technology is used successfully for softer materials where high rates of metal working are needed, and where heat generation is not a major problem. (du Plessis, 2001) These can operate at higher temperatures as they have better resistance to thermal degradation than mineral oils. (Mortier & Orszulik, 1993) They are biodegradable and do not cause dermatitis and are therefore more environmentally acceptable. In many cases phosphor and sulphur do however still form part of the cutting fluid. (FVTC, 2000)

For the water miscible fluids water quality has a large effect on the coolant. Hard water (high mineral content) can cause stains and corrosion of machines and work pieces. Water can be deionized to remove the impurities and minerals. Water is the best fluid for cooling. It has the best ability to carry heat away. Water, however, is a very poor lubricant and causes corrosion.
Oil is excellent for lubrication but very poor for cooling, and it is also flammable. It is clear that, from a lubrication point of view water and oil have strengths but also some weaknesses. If water and oil are combined and an attempt is made to minimise the weaknesses the best properties of both may be balanced to obtain desirable end properties for the cutting fluid. Water-soluble fluids have been developed which have good lubrication, cooling ability, low-flammability and corrosion resistance. These fluids are usually mixed on site. It is crucial that the mixing directions and concentrations are followed very closely to get the maximum benefit from the coolant. (FVTC, 2000)

Emulsions
An emulsion is a dispersion of oil droplets in water. Soluble oils are mineral oils that contain emulsifiers. Emulsifiers are soaps or soap-like agents that allow the oil to mix with water and stay in suspension. Emulsions (soluble oils) when mixed with water produce a milky white product. Lean concentrations (more water, less oil) provide better cooling but less lubrication. Rich concentrations (less water, more oil) have better lubrication qualities but poorer cooling properties.
There are different types of soluble cutting fluids available including extreme pressure soluble oils. These are used for extreme machining conditions like broaching and gear hobbing for example. (FVTC, 2000)

Chemical Fluids
Chemical coolants are also miscible cutting fluids. Chemical cutting fluids are pre-concentrated emulsions that contain very little oil. Chemical fluids mix very easily with water to form an emulsion. The chemical components in the fluid are used to enhance the lubrication, bacterial control, and rust and corrosion characteristics. There are several types of chemical coolants available including coolants for extreme cutting conditions.
Inactive chemical cutting fluids are usually clear fluids with high corrosion inhibition, high cooling, and low lubrication qualities. Active chemical fluids include wetting agents. They have excellent rust inhibition and moderate lubrication and cooling properties.
Sulphur-, chlorine- and phosphorous- containing compounds are sometimes added to improve the extreme pressure characteristics. These are usually in an organic form, i.e.

the sulphur, chlorine or phosphorus is grafted onto a hydro-carbon backbone. (FVTC,2000)

Straight Cutting Oils

Straight cutting oils are not mixed with water. Cutting oils are generally mixtures of mineral oil and animal, vegetable or marine oils to improve the wetting and lubricating properties. Sulphur, chlorine, and phosphorous compounds are sometimes added to improve the lubrication qualities of the fluid for extreme pressure applications. There are two main types of straight oils: active and inactive.

Inactive Straight Cutting oils

Inactive oils contain sulphur that is very firmly attached to the oil. Mineral oils are an example of straight oils. Mineral oils provide excellent lubrication, but are not very good at heat dissipation (removing heat from the cutting tool and work piece). Mineral oils are particularly suited to non-ferrous materials such as aluminium, brass, and magnesium. Blends of mineral oils are also used in grinding operations to produce high surface finishes on ferrous and non-ferrous materials. (FVTC, 2000)

Active Straight Cutting Oils

Active oils contain sulphur that is not firmly attached to the oil, i.e. it is part of the oil molecule but is only weakly bonded to the hydro-carbon backbone. Thus the sulphur is easily released during the machining operation to react with the work piece. These oils have good lubrication and cooling properties. Special blends with higher sulphur content are available for heavy duty machining operations. They are recommended for tough low carbon and chrome-alloy steels. They are widely used in thread cutting. They are also good for grinding as they help prevent the grinding wheel from loading up. This increases the life of the grinding wheel. (FVTC, 2000)

Gases and vapours

Cutting oils and water miscible types of cutting fluids are the most widely used. Compressed air, inert gases like carbon dioxide, Freon, and Nitrogen are sometimes used. A vortex tube may be used to apply gaseous lubricants or coolants (ARTX, 2002). Using this tube, it is possible to apply the gases at a very low temperature and under medium pressure thereby facilitating a higher gas density and cooling and lubrication capability. Cutting using sub-zero cold gas is known as cryogenic cutting. The gas stream also helps to blow away chips from the cutting area. (FVTC, 2000)

The further advantage of a gaseous or vapour phase cutting fluid is that the constituents are of a far finer nature than liquids or solids, and due to the way of application, namely jet application, have far greater kinetic energy, and therefore have a greater penetrative capability. Molecular exchange is much slower when flood lubrication is used. Any adhered film is static and can be penetrated by the cutting fluid when jet type application is used. This promotes convective cooling and adds capacity for evaporative cooling.

(Varadarajan, Philip and Ramamoorthy, 2001) As far as vapour phase cutting fluids are concerned carbon tetra chloride (although forbidden to use as a cutting fluid) is very volatile and vaporises easily under ambient temperature conditions. Gas phase molecules do not adhere to each other as much as the molecules of liquids and are thus far more free to move.

Paste and Solid Lubricants

Waxes, pastes, soaps, graphite and molybdenum disulphide are examples falling into this category. These are generally applied directly to the work piece or tool or in some cases impregnated directly into the tool, for example the grinding wheel of a grinder. One example of a paste lubricant is lard. Many experienced journeymen recommend lard for tapping.

Lubricants for metal cutting may be presented schematically as in figure 4.1 .

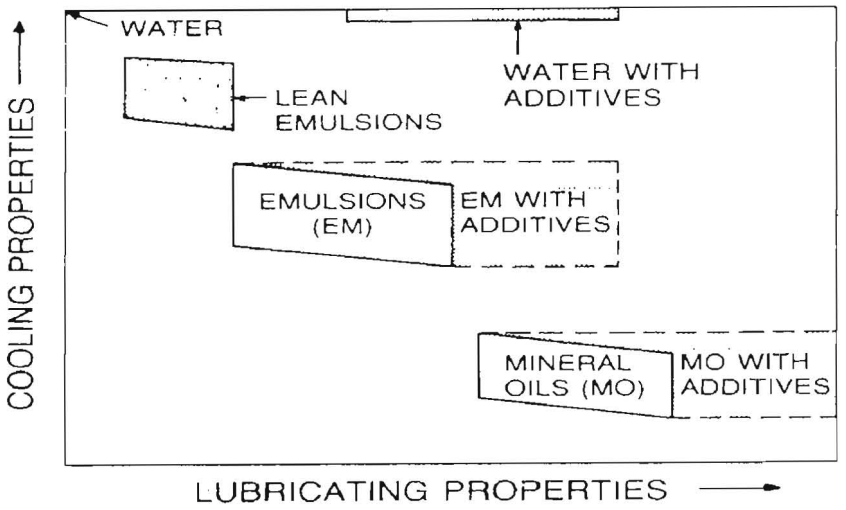

Figure 4.1 Lubricating and cooling properties of metalworking fluids.
(Mortier & Orszulik, 1993)

Coolants

The use of coolants becomes particularly essential when machining high melting point metals and alloys. Their use is most important when cutting with steel tools, but they are also used when cutting with carbide tools. (Trent, 1977).

In section 3.2 the two main sources of heat in the cutting operation were discussed – on the primary shear plane and in the flow-zone on the tool/work interface. The work done in this region is converted into heat, while the work done by sliding friction only makes a minor contribution to heating under most cutting conditions. Coolants cannot prevent the heat being generated, as they do not have direct access to the zones which are the heat sources.

Cutting fluids used in more severe operations must have very good anti-weld and lubricating properties to protect the cutting tool and to ensure proper surface finish and accuracy. (Mortier & Orszulik, 1993). More severe operations are those where the cutting

fluid cannot be in direct contact with the tool at the cutting point as for example during a band sawing operation or any other operation where the work-piece restricts access to the cutting point, hence turning is a less severe operation. More severe operations demand more active cutting fluids and usually also a decrease in cutting speed. This means that additives, particularly of the extreme pressure type, must be used under severe operational conditions. Cutting fluids contain a wide variety of speciality chemical additives designed to improve lubricity, surface activity, stability and anti-weld properties. (Mortier & Orszulik, 1993)

The Chemistry of cutting fluids : a partial overview

When the metal is cut a clean nascent surface at atmospheric pressure results that is very reactive and quickly adsorbs either by chemisorption (strong) or physisorption (weak) any substances (liquids or gases) in sufficiently close proximity to itself. Chemisorption is the adsorption onto a surface where a chemical bond such as a covalent or ionic bond forms, whereas physisorption involves lesser forces of adhesion like van der Waals forces from polar interactions between atoms. Depending on the cutting process used, the time available for chemical equilibrium to establish itself on the new metal surface varies, and this could influence the performance of the cutting fluid used. Monitoring certain cutting process parameters that will need to be determined from the experimental results should indicate cutting fluid life, i.e. how long it takes when cutting for the cutting fluid to stop aiding the cutting process.

It does seem feasible that the cutting fluid that is applied to the tool tip just before cutting can last for a short time as a protective film as its bond energy from chemisorption is typically 40 to 800 kJ/mol (Nix, 2002) and the bond energies of aluminium are typically in the region of 0.015kJ/mol to 57 kJ/mol. (Xuegang et al, 2002) The metal soaps that would originate are layers that would have a lower tendency to weld than metal. Catalysis can and often does happen, and there may be a need for the initial cutting fluid to have a specific molecular arrangement for catalysis to occur in the metal at the interface of the tool and the shear-zone. Thus it may be possible for similar cutting fluids to exhibit different results during cutting.

As limited volume lubrication uses only very little cutting fluid it is necessary that the cutting fluids must have enhanced reactivity. According to Rowe and Murphy (Rowe & Murphy, 1974), such enhanced surface activity may be represented as follows:
Enhanced reactivity = Exoelectron + Elevated temperature + High pressure.

To provide lubricants with sufficient load carrying capacity and friction characteristics for cold rolling of aluminium, additives are added to the low viscosity mineral base oils. These additives are mainly fatty alcohols, fatty acids and fatty esters. Fatty alcohols ensure better performance of the lubricant because they do not affect the annealing properties of the aluminium.

Tribochemical reactions of these additives with aluminium are very interesting. Organometallic products result from reaction of the fatty additives with fresh unoxidised metal surfaces that formed during plastic deformation. These surfaces are very reactive and are called nascent surfaces. Fatty acid soaps are well known. It is clear that esters, ethers and alcohols react with fresh aluminium surfaces. (Montgomery R.S., 1965). It has been suggested that polymeric soap formation results from reaction with esters and fatty acids, and alkoxide formation from alcohols and ethers. Fatty alcohols can lead to a similar reaction of soap formation but to a lesser extent than fatty acids. In this case, it was assumed that part of the alcohol was changed in to an acid which can react to give an ester and a blend of hybrid soaps of the general formula

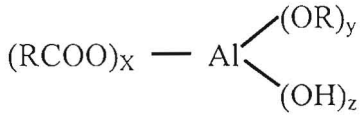

where x = 1,2 or 3 and x + y + z = 3.

The negative-ion lubrication mechanism proposed by Kajdas, (Kajdas, 1987) explains the formation of aluminium alkoxides i.e. the $Al(OR)_y$ part of the hybrid soap from alcohols. The mechanism is based on the low-energy electron emission process from the aluminium surface. The action of the emitted electrons on alcohol molecules produces negative and radical-negative ions, including $R\text{-}CH_2\text{-}CH_2\text{-}O^-$ ions which provide alkoxides by reacting with the positively charged sites on the plastically deformed aluminium surface.(Mortier & Orszulik, 1993)

The cutting fluids stabilise the nascent metal surfaces by means of reacting with them. The metal salts that form serve as a low shear strength film that reduces friction and provides improved anti-weld properties, i.e. the resulting surface has better anti-weld properties than the unreacted freshly formed nascent metal surface. The result is a shorter welded-zone or contact length and there is therefore less shear, a lower cutting force and a reduced cutting temperature. When metal is cut in a vacuum a longer contact length is observed than when it is cut in air. (Trent,1977) When air is present the oxygen reacts with the nascent metal surface instead of the tool and this reduces the contact length. The oxide layer on the tool does not form at the hottest region on the tool but a little further away in the cooler region, because the oxygen in the air reacts preferably with the nascent metal surface and is thereby removed from the cutting edge region of the tool. Similar to the oxide layer producing a shorter contact length the cutting fluids also react with the nascent metal surface produced in metal cutting to bring about a reduced contact length, i.e. the size of the welded zone is reduced.

In a paper by Kajdas (Kajdas, 1996) it is stated that metal surfaces that are coated with oxides, hydroxides and adsorbed organic contaminants are not sufficiently chemically active. The mechanical action at solid surfaces tends to promote reactivity of the surfaces by exposing nascent high reactivity surfaces that can promote chemical reactions that are entirely different to those reactions that would be observed for static systems. Friction at the nascent surfaces initiates and accelerates chemical reactions that would otherwise only occur at higher temperatures or not initiate at all.

Experiments done in a vacuum chamber of restricted volume, where 27 elemental metals were rubbed on each other, and mass spectrometry was used to show the nature of the gases being adsorbed showed the following: (Kajdas, 1996)

1) Oxygen and water molecules were adsorbed on the metal surfaces, and hydrogen molecules were desorbed from the metal surfaces during sliding. Far more adsorption of oxygen was observed during mild wear than during severe wear.
2) Oxygen adsorption on the metal surfaces during the wear process was governed by the position of the metallic element in the periodic table
3) A high gas consumption rate was observed in rare earth metals and in the transition metals, which tend to wear in a mild manner during rubbing.
4) A higher gas consumption rate for Fe/Fe rubbing in the mild wear mode than in the severe wear mode.
The chemical nature of nascent metal surfaces is one of the most important active sources for tribochemical reactions. From experiments performed in a restricted volume chamber under vacuum where nascent surfaces were produced by scratching the metal surface the following was found (Mori,S., 1995).
1) Enhanced activity on the nascent metal surfaces. The gold surface for example became so active that organic compounds chemisorbed on it.
2) Aromatic compounds decomposed catalytically on nascent transition metal surfaces even at room temperature.
3) The chemical nature of the nascent surfaces for the simple metals was different from that of the transition metals
4) According to the chemisorption activity of organic compounds, the chemical activities of nascent metal surfaces were dependent on their electronic surfaces.

The tribochemical activity of fresh metal surfaces is very complex and is still not well understood. (Kajdas, 1996).

Application of cutting fluids

Many machine tools are fitted with a system for handling the cutting fluids. For near-dry machining a spray or mist type applicator is used. The position on the tool and work-piece where the lubricant/coolant is applied plays a significant role in the temperatures and the temperature distribution that will result during metal cutting. (See figures 4.2 to 4.4 (Trent, 1977 and also figure 2..3)

Most of the heat generated on the shear plane is carried away in the chip, only very little is conducted into the work-piece which is voluminous in relation to the chip and thus the temperature rise is much lower in the work-piece. The work-piece is usually kept cool for purposes of dimensional accuracy. In relation to the tool in the cutting process all surfaces are stationary; only the tool itself is moving and in constant contact or proximity of the zones in which heat is generated. It is the tool that is damaged by the high temperatures and therefore, cooling is most effective through the tool in most cases. The

tool is cooled most effectively by directing the coolant to the accessible surfaces of the tool which are at the highest temperatures, as these are the surfaces from which the heat is most rapidly removed, and the parts of the tool most likely to suffer damage. It is helpful to know the temperature distribution in the tool for a rational approach to coolant application.

In figures 4.2 to 4.4 (Trent, 1977,) the HSS tool that was used to cut iron at 183 m/min. was etched to show temperature distribution is shown for a few cases where a) no coolant was applied, b) the tool was flooded with coolant over the rake face and c) lastly for a jet of coolant that was directed at the end clearance face.

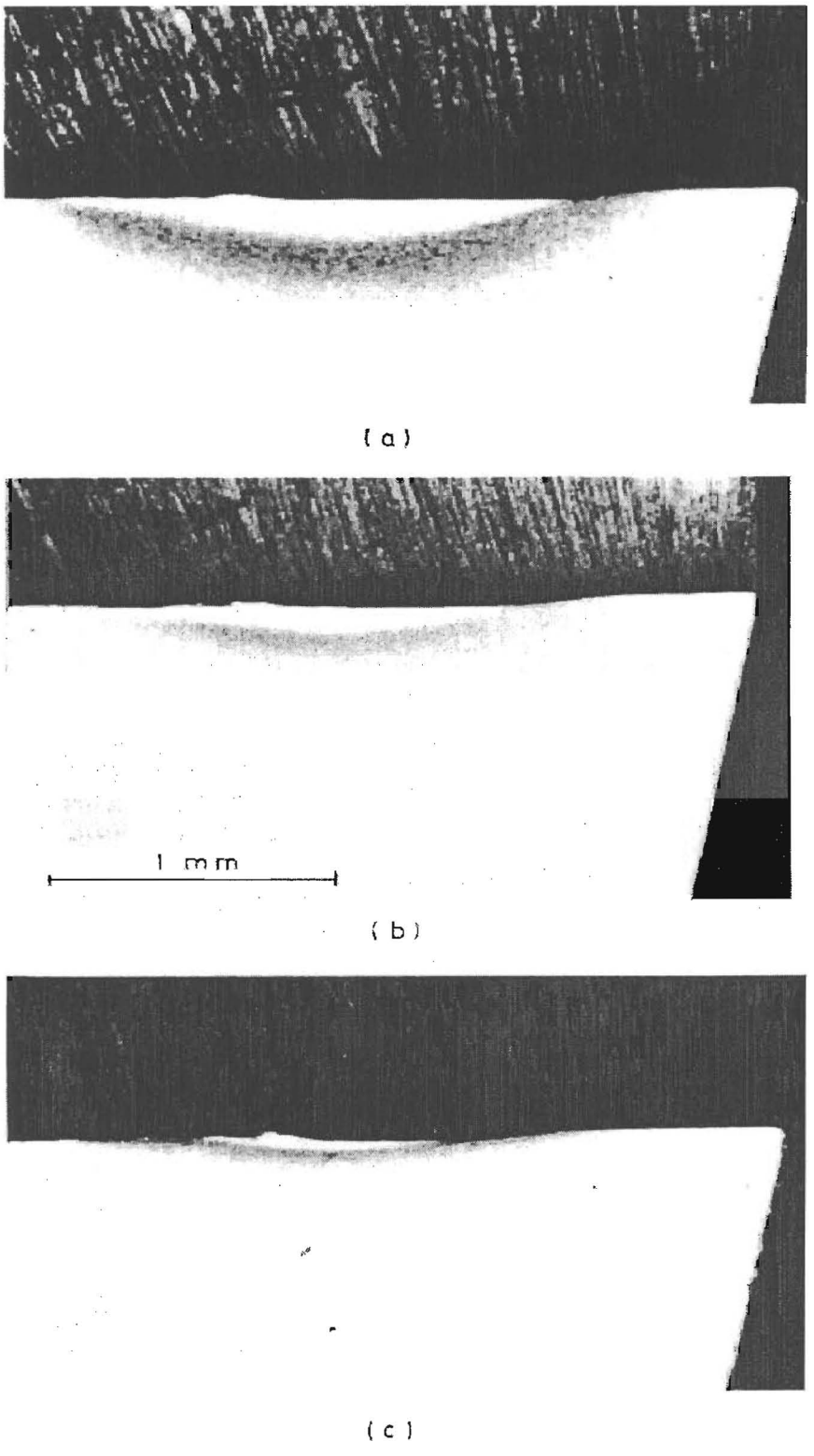

Figure 4.2 (a) Section through HSS tool after cutting iron in air at 310m/min., etched to show temperature distribution. (b) As (a) for tool flooded with coolant over rake face. (c) As (a) with jet of coolant directed at end clearance face. Trent,1977

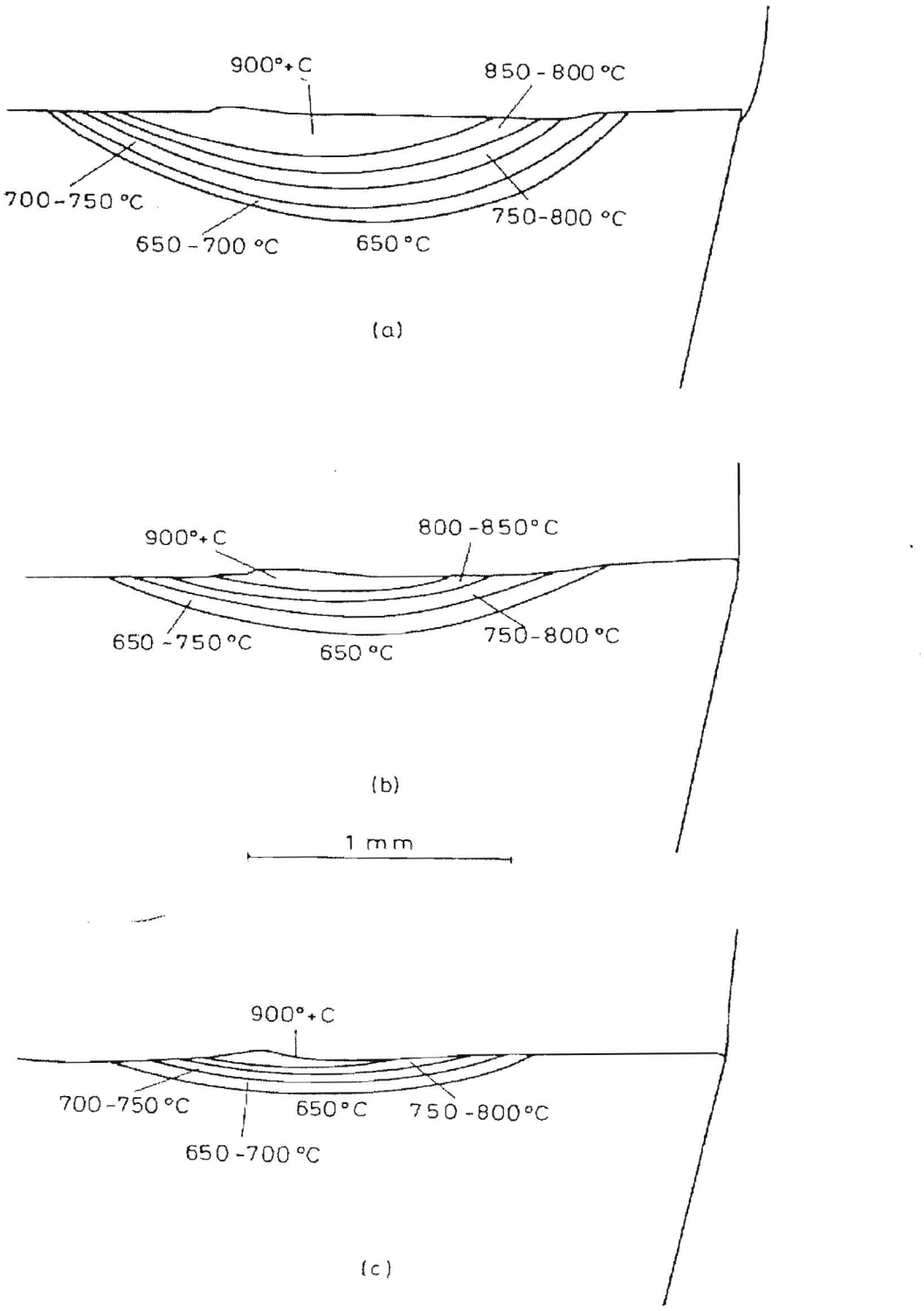

Figures 4.3 (a), (b) and (c) Temperature contours derived from Figures 4.2 (a), (b) and (c) respectively. (Trent, 1977)

The method of temperature contour derivation is by micro-hardness determinations and by metal crystal structure evaluation as was explained for structural changes in HSS tools.

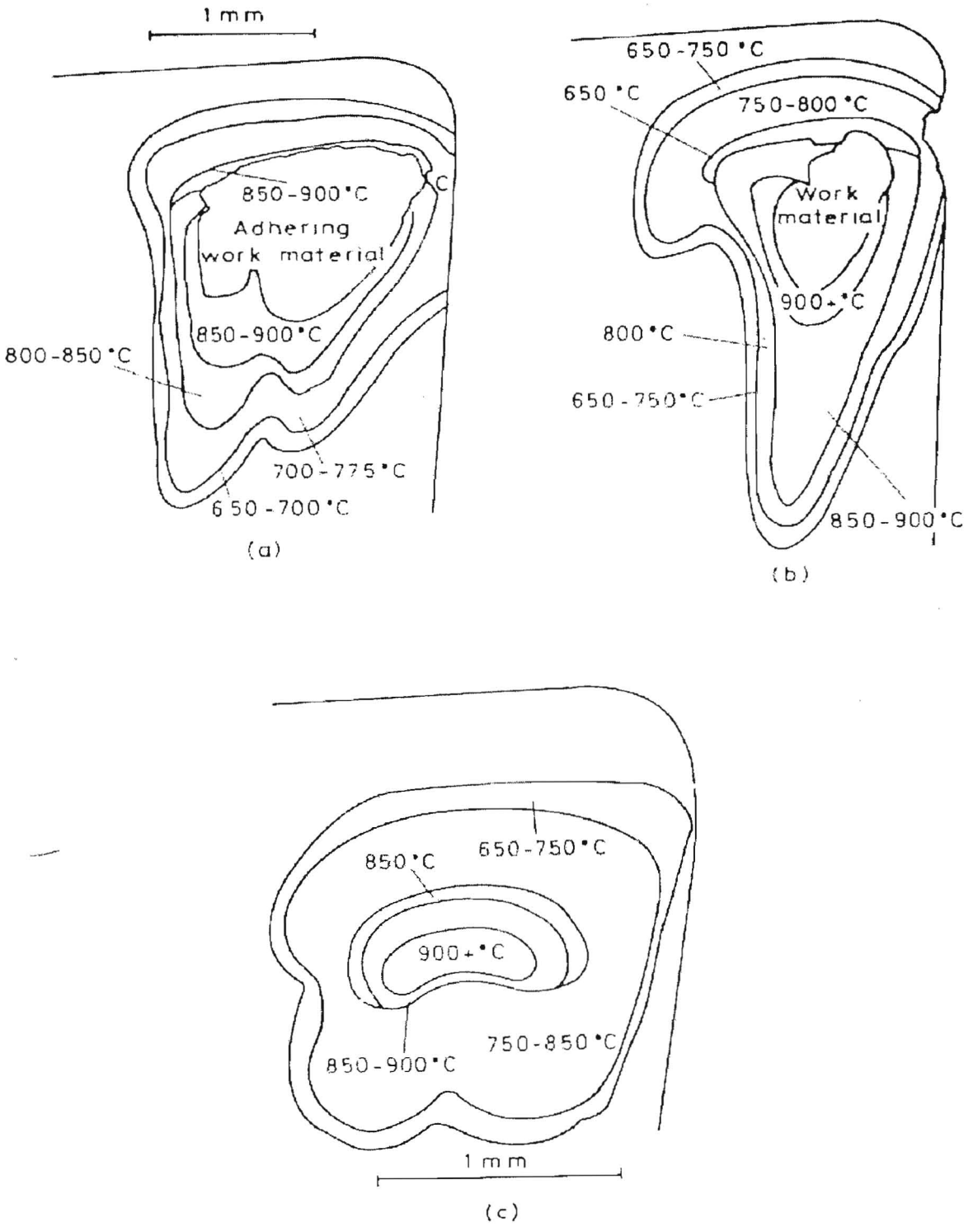

Figure 4.4 (a), (b) and (c) are rake face views of the temperature contours for figures 4.2 (a), (b) and (c) respectively of the same HSS tool used to cut iron in air (Trent,1977)

It is evident that the temperature gradients in the tool are very steep. They cover a range of about 300 °C in the space of 1 mm.

5.Metal to metal affinity

The structure of metals:

Metals have a metal lattice structure and are arranged in unit cells. Depending on the unit cell they can have a bulk co-ordination number of 8 or 12 i.e. they have 8 or 12 nearest neighbours. The fcc (face centred cubic) unit cell structure for example has a bulk co-ordination number of 12 The nearest neighbours are those atoms that are in direct contact with an atom in the bulk of the metal lattice structure. Miller indices refer to planes of symmetry through the metal lattice structure. Depending on the Miller index i.e. the plane on which the lattice is cut the co-ordination number of the surface atoms changes. Only the simplest of planes are usually considered when studying metal surfaces. (See Appendix A) Surface atoms have different co-ordination numbers than atoms in the bulk of the metal lattice. The atoms from the cutting fluids must locate on or between the surface atoms and their co-ordination number and how firmly they are attached to the metal surface depends on how they locate and attach to the metal surface.

The nature of the metallic bond:

The metal atoms in the metal lattice are bonded to each other by means of de-localised electrons. The electrons are shared between the atoms but not only between two atoms, as is the case in covalent bonds but between the nearest neighbour atoms. The metallic bond consists of a "sea" of electrons that is composed of the de-localised electrons. Depending on the atomic orbital of the atoms in the lattice there are more or less electrons that can be de-localised, and depending on the size of the atoms i.e. how many protons they have there is more attractive or less attractive force available to keep the electrons close to the atomic nucleus. The bulk co-ordination of atoms in the metal lattice can also contribute to the amount of de-localised electrons in the electron "sea" around the atoms in the metal lattice. This is why the strength of the metallic bond varies. Generally the denser the cloud or sea of electrons in the lattice the stronger the metallic bond, and the higher the melting point and boiling point of the metal will be. This is why many of the transition metal elements have a high melting point. The metallic bond is only really broken once the metal boils. When the metal melts the atoms are still loosely associated as the ordered structure has broken down, but the metallic bond is still present, hence boiling point is actually a better indication of bond strength for a metal than melting point. (Clark, 2002)

The metal to metal affinity for the development of a cutting fluid should be measured so as to establish the ability of the cutting fluid to decrease the metal to metal affinity. Lengths of welded-zone measurements give an indication to what extent seizure occurs for the various cutting fluids. The extent of seizure is an indication of the metal to metal affinity of the cutting system.

By manipulating the chemical structure of the cutting fluid it is possible to decrease the metal to metal affinity and this is evident from the difference in cutting force and cutting temperatures that are observed as the welded zone length changes for different types of cutting fluids. A case study shows this. (Vieira, Machado, & Ezugwu, 2001) In this case study the cutting temperature, tool life and power consumption changed when the cutting fluid was changed.

If the cutting temperature and the cutting forces are monitored during cutting and the contact–zone length would change then a change in the temperature and the cutting force should be observed. Taking a cutting fluid that has a high affinity for the work-piece for example and a low affinity for the tool material should result in the two materials (i.e. the tool and the work-piece material) which may have a high affinity for each other ending up displaying a lower affinity for each other in the presence of the cutting fluid. This should become obvious from the length of the welded-zone during the metal cutting operation.

A change in the length of the welded-zone should show up in a lower cutting tool temperature, a smaller chip radius, a lower cutting force and a lower current drawn by the motor. A lower cutting force is expected for a shorter welded-zone because a shorter welded-zone implies less shearing of the metal.

The cutting tool often has a carbide or nitride coating on its surface. Both carbon and nitrogen have high electronegativities and are strongly bonded to the tool surface. This is also evident from the high melting points that carbides and nitrides have. A cutting fluid has constituents such as carbon, oxygen, sulphur, phosphor and chlorine and they are highly electronegative. Chlorine for example has an elecronegativity of 3.0 and that is twice that of aluminium. The electrons in the work-piece are less tightly held than those on the tool surface because they are in an environment of atoms of lower electronegativity, and consequently are easier to take. The cutting fluid serves to decrease the electron density in the surface layer of atoms on the work-piece the moment it comes into contact with the nascent metal surface as it is formed during cutting. The bond that a cutting fluid makes with the tool is less of a polar covalent nature than the bond it makes with a nascent metal surface because the atoms of the work-piece are less electronegative. The molecules of the cutting fluid should have a lesser tendency to cling to one another; thereby they would be freer to flow over the nascent metal surfaces and weaken the metallic bond in the vicinity of the cutting edge of the tool during metal cutting. The cutting fluids should have good wetting capability and because they should flow easily they would have a low viscosity.
By weakening the metallic bond the cutting forces should decrease and therefore the work that is performed in cutting should decrease. This should lead to a lower cutting temperature and consequently a smaller welded region and reduced tool wear.

The positive aspect of the electronegative atoms weakening the metallic bonds in the vicinity of the cutting edge is that they are able to do so without themselves being in the "sea" of electrons. By being on the surface of the metal they are able to draw or attract the electrons in the "sea" of electrons in the metal lattice. If however the atoms from the cutting fluid are able to penetrate the grain boundaries on the surface of the work-piece then the weakening of the metallic bond at a greater depth in the metal lattice is possible. The reason for carbon tetra chloride being such a good cutting fluid is that it has excellent wetting properties, flows very easily and has a high chlorine density. The small size of the molecule probably contributes to ease of penetration into the metal lattice. Other than the size of the molecules of the cutting fluid, the size of the atoms and the ease with which a cutting fluid supplies them to the cutting process must also play a role in the chemistry that happens on and near the surface of the work-piece

The dynamics of the cutting process are fast and the flow or movement of the metal from the work-piece continuously disturbs the cutting fluid. The metal that moves through the flow-zone typically does so in the time span of milliseconds as was shown in section 3.2. This means that it is very likely that no equilibrium conditions become established, but the cutting fluid present can still contribute to the success or failure of the cutting process.

A background knowledge of the relevant Miller indices (see Appendix A) for the tool and the work-piece material could help to shed some light on the reasons for some observations made for the cutting process. Another possibility in metal to metal affinity is that it is the degradation products from the cutting fluid itself that change the metal to metal affinity and that if any explanation as to why a certain cutting fluid performs better than another lies in the chemistry between the degradation products and the metals involved in the cutting process. These products often form by means of catalytic decomposition.

It is possible for tough, wear resistant metal carbides to form by catalytic decomposition of ethane. (Kajdas, 1996). Cutting fluids and or their degradation products can also be catalytically affected under high temperature and pressure, as in metal cutting. These degradation products could also be wear promoting. (Trent 1977) Cutting fluid formulation is therefore very important.

The theory that was put forward in section 2.1 about the chip/tool interface and about chip flow under conditions of seizure stated that shear occurs in the weakest material. This means that the work-piece is cut or sheared off at the tooltip/work-piece interface as it is the weaker material, but as the tool heats and the work material fuses to the tool in the seizure zone it becomes weak and if it so happens that the weakest link is at the boundary layer of the tool and shear zone, then the tool can lose mass to the chip during cutting.
There is also a diffusion gradient possible at the seizure zone and the tool can thus lose mass by carbide loss to the chip by diffusion. (Trent, 1977) Diffusion occurs at higher rates as the temperature of the metals involved increases, thus cooling should counteract wear on the tool. Other wear mechanisms such as adhesive wear and attrition wear are discussed by Trent (Trent, 1977).

On metal surfaces the unfavourable contribution to the total free energy may be minimised in several ways:

1. **By reducing the amount of surface area exposed**
2. **By predominantly exposing surface planes which have a low surface free energy**
3. **By altering the local surface atomic geometry in a way which reduces the surface free energy**

The interaction of the nascent metal surfaces and the surrounding atmosphere and/or the cutting fluids that are used will thus be such as to minimise the total surface free energy.

It should also be noted that there is a direct correspondence between the concepts of "surface stability" and "surface free energy" i.e. surfaces of low surface free energy will be more stable and vice versa.

One rule of thumb, is that the most stable surfaces are those with:

1. a high surface atom density
2. surface atoms of high co-ordination number

(Nix, 2002)
(Note - the two factors are obviously not independent, but are inevitably strongly correlated).

Consequently, for example, if we consider the individual surface planes of an fcc metal in vacuum, then we would expect the stability to decrease in the order

fcc (111) > fcc (100) > fcc (110)

but the presence of a fluid above the surface (gas or liquid) can drastically affect the surface free energies as a result of the possibility of molecular adsorption onto the surface. Preferential adsorption onto one or more of the surface planes can significantly alter the relative stabilities of different planes, but will none the less be such as to minimise the total surface free energy. These effects under reactive conditions (e.g. the high pressure/high temperature conditions pertaining in metal cutting) though poorly understood are to influence the ease of metal deformation, chip formation and metal to metal affinity.

6. The machinability of aluminium

The machinability of a material depends on:
i) the type of material being machined
ii) the cutting conditions
iii) the type of machining process that is used
iv) the type of lubrication and
v) the type of lubricant that is used.

The machinability of a material may be assessed by one or more of the following criteria: (Trent,1977)
i) Tool life. The amount of material that can be removed with a tool under standardised cutting conditions, before performance becomes unacceptable or before a fixed amount of tool wear is observed.
ii) Limiting rate of metal removal. The maximum rate at which a material can be machined for a standard short tool life.
iii) Cutting forces. The forces acting on the tool as measured by an appropriate method.
iv) Surface finish and dimensional accuracy. The surface finish and dimensional accuracy of the finished work-piece that are attainable under specified cutting conditions.
v) Chip shape. The chip shape as it influences the clearance of the chips from around the tool, under standardised conditions.

In this study the key factor is to reduce the operating costs for the metal that is cut and to optimise the uptime for the cutting process. This is achievable by increasing the tool life and by decreasing secondary machining time. This may be achieved by using limited volume lubrication and a suitable cutting fluid that enhances tool life and produces a smooth surface finish.

Tool life depends on a number of factors the most common being the cutting speed, the feed rate and the depth of cut. Fracture due to mechanical fatigue or snap loading and thermal fatigue are two other noteworthy contributors to tool failure particularly in operations of an interrupted nature such as milling and shaping for example. (Trent, 1977)

Aluminium and its alloys rate highly by most of the criteria for machinability. Aluminium melts at 659°C and its alloys melt at similar temperatures. The alloy used in this study is T6082 alloy. (See Appendix B) It is a heat-treatable aluminium-silicon-magnesium wrought alloy. and melts at 570°C ± 5°C. The temperatures generated during cutting are thus never high enough to damage heat treated structures of HSS (high speed steel) tools or the structures of the tungsten carbide tool. Good tool life can be attained when cutting most aluminium alloys up to speeds of 600m/min. when using carbide tools and 300m/min. when using HSS tools. (Trent, 1977) Similar cutting speeds for turning work are recommended for HSS by Le Grand (Le Grand 1971), but in drilling speeds of up to 1200m/min are recommended.

It is in aluminium alloys of silicon content above that of the eutectic composition that high wear rates become evident, even when using carbide tools. Wear is in the form of flank wear. The silicon structures other than the eutectic silicon contain large grains of silicon, up to 70 microns across. It is these large grains, when present, that are responsible for the pronounced increase in wear rate. The drastic effect of large silicon particles is the result of high stress and temperature that these impose on the cutting edge. The silicon particles have a high melting point (1420 °C) and quite a high hardness (> 400HV) The large silicon crystals cause an attrition type of wear (see next paragraph) and demonstrates that the wear of tools depends not only on the phases present in the work material, but also on their size and distribution. In the eutectic alloy the silicon particles are fine enough to pass the cutting edge without severe damage to the tool. The machining of high silicon alloy is one of the applications for diamond and diamond-coated tools.(Trent, 1977)

Attrition wear happens at relatively low cutting speeds, temperatures are low, and wear based plastic shear or diffusion does not occur. The flow of metal past the cutting edge is more irregular, less stream-lined or laminar , a built-up edge may be formed and contact with the tool may be less continuous. Under these conditions, fragments of microscopic size may be torn intermittently from the tool surface, and this mechanism is called attrition. (Trent, 1977) Aluminium is much softer than steel and because of the high hardness of tungsten carbide abrasive wear will not be considered here. Abrasive wear is much less likely with the tungsten carbide tool than with a high speed steel tool.

As far as the cutting forces for the machinability of aluminium alloys is concerned the tool forces are generally low and decrease somewhat when the cutting speed is raised.. High forces however do occur when commercially pure aluminium is cut. This is particularly so at low cutting speeds. In this respect aluminium behaves differently from magnesium, but in a similar way to many other pure metals. The area of contact on the rake face of the tool is very large. This leads to a low shear plane angle and very thick chips, with consequent high cutting force and high power consumption. The effect on pure aluminium of most alloying additions or of cold working is to reduce the tool forces, particularly at low cutting speeds because a eutectic is present when alloying has been done.

A built-up edge is not present when cutting commercially pure aluminium, but surface finish is poor except when very high cutting speeds are used. Most aluminium alloys have structures containing more than one phase and with these a built-up edge is formed at low cutting speeds.. When the cutting speed is increased to over 60 to 90 m/min., the built-up edge may or may not develop. Tool forces are low when a built-up edge is present, and the chip is thin, but the surface finish tends to be poor.

The main machinability problems with aluminium are in controlling the chips. Extensive plastic deformation before fracture, occurs more readily with face centered cubic (fcc) structure aluminium than with hexagonally plane centered (hpc) magnesium. When cutting aluminium and some of its alloys the chips are continuous, thick, strong and not

readily broken. The actual form of the swarf varies greatly, but it may entangle the tooling and require interruption of the operation to clear the chips.

In some machine tools the designs can be modified slightly to prevent clogging as with the flutes of a drill for example. The cutting action can often be improved by modifying the rake and approach angles, or the introduction of chip breakers or curlers that deflect the chip into a tight spiral. The composition of the alloy can also be modified so as to produce chips that are fragmented and more easily broken. The standard aluminium specifications include 'free machining alloys' that contain additions of lead, lead and bismuth, or tin and antimony in proportions of up to about 0,5%. How these additions function is not certain, but the chips are more readily broken into small segments when they are present. These low melting point metals do not go into solid solution in aluminium, and are present in the structure as dispersed fine globules. They may act to reduce the ductility of the aluminium as it passes through the shear plane to form the chip. The main purpose of 'free cutting' additives in aluminium and its alloys is improvement in the chip form rather than better tool life or an increase in the metal removal rate.

7. Experimental preparation:

This chapter has the following layout:

- The type of machine tool that will be used is stated
- The choice of machine tool is motivated.
- The machine tool is described
- What parameters in the cutting process are to be measured, and how are they measured
- Other equipment, and analytical tools used are described.
- The software and communication with the cutting process is described.
- The choice of chip parameters is motivated and explained
- The choice of cutting fluids used is motivated
- The aim and significance of the experiments with reference to Appendix C is described.

The experimental setup and measurements

To evaluate the cutting process for various cutting fluids requires a test bench and a test method. A metal billet sawing operation is an operation where saw teeth engage in the work-piece intermittently, i.e. on each cycle the saw tooth has a time where it is cutting the billet and a time where it travels freely. The shaper (figure 2.3 & figure 2.4) was chosen as a test bench for the experimental work because it is easier to fit the instrumentation to this machine tool, without introducing as much noise as would be introduced on a sawing operation. This noise is with respect to the signals that are measured as an indication of the cutting force and cutting temperature. The measuring of certain cutting process parameters is necessary and they need to be analysed so as to show how different cutting fluids affect the cutting process. The main parameters that are measured and logged during the cutting process in this study are cutting force and cutting temperature. They give an indication of the success of the cutting process as discussed in the preceding chapters. The physical measurements of the properties of the chip after cutting are complementary to these parameters.

The other reasons why a shaper was chosen for the investigation were:

i) Motion is simple, i.e. forwards and backwards, not rotary. This circumvents complications with respect to the fitting of instrumentation that would otherwise have been experienced if a circular saw or band saw would have been used.
ii) to observe the effects generated during a single cut
iii) to keep cutting conditions as simple as possible, i.e. cutting in a single plane
iv) to use a straight tool edge, normal to both the cutting direction and the feed direction.
v) because it represents intermittent cutting

The shaper was built by Maskin Fabriks A.B. Thule in Malmö Sweden before 1980. It is a model S.16".S. The aluminium alloy that was cut was a heat treatable T6082 alloy. (see Appendix B for details)

The tool, in this case a tungsten carbide tool, is clamped in the tool holder on the shaper. The work-piece is stationary and the movement of the tool is simple. The electrical wiring for instrumentation to measure the cutting forces and the cutting temperature is therefore easily performed. For the tool/work-piece thermocouple that will be used for cutting temperature determination one wire needs to be attached to the tool and the other to the work-piece. This would have posed a more substantial problem if a lathe had been used, as the work-piece on a lathe rotates.

The tool is not electrically floating, but the work-piece is. One of the two must be floating otherwise the tool/work-piece thermocouple is in a dead short. The work-piece is electrically floating; i.e. it is insulated at the ends where it would have been in metal to metal contact with the shaper. The workpiece is clamped in the vice on the shaper such that the depth of cut will be constant over the length of the work-piece. This is achieved by machining a very thin layer off the top of the work-piece. After this the surface of the work-piece is parallel to the operating plane of the shaper. Because the movement of the tool is simple, it is easy to fit the strain gauge for cutting force measurement on the tool.

The simplified conditions applicable when doing laboratory investigations are known as orthogonal cutting and for this the tool edge is straight, it is normal to the cutting direction and normal to the feed direction. In figure 2.4 the push stroke is the cutting stroke and the force on the tool by the work-piece that is being cut has a moment about the bottom edge of the tool holder support. This moment maintains the tool down into the workpiece.
The **force** on the tool is the cutting force and it deforms the tool and the strain gauge mounted on the rake face of the tool. The amount of deformation of the strain gauge is an indication of the cutting force. The theory of strain gauges is discussed in detail by Hoffman (Hoffmann, 1989). The strain gauge is a type of "Wheatstone bridge". The resistance of the electrical wire changes as it is deformed and this affects the amount of current that can flow through that wire. The potential difference over the ends of this wire is amplified and the signal is logged on file by a computer program. The magnitude of this signal is directly proportional to the cutting force. The proportionality constant is determined experimentally. On the shaper this is the only force that needs to be considered. The feed force is zero because feed happens between cuts, and the tests are done with chip flow being equally restrained from both sides. The force to keep the tool down into the workpiece is provided by the moment the cutting force has about the tool holder support. The only force that needs to be measured to evaluate the cutting process therefore is the cutting force. It is evident that the cutting process has been simplified very much to facilitate ease of data- acquisition, monitoring and analysis.

The **temperature** in the metal cutting process is measured by means of a tool/workpiece thermocouple. The theory of thermocouples is discussed in detail by Considine. (Considine D.M., 1974) A thermocouple consists of two dissimilar metals, which in this case are the tool and the workpiece. A temperature dependent thermo-electric e.m.f. (electro motive force) is generated at the junction of the dissimilar metals. This e.m.f. signal is measured amplified and converted to a temperature reading that is logged on file

for later analysis. The calibration curve for the tool/workpiece thermocouple is determined experimentally.

As far as the use of the thermocouple effect for monitoring of the cutting process is concerned there are two cold junctions and one hot junction in the circuit. The two cold junctions are approximately 100mm removed from the hot junction. They are, and essentially stay at room temperature: namely 23 °C. The change of e.m.f. that would be generated if the cold junction temperatures were not constant would have to be compensated for by referencing the obtained signal to the e.m.f. that is measured at ambient temperature prior to beginning experiments. The voltages of the cold junctions would have to be added to the signal obtained during experimenting (Considine, 1974) and Capgo, 2002) to obtain the true e.m.f. that is generated relative to room temperature.

Cutting speeds in metal cutting are usually between 3 and 200 m/min., but in exceptional cases can be higher than 3000 m/min. Cutting speeds and rate of metal removal vary and depend on many factors such as:

- cutting conditions
- the type of metal that is cut
- the cutting fluid that is used and
- the type of tool and type of machine tool that is used.

Metal removal rates of nearly 0 cm^3/min. to about 1600 cm^3/min. (Trent, 1977) are encountered in metal working operations. In this study the rate of metal removal was 2.2 cm^3/min. and the range of cutting speeds available on the shaper ranged between 5.7 m/min. and 90m/min. All the experiments that were performed with cutting fluid were performed at 8m/min. A few experiments for dry cutting were done to show the influence of cutting speed on the temperature and cutting force response of the cutting process.

Other equipment and analytical tools

The optical microscope and the scanning electron microscope (SEM) are valuable in making micrographs by which analysis of the chips for metal deformation and flow-zone thickness may be performed. The optical microscope is used to make micrographs of etched cross sections of the chips. The Vickers hardness test machine is used to determine the micro-hardness profiles on the chips. The hardness profiles are complementary to the micrographs as far as determining the flow-zone thickness is concerned.

A non-etched chip sample as cut can be analysed by means of a scanning electron microscope (SEM) and/or mass spectroscopy (MS) for type of atoms that are present on the underside of the chip surface and in the chip after cutting when good cutting results are obtained. For an analysis inside the chip a longitudinal cross section should be used. By examining the cross-section of the tool work-piece interface, the work-piece finished surface, and the tool surface after cutting, under a (SEM) important information might be obtained. A SEM analysis requires extreme vacuum, and has the advantage of a great depth of focus. Two to three layers thick of atoms can be seen. If there are traces of the

constituent atoms of the cutting fluid used on these surfaces then it may be possible to postulate what happened with the chemistry. The postulate might be difficult to prove.

Likewise examining the tool cutting edge and rake face by SEM, or mass ion spectroscopy (MIS) could give an indication of which atoms are present. This could give an indication of which atoms are desired, when this examination occurs after pleasing results from a mechanical parameter investigation are obtained. If more detail is required FTIR (Fourier transform infrared) spectroscopy can be used for identification of the metal compounds that do form.

The computer applied cutting fluid for one second before every test was started and then the moment the cutting tool made contact with the work-piece temperature measurement started and this signal was used to trigger the application of cutting fluid for the rest of the duration of the cut. The applicator that was used is a mist type applicator, in which a pulsating pneumatically operated piston pumps the cutting fluid into a mixing chamber in which the cutting fluid is broken up into minute droplets and mixed with air under pressure. A jet of air/cutting fluid mist is applied to the flow-zone area in the cutting process.

For the purpose of the study of the aluminium cutting fluids a Surtronic 3P profilometer is used to determine surface roughness. (Hobson,1980). A Vickers hardness tester is used with a chart to express the Vickers hardness (VH25) before and after cutting. (Van der Voort., 1999/04)

Software

All the software that was needed to perform the experiments was self-developed. A program was written so that the sampling rate could be changed if deemed necessary. The sampling rate was however fixed at 200 ± 2Hz for all the experiments that were performed. For some unknown reason the sampling frequency varied within 1% of 200 Hz.

The instrumentation was purchased and self installed, except for the strain gauge. A PC30B A/D – D/A converter card was used for analog to digital and digital to analogue signal conversion, and two signal amplifiers were used to amplify the temperature and cutting force signals sufficiently for use in the PC30B card. The system that was constructed may be schematically represented as in figure 7.1. The software is necessary for establishing communications between the measuring sensors, (i.e. the tool/work-piece thermocouple and the strain gauge), and the computer.

Once the hardware had been installed software had to be developed and the measuring instruments and signal receiving components had to be calibrated. For the PC30B card that was used, calibration requires a high precision voltage source and a high precision multimeter. For calibration details use was made of the appropriate card user manuals (Tinker, 1990,1992). If the cards are used often it is necessary to check their calibration

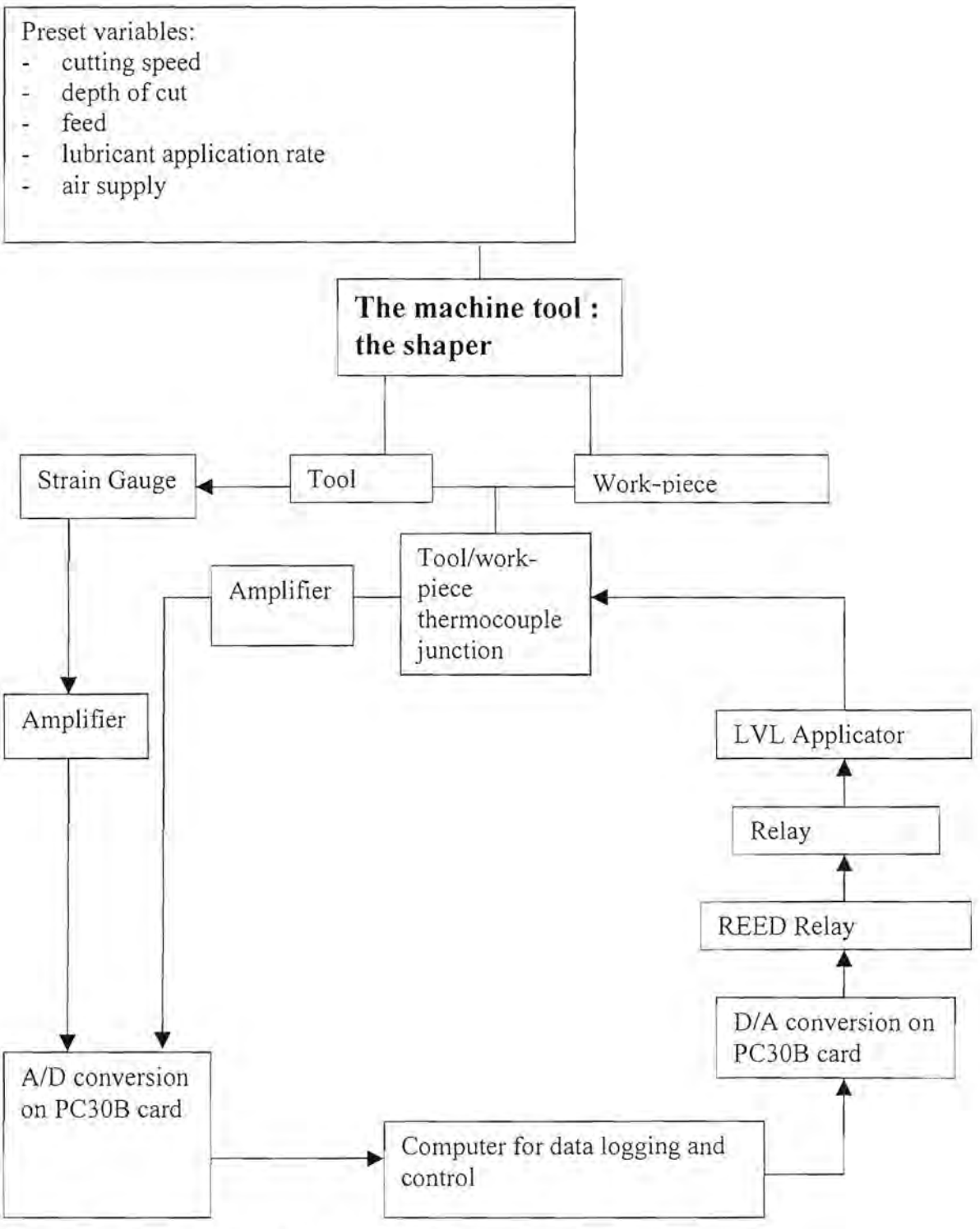

Figure 7.1 The Shaper machine hardware and data acquisition set-up

from time to time. It is important that the board is jumpered into its intended operating mode when calibration is done. The calibration software program cal.exe under C:\pc30, is run when calibration is to be done.

Establishing communications between the process hardware and the computer also requires wiring and an AD/DA card. This card requires a voltage input signal and gives a voltage output signal. The signal comes from amplifier via the measuring element on the shaper to the PC30B card. The signals come into the card as analogue voltage inputs and are converted to 12 bit digital code. More details on what needed to be done to set up the communication for the cutting process are in Appendix E.

Experimental planning

The experiments are described later and in detail in Appendix C. The **cutting force** and the **cutting temperature** in metal cutting should be measured as they give an indication of conditions during cutting. If the welded zone is large the cutting force and cutting temperature are expected to be higher than when it is smaller, because more metal will have to be sheared per unit time. The sudden decrease in cutting force with an immediate decrease in cutting temperature following should indicate that a built-up edge has formed. The length of the chip radius and the thickness of the chip should also decrease when this happens. The temperature and the cutting force measurements are very important for the cutting process experiments because many of the other parameters that were monitored were determined from cutting force and temperature data as will be shown later in this chapter.

The metal-to-metal affinity for the development of a cutting fluid should be measured so as to establish the ability of the cutting fluid to decrease the metal to metal affinity, and thereby decrease tool wear. The chip mass should be standardised because chip mass has a pronounced effect on the cutting force and cutting temperature. This means that all cuts that are performed can be compared to dry cuts or any other reference cutting fluid under the same cutting conditions. The built-up edge should not be present in the region of the cut where the comparison is made, because it is a dynamic unstable structure that changes the cutting conditions. Length of welded-zone measurements from quick-stop sections, although tedious to do, give an indication of the extent of seizure that occurs for various cutting fluids. The extent of seizure is an indication of the metal-to-metal affinity of the cutting system.

Another idea on how the length of the welded-zone may be determined is by using restricted contact tools and finding the **contact length** at which the cutting force starts to decrease for standardised cutting conditions.

Bi-directional chip flow restraint is used. This produces chips that are two dimensional that are sufficiently open when a built-up edge is not present that their surfaces may easily be inspected and their length easily determined.

In all the experiments performed, a relatively shallow cut of 0.25mm and low cutting speed of 8 m/min. will be used, so as to be able to build in a fair amount of sensitivity to the cutting fluids that are used. This should result in shorter thicker chips and this is on

the **steep part** of the shear strain vs. shear plane angle relationship graphically presented in figure 2.9. Differences in shear strain for the different lubricants used should therefore be more evident than when a higher cutting speed is used that produces longer, thinner and less strained chips.

As **surface finish** is a major objective in metal cutting and lubricants are rather more effective at low cutting speeds in the presence of a built-up edge (Trent, 1977) a low cutting speed was chosen for the experiments that were performed.

A shallow cut is used so that if there is lubricant penetration into the cutting zone from the sides where the lubricant is applied then the area affected by the lubricant as a percentage of the total area of the cutting zone will be more significant than when a deeper cut is made.

It is postulated that the e.m.f. that is generated during cutting will decrease as there is a built-up edge that is forming and then suddenly increase again if the built-up edge is sheared off. The maximum temperature occurs in the flow-zone and the flow zone moves away from the tool rake face as a built-up edge forms. It also decreases in length in the same way as it decreases in size/length when a restricted contact tool is used to cut the metal. This decreases the amount of shear that takes place when metal cutting is done, hence the e.m.f. that is generated between the dissimilar metals i.e. between the tool and the work material decreases when a built-up edge forms. The results from the experiments will help to substantiate this claim.

It is thought that the key to the chemistry involved lies in the role that the reaction products from the cutting fluid play in reducing the metal-to-metal affinity. Metal-to-metal affinity should be reduced as much as possible to prevent a large welded region in the contact-zone.

The current vs. depth of cut that is drawn by the electric motor during cutting could also be monitored in the experiments. It was decided not to do this as this is not as sensitive a method as using strain gauges, thus strain gauges were fitted to the cutting tool and cutting force in the direction of cut was monitored. The problem with the electric motor and data sampling was the associated complications in sampling.

CHOICE AND MOTIVATION FOR CHOICE OF CHIP PARAMETERS

The **average smooth fraction** on the underside of the chips will be determined. This should give an indication when stick-slip initiates and is an indication of the distance cut until seizure starts to appear. Little fine scratches on the underside of the chip should form as the chip welds to the tool face and shears loose. The better a cutting fluid, the longer the cut that can be made without stick-slip occurring.

The **shape** of the chips will be observed because the shape, the **chip radius** in particular, is an indication of when a built-up edge forms. The built-up edge will change the rake face angle and the chip will have a shorter chip radius when this happens. The cutting

force will decrease as a built-up edge will act as a restricted contact tool and the chip should become thinner.

The **length of cut until the first break** in the chip occurs will be measured because it is expected that this is related to the length cut until the built-up edge forms. It is expected that the chip will break soon after the built-up edge forms. When the built-up edge forms the chip is very much more deformed as is seen from the smaller chip radius and therefore more strain-hardened and this often leads to the chip breaking under the compressive stress. It is expected that the chip will be harder when cutting with a built-up edge than cutting when the built-up edge is not present.

The **chip shear strain and the hardness and the hardness profile** for the chip in the non-built-up edge region will be determined on a Vickers hardness tester. From the chip shear strain and the average hardness in the almost flat region of the hardness profile for the chip **the ease of chip formation** may be calculated. It is expected that the easier a chip can form and the softer it is, the less tool wear should result. To be able to confirm that the built-up edge does cause a harder chip a hardness profile on one of the chips where a built-up edge was present should be performed. The hardness profile for a chip should also serve to indicate the thickness of the flow-zone and is complementary to the SEM micrograph and the optical micrograph of an etched cross section of a chip. The thickness of the flow-zone is determined because it should reflect on the ease of deformation in the chip and the temperature that is attained at the interface of the tool and the flow-zone. If ease of deformation in the chip is high and or the temperature is high then a thicker flow-zone should be seen.

The **peak cutting** force normalised for a 200 mg chip will be determined from the cutting force data as it might be able to show a trend that is related to other cutting process parameters for a cutting fluid.

The **peak average temperature** prior to formation of the built-up edge will be determined from the cutting temperature data, as it should point out the maximum temperature up to which a cutting fluid can prevent the formation of a built-up edge.

The **five point moving average of the cutting force** prior to built-up edge formation should serve as an indicator of the contact length and the ease of chip formation at that stage of the cut. The relative contribution of these two parameters to the cutting force will however be unknown. If the contact lengths would be determined for that stage of the cut, then they could be used together with the ease of chip formation data in the interpretation of the cutting force data at that stage of the cut.

The aluminium plate that will be cut in the experiments must be marked at the ¼- , ½- and ¾- way mark so that the length of the first quarter of the chip may be determined easily and used in the calculation of the **chip thickness ratio** that will also be used for the calculation of the **chip shear strain** and the **shear plane angle**.

The **repeatability of the chip masses** will be noted for control purposes, and so that if there is a difference in the repeatability of the chip mass for different cutting fluids that this difference will be evident.

The **cutting temperature at the one quarter way mark** of the length of cut will be determined from the temperature data because it is a function of the contact length and the thickness of the flow-zone which itself is affected by the ease of chip formation and the temperature at that stage of the cut. The longer the contact length the greater the area for heat exchange with the tool, consequently the tool should heat up faster. This cutting temperature is a parameter for which the individual contributions of the contact length and the flow-zone thickness will be unknown. The complicated question is: What is the temperature in the flow-zone at the quarter way mark, and has the tool/flow-zone interface attained this temperature or not? Does the tool heat up faster due to a larger temperature gradient or due to a larger surface area for heat exchange?

Take it that the temperature for two different cutting fluids in the volume of the flow-zone above the welded zone is the same, and that the volume of the flow-zone above the welded zone is also the same. The cutting temperature at the quarter way mark would be higher for the cutting fluid with the longer welded zone because it has a larger area for heat exchange with the tool rake face, despite the fact that the temperature in the flow-zone for both cutting fluids is the same. Although this is complicated, it is desirable that the tool must be as cool as possible, and therefore the temperature at the quarter way mark is determined as a performance parameter dependent on the cutting fluid.

The **surface finish** for the different cutting fluids will be determined as a cutting fluid that produces a smoother surface finish will require less secondary machining time and this is economically desirable.

SELECTION OF CUTTING FLUIDS

The types of cutting fluids that are to be tested in this investigation are selected from a range of known types of chemistries that are, or can be used as cutting fluids. This was done so that the bench test can show the differences in cutting performance between different chemistries. More than one example of some cutting fluids with similar chemistry was chosen so that the bench test can show if there are similarities between related cutting fluids. The chemistries chosen include alkanes, esters, polyisobutylene, carbon tetra chloride (CCl_4) and dry cutting.

Dry Cutting

Dry cutting is performed as a reference against which the other cutting fluids may be compared.

Alkanes

Alkanes are widely used as cutting fluids and it is known that paraffin may also be used as a cutting fluid when cutting aluminium. Usually the alkanes are chlorinated to improve their cutting performance and they are then referred to as chlorinated alkanes or chlorinated paraffins. Chlorine is an undesirable constituent of cutting fluids because the

reaction products may be carcinogenic and because they contribute to skin disorders related to cutting fluids.

Generally the trend for cutting fluids that contain chlorinated paraffins is that the rake face and or flank face temperature decreases, and or the rate of flank wear and built-up edge formation decreases (Birmingham, Henshall & Hooper,1997). Work performed in that investigation was for intermittent cutting with a HSS tool.

Esters

Currently esters are used more and more as cutting fluids because they do not cause skin problems and have a higher thermal range across which they can be used as cutting fluids, i.e. they are thermally more stable than the alkanes. The ester linkage is an exceptionally stable one; bond energy determinations predict that it is more thermally stable than the C-C bond. (Mortier & Orzulik, 1993). Ester groups are polar and will therefore affect the efficiency of anti-wear additives.

When a base fluid that is too polar is used it and not the anti-wear additives cover the metal surfaces. This can result in higher wear characteristics. Consequently, although esters have superior lubricity properties compared to mineral oils, they are less efficient than anti-wear additives.

Esters can be classified in terms of their non-polarity. (Van der Waal,1985)

$$\text{Non-polarity index} = \frac{\text{total number of C atoms x molecular weight}}{\text{number of carboxylic groups x 100}} \qquad \text{Eqn.7.2}$$

In general the higher the non-polarity index, the lower the affinity for the metal surface. Using equation 7.2 shows that increasing molecular weight will generally improve overall lubricity. Esters terminated by normal acids or alcohols have better lubricities than those with branched acids/alcohols, while esters with mixed acids/alcohols have lubricities intermediate between esters of normal acids and esters of branched acids/alcohols. (Mortier & Orszulik, 1993)

PIB's

Poly-isobutylenes (PIB's) contribute to forming a tough lubricating film even under severe conditions and provide excellent protection against wear and scuffing. They are also suited for high temperature applications. They also have the ability to burn off cleanly. The above properties make them suitable as a metal working fluid.

Like the esters, a metal cutting fluid free of chlorine is obtained. Other than the esters, PIB is not biodegradable and this may limit its use in some applications where environmental issues are significant. In limited volume lubrication any residual PIB on the chips can be burnt off easily during recycling and PIB in metal cutting therefore has merit.

CCl_4

Carbon tetra chloride is known to be a good cutting fluid (Liew, Hutchings & Williams, 1997; Trent, 1977; Boston,1952), and it is therefore tested as a matter of confirming this, and for comparing the other cutting fluids that are tested. Carbon tetra chloride is however not used as a cutting fluid because it poses a threat to the health of the machine tool operators; it is carcinogenic and can cause permanent damage of the kidneys. By the choice of this cutting fluid a reference against which the chlorine free cutting fluids may be compared is obtained.

Experimental procedures

Before the execution of any experiments the following must always be checked:

- Fix the reference points namely 0.33 ± 0.01V at 23°C for temperature data accumulation and -0.005 ± 0.005V for 0N on the strain gauge. These readings are adjusted by tuning the trimpots on the signal amplifiers so that the signals obtained for 23 °C and 0N meet the requirements. The temperature signal is always an unfiltered signal, but the force signal is obtained with the filter on the signal amplifier in the "on" position.

A detailed explanation of how to perform the following experiments is given in Appendix C.

Experiment 1:

Aim: To see whether an e.m.f. will be generated merely by the deformation of the metal crystal structure.

Significance: If an e.m.f. would result merely by the deformation of the metal lattice structure then compensation for this fraction of the observed e.m.f. would have to be made so as to obtain the true e.m.f. that is due only to the thermo-electric effect.

Experiment 2:

Aim: To obtain data to calibrate the tool/workpiece thermocouple. This gives an indication of the temperatures that are attained when the aluminium is being cut.

The temperature is measured by using the dissimilar metal junction formed by the tool and the workpiece as a thermocouple. The e.m.f. that is generated at this junction is an indication of the temperature at the junction, i.e. the temperature is a function of the e.m.f.

Significance: If the temperature and the corresponding e.m.f for a number of temperature s between 30 °C and the melting point of the alloy is known then the temperature e.m.f. relationship may be determined by mathematical regression. This relationship can be implemented directly in the computer program so that the temperature corresponding to the generated e.m.f. can be displayed on screen and written to file. Comparisons between cutting temperatures rather than e.m.fs for different cutting fluids can therefore easily be made.

Experiment 3:
Aim: To obtain data to calibrate the strain gauge.
Significance: If the milli-volt signal and the corresponding force on the cutting tool for a number of forces is known then linear regression will give the relationship between the milli-volt signal and the cutting force. This relationship is then implemented in the computer program so that the cutting force for the particular milli-volt signal can be displayed on screen and written to file. Comparisons between cutting forces rather than milli-volt signals for different cutting fluids can therefore easily be made.

Experiment 4:
Aim: To obtain chips and the corresponding cutting force and temperature data for cutting metal when various cutting fluids are used.
Significance: By collecting the chips and their cutting force and temperature data analysis of the cutting process for a particular cutting fluid can be performed. The temperature and cutting force data together with the physical parameters that are measured on the chip, provide important information on the success of the cutting process. The important physical parameters on the chips were mentioned in the introduction. The chip masses are determined first. This is important because chip mass has a profound effect on the cutting force and temperature data. This way meaningful comparisons of parameters for the various cutting fluids may be made. Once the mass has been controlled the physical parameters of the chips may be determined as described in Appendix C. Thereafter analysis of the chips is performed.

Experiment 5:
Aim: To obtain surface roughness data for the different cutting fluids that were used.
Significance: Surface finish in metal cutting is an important parameter. A smoother surface finish requires less secondary machining time and the finished product can therefore be produced at a lower cost.

Experiment 6:
Aim: To show an etched micrograph of the built-up edge that is present and to show its affect on the micro-hardness profile for the chip.
Significance: The micrograph serves as visual confirmation that the built-up edge is present. The hardness profile shows the effect of the built-up edge on the strain hardening of the chip.

Experiment 7:
Aim: To see whether the built-up edge forms later, i.e. at a greater length of cut, when the cutting speed is increased and to see the effect of this on the cutting temperature and the cutting forces.
Significance: This experiment shows at which cutting speed and cutting temperature the shear rate becomes such that the built-up edge can no longer form. It also shows how the contact length and cutting force and cutting temperature increases when the built-up edge is not present.

8. Results and Discussion

Results from the cutting process

Nine different cutting fluids were tested including dry cutting. Ten cuts were made for every cutting fluid that was tested, of which five or six are shown per cutting fluid in Appendix D. The exception was for the dry cutting tests where thirty-five cuts were made so that comparable chip masses were available for the cuts performed with cutting fluid.

Experiment 4 (detailed in Appendix C) is the most important experiment and hence its results are presented first. The preceding experiments were necessary to establish the procedure and to set up the equipment so that experiment 4 could be performed. Results for those experiments are in Appendix C, and were used to calibrate the tool/work-piece thermocouple and the strain gauge that was used.

The first result is for carbon tetra-chloride and it shows by means of arrows, which graph **represents temperature** and which graph **represents cutting force**. This is shown once only and is relevant for all similar graphs that follow under the raw data column for each individual cutting fluid that was tested.

It must be noted that all results are **referenced to dry cuts** of comparable chip mass and that the reference graph is always the **dark coloured graph**. The chip mass must be comparable because chip mass has a profound effect on the cutting process data.

All the graphical results have a title per graph and this title aims to convey some more background information of the test to the reader. A title is discussed here for clarity of how the titles should be read. Take for example the following titles:

1) SC T3 C.force and Temperature 200 mg
2) Compare C.forces C3 200 vs. Dry2 198mg
3) Compare Temperature C3 200 and Dry2 198mg

The first title conveys that it was the third test that was done for cutting fluid sample C, hence SC T3, and that the cutting force and the temperature data for this cut are displayed, and that the mass of the chip was 200 mg.

The second title conveys that cutting force data for the third test of sample C of chip mass 200mg is compared to the second dry cutting test with a chip mass of 198mg.

The third title conveys that the temperature data of the third cut for sample C of chip mass 200mg is compared to the second dry cutting test with a chip mass of 198 mg.
The two to three mg mass difference for the chips that are compared, is due to the chip that was cut with cutting fluid being wet. It was found that a dried chip had a mass of about two-mg less than a wet chip after cutting.

The graphs shown in Appendix D are arranged in three columns. The graphs in column one are the raw results. In column two a five point moving average of the cutting forces is presented and in the last column the temperature comparisons are presented. Furthermore, the results for a particular number of test are displayed in the same row of

graphs, i.e. the third test for cutting fluid sample A, for example, is displayed in the third row of graphs for sample A.

In viewing each of the sets of graphs of the cutting fluids that were tested on the shaper it is apparent that there is a high degree of repeatability of the results. Each cut is 205mm long. The duration of each cut at 8m/min. is 1,55 seconds. At 200 Hz sampling rates therefore about 310 data points are available for each cut when a cutting speed of 8m/min is used. This is equivalent to one data point or one sample every 5 milliseconds. The x-axis in the graphical results is the sample number and essentially constitutes a time scale. To convert sample number to time divide the sample number by the sampling rate.

The distance cut in 5 milliseconds is 0.66mm. The rate of cutting fluid application in each test was 0.2 ml/min and the amount per cut of 1,55 seconds is thus slightly more than 5 micro-liters.

The different cutting fluids that were tested were:
- dry cutting
- carbon tetra-chloride
- paraffin as common illuminating paraffin
- a light fraction and a heavy fraction alkane
- three different types of esters and
- poly-isobutylene

The reason for this selection was given under the experimental planning section

For every cutting fluid the graph for cutting force first rises very rapidly to a maximum and then rapidly decreases slightly. (Figure 8.1 and figure 8.2) Initially the cutting force is low because the workpiece material is ductile and soft, but metal accumulates very rapidly in the chip that forms and the chip formation zone rapidly increases in size from $0mm^3$ to close to its maximum size. As the chip formation zone and the chip volume increase the cutting force increases. The metal is still cold and has not reached its maximum temperature yet (Figure 8.1 and figure 8.3), and is therefore severely cold-worked and strain hardened. This is when the maximum cutting force is observed.

As metal cutting continues, the temperature rapidly approaches the maximum and the metal in the chip formation zone becomes softer and a corresponding decrease is seen in the cutting force. The cutting force would stabilise then if the contact length could stay constant, but instead the maximum temperature for the cut is reached and metal to metal affinity increases resulting in metal welding/seizure.

In this case a rapid metal build-up occurs on the welded length/ contact length resulting in built-up edge formation (Figure 2.12). When a built-up edge forms the effective rake face angle changes. The tendency is towards a more negative rake face angle. This results in increased chip strain, as is evident from figure 2.9 and as will be shown in the micro-hardness test that was done for poly-isobutylene where chip formation occurred in the presence of a built-up edge. It also results in a restricted contact. This is like the tool in figure 3.2. A shorter contact length results in a shorter flow-zone and therefore less shear and therefore a further decrease in cutting force and temperature is observed. The built-up edge is however not a stable structure and can shear off unpredictably to varying extents.

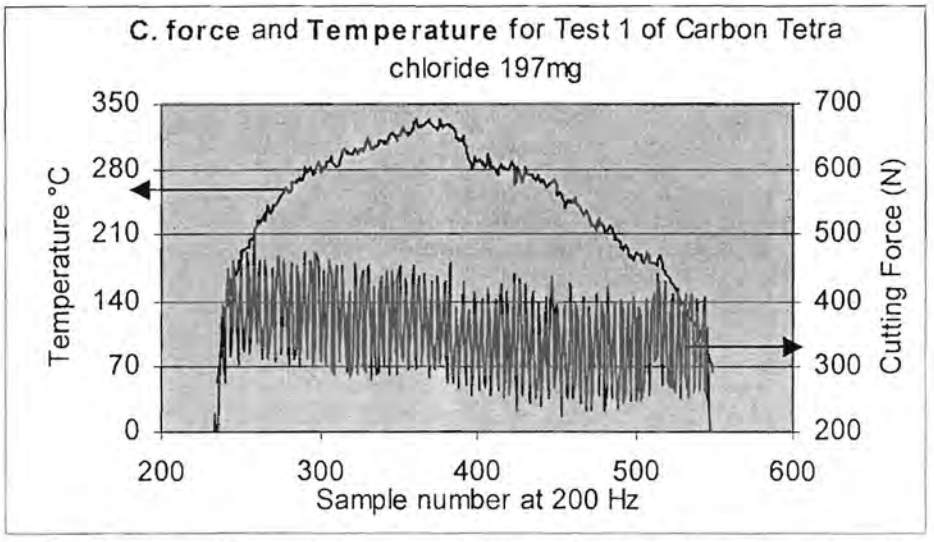

Figure 8.1 General form of the graphical results for the raw cutting force and temperature data

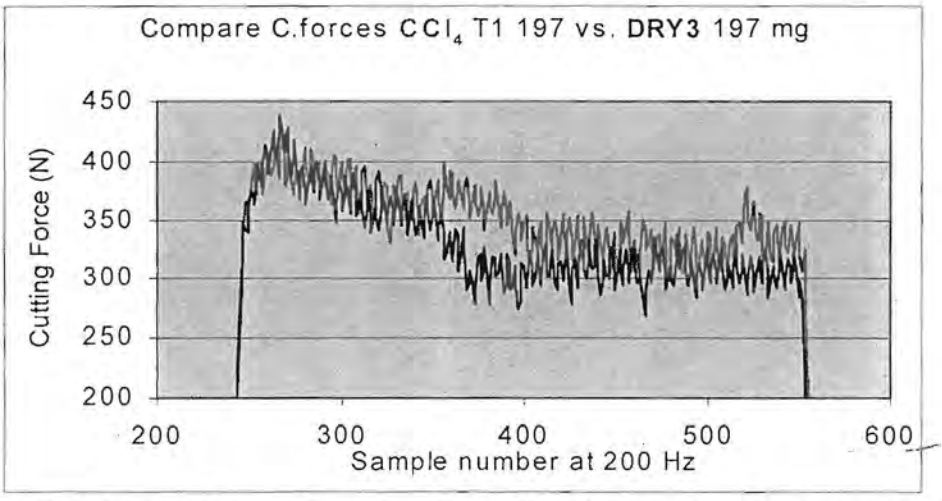

Figure 8.2 General form of graphical result of five point moving average for cutting Force

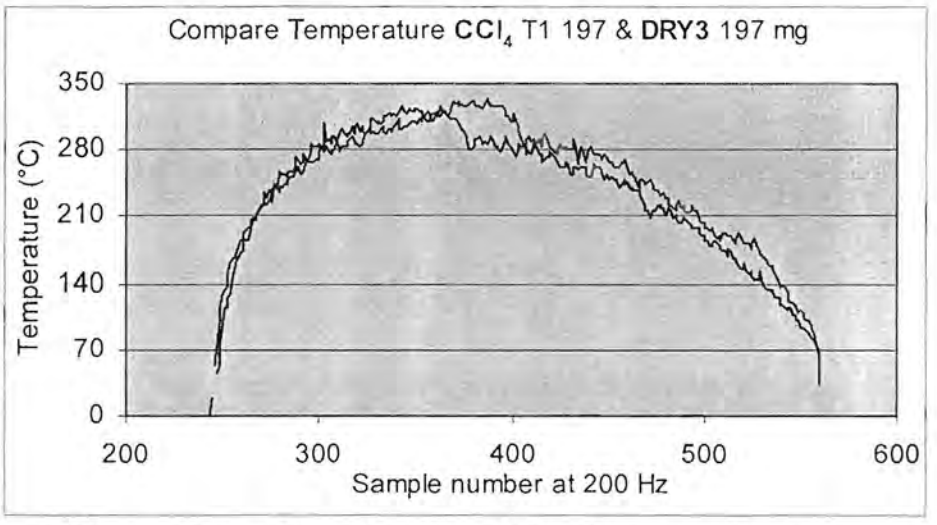

Figure 8.3 General form of graphical result for the temperature response

This is like having a tool for which the cutting geometry is forever changing and leads to a fluctuation of results during metal cutting. The efficiency of a metal cutting operation is also dependent on the tool geometry and therefore the built-up edge is unacceptable.

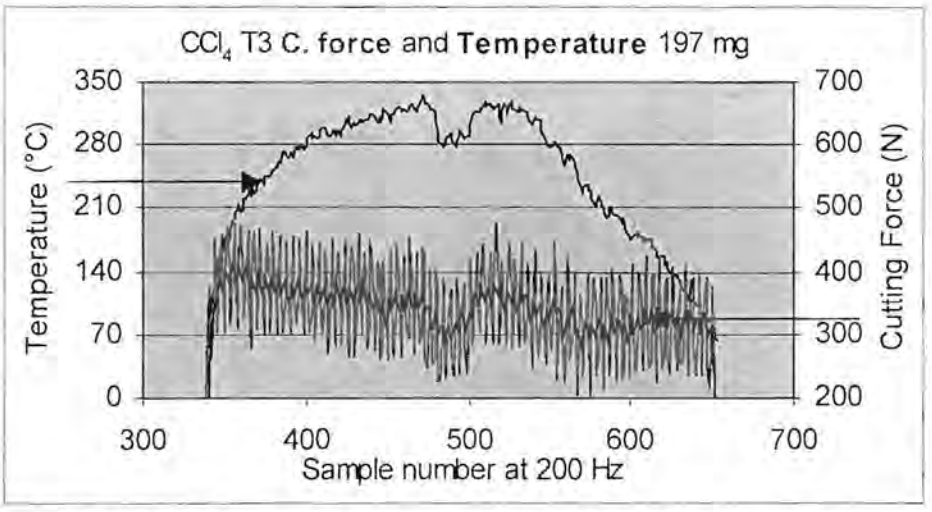

Figure 8.4 Temperature and cutting force response when a built-up edge forms and is sheared off and forms again.

In figure 8.4 the same initially happens as with the other cuts that were made, but about half way through completing the cut a built-up edge forms and the cutting force decreases rapidly and the temperature decreases immediately afterwards. This shows that the temperature response for the cut lags the cutting force response, but only slightly and this is probably more evident from when the cutting force suddenly increases again thereafter.

The dark curve in the middle of the cutting force of figure 8.4 is a superimposed 5 point moving average of the cutting force and emphasises the change in cutting force when a built-up edge forms or is sheared off. Immediately after the built-up edge had formed it was sheared off again and the cutting force immediately increased and immediately afterwards the cutting temperature increased as well, only to steadily decrease again thereafter as the build up of a new built-up edge started.

That the temperature lags the cutting force also makes sense from a dynamic point of view, since the dynamics of force measurement should be faster than that of the energy measurement via temperature of the tool/work thermocouple.

It is important to remember that temperature measurement is by means of the tool/workpiece thermocouple and is measured at the junction of the dissimilar metals. The observed temperature when a built-up edge forms will therefore decrease because the flow-zone is slightly removed from the dissimilar junction as it is situated on top of the built-up edge.

The flow-zone has a very high area to volume ratio and as metal, especially aluminium, is a very good conductor of heat, this facilitates very efficient heat loss from the flow-zone. All three components necessary for efficient heat transfer are present namely good

conductivity, a large temperature gradient between the flow-zone and the surrounding metal and a large surface area. This is evident from very large temperature gradients that exist at and around the flow-zone. (See figure 4.4 for a temperature profile on the tool when steel is cut) Further away from the flow-zone the temperature gradient becomes less steep because the volume of metal into which the heat is dissipated increases. Evidence for the steep temperature gradients may be found from optical micrographs taken after etching the tool and from micro-hardness tests done on high-speed steel tools. The hardness and the change in the metal structure at and near the rake face of the tools after metal cutting is indicative of the temperatures that were present for the structures to form.

It must be pointed out that the time interval for a change in temperature in the flow-zone is very short. This is evident from figure 8.3 for example, (and all other temperature graphs), where it is noted that at a sampling interval of 5 milliseconds, significant temperature changes are sometimes seen over intervals of ± 10 to 20 milliseconds, as for example when a built-up edge forms. This shows that the tool-workpiece thermocouple has very fast dynamics.

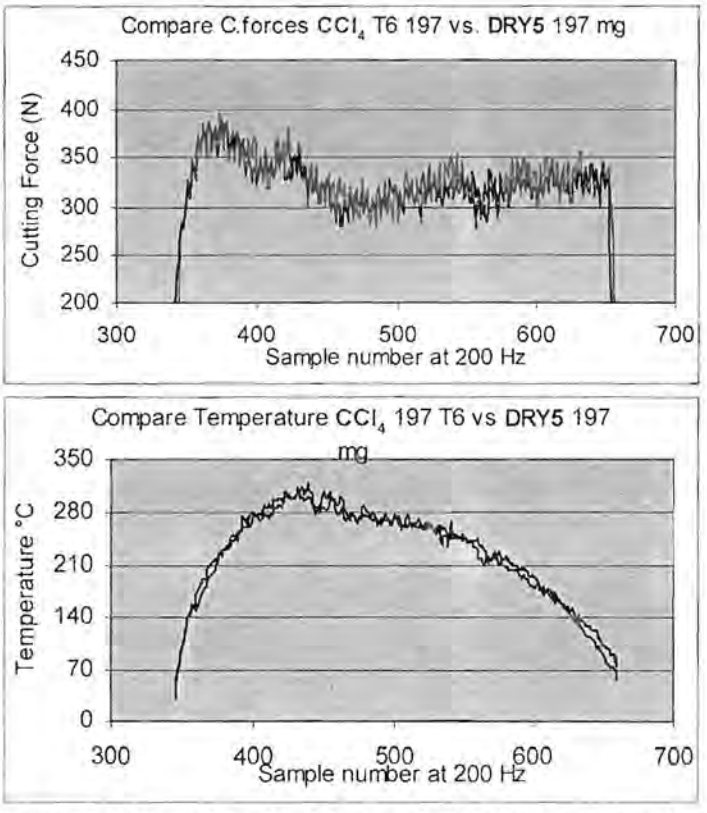

Figure 8.5 Graphical evidence that lubricant application failed

Another interesting observation is the fact that the cutting force signal fluctuates much more than the temperature signal. The temperature signal is an unfiltered signal whereas the cutting force is a filtered signal. The reason for the cutting force signal fluctuating so much is because of the three phase alternating current motor, (a.c.motor). The motor

cannot supply a constant force, i.e. the force varies with the 50Hz sine wave of the a.c. current, thus the oscillations in the cutting force that is recorded are at 50 Hz
The temperature signal has very little noise because good electrical contact at the cold and hot junctions was ensured.

In figure 8.5 it is seen that the cutting force and the temperature for a dry cut and a cut performed with CCL_4 are very similar, yet when comparing the result to that of figure 8.2 and figure 8.3 there is a significant difference between the cutting force and temperature for dry cutting and CCl_4 cutting, i.e. the cutting force and temperature curves lie further apart. The comparison must be done for data points that lie vertically above each other. From this comparison it should be clear that lubricant application malfunctioned for the test performed for figure 8.5. The built-up edge for CCl_4 also formed later in figure 8.3 than in figure 8.5.

It was stated under the experimental planning section that the chip mass must be determined after a cut is performed before the determination of the physical chip parameters and that the masses of chips that are compared for different cutting fluids must be the same. This was so because chip mass significantly increased the difference in cutting force as is evident from figure 8.6. The cutting force was more than 20% lower for the lighter chip and, although not shown here the temperature that was recorded, was also lower. A decrease in the amplitude of oscillation for the cutting force was also noted for a lighter chip.

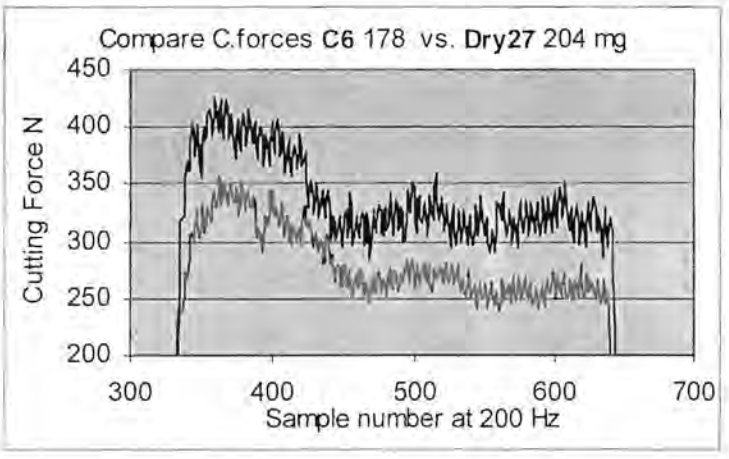

Figure 8.6 Difference in cutting force due to difference in chip mass

In figures 8.1 to 8.6 the pronounced decreases in cutting force and corresponding temperature, depending on which graphical result is considered, is clearly visible. The sudden decrease in cutting force **and** temperature signals that a built-up edge has formed, and when the chip radius and/or the chip thickness ratio for that stage of the cut also shows a sudden decrease it helps to confirm that the built-up edge has indeed formed.

The length cut to formation of built-up edge parameter in Table 8.1 was calculated from the graphical results. In figure 8.6 for the dry cut for example, approximately (430-330) i.e. 100 samples had been taken when the cutting force decreased markedly. The same is

seen on the temperature response for that particular cut. (See the sets of results for the individual cutting fluids in Appendix D, where the results for sample C are given).

The total number of samples taken in the cut are 311. The length of each cut was 205 mm and in this case the product of 100/311 and 205mm gives the length cut until the built-up edge forms. For the particular cut of Dry27 the built-up edge formed at a distance of 66mm. Applying the same method to calculate the distance cut to formation of built-up edge for CCl_4 in figure 8.2 and figure 8.3 gives a distance of ((380 – 240)/311)*205 = 92 mm.

Once the built-up edge has formed, no comparisons of the graphical results should be made between the different cutting fluids for that region, as the built-up edge is an unstable continuously changing and thus unpredictable structure, i.e. all comparisons must be done for the non-built-up edge region.

The built-up edge was a contributing factor to the results for the various cutting fluids not being absolutely repeatable in every respect as is evident from the cutting force - and temperature vs. time graphs, (see Appendix D) and to a lesser degree from Table 8.1 and Table 8.3 where the influence of the built-up edge has been avoided as far as possible.

For analysis of the other parameters (i.e. other than cutting force and temperature) during the cutting process, the region of the chip before the sudden decrease in cutting force and the maximum temperature are used, in other words the first quarter of the chip. In this way the unpredictable influence of the built-up edge may be avoided. Despite the built-up edge a high degree of repeatability is attained in the tests for the various cutting fluids, in that the general shape of the graphical results for cutting force and temperature is very repeatable. (see Appendix D).

In Table 8.1 the following parameters were determined from the graphical results:
- the average peak cutting force
- the average peak temperature prior to formation of the built-up edge
- the average of the 5 point moving average of the cutting force at formation of the built-up edge
- the average distance cut to formation of the built-up edge
- the average temperature at the quarter fraction of length of cut

The order in which the results are presented is dry, carbon tetra-chloride, the alkanes, the esters and lastly a poly-isobutylene formulation. The alkanes are paraffin or common illuminating paraffin, a heavier alkane fraction formulation referred to as C or SC and a light alkane fraction displayed or referred to as sample D (SD or D) in the results. The three ester formulations are also referred to as P8, SA and SE and the poly-isobutylene as SB or PIB.

Lubricant	Peak Cutting Force (N) (Average of 5 tests) + 1	Peak average Temperature (°C) prior to BUE formation 2	5 pt. MA Cutting force (N) prior to BUE formation 1	Average distance (mm) cut to formation of BUE ** 2	Temperature (°C) at quarter fraction of length cut 2	Smooth fraction on chip 2	Chip thickness ratio
Dry	494 7	312 ±4 3	324, 323±3 1	69, 72±14 4	304 8	5/16 5	3.66 8
CCl_4	490 5	333 ±4 1	370, 370±2 7	89 2	296 2	4/8 3	4.27 2
Paraffin	508 9	305 8	364, 363±6 4	100; 95±12 1	301 5	5/8 2	4.27 2
Heavier alkane fraction	488, 489±7 4	312 ±5 4	385, 383±9 8	61; 62±6 6	307 9	2/8 6	3.942 4
Lighter alkane fraction	503, 502±12 8	308 ±7 5	366, 372±15 6	80; 80±10 3	293 1	7/10 1	4.457 1
Ester P8	490 5	306 ±4 7	350, 350±10 2	61; 60±6 7	302 6	5/16 4	3.80 7
Ester A	486 3	307 ±4 6	417, 417±10 9	59; 57±5 8	302 7	2/8 6	3.58 9
Ester E	484, 481±27 2	304 ±11 9	365, 364±8 5	49; 49±3 9	301 4	2/8 6	3.942 4
PIB	482, 479±11 1	315 ±4 2	354, 358±14 3	66; 63±6 5	299 3	2/8 6	3.87 6

Table 8.1 Comparison of results for different cutting fluids used.

+ Average of the peak cutting force adapted to a 200mg chip with the assumption of linearity as the region around 200mg is small
**Top figure indicates average and bottom figure indicates mean and range.

Lubricant	Average length cut (mm) to first break 2	Average chip hardness (HV25) 2	Shear strain per Average chip hardness 2	Chip shear strain (dimension-less) 1	Shear plane angle (°) 1	Repeatability of chip mass (mg)	Approximate Flow zone thickness ** (µm)	Overall per-formance ranking
Dry	62 9	119 9	0.031 9	3.717 8	15.67 2	196±2	20 16	6.22
CCl_4	154 2	109 4	0.039 2	4.29 2	13.45 7	198±1	20 13	2.94
Paraffin	156 1	114 6	0.038 4	4.29 2	13.45 7	197±4	18 5	4.22
Heavier alkane fraction	74 7	115 8	0.035 6	3.98 4	14.57 5	207±2 * 198	10 12	6.28
Lighter alkane fraction	147 3	114 6	0.039 2	4.47 1	12.90 9	198.5±2.5	15 28	3.67
Ester P8	87 4	90 1	0.043 1	3.848 7	15.10 3	201±2	15 14	4.28
Ester A	87 4	104 2	0.035 6	3.646 9	16.0 1	197±2	20-30 3	5.55
Ester E	65 8	108 3	0.037 5	3.98 4	14.57 5	197±4	18 22	5.78
PIB	79 6	113 5	0.035 6	3.912 6	14.84 4	193.5±3.5	10 26	4.44

Table 8.1 continued Comparison of results for different cutting fluids used.

* Data from a separate repeatibility test with no other data logging, and 198mg is the average chip mass from the test chips
** First measurement before BUE region and second measurement in BUE region

Ranking the cutting fluids

The bold numbers in Table 8.1 rank the cutting fluids according to the parameter that is investigated on a scale of 1 to 9, where 1 is most desirable and 9 is least desirable for the particular parameter. The bold numbers in the centre at the top of the columns are the weight of importance of the parameter.

Multiplying the weight factor by the rank and adding the values for all the parameters used for the weighing and dividing by the sum of the weight factors gives the overall performance rating for the cutting fluid. This is summarised in the following formula:

$$OPR = \sum_{i=1}^{n} \omega_i \cdot rank_i \; / \; \sum_{i=1}^{n} \omega_i \qquad \text{Eqn 8.1}$$

Where OPR is the overall performance rating
ω_i is the weight of the i-th parameter
$rank_i$ is the rank of the i-th parameter

The chip shear strain and chip thickness ratio parameter could be ranked the other way round as a smaller chip shear strain may be more desirable, argued from the viewpoint that less chip shear strain means less metal deformation and less metal deformation means less energy needed to perform the cut, but this is not done because chip shear strain on its own without chip hardness data can be misleading.

For example a small chip shear strain is more desirable, consequently because CCl_4 has the second largest chip shear strain it is the second worst cutting fluid.?? Compare the energy for performing the cuts for the different cutting fluids given in Table 8.2, and compare the chip shear strain from Table 8.1.

	CCl_4	% of Total Energy	P8	% of Total Energy	SC	% of Total Energy
Work on rake face	4.51J	19	5.08J	21.2	4.88J	20.6
Work on shear plane	18.84J	81	18.84J	78.8	18.77J	79.4
Total work	23.35J		23.92J		23.65J	

Table 8.2 Average of the work done in cutting the aluminium plate for 0.375 seconds at 0.133m/s and 0.25mm deep.

Calculating the energy of the work on the shear plane and the work on the rake face and the combined energy to cut the aluminium plate for 0.375 seconds (Eqn 2.7 and eqn. 2.11) yields the results as shown in Table 8.2. In all three cases the distribution of the results before calculating the averages was very narrow showing that the data is very repeatable. Five tests were used for each cutting fluid. The energy involved at the

junction between the tool and the work-piece was not taken into account for the total work in Table 8.2.

Cutting process parameter interpretation
Some of the parameters listed in Table 8.1 require further explanation:

- The **peak average temperature prior to built-up edge formation**: This gives an indication of the cutting fluids ability to reduce metal to metal affinity and thereby to prevent metal to metal seizure and to delay or prevent the formation of a built-up edge. The higher this temperature the better.

- The **5 point moving average of the cutting force prior to built-up edge formation** has potential to give an indication of how long the welded zone is i.e. it attempts to show the extent of metal to metal seizure prior to the forming of a built-up edge.

- The **average distance cut until the built-up edge forms** is also an indication of the cutting fluids ability to defer or prevent metal to metal seizure. The longer this distance the better.

- The **temperature at the quarter way mark of the length of cut** is an indication of how quickly the cutting tool heats up. The lower this temperature the longer the cutting time should be before the tool becomes too hot. The lower this parameter the better.

  The temperature at the quarter way mark is an attempt at obtaining an indication of the length of the contact-zone, it tries to show to what extent seizure has taken place relative to another cutting fluid. As far as the temperature determination at the quarter way mark of the cut is concerned (see also the motivation for choice of parameters, under the experimental planning section), for determining the different parameters. It would be more meaningful if the volume of the flow-zone directly above the welded-zone/contact length would be determined at that stage of the cut. It is possible that the intensity of shearing metal atoms over metal atoms in the flow-zone varies from one cutting fluid to another. This is because of a variation of the electronegativity of its constituent atoms and because of the variation of the number of electronegative atoms that adhere to the nascent metal at the cutting edge, thereby weakening the metallic bond. Comparing the volume of the flow-zone above the welded region is therefore incomplete if the ease of chip formation is not taken into account.

- The **smooth fraction** on the underside of the chip shows how long it takes until stick-slip develops. Stick-slip is the result of small welded regions that form and break loose again. The larger this fraction the better the ability of the cutting fluid to prevent welding.

- The **chip thickness ratio** is useful for the calculation of shear plane angle, chip shear strain and the work involved in performing the cut. It also changes when the cutting conditions change suddenly as they do when a built-up edge forms.

- The **average length cut until the chip breaks for the first time** is also an indication of how well a cutting fluid can promote ease of metal deformation. The chip will break in compression due to it having no more plastic capacity. A chip is strained more when a built-up edge forms and it often breaks suddenly when a built-up edge forms. The longer the length of cut the better the ability of the cutting fluid to prevent built-up edge formation and the better the ability to promote ease of metal deformation.

- The **average chip hardness** indicates the ability of the cutting fluid to prevent strain hardening. If the chip is softer then more metal should be cut before the tool becomes worn out. This should promote up-time and save on tool costs.

- **Chip shear strain per average chip hardness** is a measure of how easily chip flow/deformation can take place. If the metal can deform more and exhibit less work hardening then it should be easier to cut. This should enhance tool life and promote up-time or production rate. The greater the value for this parameter the better.

- The **chip shear strain** is used to calculate the previous parameter and indicates the same as the chip thickness ratio.

- The **shear plane angle** is used to calculate the energy used when a cut is made. The energy necessary to perform a cut follows a more or less parabola shaped function. The closer to 0°, and the closer to 90° the shear plane angle the more work is done on the shear plane and also in total. The minimum amount of work needed is at a shear plane angle somewhere in between, and the angle decreases for the minimum when the contact length increases. The minimum however also increases. The cutting fluid can influence the amount of work that is done in total. (see Table 8.2)

- The **repeatability of chip mass** is recorded for control purposes and because it may well be that tolerances are more closely attainable for cutting fluids that exhibit a high degree of repeatability.

- A thicker **flow-zone** shows either hotter cutting conditions, due to a longer welded zone, or greater ease of metal deformation or both. This parameter actually requires the length of contact so that the flow-zone volume may be calculated. The smaller this volume the better, as less metal over metal shearing will occur and therefore less heat will be generated, which will promote tool life.

- The other parameters that were monitored although not shown in Table 8.1 were **surface roughness** (Table 8.3) and **chip shape** (figure 8.7). Chip shape includes the visual observation of the **chip radius**. A sudden decrease in the chip radius is an indication that the effective rake face angle changed as it does when a built-up edge forms.

- **Surface roughness** shows the ability of the cutting fluid to produce a smooth finish. A smooth finish will require less secondary machining time to attain the required end

finish and this will increase the production rate as it decreases the production time. A cost savings is thus realised for a cutting fluid that can produce a smoother surface finish.

The readings in Table 8.3 are the minimum readings measured in microns (μm) that were obtained from experiment 6 when measuring the R_a value at a cut-off length of 0.8 and over a length of 13mm at various cuts for the different cutting fluids. The width of these cuts was measured to be 50 microns and by searching for the minimum readings possible on the work-piece in the length wise direction it was taken that the alignment of the Taylor Hobson Surtronic 3P profilometer was such that a measurement would be made in the same groove and not across two grooves. (For more detail on the method see Appendix C, Experiment 6.)

		Dry	Ester 8	Paraffin	Ester A	PIB	Heavy alkane	Light alkane	Ester E
Start	Across	1.28	1.41	1.34	1.36	1.46	1.35	1.31	1.41
	Length wise	0.14	0.13	0.13	0.12	0.12	0.14	0.12	0.13
Middle	Across	1.46	1.41	1.32	1.39	1.40	1.36	1.40	1.39
	Length wise	0.14	0.12	0.11	0.10	0.10	0.11	0.06	0.11
End	Across	1.28	1.41	1.37	1.42	1.38	1.39	1.35	1.38
	Length wise	0.12	0.14	0.12	0.14	0.12	0.12	0.11	0.13

Table 8.3 Comparison of surface roughness values measured in microns for different cutting fluids used.

It was found that the length-wise measurements, i.e. the measurements made in the direction of the cut, are more repeatable than the measurements made across the cuts.
Again, as for the longest smooth distance on the underside of the chip (Table 8.1), the non-polar compounds i.e. the alkanes and paraffin appear to render the smoother overall surface finish the exception being the heavy alkane, that in Table 8.1 also did not have a large smooth fraction on the underside of the chip. Table 8.3 shows that the difference in the minimum surface roughness values varies little for the different cutting fluids, the range being from 1.28 microns to 1.46 microns for the transverse measurements and 0.06 microns to 0.14 microns for the longitudinal measurements.

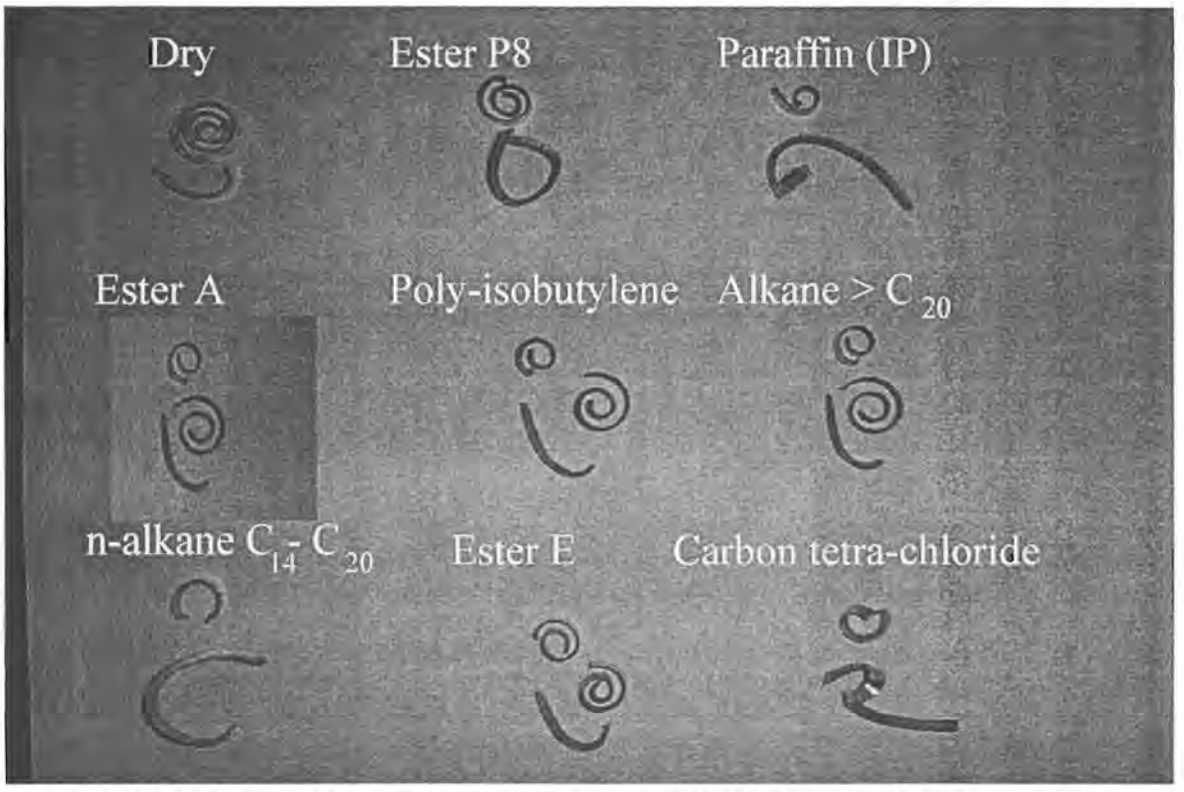

Figure 8.7 Most commonly observed chip shapes for the cutting fluids indicated

For paraffin, the lighter alkane, namely the n-alkane, and carbon tetra-chloride the longer chip is the first chip produced from the cut. Only ester P8 ranks higher in the ease of chip flow parameter of Table 8.1, than these cutting fluids. It is obvious that the decrease in chip radius occurs later for these three cutting fluids than for the other cutting fluids, where the first chip produced in those cuts is the most open shaped chip. This chip is comma shaped for Ester E, the heavier alkane, the PIB, Ester A and the dry cut. Once the effective rake face angle becomes more negative as it does for the built-up edge the chip is curled more tightly, i.e. the chip radius decreases significantly. With ester P8 a built-up edge forms more or less at the same length of cut as for the other esters. Ester A and ester P8 showed both the chip forms given, i.e. the chips of ester A sometimes also looked like those of ester P8 and vice versa. Because these chips are the softest of all the chips (Table 8.1) they have a longer length of cut to first break than ester E. They also display a longer length of cut to formation of the built-up edge.

CCl_4

From literature it is known that CCl_4 is a good metal working lubricant and that it is toxic and therefore cannot be used as a cutting fluid in industrial cutting.(Trent, 1977),(Boston 1952). It is a volatile low viscosity fluid. A molecule of CCl_4 is much smaller than the molecules of most cutting fluids that are used. It consists of five atoms only. In tests done by Trent at low cutting speed namely 8m/min. CCl_4 produced a smoother surface finish than either water or air. The reason for CCl_4 being a good cutting fluid probably lies in the fact that it has i) a small molecule ii) is rich in electronegative

atoms and iii) is volatile, thereby aiding evaporative cooling in addition to convective cooling. The high concentration of electronegative atoms at the cutting edge helps to weaken the metallic bond.

When the results (Table 8.1 and Appendix D) from the tests on the shaper are viewed it becomes apparent that the cutting force for CCl_4 is generally somewhat higher than for the dry cut. It is emphasised again that comparisons must be done for data points that lie vertically above each other on the graphs. Furthermore the cutting temperature is also generally somewhat higher than for the dry cut and it could therefore easily happen that the incorrect conclusion is drawn: namely that CCl_4 is not a good cutting fluid because both the cutting force and the temperature are higher which should result in increased operating costs and reduced tool life. The way to actually interpret these results is once again to look at the **non built-up edge region** of the graph. Now in this region the operating temperature is generally slightly lower for CCl_4 than for the dry cut once the quarter way mark of the length of cut has almost been attained, although not much difference is seen between the cutting forces for the same region. In the first five cuts the maximum temperature is reached at a later stage than for the dry cut and the sudden decrease in the cutting force is also at a later time. This shows that CCl_4 is able to resist metal to metal seizure for longer than the dry cut and that the length of the welded-zone in the non built-up region for CCl_4 is shorter. It is therefore clear that CCl_4 is able to decrease metal to metal affinity. It is also clear that the lubricant applicator malfunctioned in test 6, because the built-up edge formed at the same time as for the dry cut. This was already shown and discussed for figure 8.5. In the first column of graphs for CCl_4 graphs 2 to 4 show a 5 pt. moving average in addition to the raw data as presented in all other graphs in the first column.

The next enlightening bit of information about CCl_4 as a cutting fluid is found in Table 8.1. The third best performance in terms of the smooth fraction on the underside of the chip determined as an average for the tests is found for CCl4. Interestingly enough there seems to be a correlation between smooth distance cut and length to first break for which CCl_4 fares second best. It also, together with paraffin, shows the second highest chip shear strain. In the continuation of Table 8.1 in the column for chip shear strain per average chip hardness CCl_4 also fares second best. It produces the fifth hardest chip of the cutting fluids tested. The dry cuts fare poorest, the chips are the hardest and the ease of chip flow is the lowest.

As far as the temperature at the quarter way mark is concerned CCl_4 once again fares second best at 296°C. The maximum temperature of 333°C at which the built-up edge forms is the highest for CCl_4 from which it follows that CCl_4 has the best ability to prevent metal to metal seizure or put another way, to reduce metal to metal affinity. It is therefore expected that CCl_4 will show one of the longer distances of cut before formation of the built-up edge, and it does. CCl_4 has the second longest distance to formation of the built-up edge. CCl_4 produced the most repeatable chip masses. As far as chip shape is concerned CCl_4 was one of two cutting fluids tested that was sometimes able to produce a single contiuous chip over the full length of cut (see figure 8.7). The

other cutting fluid was the light alkane (SD). The overall performance rating for CCl_4 is 2.94 and this is also the best of all the cutting fluids that were tested.

Alkanes: (Paraffin, SC, SD)

The next analysis of cutting fluids is that of the alkanes and they are treated as a group. See appendix D for the results of paraffin. Looking at the graphs in columns two and three it is clear that the applicator worked in each test that was conducted, because the vertical difference in cutting force and temperature data points is not almost zero. The heaviest chip seen in test 4 produced the highest peak cutting force.

The cutting force for paraffin is also generally somewhat higher than for the dry cuts. The cutting temperature for paraffin in the non built-up edge region graphs 1 to 5 is also somewhat higher for paraffin than for dry cutting. It is inferred that there is a longer contact-zone for paraffin than for dry cutting as the flow-zone thickness is close to the same; for dry cutting it is 18 μm compared to 20 μm for paraffin, therefore for the same same contact-zone length the cutting temperatures should have been close to the same. The forming of the built-up edge is delayed longer with paraffin than for dry cutting. This is especially clear from the graphs for tests 1 and 2. In graphs 2 and 3 as the built-up edge was forming (slower than for the dry cut) at more or less sample 500 and 540 respectively there is a sudden increase in the cutting force. This is because the built-up edge, or part of it was sheared off. The flow-zone is immediately closer to the dissimilar metal junction of the tool and the chip and the temperature immediately responds. The graphs for paraffin, especially the temperature graphs, have a high degree of repeatability for the non built-up edge region.

- Many more cuts were done with dry cutting than for any other cutting fluid and the fact that built-up edges were sheared off six times in ten runs with paraffin, shows that the built-up edge is weaker when cutting with paraffin than when dry cutting.
- CCl_4 also showed the shearing off of the built up edge namely three times in six tests that were done.
- The shearing off of a built-up edge was far less frequent for dry cutting.
- Paraffin produced the highest peak cutting force for a 200 mg chip: namely 508N compared to the lowest peak of 482N produced for the poly-isobutylene chip.
- The cutting fluid related to paraffin namely the light fraction alkane produced a similar peak cutting force result as paraffin and both of these cutting fluids had a good length of cut to first break, distance cut to formation of built-up edge and a good smooth fraction on the underside of the chip. (See Table 8.1)
- Paraffin for length to first break and length to formation of built-up edge fared best overall and the light fraction alkane third best, but the light fraction alkane fared best for smooth fraction and paraffin fared second best.
- For ease of chip flow the light fraction together with CCl_4 fared second best and paraffin third best.
- The temperatures at the quarter way mark for paraffin and the light fraction alkane are 301 (fourth lowest) and 293°C (lowest) respectively.

For paraffin and the lighter fraction alkane the average peak temperature at the time where the built up edge forms is 305°C and 308°C respectively, which is the same temperature region as for the ester formulations that were tested, but the built-up edge forms later and therefore these temperatures are attained later and the cutting process runs cooler for longer with these cutting fluids than for the esters. This is not pronouncedly so when viewing the graphical results, but the difference is there. It is apparent that the temperature stays higher for longer with paraffin, CCl_4 and the lighter fraction alkane because the built-up edge forms later, and it appears that the initial rate of temperature increase is nearly the same regardless of which cutting fluid is used. If however, the temperatures are compared at regular intervals as the cut develops, the differences are apparent. The quarter way mark temperature comes in useful here. The heavier alkane had the highest temperature at the quarter way mark. It also fared poorly as far as length cut to first break and smooth fraction are concerned. It is in position seven. Together with some other cutting fluids it fares second poorest as far as ease of chip flow is concerned. Only the dry cut fares poorer. Unlike paraffin and its lighter relative, it is not able to delay the formation of the built-up edge for long. The built-up edge sheared off five times in eleven tests. The result for the first test is very similar to the tests where the built-up edge did not prominently shear off and form again.

The quarter-way temperature for this product interestingly is the highest of all the cutting fluids. When the temperature response is compared to the graphs for the dry runs of comparable chip mass in the non built-up edge region the behaviour is similar to that of paraffin and the light fraction alkane in that the temperature is higher than for the dry run. The temperature difference is however less pronounced for the heavier alkane than for paraffin and the lighter alkane. The built-up edge did not shear off and form again when cutting with the light alkane. The shape of the graphical results for the light alkane is the most repeatable of all the results for the cutting fluids that were tested. This once again indicates that the results on the shaper are generally very repeatable.

The shape of the last graphical result for the heavier alkane shows a similar result as for the rest of the tests done for the heavier alkane, but it is clearly noted that the peak temperature and the cutting force are lower over the full duration of the cut because the chip is lighter. Also the amplitude of the oscillation of the cutting force signal decreases when the chip is lighter. This was also shown in figure 8.6.

Based on the results for the light fraction alkane and paraffin it is clear that they perform well as a cutting fluid for aluminium cutting. Their overall performance ratings are 3.67 and 4.22 respectively and these are the second and third best overall ratings (see Table 8.1). The heavier fraction alkane was not able to perform as well as paraffin and the light fraction alkane. The rank it attains for the various cutting process parameters investigated is generally much lower. Its overall performance rating is 6.28 and is the lowest performance rating of all the cutting fluids.

The performance ranking is dependent on the weight that is assigned to the different performance parameters.

Esters: (P8, SA, SE)

The ester cutting fluids that were used generally performed weaker than CCl_4 , paraffin and the light fraction alkane.

- The distance cut to first break, the smooth fraction on the underside of the chip and the distance to formation of the built-up edge are markedly shorter.

Looking at the distance cut to first break and the smooth fraction on the underside of the chip ester P8 performs the best when compared to the other esters.

- Ester P8 has the best ease of chip flow of all the cutting fluids that were tested, but the built-up edge unfortunately appears too early.
- In all the tests the esters display a built-up edge that forms earlier than for any other cutting fluids that were tested.
- The esters have a lower peak cutting force for a 200mg chip than the other cutting fluids, probably because they produced the softest chips although in the ease of chip flow SE performed intermediate and SA performed of the second poorest.
- The esters have a lower peak temperature than for the other cutting fluids because the built-up edge forms too early, but it is noted that the quarter way temperature at 302, 302 and 301°C for P8,SA and SE respectively are intermediate and compare well with that of paraffin which is also at 301°C.
- They all display a poor smooth fraction of ¼, except for P8, on the underside of the chip. P8 dispays 5/16, which is only marginally better.
- The esters and PIB typically give two or three chip fragments from one cut whereas one or two fragments result for paraffin, CCl_4 and the light fraction alkane (see figure 8.7).

Poly-isobutylene:

- Poly-isobutylene had the lowest peak cutting force and a slightly better average distance cut to formation of built-up edge than the esters. There was however no correlation found between ease of chip flow and peak cutting force.
- The length cut to first break was more or less the same as seen for the esters.
- The smooth fraction on the underside of the chip was just as poor as for the esters.
- The temperature at the built-up edge was higher, namely 315°C than for the other cutting fluids and if it is taken into consideration that this is at a short distance to formation of built-up edge, the temperature rise is more rapid for this cutting fluid than for the others.
- At the quarter way mark it was third coolest at 299°C.
- When the built-up edge forms it has the second hottest temperature. A question that one may ask is whether this temperature is an indication of the maximum temperature up to which a cutting fluid can withstand built-up edge formation? The answer is probably yes. One problem with PIB is therefore that because this temperature is reached too soon, built-up edge formation happens early: after 66mm of cutting.
- The ease of chip flow is the second poorest.

An explanation to the higher chip thickness ratios when lubricants are used is that the metal grains are able to flow more readily and when the cutting speed is increased the ratios decrease because time to flow decreases and the contact length, or flow-zone length decreases slightly and so the shear in this zone is less. As a result the cutting force

decreases, therefore there is less potential for the chip to flow. Another contributing factor is that the tensile strength of the work material is time dependent. This means that it will present stronger when the time over which the force is applied is shortened, but this effect is probably offset by the decrease in tensile strength due to an increase in temperature when the cutting speed is increased. There is a point though, when the cutting speed is increased sufficiently where the temperature in the flow zone increases sufficiently to promote welding of the chip to the tool and then the flowzone length starts to increase again. Severe cratering and tool wear becomes manifest at these speeds. The tool may also break.

Softer materials are more ductile and therefore yield thicker chips. If a cutting fluid is able to better lubricate the metal grains that constitute the work-piece then the chip thickness should increase as lubrication improves. For CCl_4, paraffin and the light fraction alkane good ease of chip flow figures were obtained and the chip shear strains were also high, showing that the chips obtained were thick.

If the cooling effect is dominant over the lubrication as it could be with a high air flow or with cryogenic cutting, then the chip is cooled more intensely than with LVL with a lower air flow, and the material becomes less ductile than it is during dry machining, as a result a thinner chip could be expected.

The results from experiment 4 for the lubricated cuts were presented first with the exception of the hardness tests and the etching work that was done. The results for the hardness tests and the etched micrographs appear on the pages that follow.

Micro-hardness profiles and micrographs

The results for the average hardness were shown in Table 8.1. The micro-hardness test results complemented by optical micrographs were as follows.
All tests were performed using a 25g mass piece on the Vickers Hardness test machine. The first quarter region of the chip was examined in all the tests. This is the region where the underside of the chip is still smooth for all the cutting fluids that were used and no built-up edge was present. All micrographs were at 250X magnification unless otherwise stated.

Cutting dry

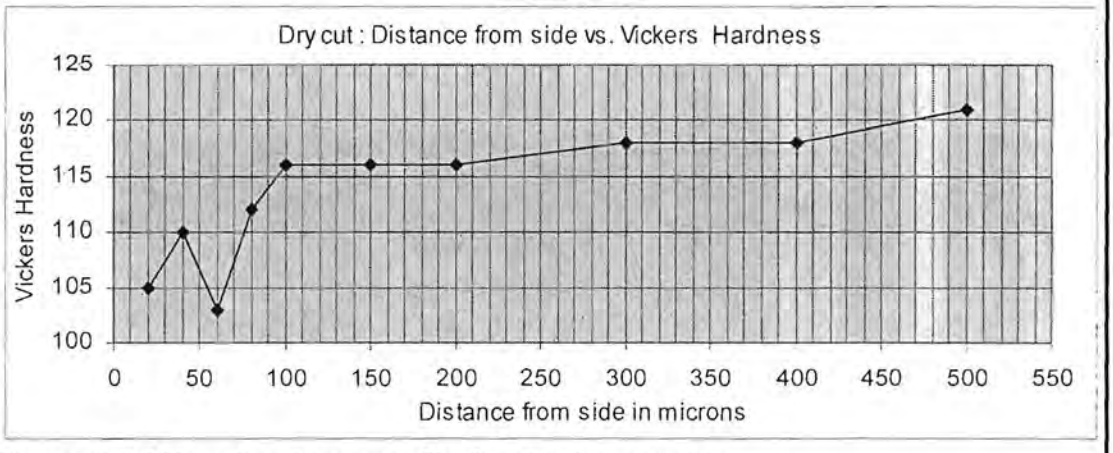

Figure 8.8 Micro hardness profile for the dry cut chip

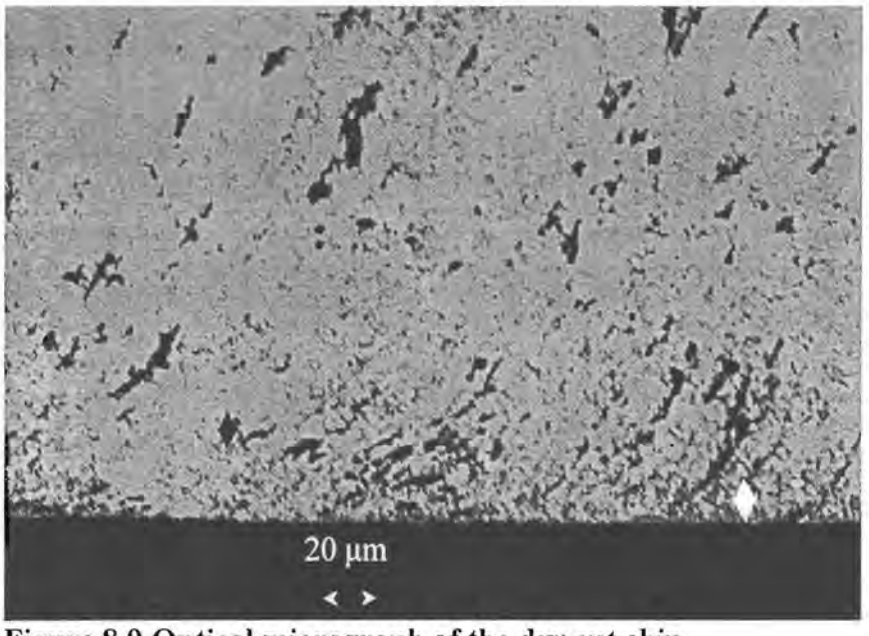

Figure 8.9 Optical micrograph of the dry cut chip

The flow-zone is just less than 20 microns on the micrograph in figure 8.9 and is indicated by the diamond shape. The hardness test prediction (figure 8.8) would have been 20 microns at the most. In all of the following results it will be seen that the chip hardness is fairly uniform and hard in the cold worked region, but when the flow-zone is

reached the hardness drops off very steeply because the chip was much hotter in this region and could therefore deform much easier without undergoing severe strain hardening. It is still strain hardened, but less so than in the colder region. Between the cold region and the hot region is a not so clear-cut transition and the hardness in this region sometimes tends to vary slightly. One reason for this could be micro-cracks in the subsurface.

Note how the hardness in the cold worked region differs for each cutting fluid that was used. (See figures 8.8, 8.10, 8.12, 8.14, 8.16, 8.18, 8.20, 8.22, 8.24)

Cutting with Carbon tetra chloride

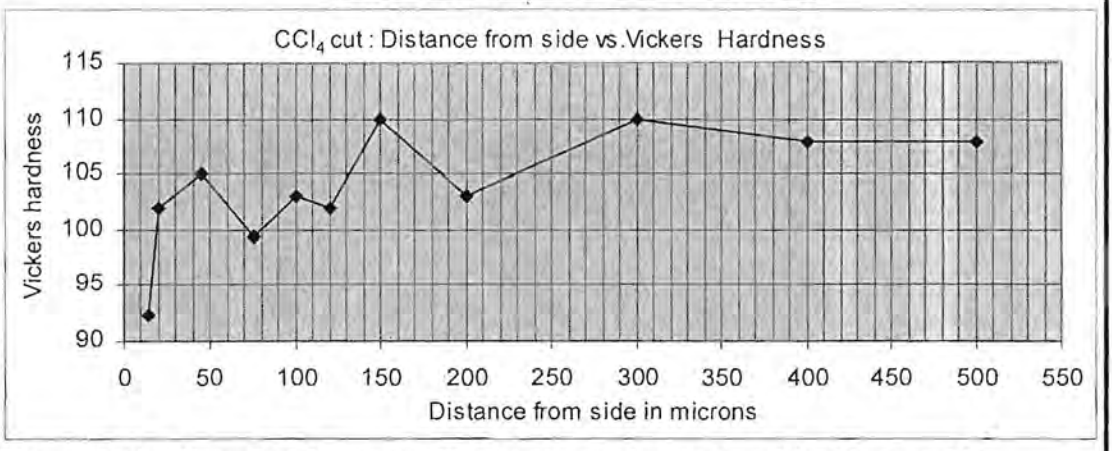

Figure 8.10 Micro hardness profile for the carbon tetra chloride cut chip

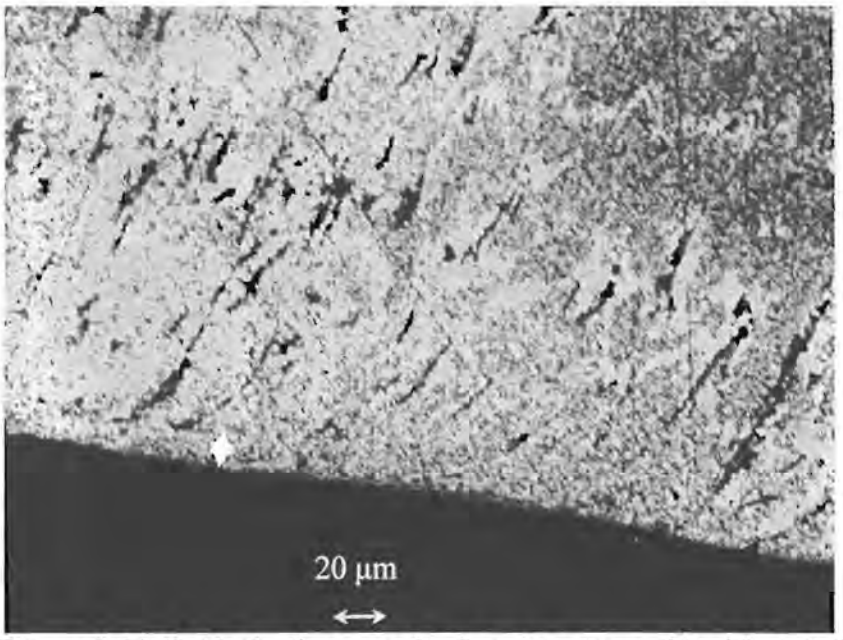

Figure 8.11 Optical micrograph of carbon tetra chloride cut chip

The flow-zone or deformed zone appears at the bottom of the micrograph (figure 8.11) and it is less than 20 microns thick. The diamond shape on the indicates the flow-zone thickness and is used as such on all the micrographs. What is difficult to determine is the point where the flow-zone ends. This is why the micro-hardness test results come in

handy so that the flow-zone thickness may be estimated. (figure 8.10) The first data point is at 14 microns from the edge and is definitely in the flow-zone. Its hardness is much less than that of the cold worked region. The second point is at 20 microns. The drop off is very sharp and will be seen again for other hardness graphs. This is why the flow-zone thickness in figure 8.8 was taken as less than 20 microns.

Cutting with Paraffin

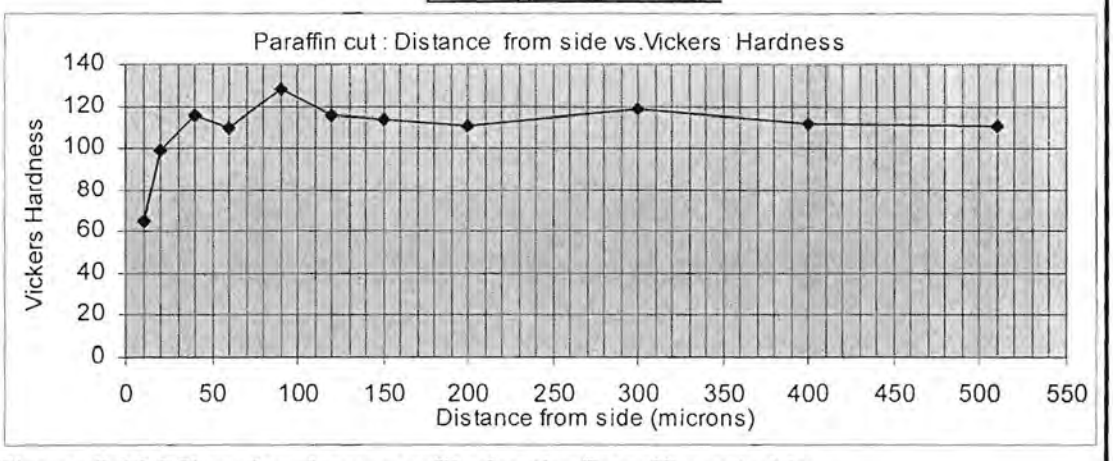

Figure 8.12 Micro hardness profile for the Paraffin cut chip

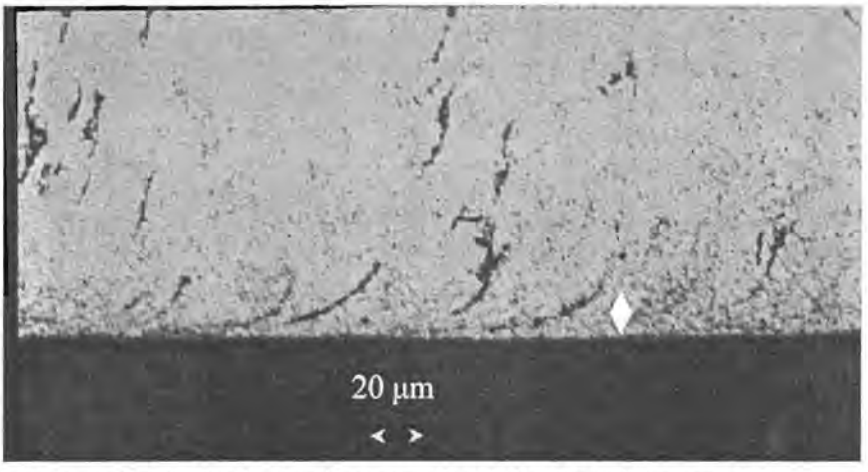

Figure 8.13 Optical micrograph of the Paraffin cut chip

The micrograph (figure 8.13) indicates a flow-zone of slightly less than 20 microns. From the micro-hardness graph (figure 8.12) the flow-zone boundary is taken as close to 20 microns.

Cutting with the heavier alkane

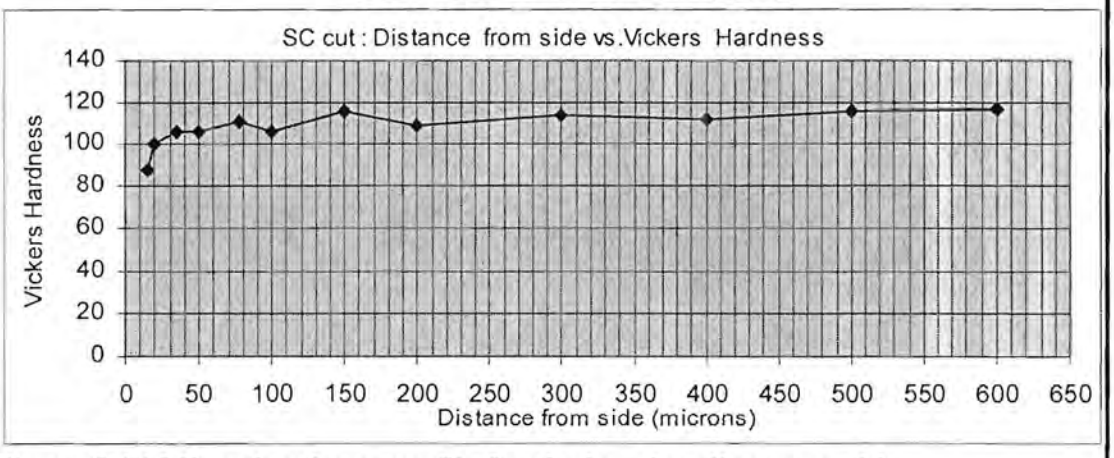

Figure 8.14 Micro-hardness profile for the heavier alkane cut chip

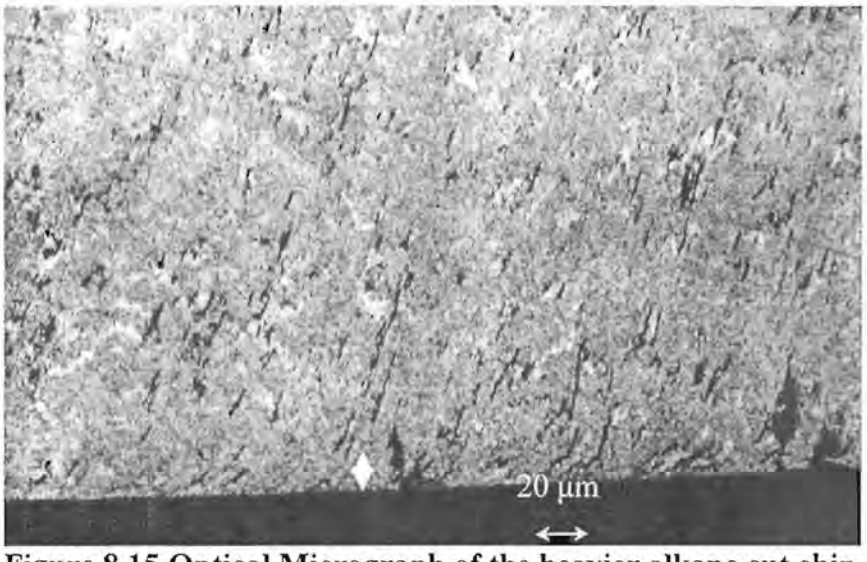

Figure 8.15 Optical Micrograph of the heavier alkane cut chip

The micrograph (figure 8.15) shows a flow-zone thickness of about 15 microns. This estimation is substantiated by the 15 microns that would have been predicted from the hardness test (figure 8.14). The 20 micron is just outside of the flow-zone. This micrograph came out very clearly. The metal in the deformation zone lies more in the horizontal direction slanting up to the right slightly, but outside the flow-zone the metal lies more in the vertical direction slanting a little to the right. This is the case on all the micrographs, only some micrographs are less clear.

Cutting with the light alkane

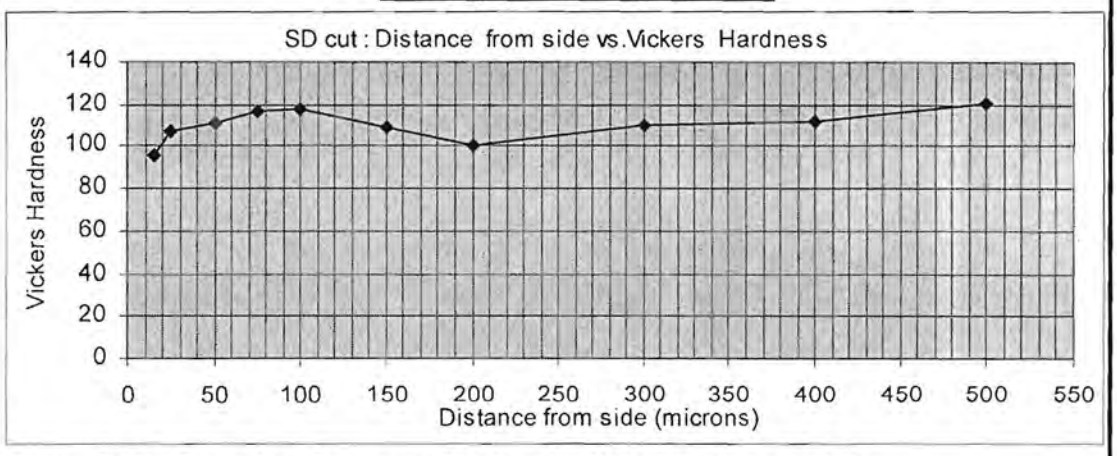

Figure 8.16 Micro-hardness profile for the light alkane cut chip

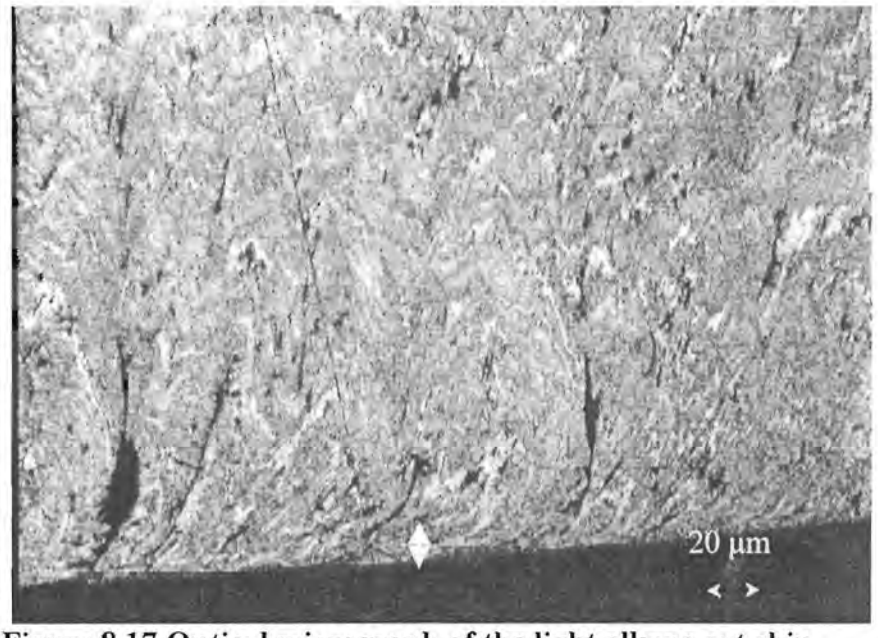

Figure 8.17 Optical micrograph of the light alkane cut chip

The flow-zone thickness from the micrograph (figure 8.17) is about 15 microns. From the hardness test (figure 8.16) it is expected that the flow-zone is close to 15 microns thick. It is clear that the etching process was a success as this micrograph also shows the metal deformation very clearly.

Cutting with Ester P8

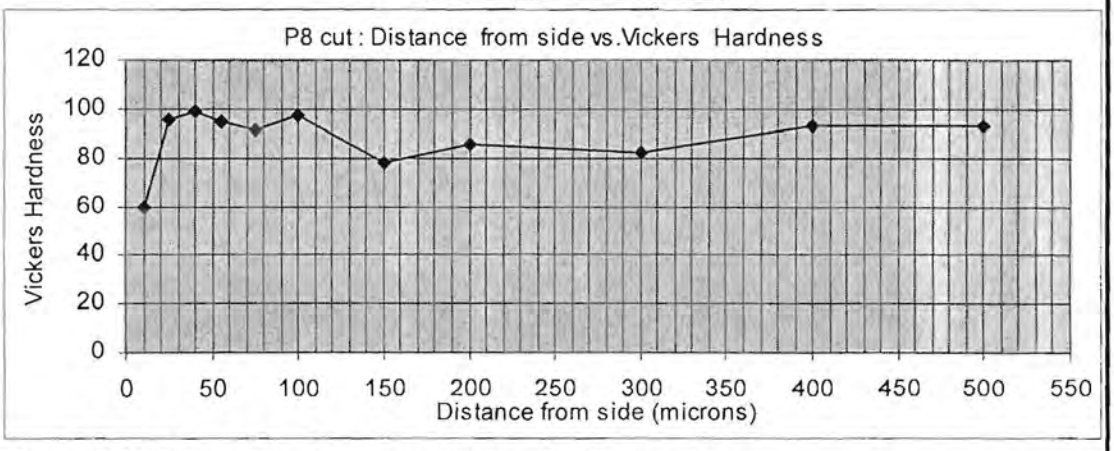

Figure 8.18 Micro hardness profile for the P8 cut chip

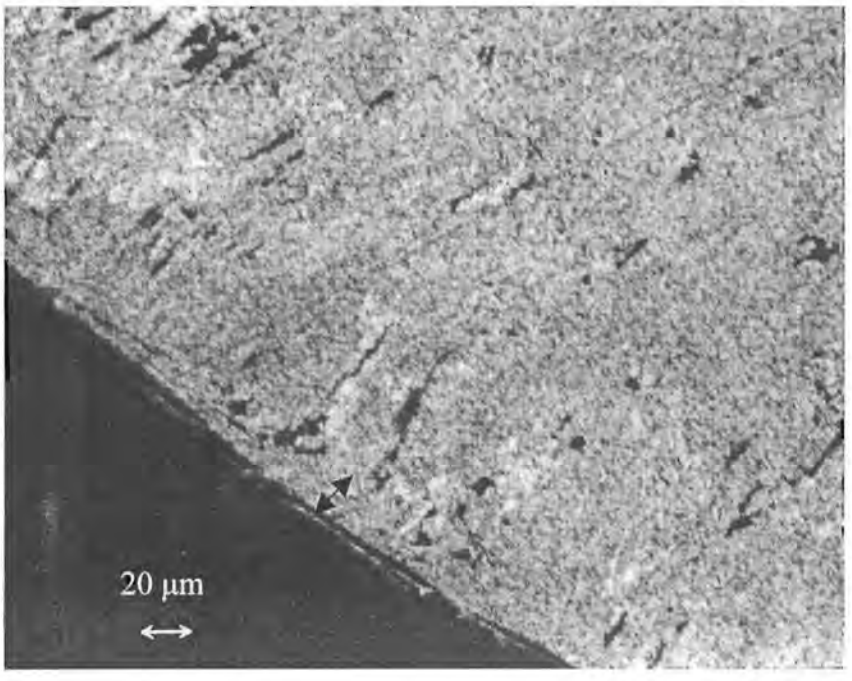

Figure 8.19 Optical micrograph of the P8 cut chip

The flow-zone on the micrograph (figure 8.19)is 10 to 15 microns thick as opposed to less than 25 microns from the hardness test figure 8.18). Another test at 15 microns would have been useful.

Cutting with Ester A

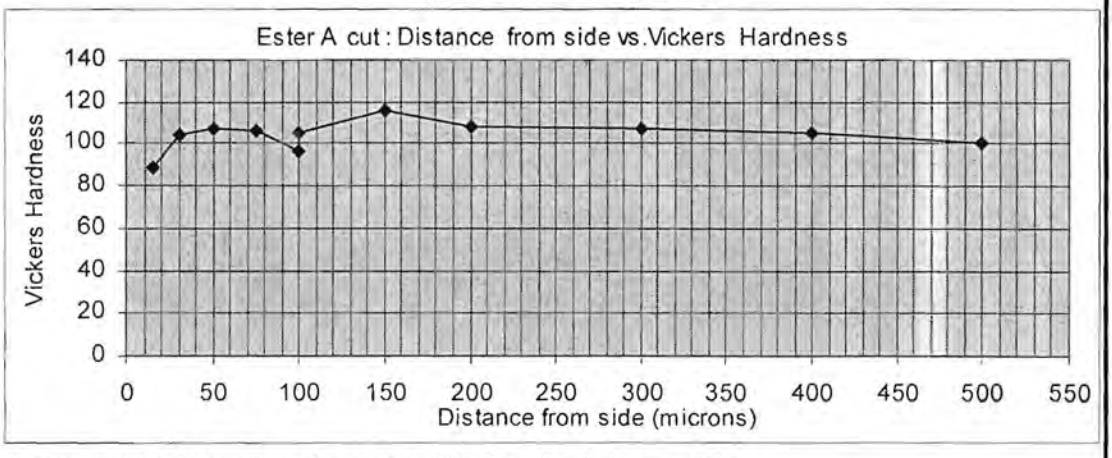

Figure 8.20 Micro hardness profile for the SA cut chip

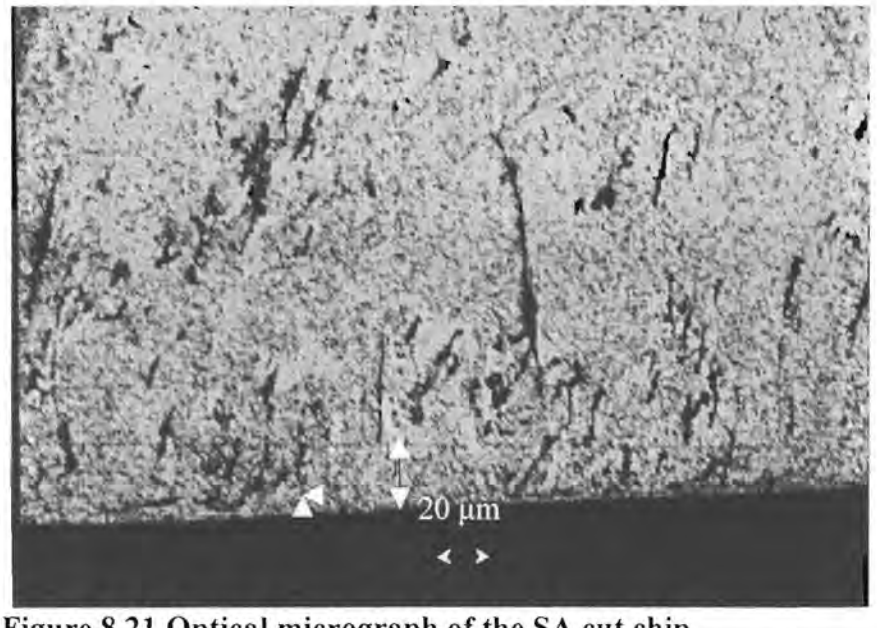

Figure 8.21 Optical micrograph of the SA cut chip

The micrograph (figure 8.21) shows that the flow-zone is between 10 and almost 30 microns thick. It is difficult to determine precisely where the boundary is. The test point at 100 microns appears twice on the hardness graph (figure 8.20). The lower value is for a shot that was placed on a micro-crack in the chip. From the micro-hardness test a little less than 15 microns would have been predicted for the flow-zone thickness. In cases like this one it is very useful to have a micro-hardness profile for the chip.

Cutting with Ester E

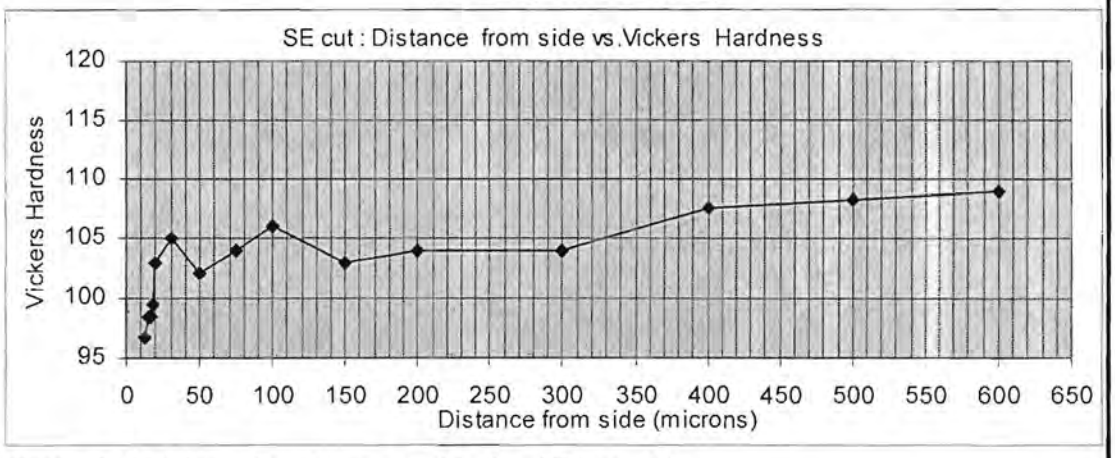

Figure 8.22 Micro-hardness profile for SE cut chip

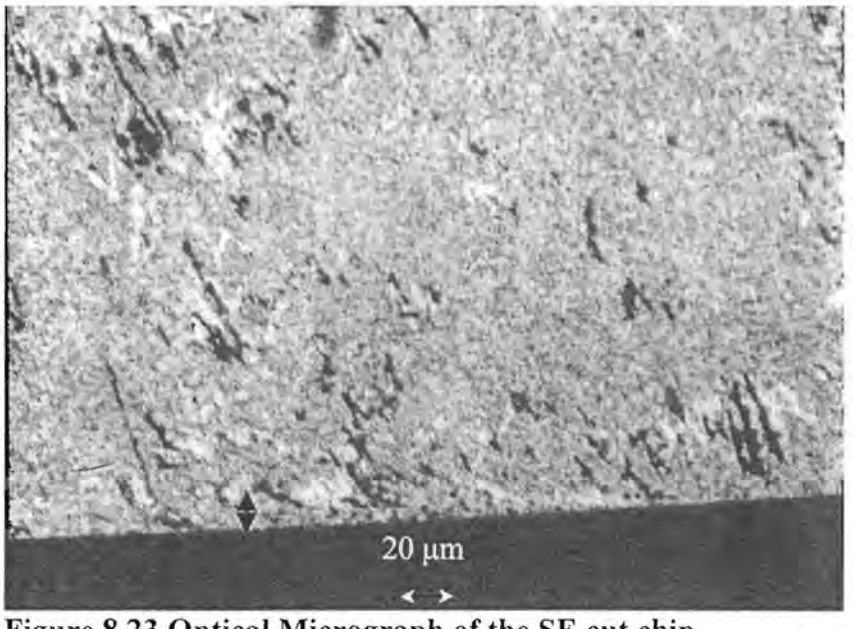

Figure 8.23 Optical Micrograph of the SE cut chip

From the micrograph (figure 8.23) a flow-zone thickness of about 15 microns is expected. The hardness test (figure 8.22) predicts it as 18 microns. This time it can be said with certainty that the flow-zone thickness is 18 microns as many hardness measurements in the immediate vicinity of the flow-zone boundary were made. It is once again apparent how steeply the hardness drops when the flow-zone is entered. Another interesting observation with the chip profiles is that in many cases it is evident that the chip becomes harder as one moves further away from the flow-zone. The reason for this is that the chip is deformed more as it has a tighter chip radius on this side of the chip and is therefore more strain hardened.

Cutting with PIB

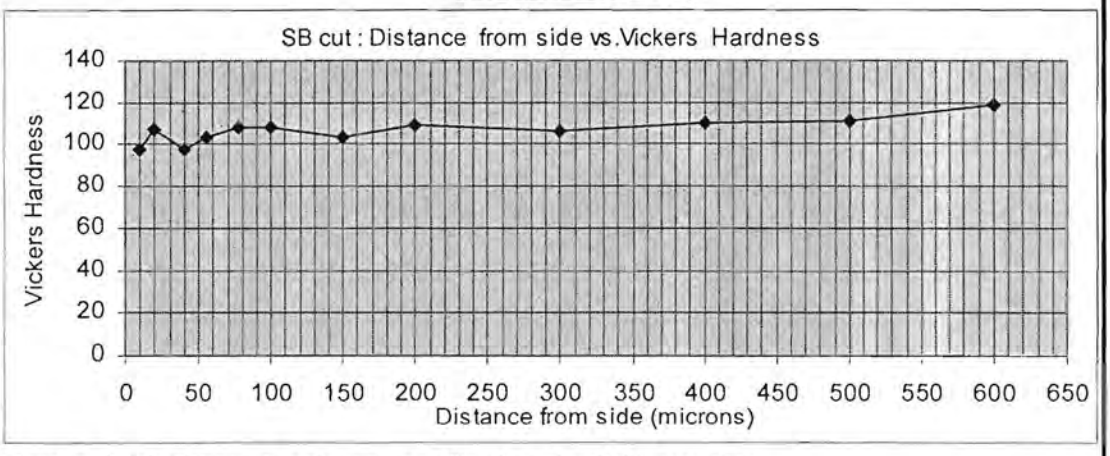

Figure 8.24 Micro-hardness profile for the PIB cut chip

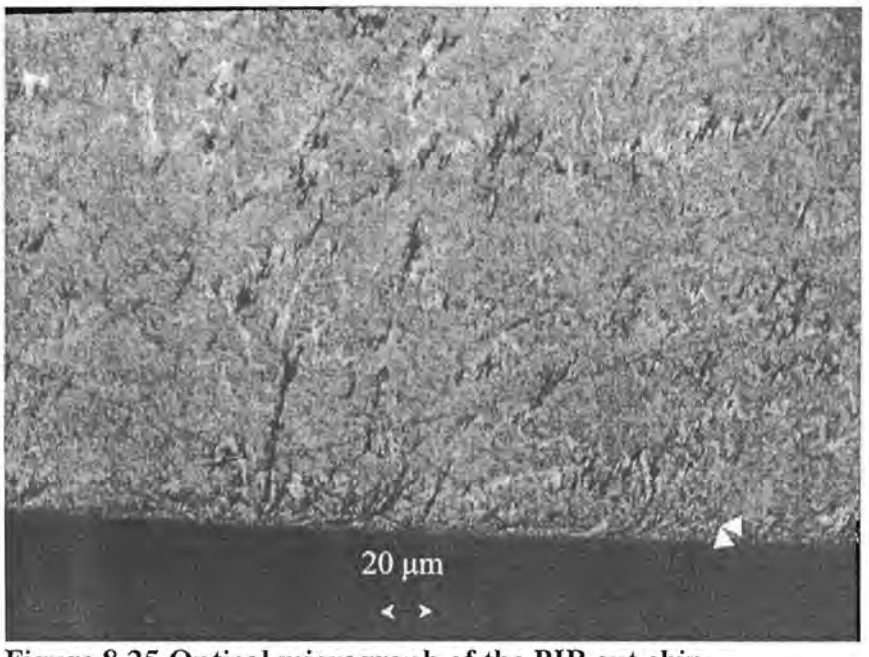

Figure 8.25 Optical micrograph of the PIB cut chip

The micrograph (figure 8.25) shows that the flow-zone is very thin generally less than 10 microns. It is not possible to do a micro-hardness measurement closer than 10 microns from the edge, therefore it is not possible to use the micro-hardness test result (figure 8.24) as a means to verify that the flow-zone is less than 10 microns thick, but it does show that it is not thicker than 13 microns.

The temperature in the non built-up edge region for poly-isobutylene was cooler than the dry cut in 3 of the 5 tests presented. The reason for this is quite likely the fact that the flow-zone is very thin, and as a result less shear is involved.

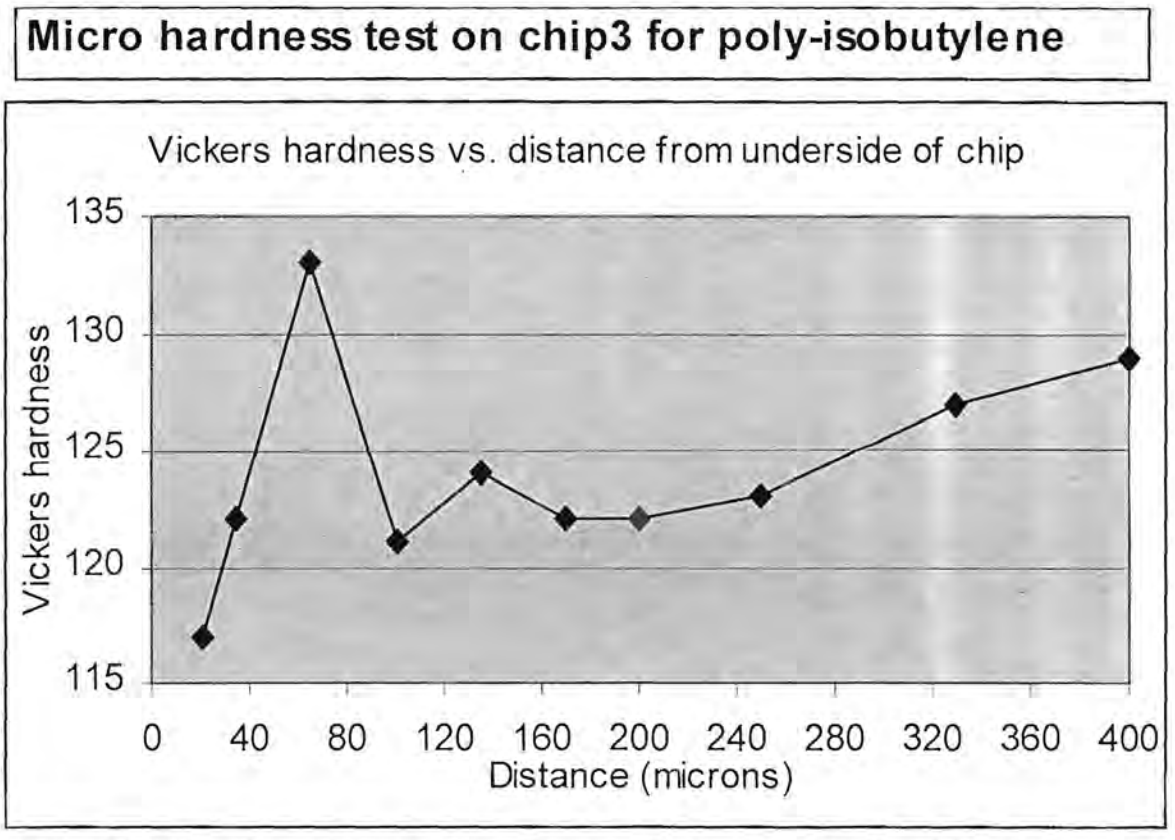

Figure 8.26 The effect of the Built-up edge on the hardness profile of the chip.

The chip becomes significantly harder when a built-up edge is present. It is curled tighter and thereby deformed more thus undergoing severe cold working. From the micro-hardness test depicted in figure 8.26 it appears as if there is a sandwiched layer between the flow-zone and the cold worked region. This high peak hardness is probably the result of the outer part of the chip being colder and therefore more resistant to deformation and on the other side of this peak is a hard tool that harshly pushes against this layer. The outer part of the chip further away from the flow-zone has less bulk that must deform; it can therefore deform easier and probably therefore has a lower chip hardness. As one goes even further away from the flow-zone the chip hardness increases again as a result of a tighter chip radius. The end hardness for SB was 119 before the built-up edge was present (see figure 8.24) after that it is 129. The hardness increases by more than 8 %. The prediction for the thickness of the flow-zone for this hardness profile would be approximately 20 microns. See the SEM micrograph figure 8.27 for comparison.

Generally the thickness of the flow-zone determined from micro-hardness test profiles correlates well with the results obtained from the optical micrographs. It is clear that micro-hardness testing works well to substantiate the results that are obtained from etching and optical micrographs. The two methods are complementary. The third method that was used for the quantification of the flow-zone thickness was to take SEM micrographs.

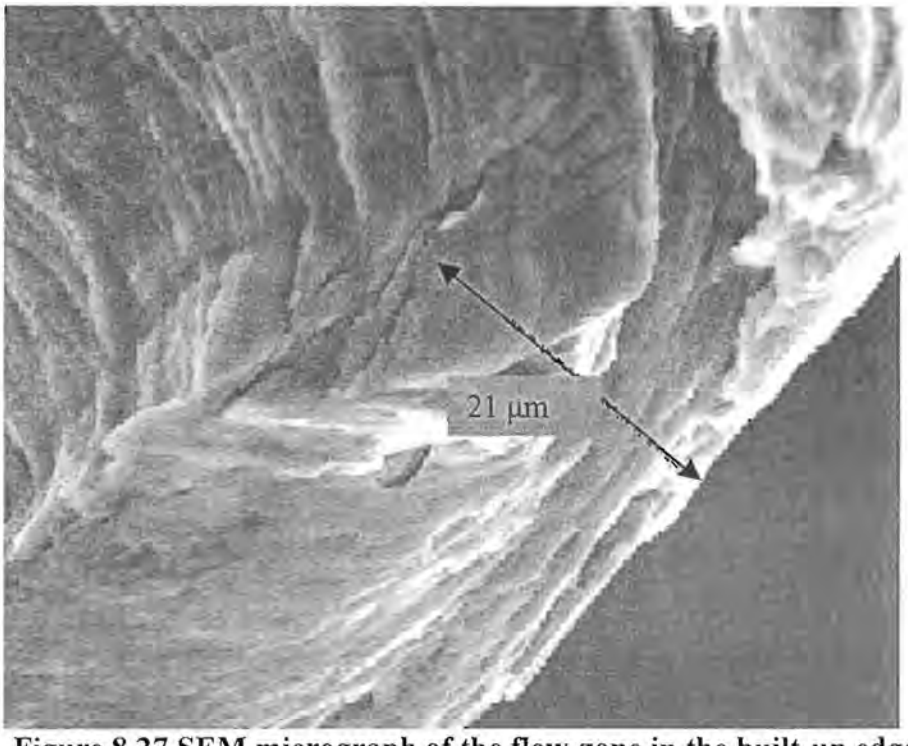

Figure 8.27 SEM micrograph of the flow-zone in the built-up edge region for poly-isobutylene at 2500 X magnification.

The prediction of the flow-zone thickness for this micrograph (figure 8.27) is also close to 20 microns. It once again depends on where the flow-zone will be measured, as the thickness of the flow-zone varies a little with position on the chip. The transition between the flow-zone and the rest of the chip in this micrograph is more clear-cut than on the optical micrographs. Compared to figure 8.22 where a prediction was made based on the hardness profile there is little difference. Both show the thickness as close to 20 microns. This confirms the validity of using SEM micrographs for determining the thickness of the flow-zone.

An indication of what the chip typically looked like at the end of a cut is given in figure 8.28. There was always a little tail at the base of the built-up edge in the chip. SEM micrographs of quick-stop sections would have served well to indicate the length of the welded zone on the rake face of the tool. For this particular chip the length of the flow-zone on top of the built-up edge is about 400 microns. The chip end that is shown is that of Ester P8. It is unlikely that the length of the tail gives an indication of the welded-zone length prior to built-up edge formation as the built-up edge could influence the length of the tail as the cut progresses. The tail does however substantiate that the flow-zone was not in direct contact with the rake face of the cutting tool. The thickness of the tail (figure 8.30) at the point where it departs from the chip is approximately 30 microns, and the thickness of the flow-zone was determined as approximately 15 microns from another SEM micrograph near the end of this chip.

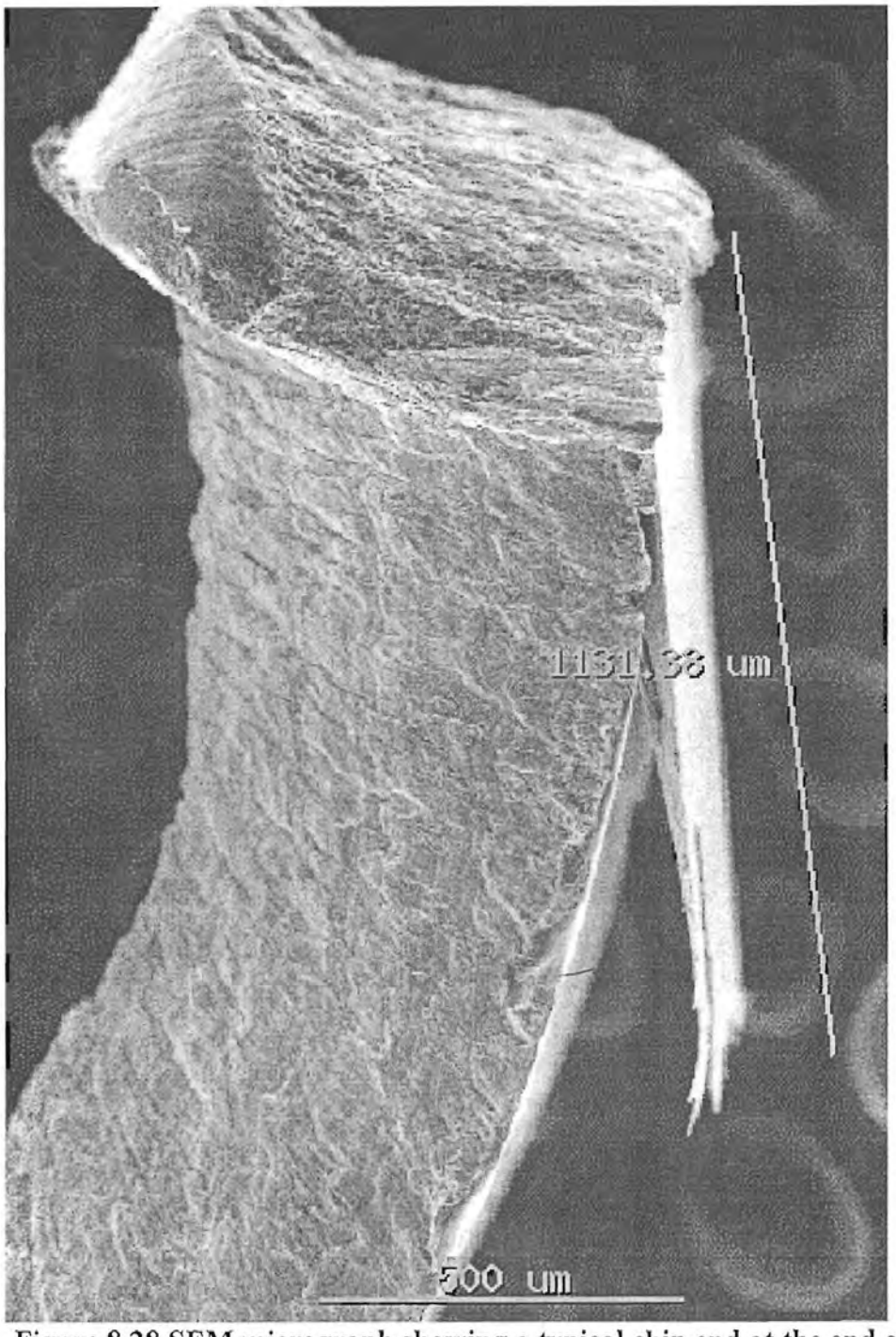

Figure 8.28 SEM micrograph showing a typical chip end at the end of a cut 2500X

From etching and micrography it is substantiated that the built-up edge is present when cutting aluminium. (See figure 8.29)

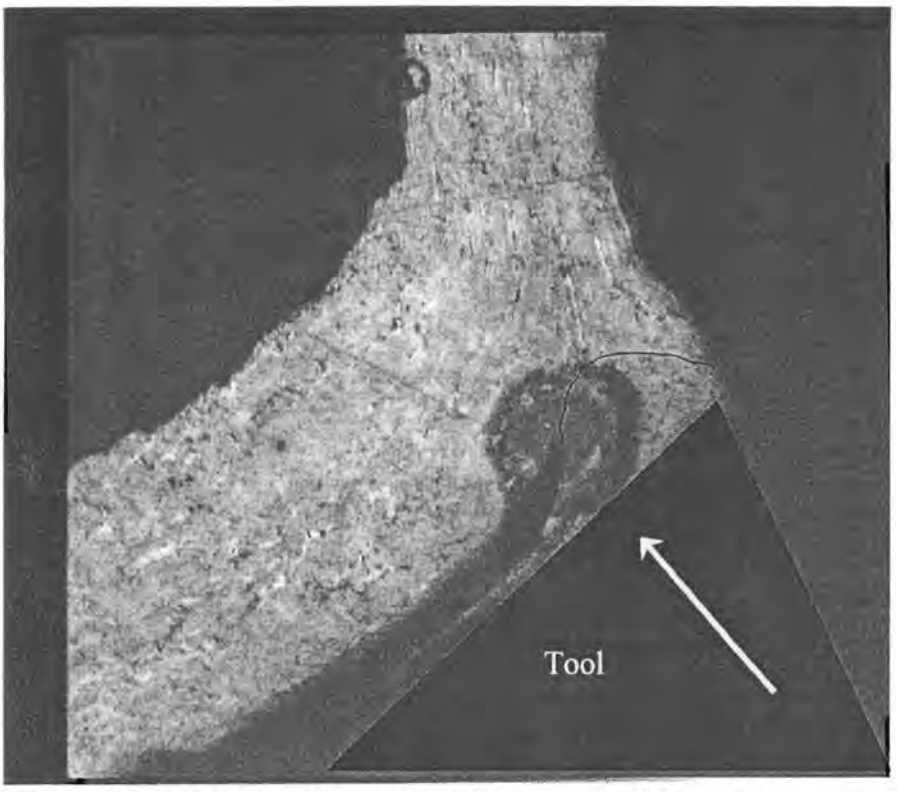

Figure 8.29 Micrograph of the built-up edge obtained when cutting with PIB 125X

It is evident that the chip is much thicker after leaving the tool than when it flows onto the tool. The chip is bent down a little at the part where it was removed from the work-piece. The white arrow on the tool indicates the direction of cut. The built-up edge is not so clearly visible but its boundary has been indicated by means of a black line. The built-up edge is about 400 microns high. The tail part of the built-up edge was originally fused to the rake face of the tool. The dark spot in the middle is where the etchant worked a little too deeply and has nothing to do with the cutting process.

The effect of the built-up edge on the hardness profile of the chip was presented in figure 8.26

For experiment 7 it was found that the cutting force decreases, and the temperature increases with an increase in cutting speed. (See figure 8.30)

Take note of the sampling rate for these experimental results. The time scale may be computed as previously, by dividing the sample number by the sampling rate. The sampling rate is close to 200 Hz in all the experiments.

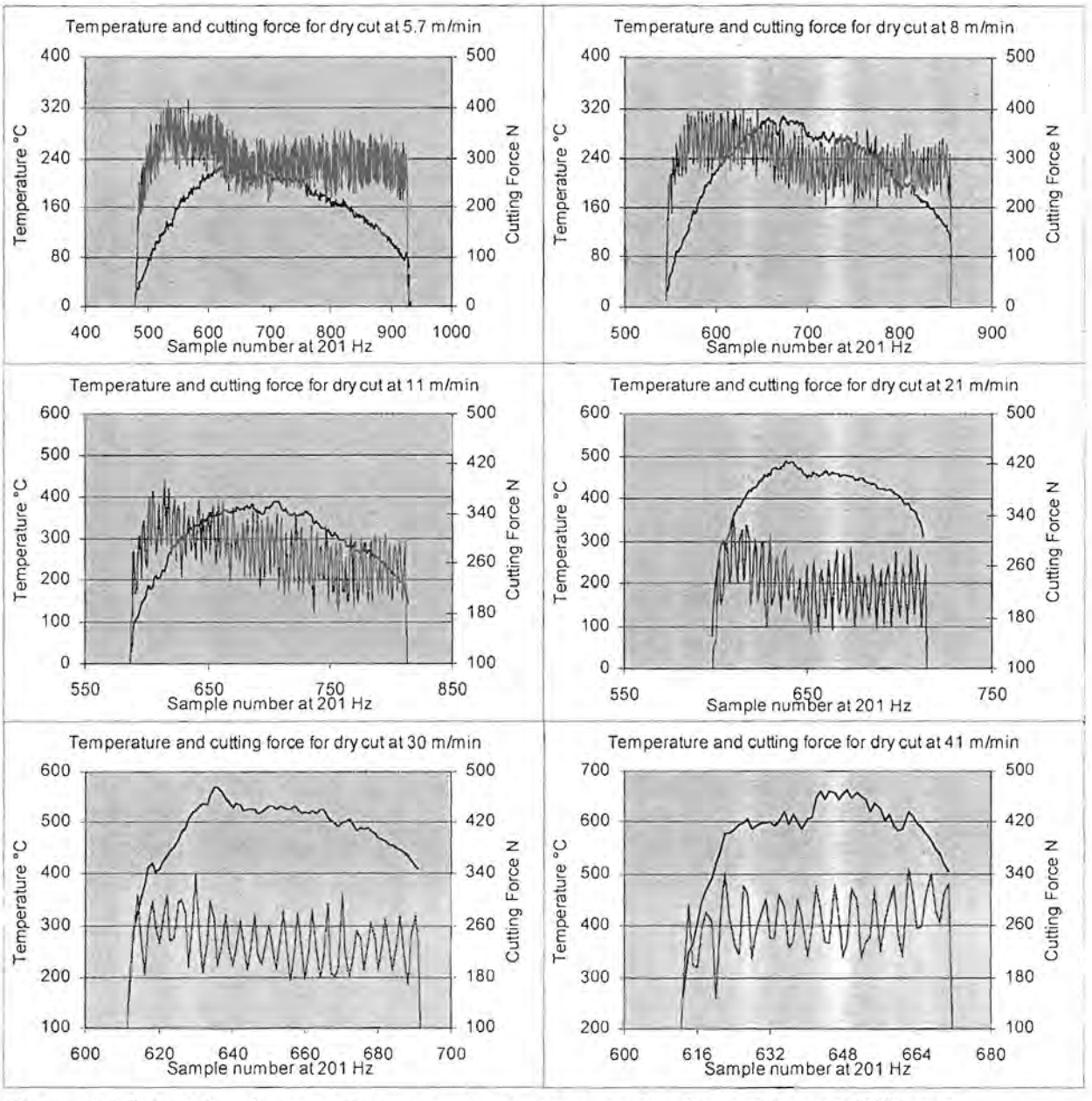

Figure 8.30 Cutting force and temperature response for dry cutting at different cutting speeds

From the graphical results it is clear that the temperature is higher throughout the test with increasing cutting speed. At the higher cutting speeds the cutting force starts to increase again because the built-up edge is being sheared off and thus forms less easily,

resulting in a longer welded zone on the rake face of the tool. See also Figure 8.31. At 41 m/min the temperature stays higher for a longer length of cut than any of the other tests done because the built-up edge has the least ease to form at this cutting speed and temperature when compared to the other tests.

When the cutting speed on the shaper is increased to over 60 to 90 m/min. then the built-up edge may or may not occur. This confirms Trent's observations in this regard. (Trent, 1977) (See section 6.1).

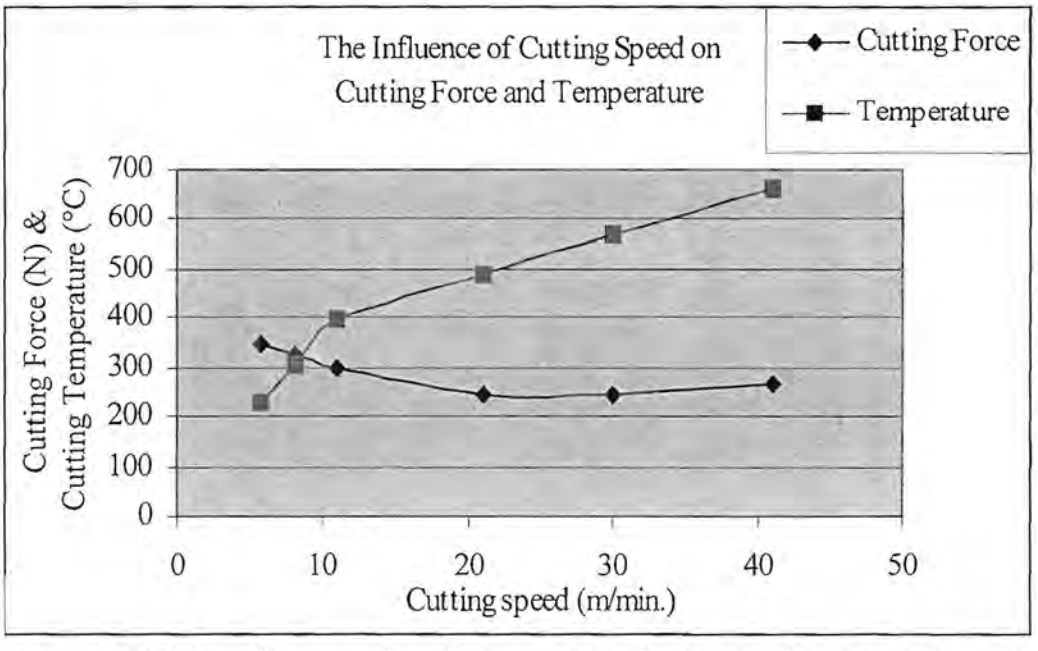

Figure 8.31 The influence of cutting speed on the cutting force and the cutting temperature

9.Conclusions:

The aim of the investigation was to establish a bench test, and to identify parameters that can be measured so that cutting fluid performance during aluminium cutting, when using limited volume lubrication can be evaluated.

1) The results from the tests on the shaper with the tool/workpiece thermocouple set-up and the cutting force measurements show that the test bench serves well for the evaluation of different cutting fluids.
2) The temperature and the cutting force responses are useful in determining when the built-up edge forms, and a micrograph of the etched longitudinal cross section of the chip serves well to substantiate the presence of the built-up edge.
3) The test method is useful for the evaluation of limited volume lubrication cutting fluids, but also has merit for the evaluation of cutting fluids other than limited volume lubrication cutting fluids.
4) The physical measurements of the chips are very useful in distinguishing the various cutting fluids from each other. All other parameters have been kept constant, i.e. the cutting speed and the depth of cut and any other parameters. The only parameter that changes from one test to the next is the cutting fluid that is used; hence **cutting fluids can be compared meaningfully**.

The most important parameters when comparing the different cutting fluids are:
- 1) the smooth fraction on the underside of the chip, this seems to be related to the distance that can be cut until the built-up edge forms
- 2) the distance cut to formation of the built-up edge,
- 3) the chip shape, specifically the chip radius
- 4) the distance cut to first break
- 5) the ease of chip flow,
- 6) the temperature at the quarter way mark at 52mm length of cut,
- 7) the temperature at which the built-up edge forms.

The surface finish obtained in this work was less enlightening as to the performance of the cutting fluids because the difference in surface finish is small, but usually surface finish is also used as a cutting performance parameter. Based on the above parameters CCl_4, the light fraction alkane, paraffin and Ester P8 are the best cutting fluids of the cutting fluids that were tested. One should have tested a product which is **not** a cutting fluid to confirm that surface finish is unacceptable.

Obtaining results such as that CCl4 is a good cutting fluid and that the cutting force decreases and the cutting temperature increases with an increase in cutting speed substantiates that the work done on the shaper can verify the results that are commonly observed during metal cutting.

Tremendous temperature gradients are involved in metal cutting. When a built-up edge forms, the welded-zone length decreases leading to reduced shearing of the metal. The maximum temperature and hence emf that is attained in the cutting process should be found in the flow-zone directly above the welded zone as this is the region of maximum

deformation rate. Due to the built-up edge the flow-zone is somewhat removed from the dissimilar metal junction at the interface of the tool rake face and the chip where the thermocouple e.m.f. is generated. Thus it was expected that temperature would decrease significantly when a built-up edge forms and it is exactly what was found from the experiments. The signal that is measured varies as the built-up edge changes. The larger the built-up edge the lower the temperature that is observed.

The built-up edge is undesirable, because if it is sheared off and passes on the underside of the tool, it causes surface defects on the worked material and it contributes to tool wear. If the formation of a built-up edge could be prevented such defects could be avoided, and this can be achieved by increasing cutting speed. The built-up edge is a type of seizure phenomenon. The longer it can be prevented from forming the better the anti-seizure properties of the cutting fluid are, and if cutting speed is increased, then these anti-seizure properties should aid the cutting process by decreasing cutting forces, tool temperatures and wear.

To complement monitoring of the flow-zone, micro-hardness tests may be done on the chip in addition to optical micrography. The hardness tests are also used when the ease of chip flow parameter is calculated. The work-piece material of aluminium was etched with 0.5%HF (hydro flouric acid) in distilled water (van der Voort, 1999). This helps to give an indication of the thickness of the flow-zone and whether a built-up edge was present or not, therefore if the experiment is performed with a quick-stop the length of the welded zone can also be determined by etching and micrographs. The SEM micrograph was also useful in complementing the result from the micro-hardness test. The hardness alone does not quantify whether a cutting fluid has good performance - it is the hardness in combination with the chip shear strain that seems to matter, as the cutting fluids that had the best performance also had good ease of chip flow figures. No parameter should be used on its own to evaluate cutting fluid performance. The full scope of performance parameters should be evaluated before a decision to use a certain cutting fluid is made.

The limitations into an investigation of the chemistry involved are severe, as the conditions that prevail in the contact-zone, (the region of maximum shear-rate and therefore the hottest region in the cutting process) are very harsh and the cutting fluids used are organic compounds with additives. The harsh conditions cause thermal degradation and mechanical breakage of the carbon chains of the cutting fluid. The contact-zone is often a continuous phase as welding between the tool and the work-piece is so complete. The only way that a chemical may penetrate the boundary of this region is by means of small molecules in the gas phase, thereby slightly decreasing the contact-zone area and thus reducing shear which becomes evident in a decrease in the cutting force, the e.m.f. generated and the shorter radius of the chip that is produced by the machining process.

The electronegativity and population density of the electronegative atoms of the cutting fluid seem to play a role in the cutting performance of the cutting fluids. They serve to weaken the metallic bond in the vicinity of the cutting edge. CCl_4 performed the best and has the highest population density of highly electronegative atoms of all the cutting fluids

that were tested. A weakening of the metallic bond will also lead to reduced cutting force and cutting temperature. The carbide or nitride coating on many tools helps to protect the tool against seizure to the chip, i.e. the welded zone is shorter, therefore lower cutting temperatures and consequently higher cutting speeds are possible with these tools than with HSS tools. The electronegative atoms of the cutting fluid compete as much or more for the electrons of the work-piece as the carbon and nitrogen atoms of the tool coating, because they have similar or higher electronegativity. The carbon and nitrogen atoms on the tool already hold onto the electrons of the substrate of the tool and therefore have a lower affinity for the electrons of the work-piece. The work-piece electrons are therefore attracted more by the cutting fluid and this demotes the affinity of the cutting tool for the work-piece material.

All tests were compared to dry machining for the same tool and work-material combination, and the temperature from the tool/work-piece thermocouple and the cutting force were monitored for different cutting fluids. The significant change in cutting force and temperature are useful in determining when the built-up edge forms and from this it is seen that some cutting fluids can delay the formation of the built-up edge for longer. The temperature and the distance cut at which the built-up edge forms are an indication of the ability of the cutting fluids ability to prevent metal-to-metal seizure.

When using limited volume lubrication for metal cutting it is important that the correct cutting fluid is found for the tool and work-piece combination of metals, as this influences the success of the metal cutting operation.

Metal cutting is an extremely complex operation. There are many parameters that play a role, and by also quantifying parameters that are not normally measured in an industrial operation it becomes possible to gain more insight on the efficiency of various cutting fluids. Test work in the laboratory can save on a lot of downtime in the industry because cutting fluid evaluation can be done without interfering with the industrial cutting operation.

Limited volume lubrication has a lot of merit in metal cutting in that it is more environmentally friendly than conventional flood type lubrication for metal cutting, requires substantially less cutting fluid, can deliver the same performance or better than flood lubrication by increasing tool life and producing acceptable end finishes on the metal surfaces. It also has merit for producing good finished surfaces in that there is less chance that the finished work-piece surface will be blemished or stained by residual cutting fluid, because very small volumes of cutting fluid are used. This also helps to facilitate ease of chip recovery. As very limited volumes of cutting fluid are used and no recycling of cutting fluid occurs, maintenance of cutting fluids and disposal of used cutting fluids are not issues. All these positive attributes of limited volume lubrication help to promote production up-time.

10. Recommendations:

Now that a test method is available, that can distinguish between different types of cutting fluids, a lot of future work can be done.

All the experiments performed in this investigation took a mechanical approach towards experimentation for the acquisition of data for analysis of the cutting process, and they are definitely necessary for cutting fluid evaluation. More tests on the shaper should be performed, both for a cutting speed where the built-up edge does form **and** for a cutting speed where it does not form.

The cutting fluids should be divided up into the various chemical families and an investigation into the effects of chain length, polarity and steric hindrance of the molecules can be done.

As far as analysis of chemistry involved in metal cutting is concerned, an identification of the types of metal salts that form and of the atoms or molecules that occur on the underside of the chip and on the rake face of the tool can be made. The physical parameters that are measurable to verify good cutting performance have been identified, and an investigation into the type of metal salts and or atoms or molecules on the surfaces should be made. This can be done by MS, SEM or FTIR.

When using limited volume lubrication for metal cutting it is important that the correct cutting fluid is found for the tool and work-piece combination of metals, as this influences the success of the metal cutting operation, therefore limited volume lubrication should not be written off in a hurry as a technology that does not work. It is recommended that the correct cutting fluid is found.

Appendix A:

Miller Indices

(Nix, 2002)

5.2.1 Surface Structure of Metals

In most technological applications, metals are used either in a finely divided form (e.g. supported metal catalysts) or in a massive, polycrystalline form (e.g. electrodes, mechanical fabrications). At the microscopic level, most materials, with the notable exception of a few truly amorphous specimens, can be considered as a collection or aggregate of single crystal crystallites. The surface chemistry of the material as a whole is therefore crucially dependent upon the nature and type of surfaces exposed on these crystallites. *In principle*, therefore, the surface properties of any material may be understood if

1. the amount of each type of surface exposed is known, and
2. detailed knowledge of the properties of each and every type of surface plane is available.

(This approach assumes that the possible influence of crystal defects and solid state interfaces on the surface chemistry may be neglected)
It is therefore vitally important to study different, well-defined surfaces independently. The most commonly employed technique is to prepare macroscopic (i.e. size ~ cm) single crystals of metals and then to deliberately cut them in a way which exposes a large area of the specific surface of interest.

Most metals only exist in one bulk structural form - the most common metallic crystal structures being:

bcc	**Body-centred cubic**
fcc	**Face-centred cubic**
hcp	**Hexagonal close packed**

For each of these crystal systems, there are in principle an infinite number of possible surfaces which can be exposed. In practice, however, only a limited number of planes (predominantly the so-called "low-index" surfaces) are found to exist in any significant amount and attention is thus focussed on these surfaces. Furthermore, it is possible to predict the ideal atomic arrangement at a given surface of a particular metal by considering how the bulk structure is intersected by the surface. Firstly, however, look in detail at the bulk crystal structures.

I. The *hcp* and *fcc* structures

The *hcp* and *fcc* structures are closely related: they are both based upon stacking layers of atoms, where the atoms are arranged in a close-packed hexagonal manner within the individual layer.

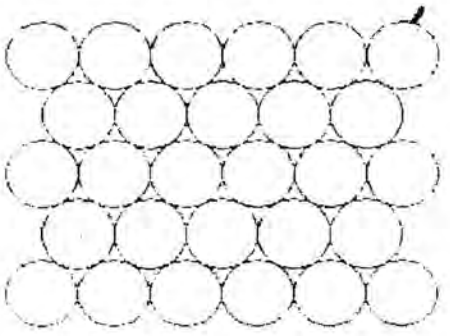

Figure A1. First layer of hcp and fcc structures

The atoms of the next layer of the structure will preferentially sit in some of the hollows in the first layer - this gives the closest approach of atoms in the two layers.

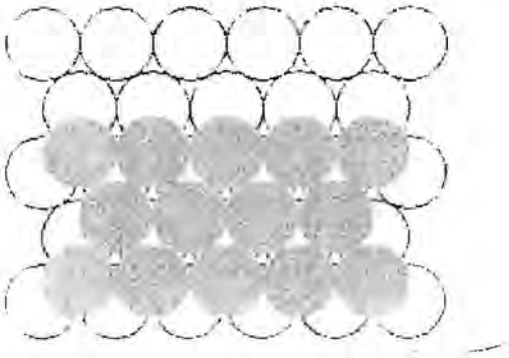

Figure A2. Second layer atoms of hcp and fcc structures

When it comes to deciding where the next layer of atoms should be positioned there are two choices - these differ only in the relative positions of atoms in the 1st and 3rd layers.

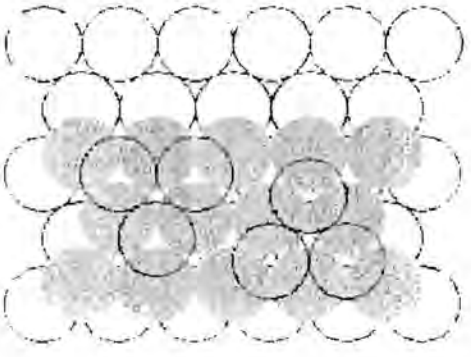

In the structure on the left the atoms of the 3rd layer sit directly above those in the 1st layer - this gives rise to the characteristic. ABABA. packing sequence of the hcp structure.
In the structure on the right of the last figure on the previous page the atoms of the 3rd layer are laterally offset from those in both the 1st and 2nd layers, and it is not until the 4th layer that the sequence begins to repeat. This is the ..ABCABC.. packing sequence of the fcc structure.
Because of their common origin, both of these structures share common features:

1. The atoms are close packed
2. Each atom has 12 nearest neighbours (i.e. CN = 12)

(a) *fcc* structure

Although it is not immediately obvious, the ..ABCABC.. packing sequence of the *fcc* structure gives rise to a three-dimensional structure with cubic symmetry (hence the name !).

fcc structure

Figure A3. The fcc structure

It is the cubic unit cell that is commonly used to illustrate this structure - but the fact that the origin of the structure lies in the packing of layers of hexagonal symmetry should not be forgotten.

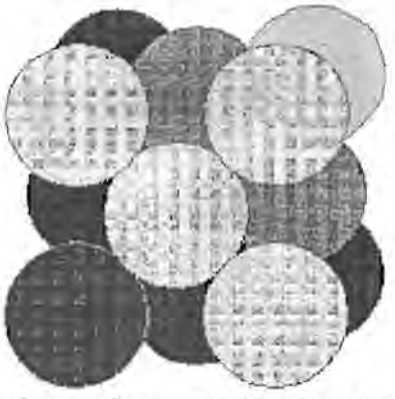

Figure A4. Different layers hexagonally close packed

The above diagram shows the atoms of one of the hexagonal close-packed layers highlighted in shades of grey (except for the top right corner atom), and the atoms of another highlighted in black.

(b) *hcp* structure

The ..ABABA.. packing sequence of the *hcp* structure gives rise to a three-dimensional unit cell structure whose symmetry is more immediately related to that of the hexagonally-close packed layers from which it is built, as illustrated in the diagram below.

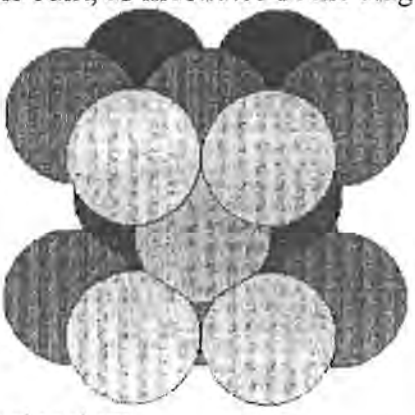

Figure A5. The hcp structure

II. The *bcc* structure

The *bcc* structure has very little in common with the *fcc* structure - except the cubic nature of the unit cell. Most importantly, it differs from the *hcp* and *fcc* structures in that it is not a close-packed structure.

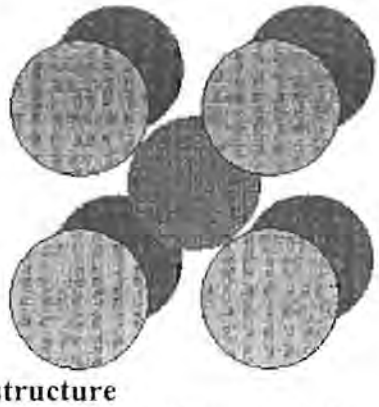

bcc structure

Figure A6. The bcc structure

The bulk co-ordination number of atoms in the bcc structure is 8

Rationale

Consider the atom at the centre of the unit cell as it is conventionally drawn. The nearest neighbours of this atom are those at the corners of the cube which are all equidistant from the central atom. There are eight such corner atoms so the CN of the central atom (and all atoms in the structure) is eight.

Whereto from here?

An ordered surface may be obtained by cutting the three-dimensional bulk structure of a solid along a particular plane to expose the underlying array of atoms. The way in which this plane intersects the three-dimensional structure is very important and is defined by using Miller Indices this notation is commonly used by both surface scientists and crystallographers since an *ideal*

surface of a particular orientation is nothing more than a lattice plane running through the 3D crystal with all the atoms removed from one side of the plane.
In order to see what surface atomic structures are formed on the various Miller index surfaces for each of the different crystal systems consider how the lattice planes bisect the three-dimensional atomic structure of the solid. As it might be expected, however, the various surfaces exhibit a wide range of:

1. Surface symmetry
2. Surface atom co-ordination , and most importantly this results in substantial differences in : 3) and 4)
3. Physical properties (electronic characteristics etc.), and
4. Surface chemical reactivity (catalytic activity, oxidation resistance etc.)

5.2.2 Surface Structure of fcc Metals

Many of the technologically most important metals possess the fcc structure: for example the catalytically important precious metals (Pt, Rh, Pd) all exhibit an fcc structure.
The low index faces of this system are the most commonly studied of surfaces: they exhibit a range of

1. **Surface symmetry**
2. **Surface atom co-ordination**
3. **Surface reactivity**

I. The fcc (100) surface

The (100) surface is that obtained by cutting the fcc metal parallel to the front surface of the fcc cubic unit cell - this exposes a surface (the atoms in the darkest colour) with an atomic arrangement of 4-fold symmetry

Figure A7. The fcc (100) surface

The diagram in figure A8 shows the conventional birds-eye view of the (100) surface - this is obtained by rotating the preceding diagram through 45° to give a view which emphasises the 4-fold symmetry of the surface layer atoms.

Figure A8. Birds-eye view of the fcc(100) surface
The tops of the second layer of atoms are just visible through the holes in the first layer, but would not be accessible to molecules arriving from the gas phase. The co-ordination number of the atoms on the surface is 8.

There are several other points worthy of note :

1. All the surface atoms are equivalent
2. The surface is relatively smooth at the atomic scale
3. The surface offers various adsorption sites for molecules which have different local symmetries and lead to different co-ordination numbers :
    - On-top sites (CN=1)
    - Bridging sites, between two atoms (CN=2)
    - Hollow sites, between four atoms (CN=4)

(In the above context, the CN is taken to be the number of surface metal atoms to which the adsorbed species would be directly bonded)

II. The fcc(110) surface

fcc unit cell
(110) face

Figure A9. The fcc (110) surface
The (110) surface is obtained by cutting the fcc unit cell in a manner that intersects the x and y axes but not the z-axis - this exposes a surface with an atomic arrangement of 2-fold symmetry. The next diagram shows the conventional birds-eye view of the (110) surface - emphasising the rectangular symmetry of the surface layer atoms. The diagram has been rotated such that the rows of atoms in the first atomic layer now run vertically, rather than horizontally as in the previous diagram.

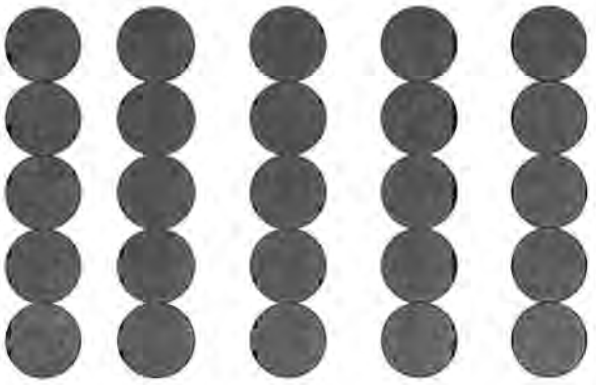

Figure A10. Atoms in topmost layer

It is clear from this view that the atoms of the topmost layer are much less closely packed than on the (100) surface - in one direction (along the rows) the atoms are in contact i.e. the distance between atoms is equal to twice the metallic (atomic) radius, but in the orthogonal direction there is a substantial gap between the rows.

This means that the atoms in the underlying second layer are also, to some extent, exposed at the surface

(110) surface plane
e.g. Cu(110)

Figure A11. The fcc (110) surface plane

The preceding diagram illustrates some of those second layer atoms, exposed at the bottom of the troughs.

In this case, the determination of co-ordination numbers requires a little more careful thought: one way to double-check the answer is to remember that the CN of atoms in the bulk of the fcc structure is 12, and then to subtract those which have been removed from above in forming the surface plane.

If one compares this co-ordination number (CN = 7) with that obtained for the (100) surface, it is worth noting that the surface atoms on a more open ("rougher") surface have a lower CN - this has important implications when it comes to the **chemical reactivity** of surfaces.

The fact that they are clearly exposed (visible) at the surface implies that they have a lower CN than they would in the bulk.

In summary, we can note that

1. All first layer surface atoms are equivalent, but second layer atoms are also exposed
2. The surface is atomically rough, and highly anisotropic
3. The surface offers a wide variety of possible adsorption sites, including :
    - On-top sites (CN=1)
    - Short bridging sites between two atoms in a single row (CN=2)
    - Long bridging sites between two atoms in adjacent rows (CN=2)
    - Higher CN sites (in the troughs)

III. The fcc (111) surface

The (111) surface is obtained by cutting the fcc metal in such a way that the surface plane intersects the x-, y- and z- axes at the same value - this exposes a surface with an atomic arrangement of 3-fold (apparently 6-fold, hexagonal) symmetry. This layer of surface atoms actually corresponds to one of the close-packed layers on which the fcc structure is based.

fcc unit cell
(111) face

Figure A12. The fcc unit cell (111) face

The diagram below shows the conventional birds-eye view of the (111) surface - emphasising the hexagonal packing of the surface layer atoms. Since this is the most efficient way of packing atoms within a single layer, they are said to be "close-packed".

(111) surface plane
e.g. Pt(111)

Figure A13. The fcc (111) surface plane

The following features are worth noting;

1. All surface atoms are equivalent and have a relatively high CN
2. The surface is almost smooth at the atomic scale

3. The surface offers the following adsorption :
    - On-top sites (CN=1)
    - Bridging sites, between two atoms (CN=2)
    - Hollow sites, between three atoms (CN=3)

IV. How do these surfaces intersect in irregular-shaped samples?
Flat surfaces of single crystal samples correspond to a single Miller Index plane and it was seen that, each individual surface has a well-defined atomic structure. It is these flat surfaces that are used in most surface science investigations, but it is worth a brief aside to consider what type of surfaces exist for an irregular shaped sample (but one that is still based on a single crystal). Such samples can exhibit facets corresponding to a range of different Miller Index planes.

SUMMARY
Depending upon how an fcc single crystal is cleaved or cut, flat surfaces of macroscopic dimensions which exhibit a wide range of structural characteristics may be produced.
The single crystal surfaces discussed here ((100), (110) & (111)) represent only the most frequently studied surface planes of the fcc system - however, they are also the most commonly occurring surfaces on such metals and the knowledge gained from studies on this limited selection of surfaces goes a long way in propagating the development of our understanding of the surface chemistry of these metals.

5.2.3 Surface Structure of hcp Metals

This important class of metallic structures includes metals such as Co, Zn, Ti & Ru.
The Miller Index notation used to describe the orientation of surface planes for all crystallographic systems is slightly more complex in this case since the crystal structure does not lend itself to description using a standard Cartesian set of axes- instead the notation is based upon three axes at 120 degrees in the close-packed plane, and one axis (the c-axis) perpendicular to these planes. This leads to a four-digit index structure; however, since the third of these is redundant it is sometimes left out!

I. The hcp (0001) surface
This is the most straightforward of the hcp surfaces since it corresponds to a surface plane which intersects only the c-axis, being coplanar with the other 3 axes i.e. it corresponds to the close packed planes of hexagonally arranged atoms that form the basis of the structure. It is also sometimes referred to as the (001) surface.

(0001) surface plane
e.g. Ru(0001)

Figure A14.The hcp (0001) surface plane

This conventional plan view of the (0001) surface shows the hexagonal packing of the surface layer atoms. This is very similar to the fcc(111) surface.

We can summarise the characteristics of this surface by noting that:

1. All the surface atoms are equivalent and have CN=9
2. The surface is almost smooth at the atomic scale
3. The surface presents adsorption sites which are locally :
    - On-top sites (CN=1)
    - Bridging sites, between two atoms (CN=2)
    - Hollow sites, between three atoms (CN=3)

5.2.4 Surface Structure of bcc Metals

A number of important metals (e.g. Fe, W, Mo) have the bcc structure. As a result of the low packing density of the bulk structure, the surfaces also tend to be of a rather open nature with surface atoms often exhibiting rather low co-ordination numbers.

I. The bcc (100) surface

Figure A15. The bcc unit cell (100) face

bcc unit cell
(100) face

The (100) surface is obtained by cutting the metal parallel to the front surface of the bcc cubic unit cell - this exposes a relatively open surface with an atomic arrangement of 4-fold symmetry. The diagram below shows a plan view of this (100) surface - the atoms of the second layer (shown on left) are clearly visible, although probably inaccessible to any gas phase molecules other than smaller atoms or molecules like N_2, H_2 or ions that result during cutting.

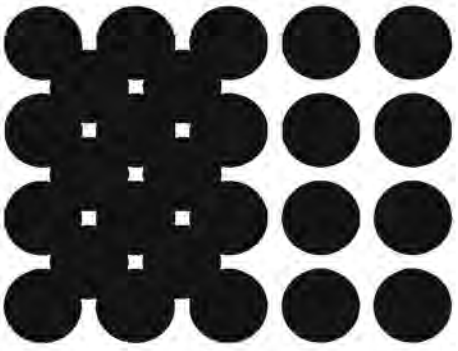

bcc (100) surface plane
e.g. Fe(100)

Figure A16. The bcc(100) surface plane

The co-ordination number for the surface atoms is 4. The nearest neighbours are at a distance of 0.87a.

The CN of metal atoms in the bulk of the solid is 8 for a bcc metal and the second layer of atoms clearly have 4 nearest neighbours in the 1st layer and another 4 in the 3rd layer.

II. The bcc (110) surface

The (110) surface is obtained by cutting the metal in a manner that intersects the x and y axes but creates a surface parallel to the z-axis - this exposes a surface that has a higher atom density than the (100) surface.

bcc unit cell
(110) face

Figure A17. The bcc unit cell (110) face

Figure A18 shows a plan view of the (110) surface - the atoms in the surface layer strictly form an array of rectangular symmetry, but the surface layer co-ordination of an individual atom is quite close to hexagonal.

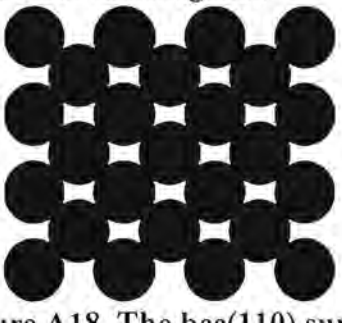

bcc(110) surface plane
e.g. Fe(110)

Figure A18. The bcc(110) surface plane

The co-ordination number of the surface layer of atoms is 6. Think in 3 dimensions.

Rationale

Each surface atom has four nearest neighbours in the 1st layer (the remaining two "near-neighbours" in this surface layer being at a slightly greater distance), but there are also two nearest neighbours in the layer immediately below.

III. The bcc (111) surface

The (111) surface of bcc metals is similar to the (111) face of fcc metals only in that it exhibits a surface atomic arrangement exhibiting 3-fold symmetry - in other respects it is very different.

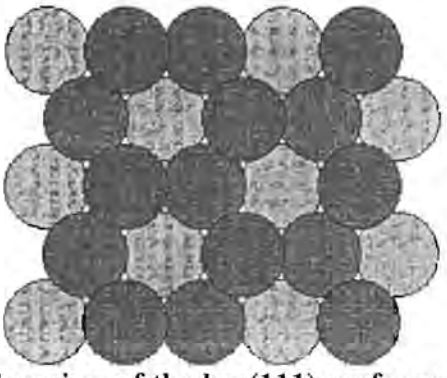

Top View:
bcc(111) surface plane
e.g. Fe(111)

Figure A19. Top view of the bcc(111) surface plane

In particular it is a very much more open surface with atoms in both the second and third layers clearly visible when the surface is viewed from above. This open structure is also clearly evident when the surface is viewed in cross-section as shown in figure A20 in which atoms of the various layers have been annotated.

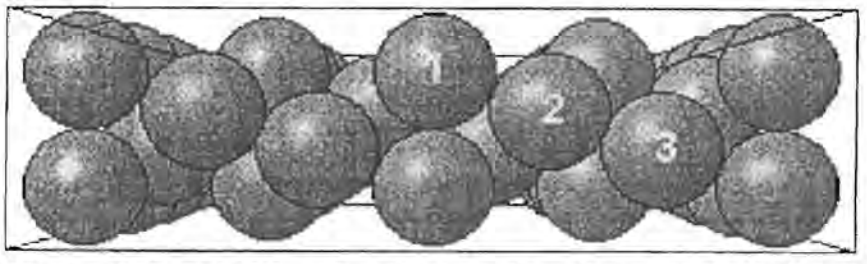

Figure A20. Side View: bcc(111) surface plane e.g. Fe(111)

Appendix B:

The aluminium alloys are given a letter designation to indicate the processes that they have been through prior to resulting in the plate, sheet or extrusion.
The designations are as follows: (Follette, 1980)

- O - annealed wrought aluminium
- F - as cast or as fabricated
- H - cold worked
- T - heat treated

The T group indicates heat treated aluminium alloys and the Table A2.1 indicates the type of heat treatment.

T2	Annealed for ductility and dimensional stability (Cast only)
T3	Heat treated and cold worked. (Wrought only)
T4	Heat treated and naturally aged to stability. (Wrought or cast)
T5	Artificially aged. (Wrought or cast)
T6	Heat treated and artificially aged. (Wrought or cast)
T7	Heat treated and stabilised. (Cast only)
T8	Heat treated, cold worked, and artificially aged. (Wrought only)
T9	Heat treated, artificially aged, and cold worked. (Wrought only)
T10	Artificially aged, and cold worked. (Wrought only)

Table A2.1 Type of heat treatments for aluminium alloys.

As the number increases the hardness increases.

Heat-Treatable Al-Si-Mg Wrought Alloy 6082

Chemical Composition Limits (in %)

Cu	Mg	Si	Fe	Mn	Zn	Ti	Cr	Other elements Each	Other elements Total
0,1	0,6 1,2	0,7 1,3	0,5	0,4 1,0	0,2	0,1	0,25	0,05	0,15

Outstanding Characteristics:

Medium strength alloy with good corrosion resistance.

Standard Commodities:

Plate; sheet; extrusions.

Typical Uses:

For stressed structural applications, such as bridges, cranes, roof trusses, transport applications. Beer barrels; milk churns. Bridle plates for man cages and ore skips.

Typical Physical Properties

Density	2,70	g/cm³
Modulus of Elasticity	70	GPa
Modulus of Rigidity	26,5	GPa
Melting Range	555–650	°C
Specific heat between 0–100 °C (273–373 K)	0,88	J/gK
Coefficient of linear expansion between 20–200 °C (293–473 K)	24×10^{-6}	/K
Thermal Conductivity at 100 °C (373 K)	180–189	W/mK
Resistivity at 20 °C (293 K)	$0{,}038 \times 10^{-8}$	Ω m

Other Characteristics

Corrosion Resistance	: Good
Weldability	: Good
Formability	: Good
Machinability	: Good
Anodizing	: Good
Brazeability	: Good

Mechanical Properties

Commodity and Temper	Gauge mm	0,2 % Proof Stress MPa	Ultimate Tensile Strength MPa	Elongation A_5 %	Brinell Hardness HB	Ultimate Shear Strength MPa
Sheet						
O	0,2–3,0	(60)	(125) 155	16 (30)	(32)	
T4	0,2–3,0	120 (200)	200 (250)	15 (18)	(70)	120 (155)
T6	0,2–3,0	255 (305)	295 (330)	8 (13)	(100)	175 (205)
Plate						
T4	up to 25	115 (185)	200 (230)	15 (22)	(60)	120 (160)
T6	up to 25	240 (280)	295 (325)	8 (10)	(95)	175 (205)
Extrusions						
O	up to 130		(170)	14		
F	up to 75		110	12		
T4	up to 75	120 (190)	190 (275)	14 (18)		
T6	up to 20	255 (315)	295 (330)	7 (10)		
T6	20–75	270 (320)	310 (345)	7 (12)		
T3	up to 6	115	215	12		
T3	6–10	115	215	14		
T8	up to 6	255	310	7		

Heat Treatment

Solution Heat Treatment				Ageing	
Temper	Temperature °C	Time h	Quenching	Temperature °C	Time h
T6	520 ± 3		In water	175 ± 3	10

Annealing

Temperature °C	Time h	
340–360	2	To soften partially.
340–360	2*	To soften fully.

*Cool not faster than 15 °C/hour to 250 °C and withdraw from furnace.

Appendix C:

Experiment 1: Relationship between metal deformation and e.m.f.
Aim: To see whether an e.m.f. will be generated merely by the deformation of the metal crystal structure
Action: The shaper was set up to confirm whether there is a significant e.m.f. change in the e.m.f. signal that is observed when the tool work-piece junction is stressed:

- The tool is brought into contact with the work-piece so that it gently touches
- The computer data sampling is started and the load on the tool is gradually increased by manually feeding the work-piece against the tool. By doing this the tool-work-piece junction is stressed and the metal at the junction is gradually deformed.
- The sampled data is then analysed after the experiment is complete by checking if the e.m.f. changed when the junction was loaded.

Experiment 2: Calibration of thermocouple
Aim: To obtain data to calibrate the tool/workpiece thermocouple. This gives an indication of the temperatures that are attained when the aluminium is being cut.
The temperature is measured by using the dissimilar metal junction formed by the tool and the workpiece as a thermocouple. The e.m.f. that is generated at this junction is an indication of the temperature at the junction, i.e. the temperature is a function of the e.m.f.
Action:

- The workpiece is cast in light weight concrete
- The cast with the workpiece in it is clamped in the chuck on the shaper.
- A hole is drilled at both ends of the workpiece
- The tool is manually fed into the workpiece
- An RTD (resistance temperature device) is inserted in the hole closest to the point where the tool/workpiece junction is and an aluminium lead into the other. The RTD was very close to the junction i.e. 5mm.
- The cold junctions are kept at 23°C.
- The data sampling program on the computer is started and the workpiece is heated gradually with a blow torch.
- The computer writes both the RTD measured temperature and the e.m.f. that is generated at the junction on a file for later use for tool/workpiece thermocouple calibration.
- The blow torch is never closer than 40mm to the junction and the RTD.
- When the workpiece starts to melt heating is stopped and the workpiece is left to cool down.
- Plot the e.m.f. vs. temperature data and obtain the appropriate polynomial by regression by which the two variables are related.

Experiment 3: Calibration of strain gauge
Aim: To obtain data to calibrate the strain gauge.
Action:

- Clamp the tool on a robust flat metal surface so that the distance between the cutting edge and the last point of support of the tool is the same as it will be when cutting metal on the shaper.
- Tune the trimpot on the strain amplifier/signal amplifier so that the output is 0.000V for 0N load.
- Use a specially adapted hanger of known mass and hang it on the tool tip.
- Measure the voltage after it has been amplified by the signal amplifier and write down the load on the tool and the corresponding voltage.
- Repeat increasing the load and writing down the load and the corresponding voltage until five data points have been accumulated.
- The relationship between the load and the voltages observed is linear. Do linear regression and find it.
- Use the mathematical relationships determined in experiments 2 and 3 in the computer program to output the temperature and cutting force data directly to screen and to file.

Experiment 4: Cut characterisation
Aim: To obtain cutting force and temperature data for cutting metal when various cutting fluids are used.
Action:

- Mark the workpiece at the quarter-, half- and three quarter- way mark with permanent marking ink of different colours.
- Know the length of the cut that will be made and the rake face angle.
- Remember to check the reference points
- Keep all cutting parameters constant
- Use bi-directional restraint of chip flow, i.e. choose a feed on the shaper such that the material flow during chip formation is restrained from both sides and so that no cut will overlap with a previous cut.
- Change only the type of cutting fluid used in each experiment
- Make sure that the cutting fluid applicator applies cutting fluid to the tool before the tool is engaged into the workpiece.
- Make sure that the cutting fluid used is the cutting fluid used and does not have residual cutting fluid or cleaning solvent from the previous test in it. This may be ensured by letting the applicator spray for a while after changing cutting fluids.
- Make sure that the tool is clean, i.e. that it has no residual metal left on it or cutting fluid from a previous test.
- Set the tool on the shaper so that it has some time to travel freely before it starts cutting the metal.
- Activate the computer program for data sampling
- Switch on the lubricant applicator if cutting fluid is used.
- Switch on the shaper and once the cut is complete switch it and the lubricant applicator off again.

- Perform the dry cuts first. Then do the cuts for the different cutting fluids. Ten per cutting fluid should suffice.
- Do one cut at a time so that the chip can be collected without confusion between chips from different cuts.
- Store each chip with a reference to the file on which the cut data appears.
- Check that the chip masses are more or less the same, say 200mg. This way it is ensured that the depth of cut is constant.
- Plot the cutting force and temperature data from the tests and check for repeatability
- Next measure the length of the first quarter of the chip. The ratio of the original one quarter length to this quarter length is the mean chip thickness ratio
- Calculate and tabulate the shear plane angle and the chip strain
- Photograph the chips as a group for the different cutting fluids used.
- Visually inspect the underside of the chips and note the smooth fraction of the chip i.e. where no marked scratching or dulling of the underside surface appears.
- Do this for each chip series in each cutting fluid
- Calculate the average smooth fraction from this for each cutting fluid
- Tabulate the data
- Similarly as for the smooth fraction determine the average fraction to first break for the chips and compute the average distance to first break from this.
- Tabulate the data
- Choose a representative chip from each group and make SEM micrographs
- Observe and tabulate the deformation / flow-zone thickness
- Choose a chip from each group and mount it in thermoset resin
- Sand the mount down until the longitudinal lateral mid cross-section of the chip is exposed and polish this section to a high fineness.
- View the cross section under an optical microscope
- If nothing is observed in terms of metal deformation etch the chip with 0,5% HF in distilled water for 30 seconds
- Immediately after that flush the chip with alcohol and blow it dry
- View it again under the optical microscope and if still nothing is seen etch again for ten seconds
- Repeat the previous step until the metal deformation becomes clear.
- Make micrographs of the metal deformation in the chip.
- Compare the deformation with that observed on the SEM micrographs.
- Make micro-hardness measurements on the mounted chips close to the one quarter mark and set up chip hardness profiles for each mounted chip.
- Plot the hardness profiles and tabulate the flow-zone thickness that may be determined from these profiles and compare this to the results obtained from the micrographs
- Tabulate the average chip hardness, as calculated from the last three hardness measurements furthest away from the flow-zone.
- Compare all the accumulated data for all the cutting fluids.

Experiment 5: Surface roughness determination
Aim: To obtain surface roughness data for the different cutting fluids that were used.
Action:

- Be sure that the cutting fluid that is to be used is uncontaminated
- Make sure the tool is clean
- Use a fine feed
- Switch on the cutting fluid applicator and the shaper
- Perform metal cutting until a 15 mm width has been cut off the surface of the workpiece
- Mark this width on the work piece
- Bleed the cutting fluid applicator and change the cutting fluid and repeat the above exercise for each cutting fluid that is to be tested.
- Use a profilometer and determine the surface roughness at the beginning middle and end of each surface produced for the different cutting fluids that were used.
- Do these surface roughness measurements longitudinally and transversely
- When doing the longitudinal measurements be careful not to cross over ridges on the machined surface. These ridges can be avoided by taking many measurements. The lowest of these can be taken as measurements where no ridge was crossed.
- Tabulate the data and compare it for the different cutting fluids that were used.

Experiment 6: Micrographic observation and micro-hardness determination
It is suspected that the BUE phenomenon is present and therefore a lateral cross-section of the tool chip interface should be made. This should be etched with an appropriate solution such as hydrofluoric acid until the metal deformation can be seen clearly when it is examined under the optical microscope. This cross-section could also be examined under the scanning electron microscope (SEM). Micro-hardness tests should also be done on this chip to see what the effect of the built-up edge is on the hardness profile of the chip.

A non-etched chip sample can be analysed by SEM and/or MS for type of atoms that are present on the underside of the chip surface and in the chip after cutting when good cutting results are obtained. For an analysis in the chip a longitudinal cross section should be used.

Likewise examining the tool cutting edge and rake face by SEM, or mass ion spectroscopy (MIS) could give an indication of which atoms are present. This could give an indication of which atoms are desired when this examination occurs after pleasing results from a mechanical parameter investigation are obtained. If more detail is required FTIR (Fourier transform infrared) spectroscopy can be used for identification of the metal compounds that do form.

Experiment 7: Effect of cutting speed on built-up edge
Aim: To see whether the built-up edge forms later, i.e. at a greater length of cut when the cutting speed is increased and to see the effect of this on the cutting temperature and the cutting forces.
Action:
- Perform cuts and increase the cutting speed for each cut that is made
- Keep all other parameters constant
- Present the results graphically

Results and Discussion of Experiments for Preparation of Equipment

The main results for the cutting process investigation were presented in chapter 8 and are the results of experiments 4 -7.

As regards experiment 1 that was used to show the effect of stressing the tool on the e.m.f. that is generated it was found that the e.m.f. is unaffected. The tool was gradually statically loaded and no change in the e.m.f. was seen.

In experiment 2 that was done to calibrate the tool workpiece thermocouple the following was found: (see figure C.1). The lower of the two curves in figure C.1(b) is the same as the curve in figure C.1(a). The hysteresis that resulted is interesting. It is due to the temperature sensor being imbedded in the aluminium workpiece cooling at a slightly slower rate than the tool/workpiece junction that is situated on the surface of the workpiece. The actual temperature of the top curve should thus have been lower and the top curve would have been very much closer to the bottom curve.

Curve fitting on the data points resulted in a fourth order polynomial of very good fit over the temperature range 30°C to 523°C, i.e. 0.4 to 2.0V. The regression coefficient was 0.9903. For temperatures above 520°C the slope of the line between 1.5V and 1.9V was used to extrapolate the temperature for the measured e.m.f.
The alloy melts at 565±5°C as measured by the RTD.
In experiment 3 the relationship (eqn. C.1) between the cutting force and the microvolt signal was found as:

$$Cutting\ \ Force = 232.2/1000000 \cdot X \qquad \text{Eqn.C.1}$$

Where X is the microvolt signal.
For the method used see Appendix C, experiment 3.

Both the results of experiments 2 and 3 were applied to get results in experiment 4 and satisfactory results were obtained as is evident from the results presented for experiment 4. (See chapter 8)

a)

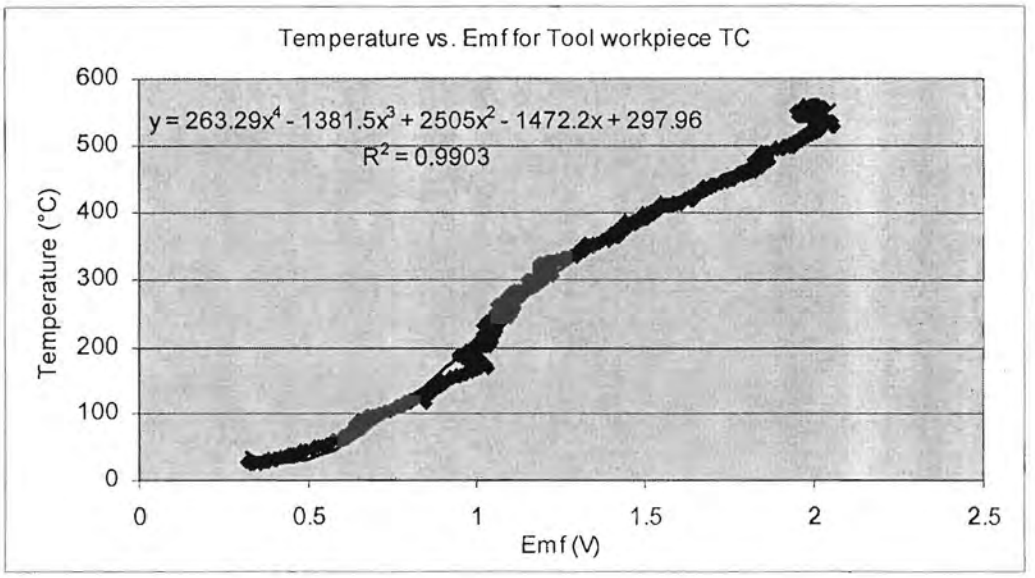

b)

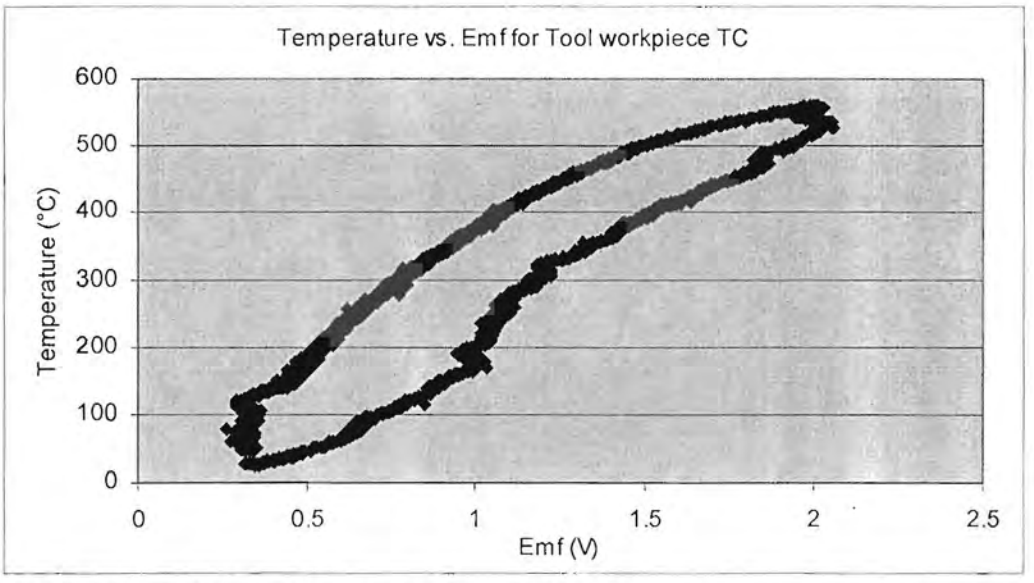

Figure C.1 Tool/workpiece thermocouple e.m.f. vs. Temperature response.

Cutting Force and Temperature: raw data	Cutting Force 5 point moving average : Sample and Dry	Cutting Temperature : Sample and Dry
C. force and Temperature for Test 1 of Carbon Tetra chloride 197mg	Compare C.forces CCl_4 T1 197 vs. DRY3 197 mg	Compare Temperature CCl_4 T1 197 vs DRY3 197 mg
CCl_4 T2 C. force and Temperature 197 mg	Compare C.forces CCl_4 T2 197 vs DRY3 197 mg	Compare Temperature CCl_4 T2 197 vs DRY3 197 mg
CCl_4 T3 C. force and Temperature 197 mg	Compare C.forces CCl_4 T3 197 vs DRY3 197 mg	Compare Temperature CCl_4 T3 197 vs DRY3 197 mg

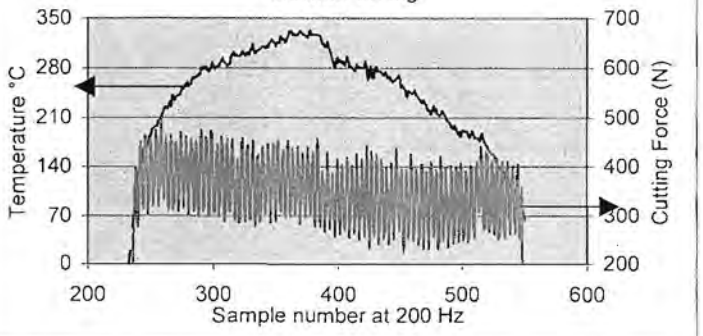

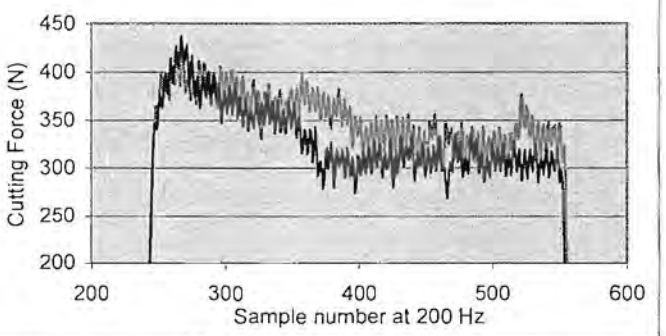

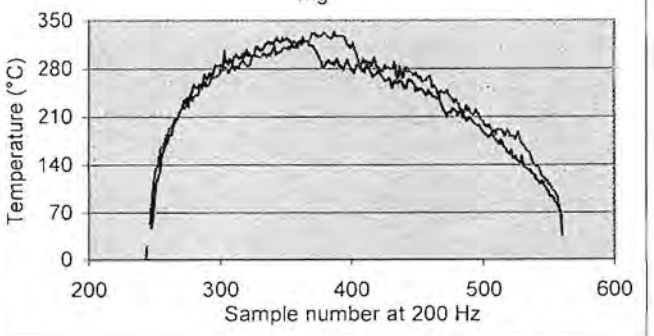

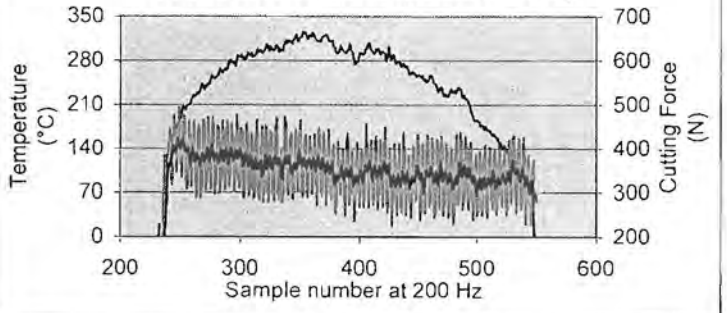

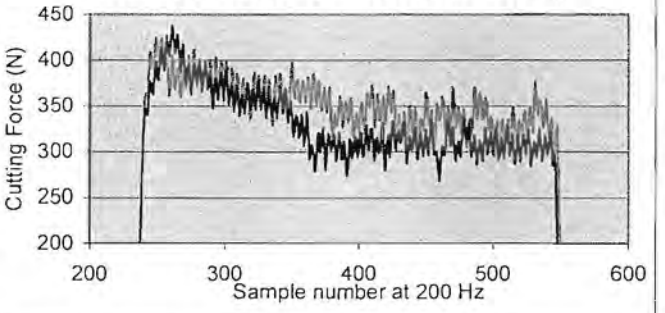

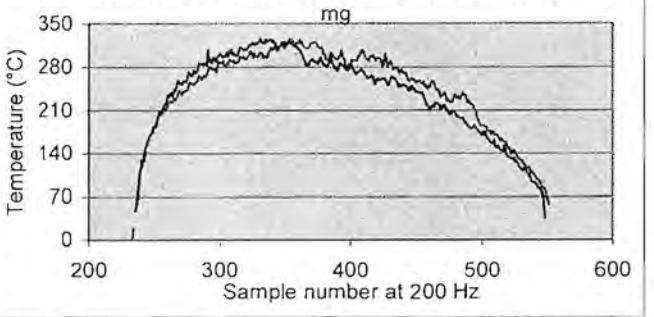

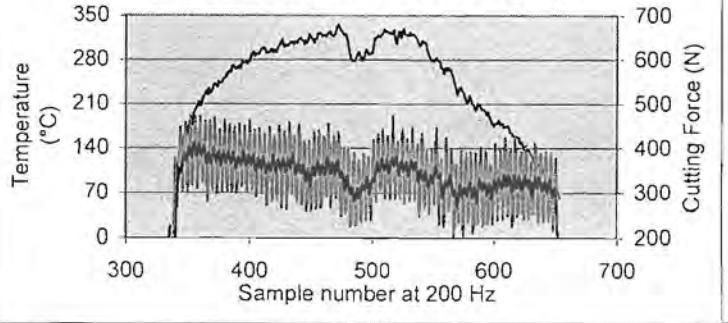

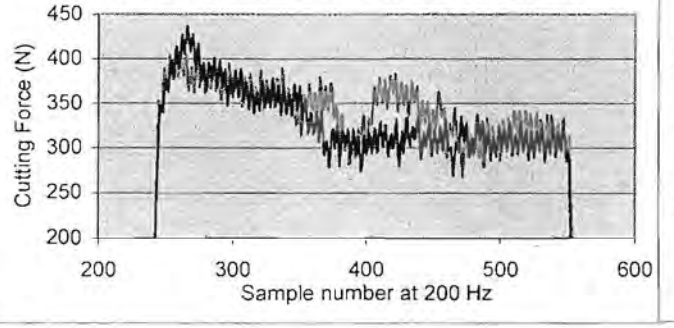

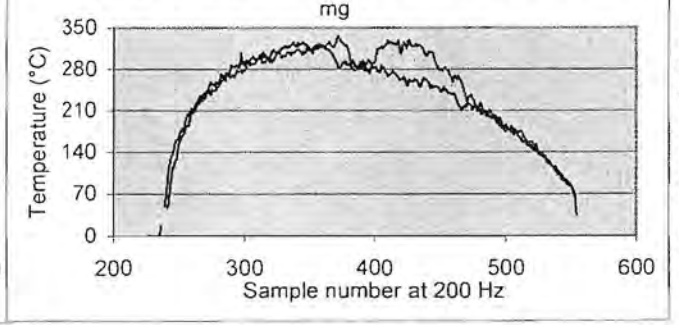

Appendix D

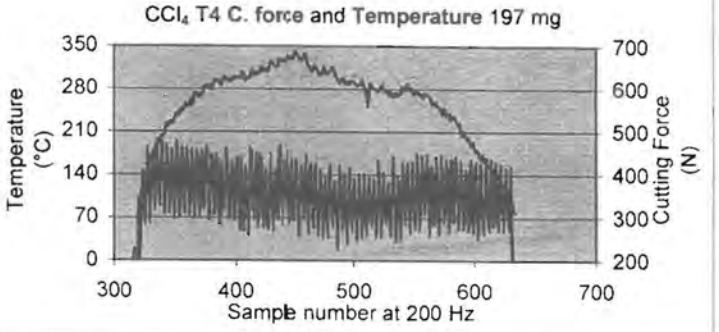
CCl4 T4 C. force and Temperature 197 mg
Temperature (°C)
Cutting Force (N)
Sample number at 200 Hz

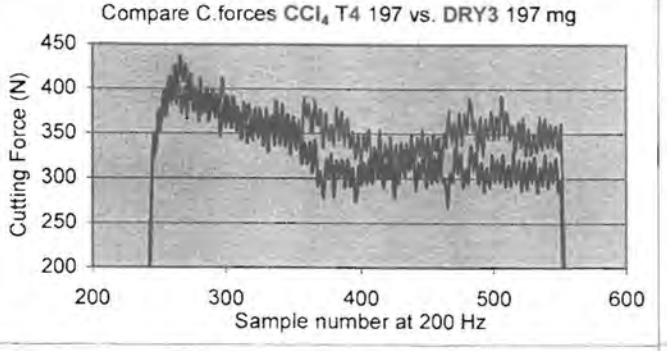
Compare C.forces CCl4 T4 197 vs. DRY3 197 mg
Cutting Force (N)
Sample number at 200 Hz

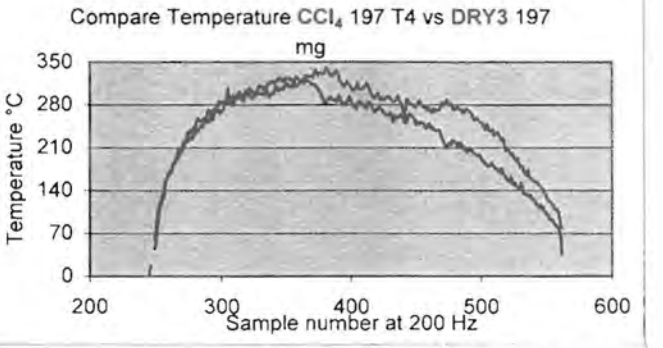
Compare Temperature CCl4 197 T4 vs DRY3 197 mg
Temperature °C
Sample number at 200 Hz

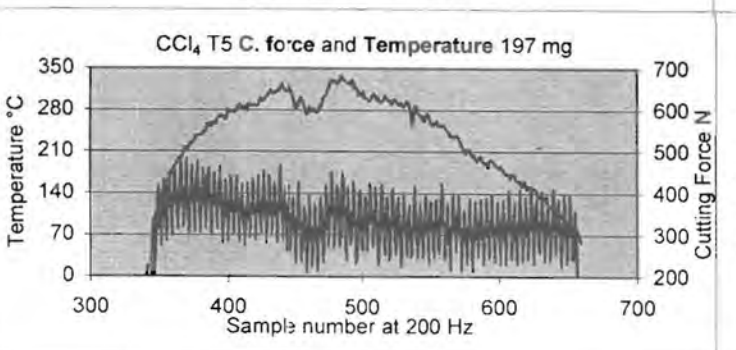
CCl4 T5 C. force and Temperature 197 mg
Temperature °C
Cutting Force N
Sample number at 200 Hz

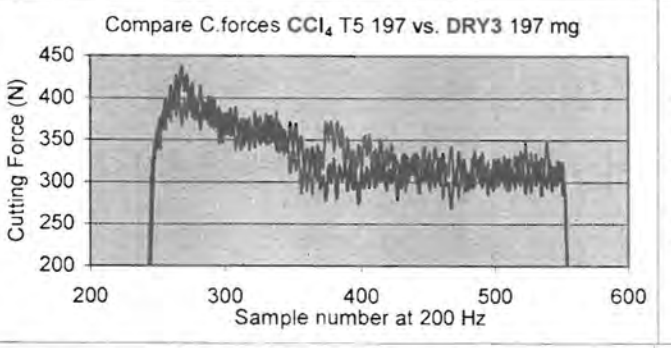
Compare C.forces CCl4 T5 197 vs. DRY3 197 mg
Cutting Force (N)
Sample number at 200 Hz

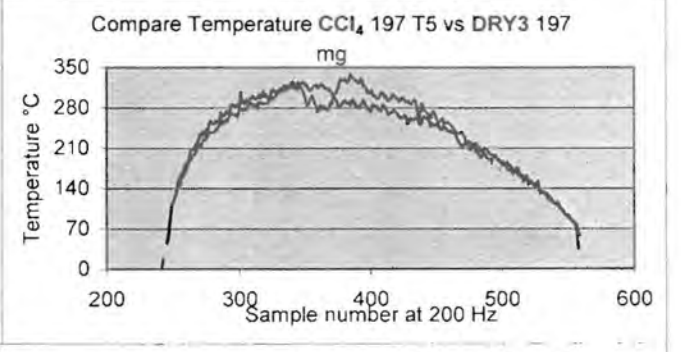
Compare Temperature CCl4 197 T5 vs DRY3 197 mg
Temperature °C
Sample number at 200 Hz

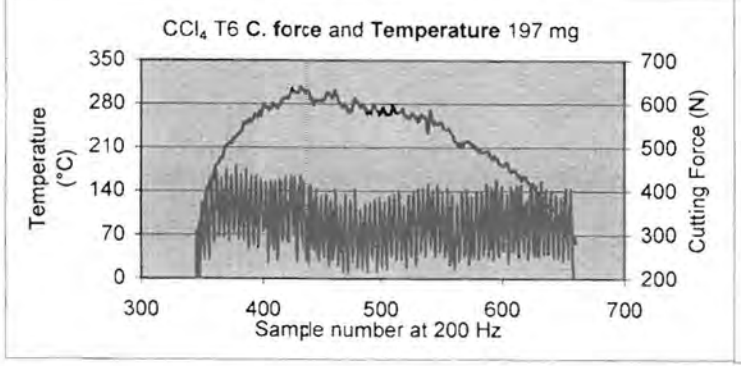
CCl4 T6 C. force and Temperature 197 mg
Temperature (°C)
Cutting Force (N)
Sample number at 200 Hz

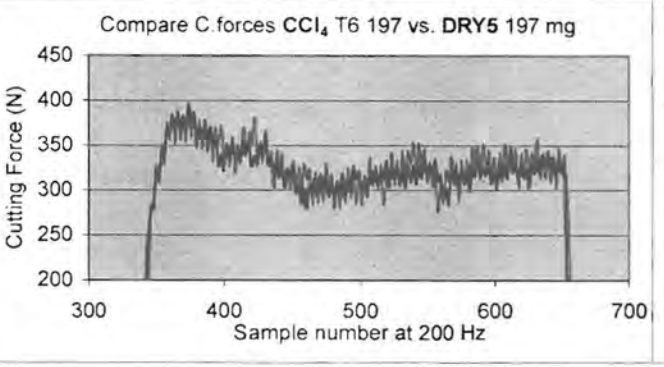
Compare C.forces CCl4 T6 197 vs. DRY5 197 mg
Cutting Force (N)
Sample number at 200 Hz

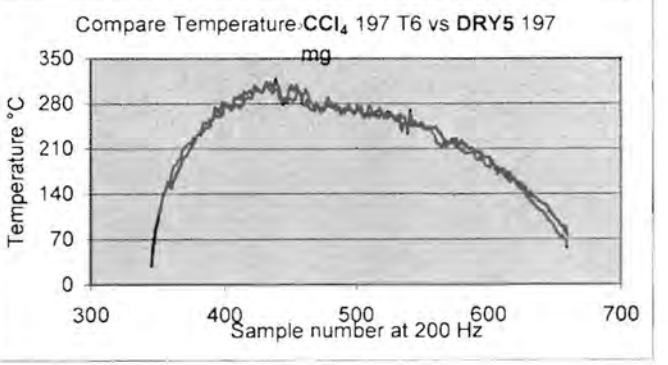
Compare Temperature CCl4 197 T6 vs DRY5 197 mg
Temperature °C
Sample number at 200 Hz

Cutting Force and Temperature: raw data	Cutting Force 5 point moving average : Sample and Dry	Cutting Temperature : Sample and Dry
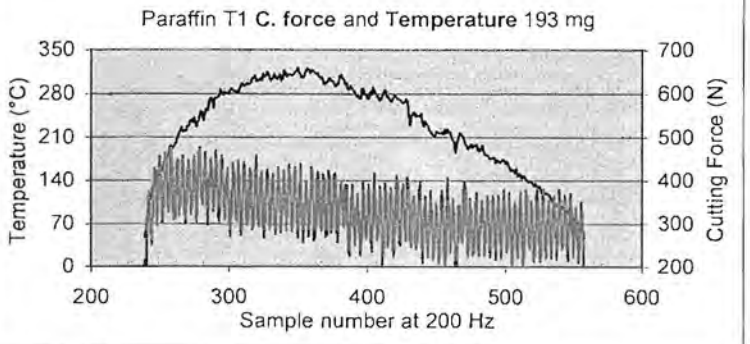	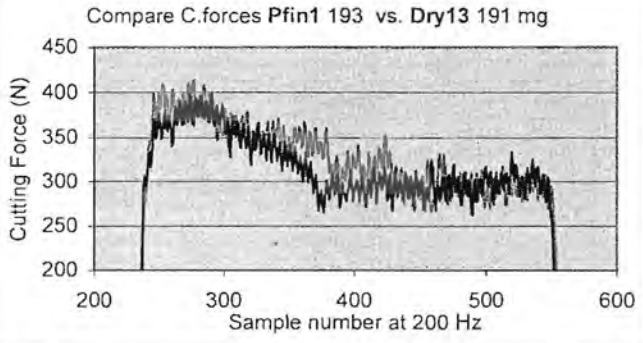	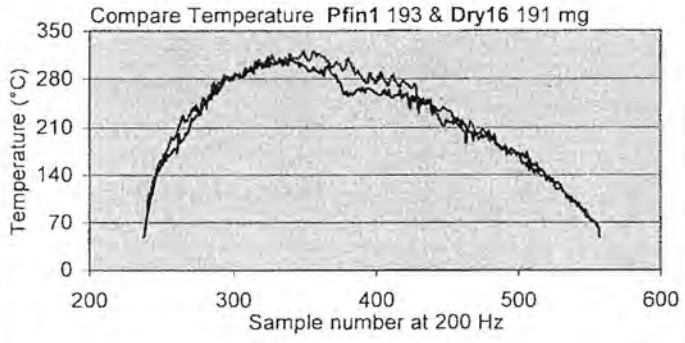
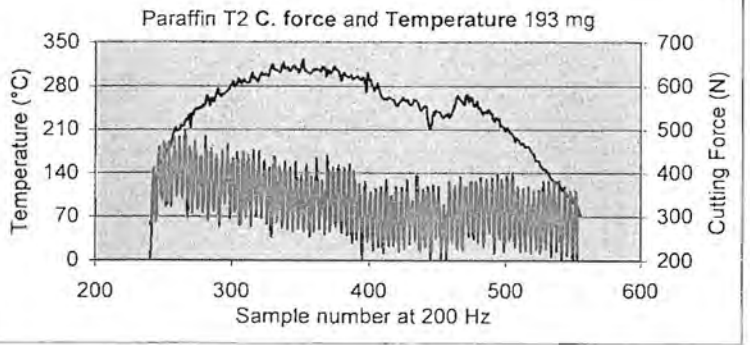	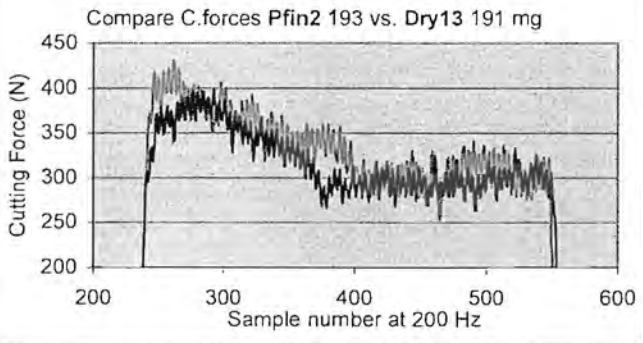	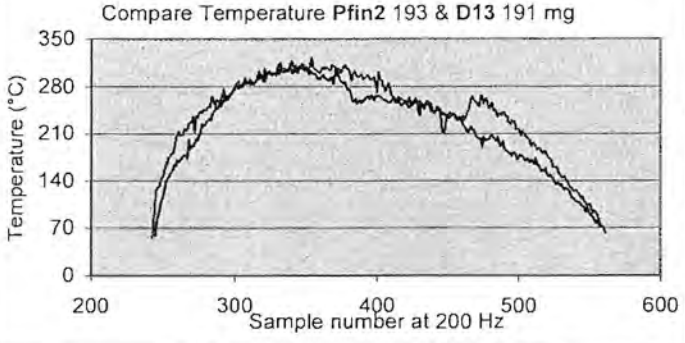
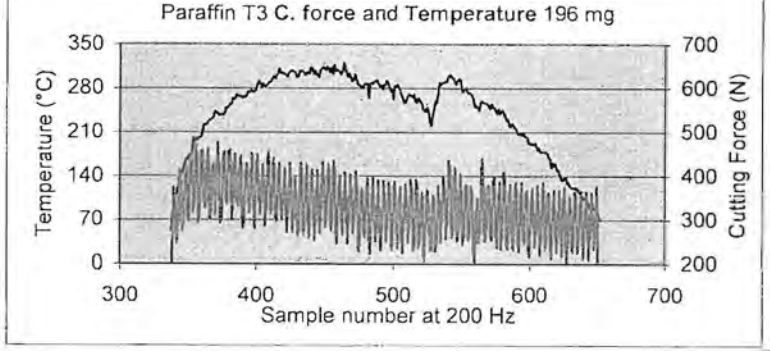	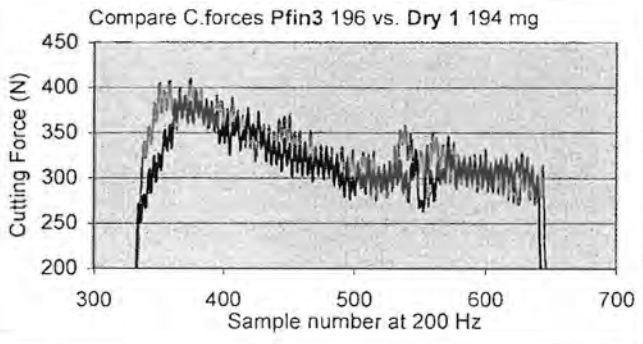	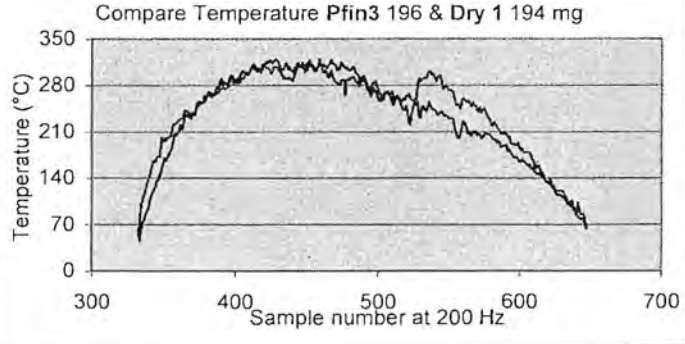

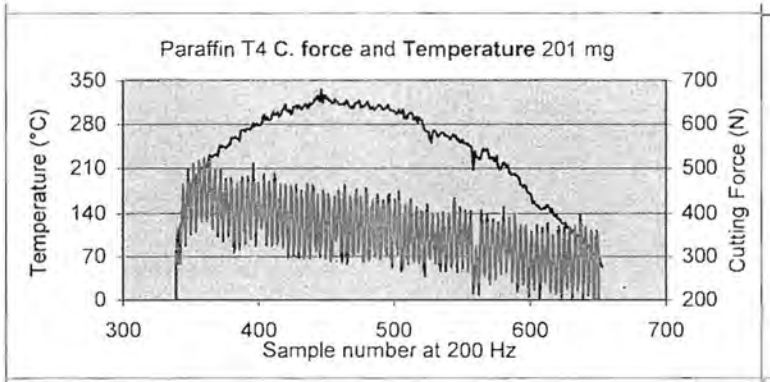
Paraffin T4 C. force and Temperature 201 mg
Temperature (°C)
Cutting Force (N)
Sample number at 200 Hz

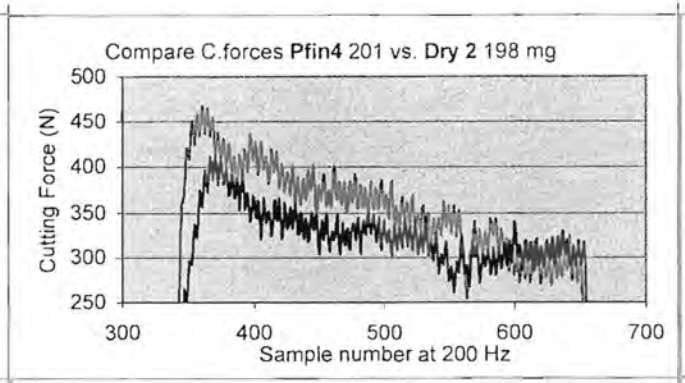
Compare C.forces Pfin4 201 vs. Dry 2 198 mg
Cutting Force (N)
Sample number at 200 Hz

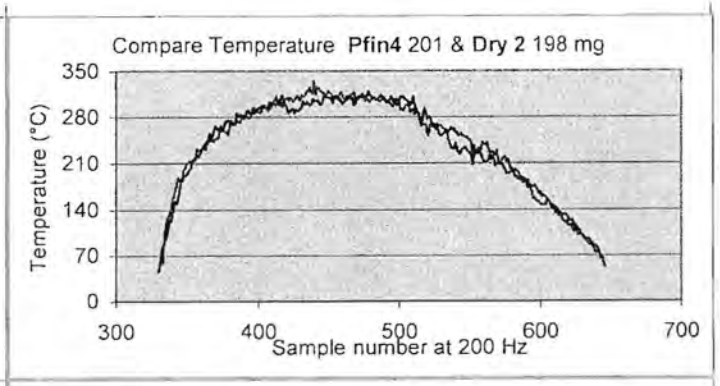
Compare Temperature Pfin4 201 & Dry 2 198 mg
Temperature (°C)
Sample number at 200 Hz

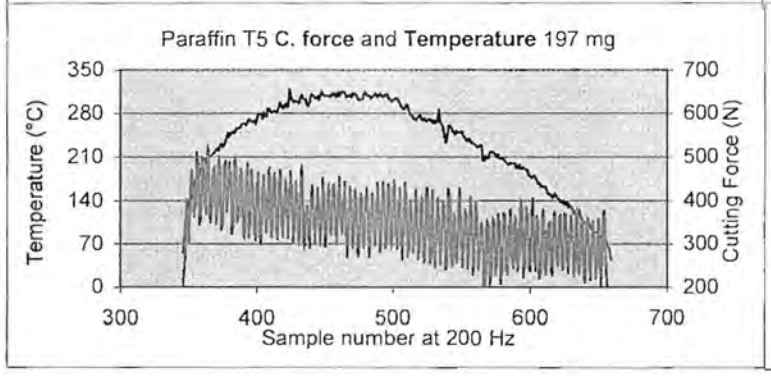
Paraffin T5 C. force and Temperature 197 mg
Temperature (°C)
Cutting Force (N)
Sample number at 200 Hz

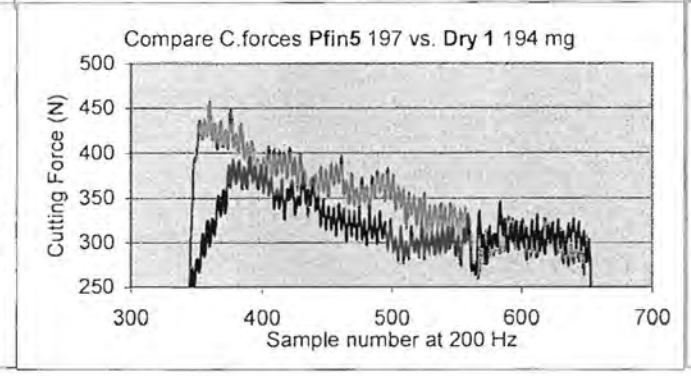
Compare C.forces Pfin5 197 vs. Dry 1 194 mg
Cutting Force (N)
Sample number at 200 Hz

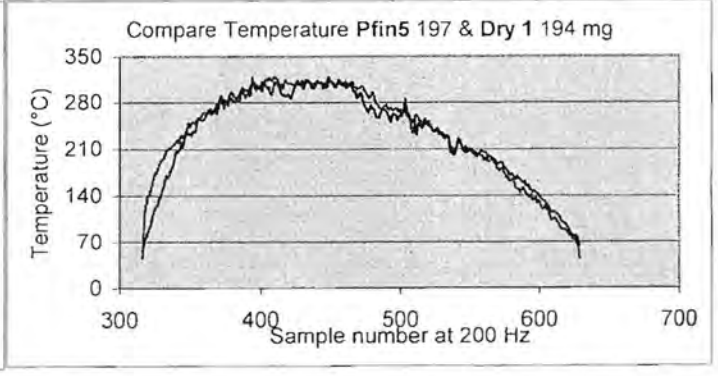
Compare Temperature Pfin5 197 & Dry 1 194 mg
Temperature (°C)
Sample number at 200 Hz

Cutting Force and Temperature: raw data	Cutting Force 5 point moving average : Sample and Dry	Cutting Temperature : Sample and Dry
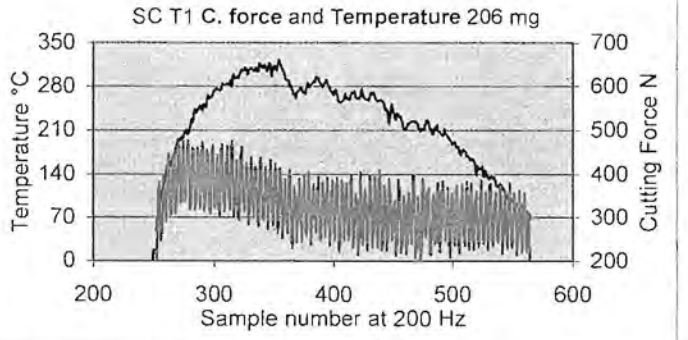	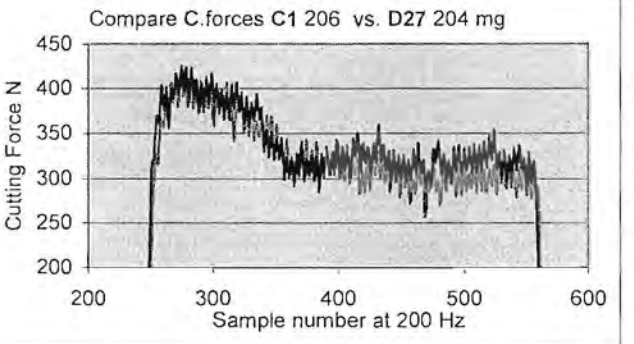	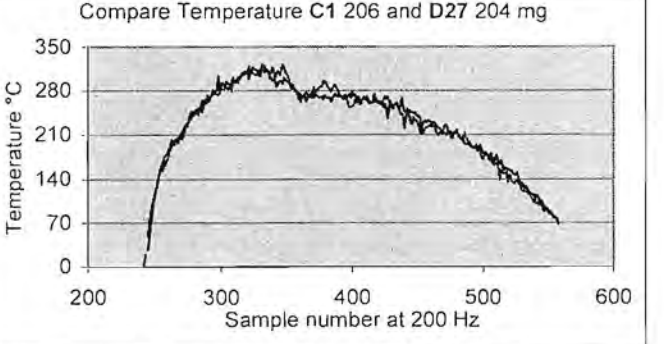
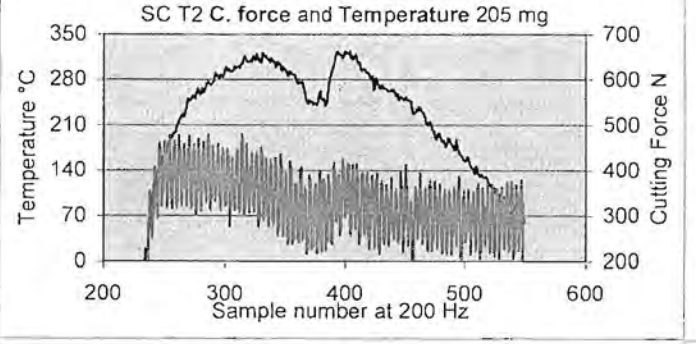	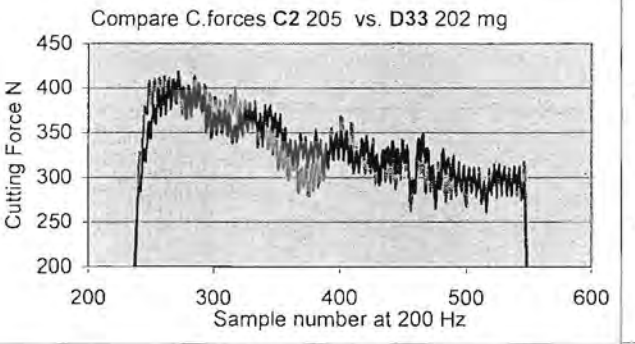	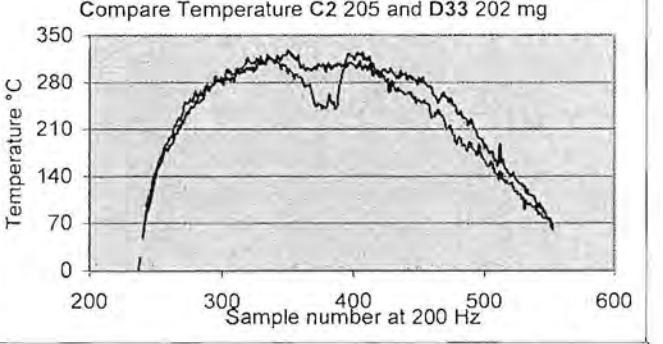
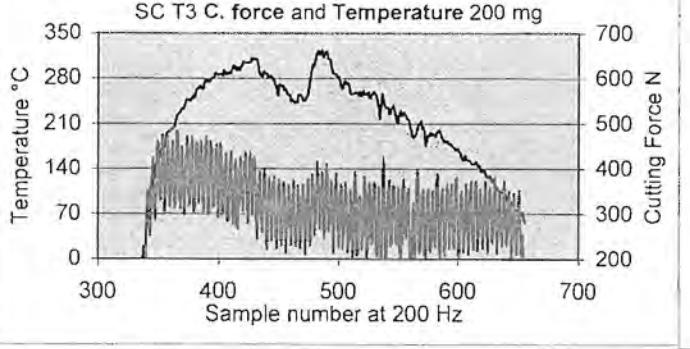	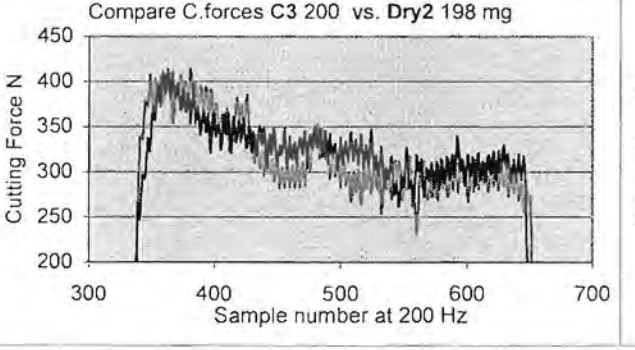	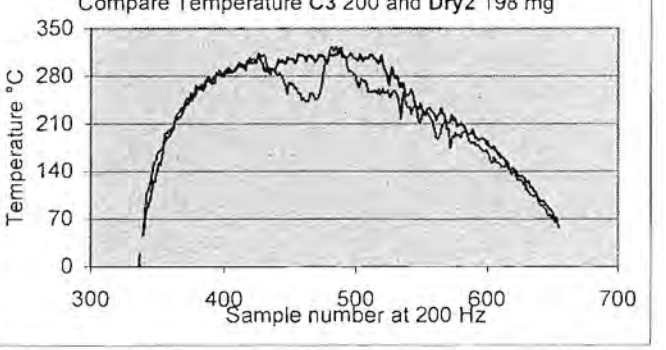

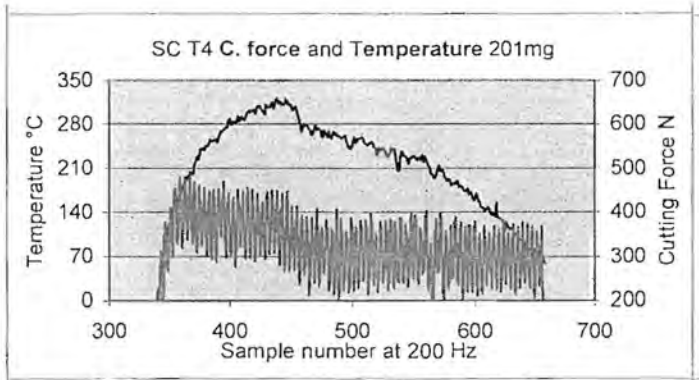
SC T4 C. force and Temperature 201mg
Temperature °C
Cutting Force N
Sample number at 200 Hz

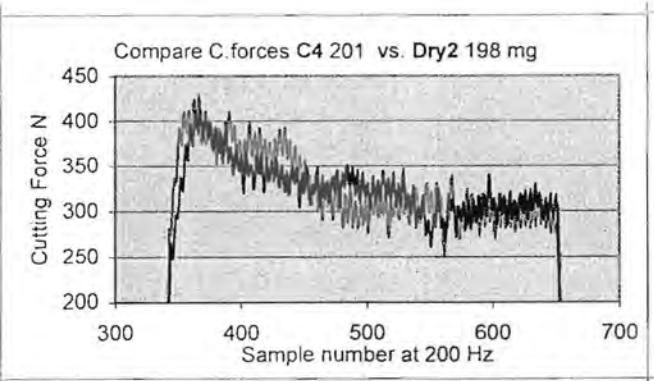
Compare C.forces C4 201 vs. Dry2 198 mg
Cutting Force N
Sample number at 200 Hz

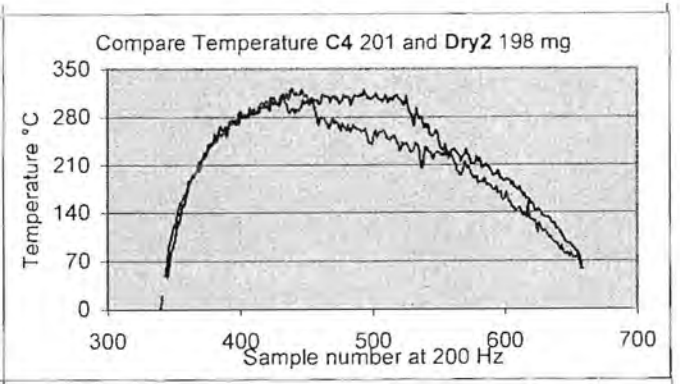
Compare Temperature C4 201 and Dry2 198 mg
Temperature °C
Sample number at 200 Hz

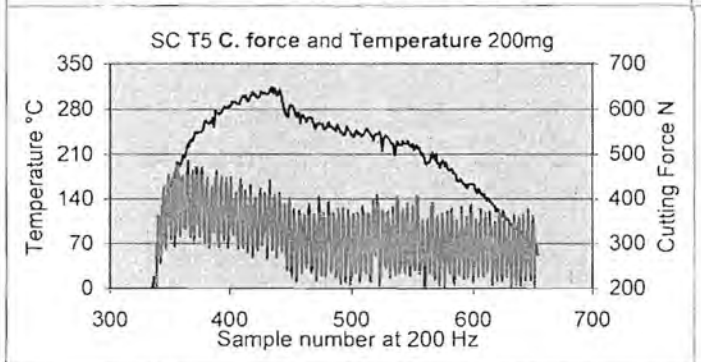
SC T5 C. force and Temperature 200mg
Temperature °C
Cutting Force N
Sample number at 200 Hz

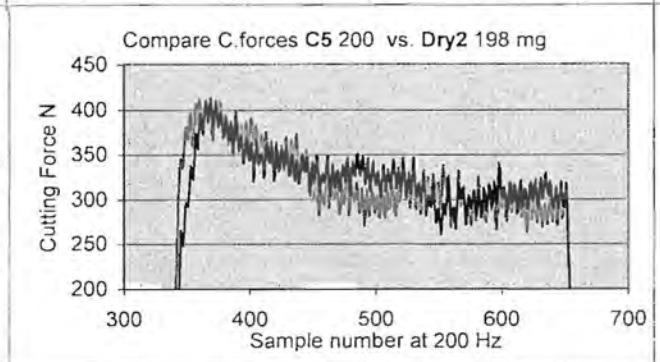
Compare C.forces C5 200 vs. Dry2 198 mg
Cutting Force N
Sample number at 200 Hz

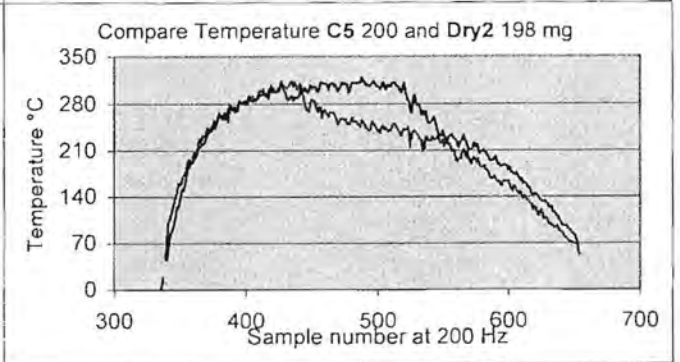
Compare Temperature C5 200 and Dry2 198 mg
Temperature °C
Sample number at 200 Hz

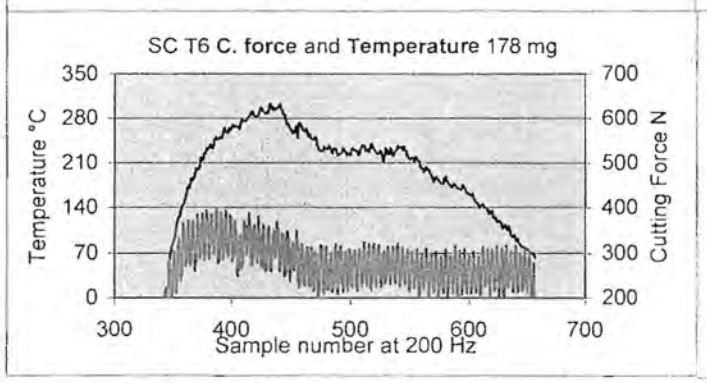
SC T6 C. force and Temperature 178 mg
Temperature °C
Cutting Force N
Sample number at 200 Hz

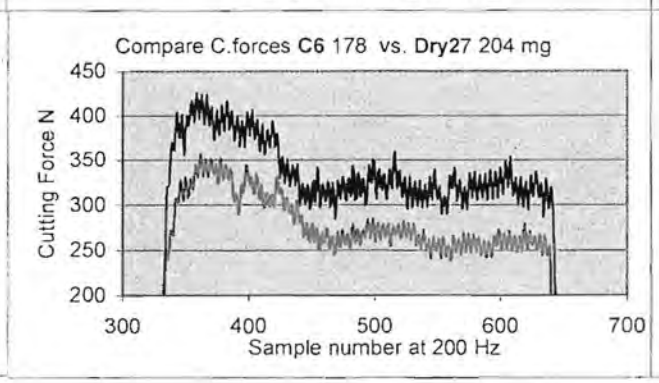
Compare C.forces C6 178 vs. Dry27 204 mg
Cutting Force N
Sample number at 200 Hz

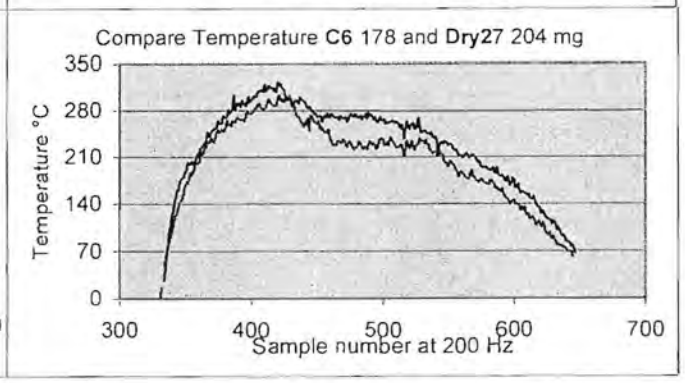
Compare Temperature C6 178 and Dry27 204 mg
Temperature °C
Sample number at 200 Hz

Cutting Force and Temperature: raw data	Cutting Force 3 point moving average : Sample and Dry	Cutting Temperature : Sample and Dry

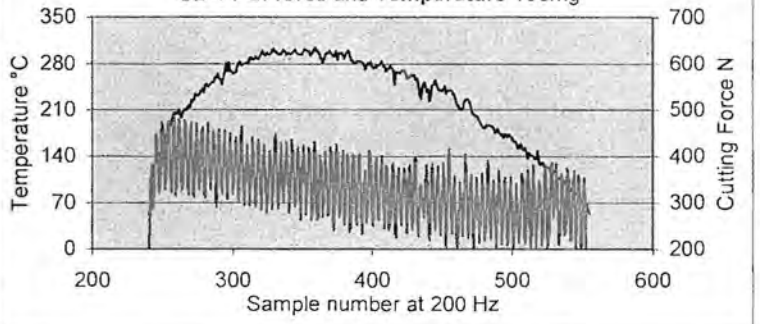

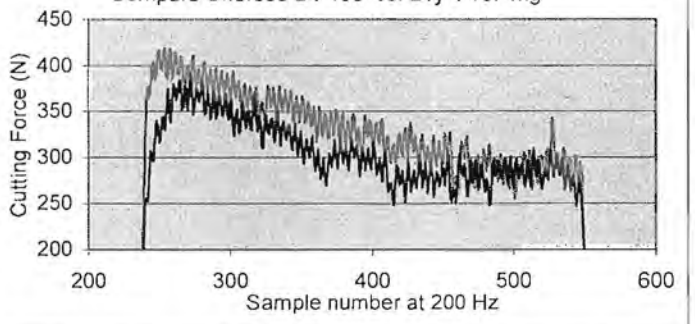

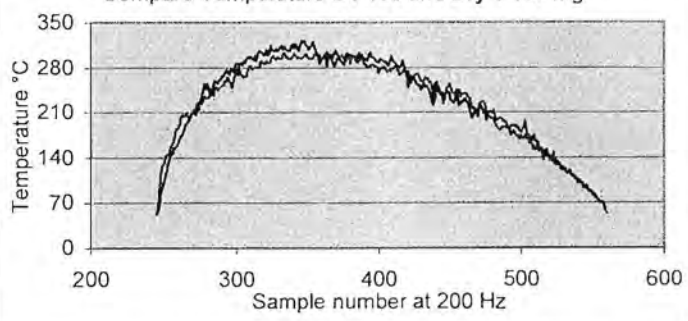

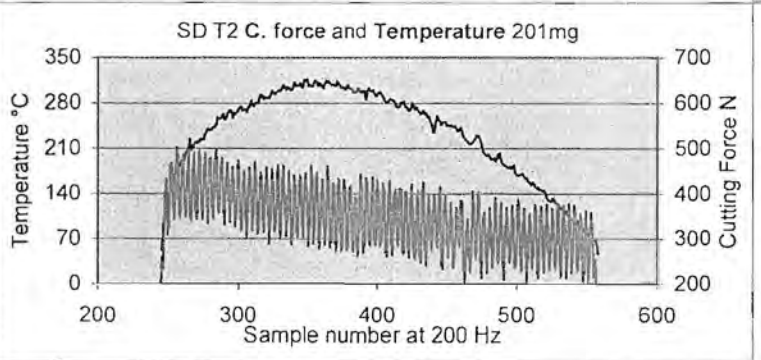

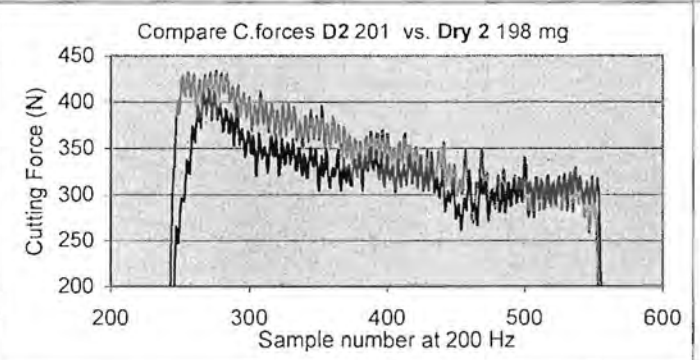

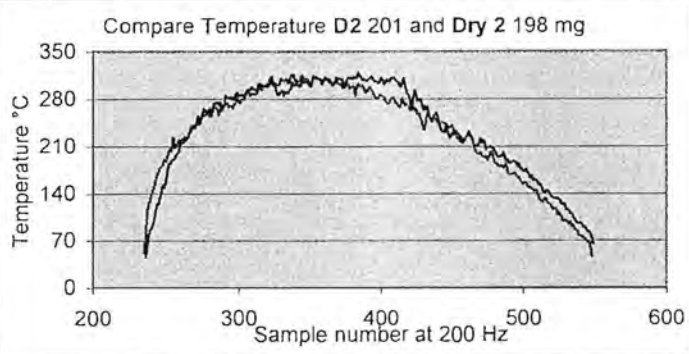

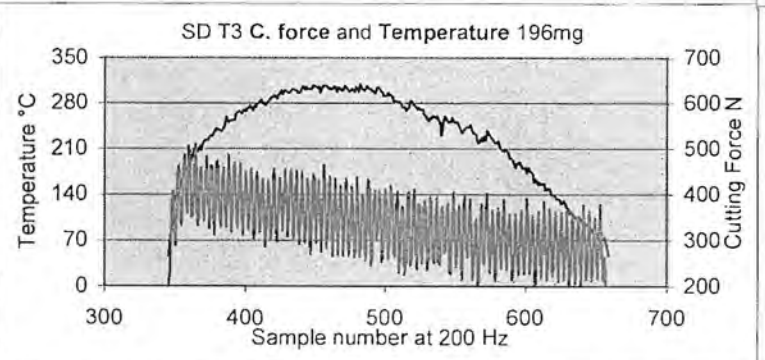

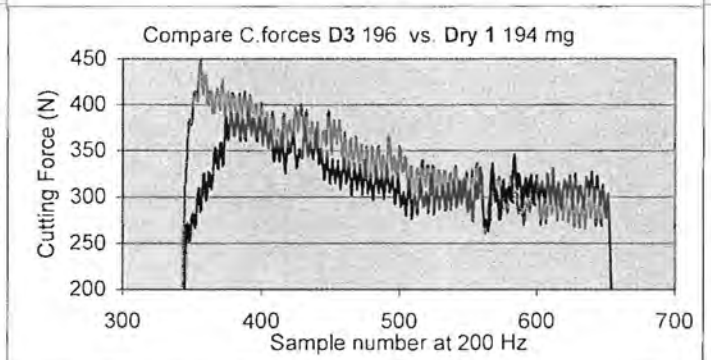

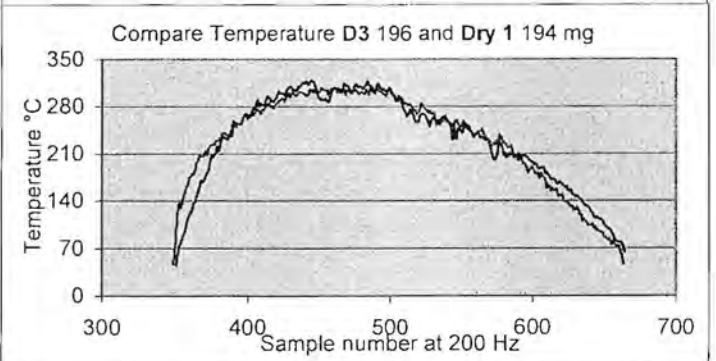

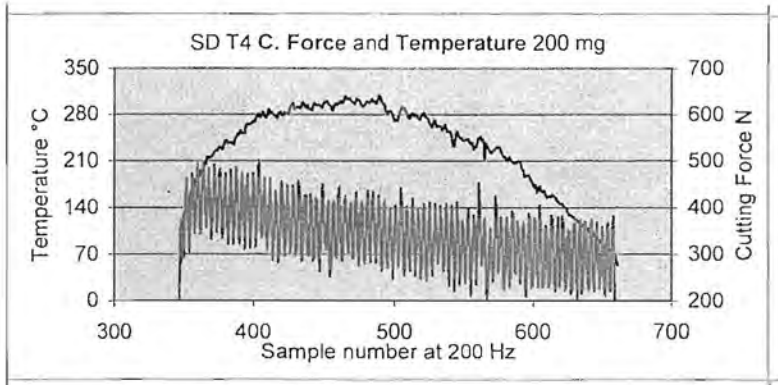

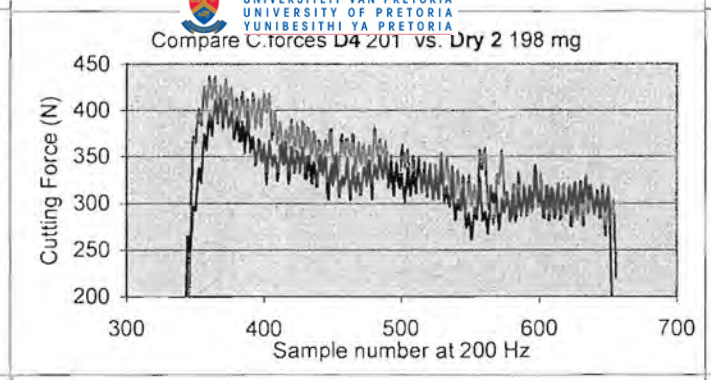

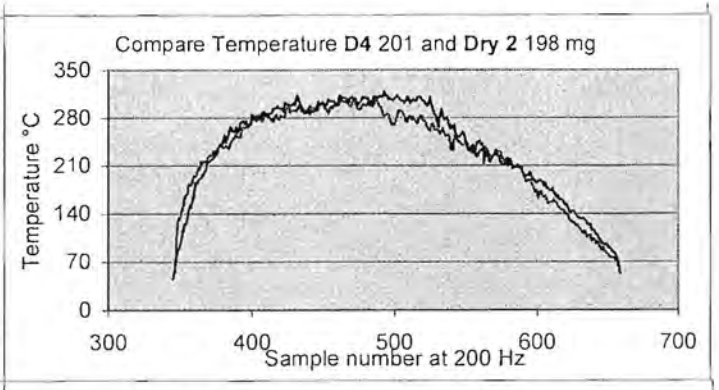

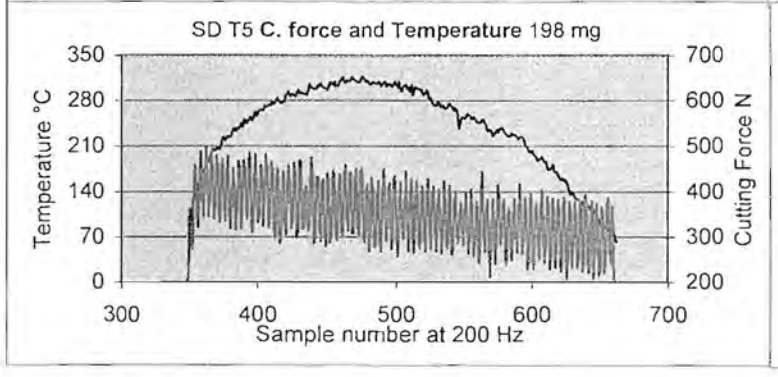

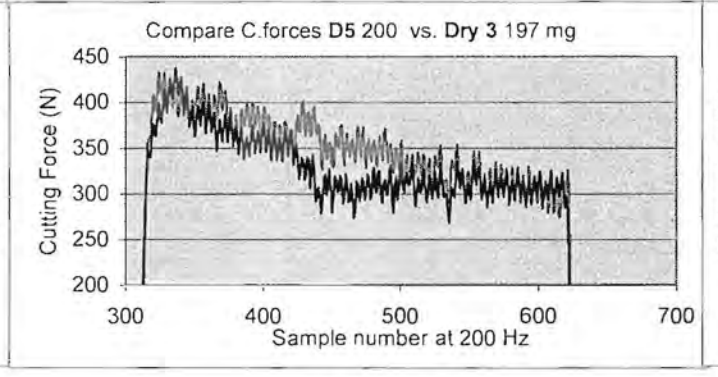

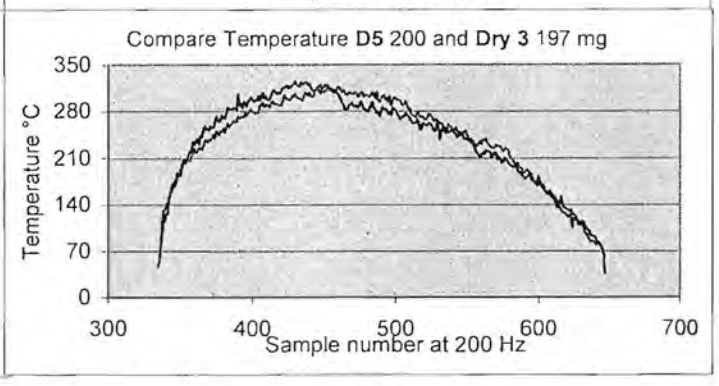

Cutting Force and Temperature: raw data	Cutting Force 5 point moving average : Sample and Dry	Cutting Temperature : Sample and Dry

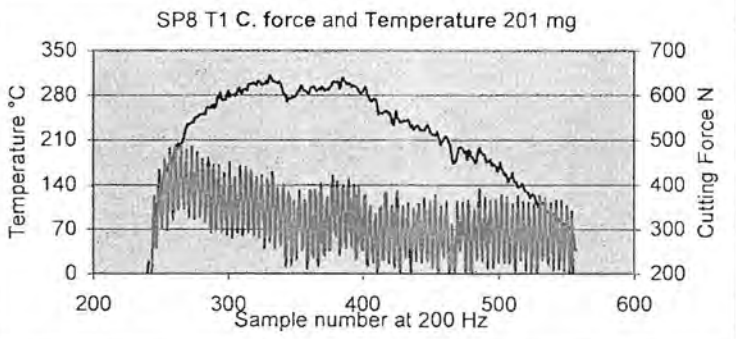

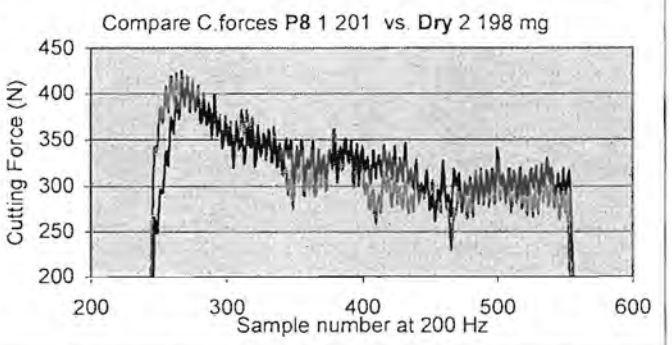

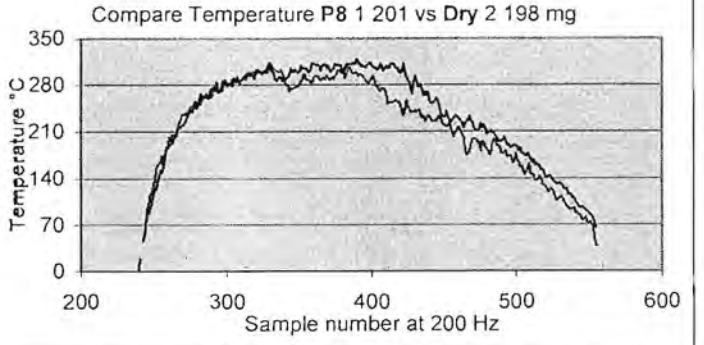

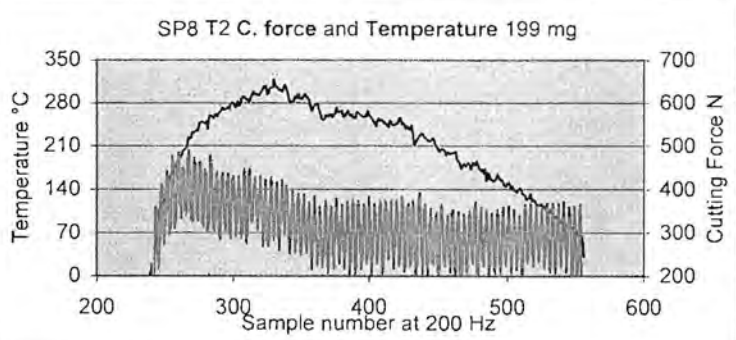

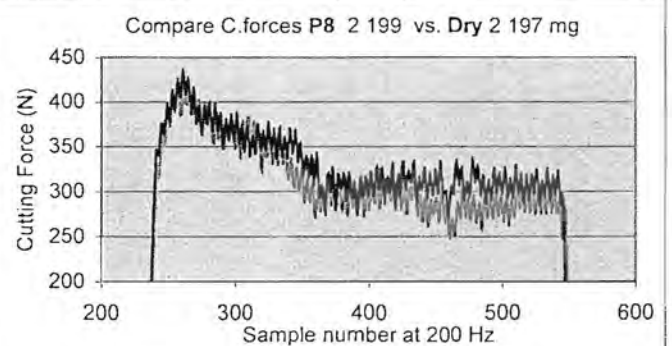

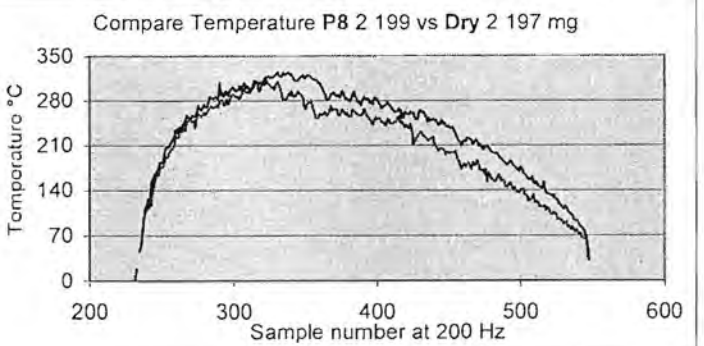

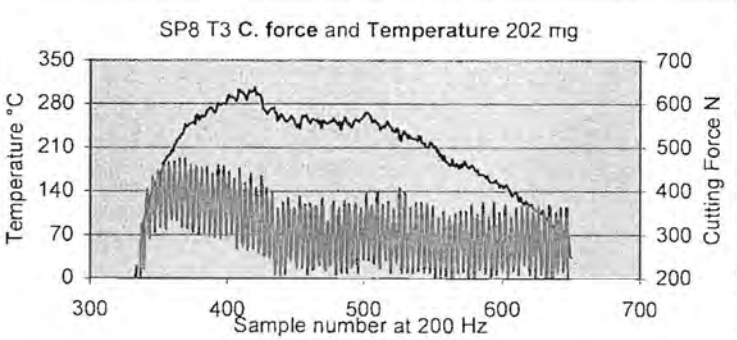

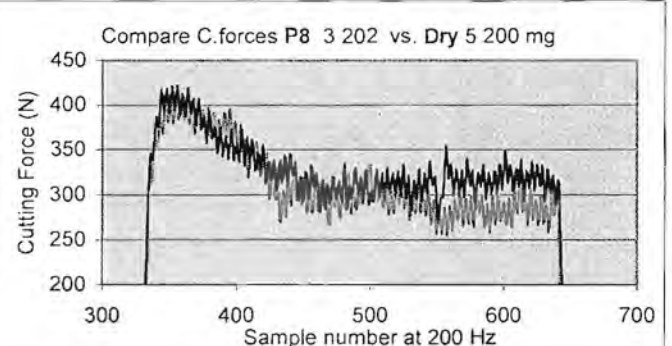

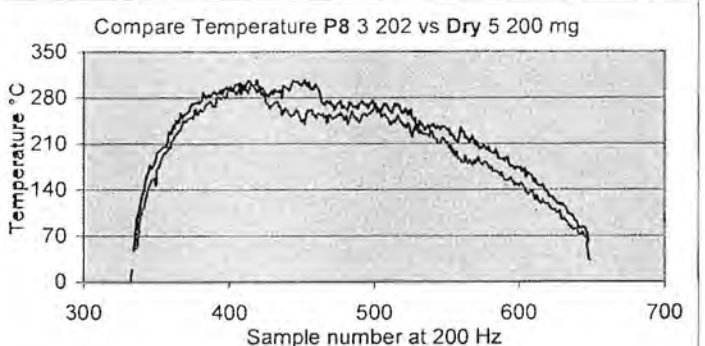

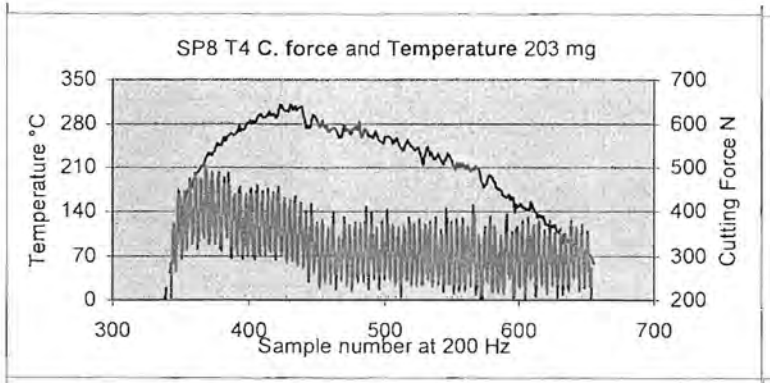
SP8 T4 C. force and Temperature 203 mg
Temperature °C
Cutting Force N
Sample number at 200 Hz

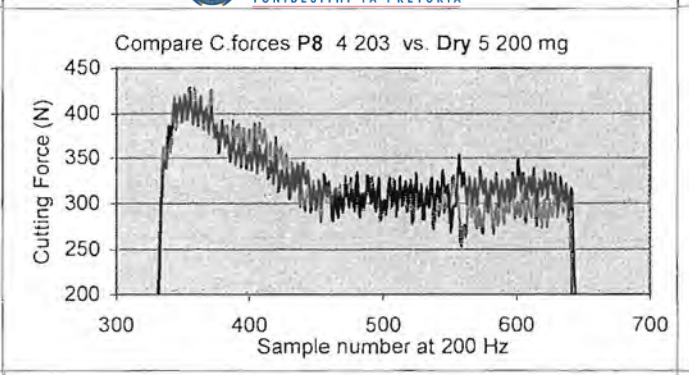
Compare C.forces P8 4 203 vs. Dry 5 200 mg
Cutting Force (N)
Sample number at 200 Hz

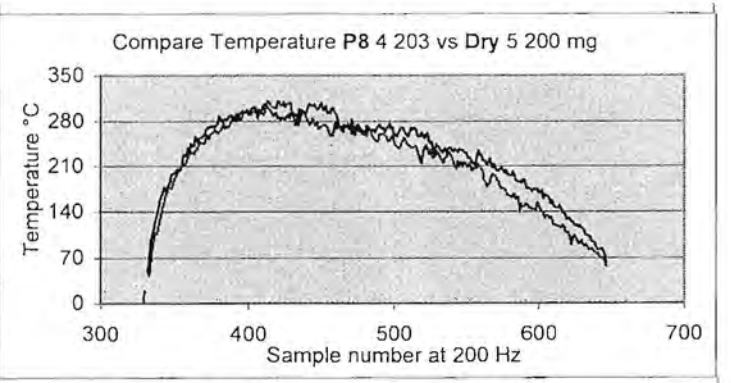
Compare Temperature P8 4 203 vs Dry 5 200 mg
Temperature °C
Sample number at 200 Hz

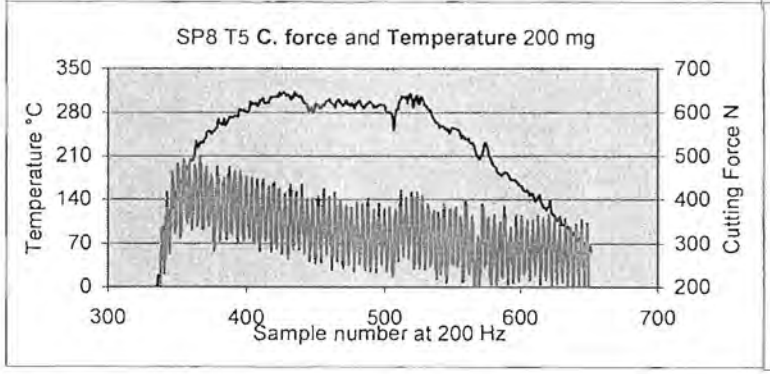
SP8 T5 C. force and Temperature 200 mg
Temperature °C
Cutting Force N
Sample number at 200 Hz

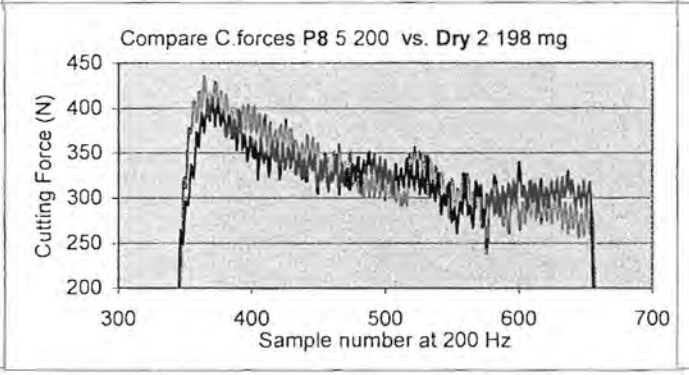
Compare C.forces P8 5 200 vs. Dry 2 198 mg
Cutting Force (N)
Sample number at 200 Hz

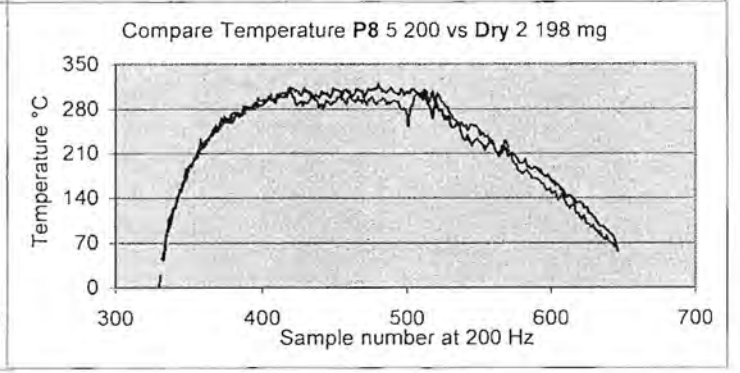
Compare Temperature P8 5 200 vs Dry 2 198 mg
Temperature °C
Sample number at 200 Hz

Cutting Force and Temperature: raw data	Cutting Force 5 point moving average : Sample and Dry	Cutting Temperature : Sample and Dry

20

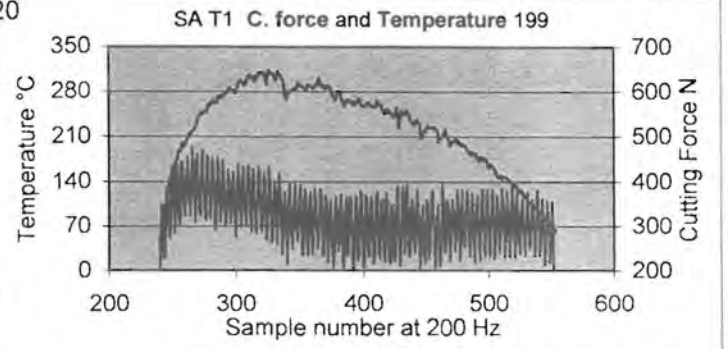

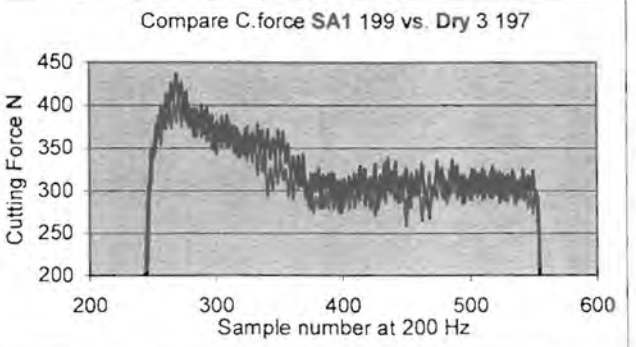

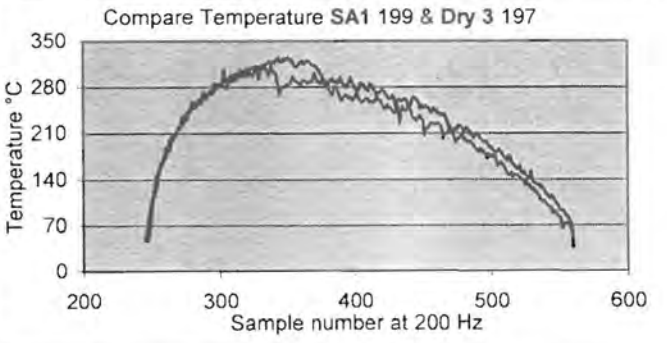

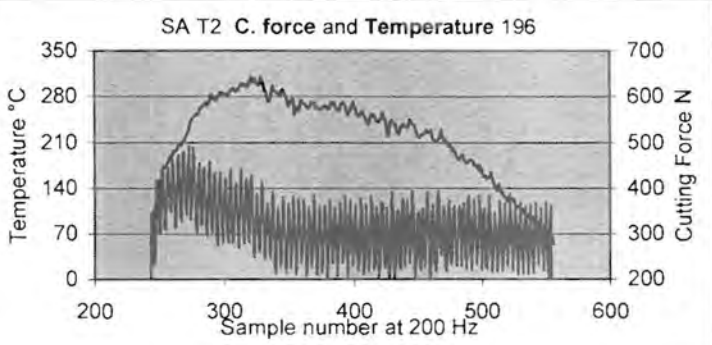

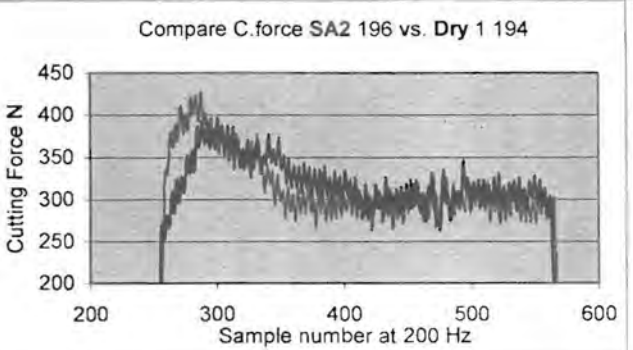

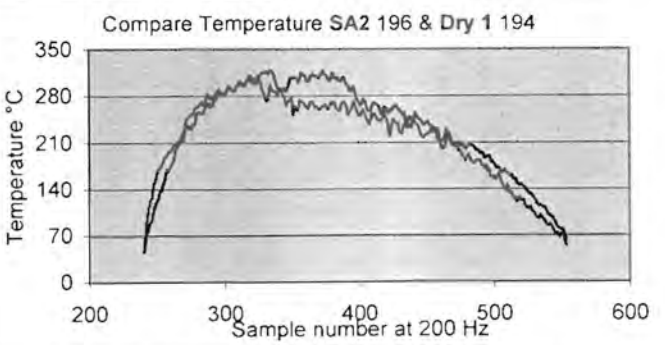

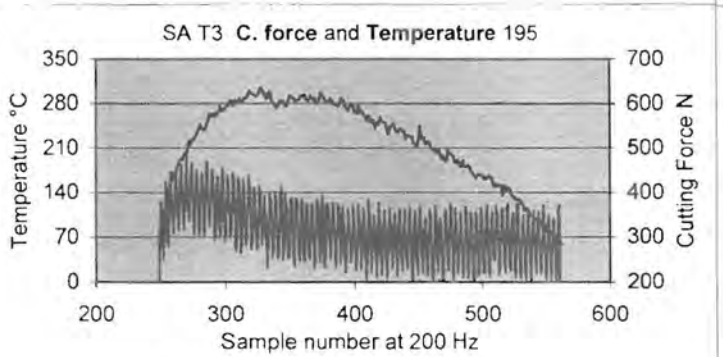

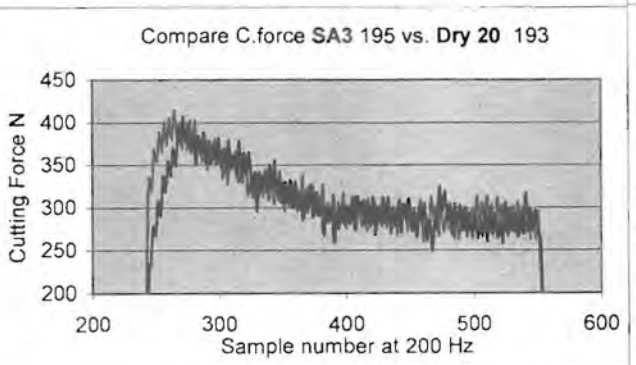

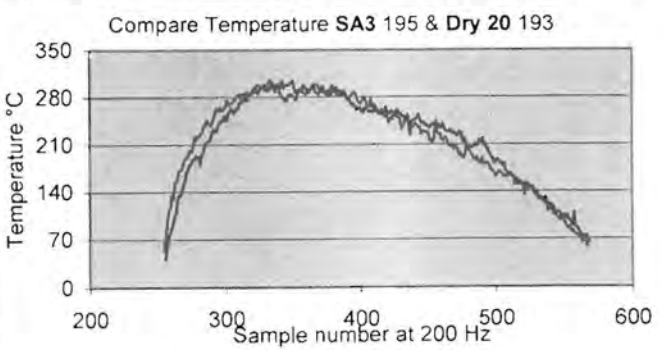

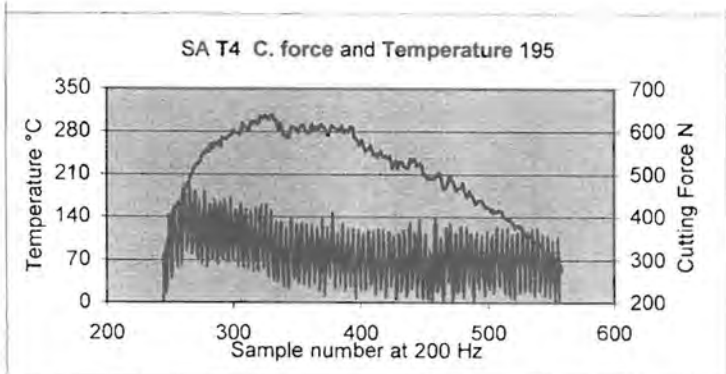
SA T4 C. force and Temperature 195
Temperature °C
Cutting Force N
Sample number at 200 Hz

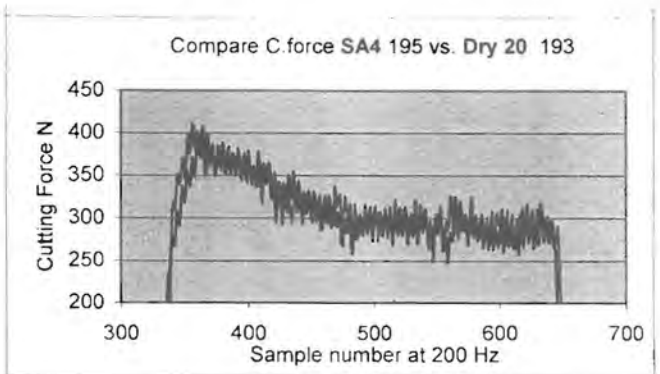
Compare C.force SA4 195 vs. Dry 20 193
Cutting Force N
Sample number at 200 Hz

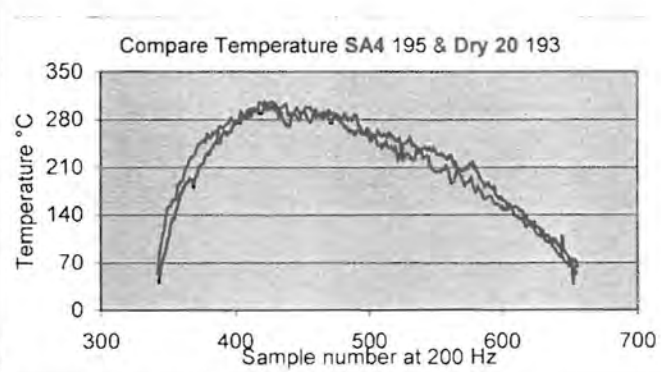
Compare Temperature SA4 195 & Dry 20 193
Temperature °C
Sample number at 200 Hz

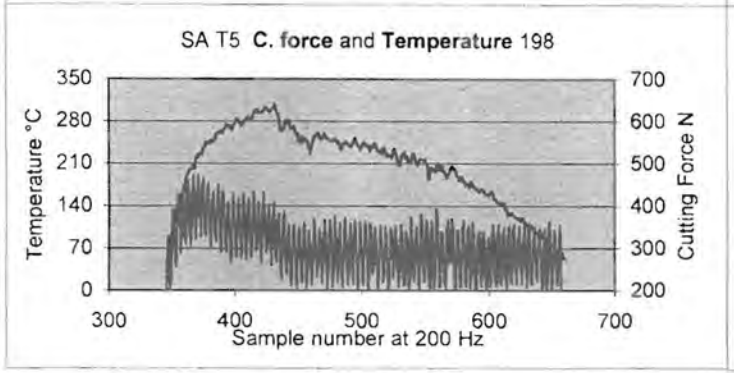
SA T5 C. force and Temperature 198
Temperature °C
Cutting Force N
Sample number at 200 Hz

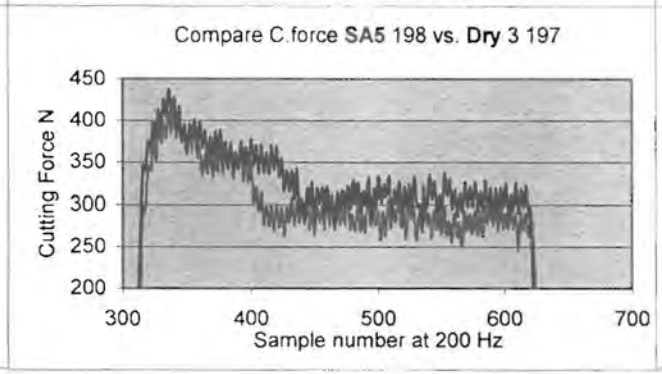
Compare C.force SA5 198 vs. Dry 3 197
Cutting Force N
Sample number at 200 Hz

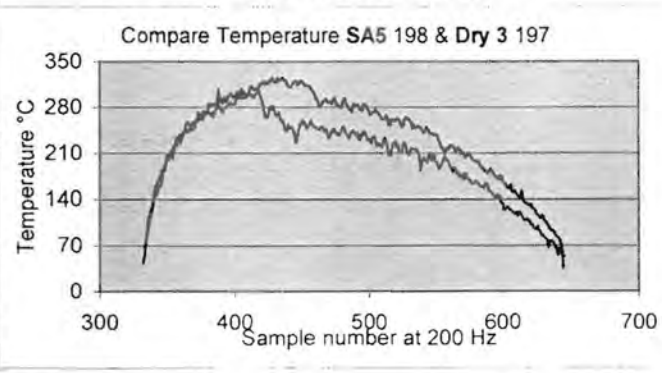
Compare Temperature SA5 198 & Dry 3 197
Temperature °C
Sample number at 200 Hz

Cutting Force and Temperature: raw data

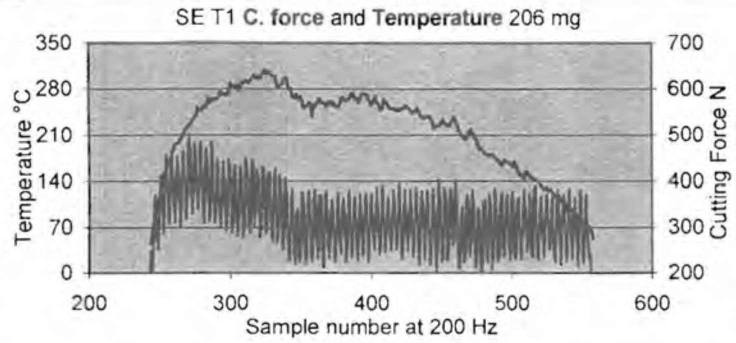

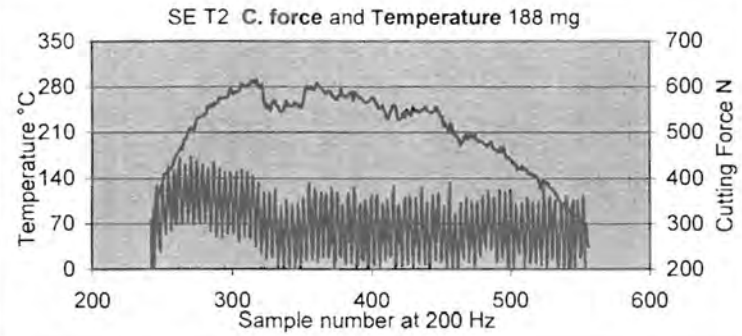

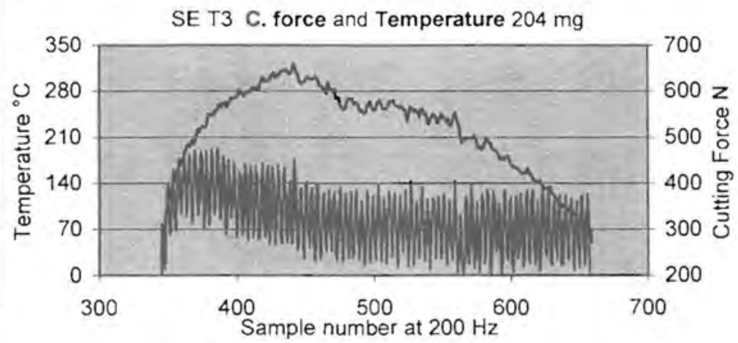

Cutting Force 5 point moving average : Sample and Dry

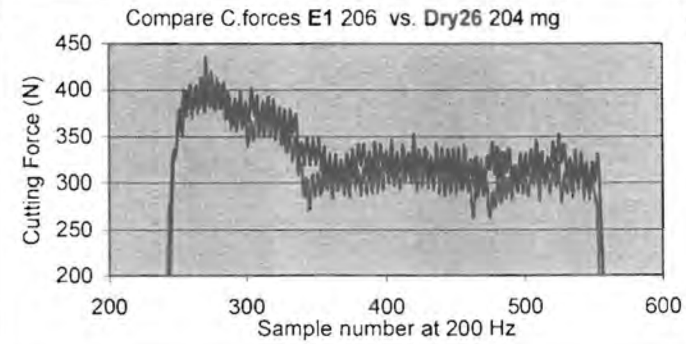

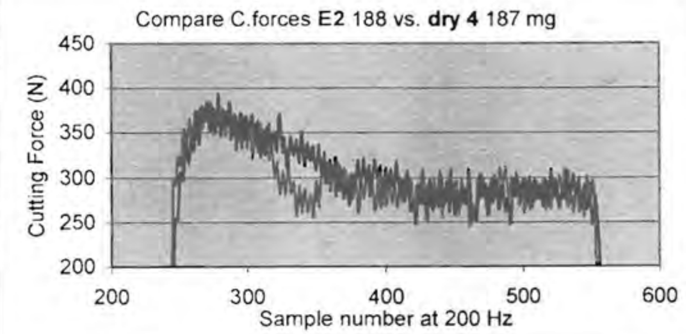

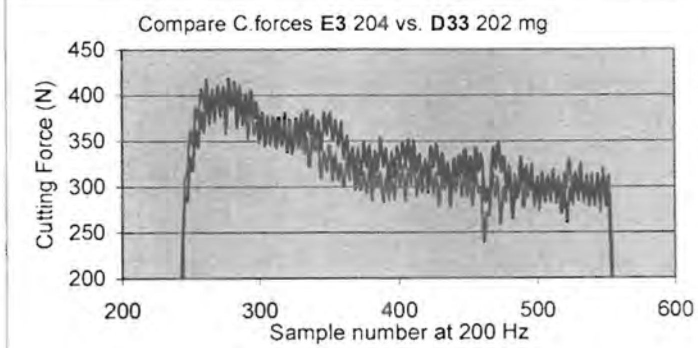

Cutting Temperature : Sample and Dry

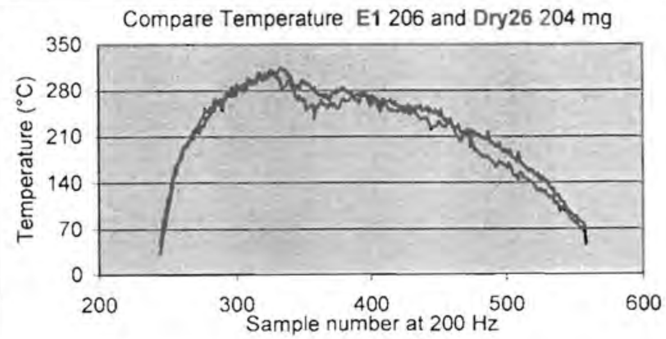

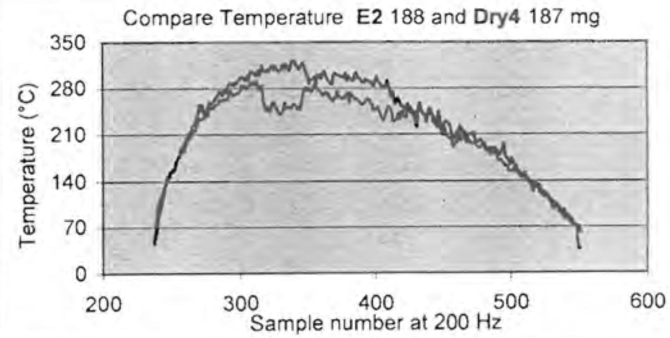

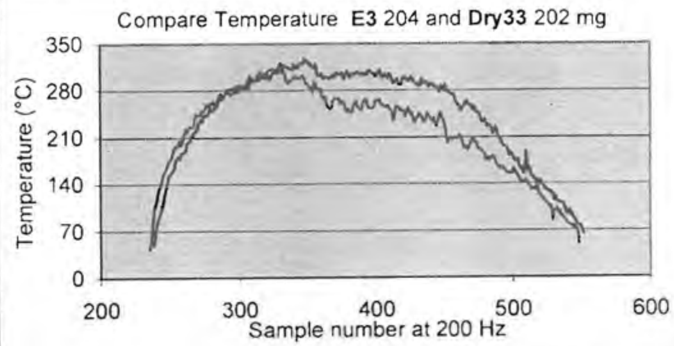

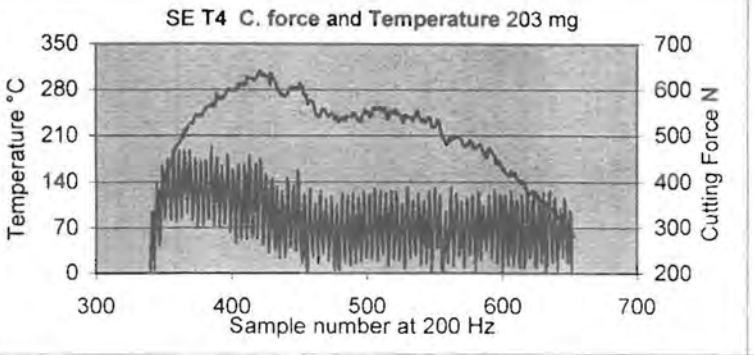
SE T4 C. force and Temperature 203 mg
Temperature °C
Cutting Force N
Sample number at 200 Hz

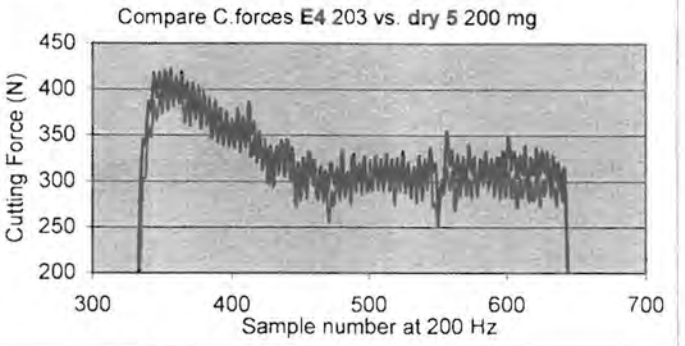
Compare C.forces E4 203 vs. dry 5 200 mg
Cutting Force (N)
Sample number at 200 Hz

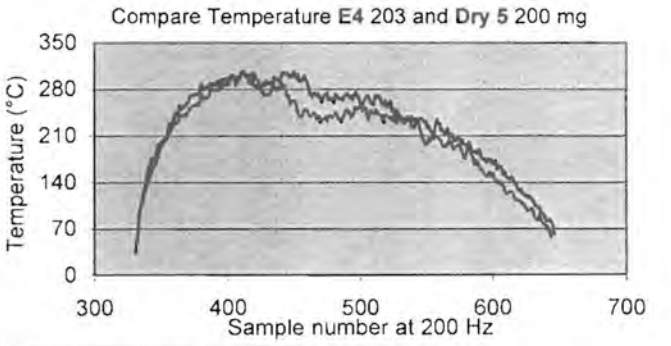
Compare Temperature E4 203 and Dry 5 200 mg
Temperature (°C)
Sample number at 200 Hz

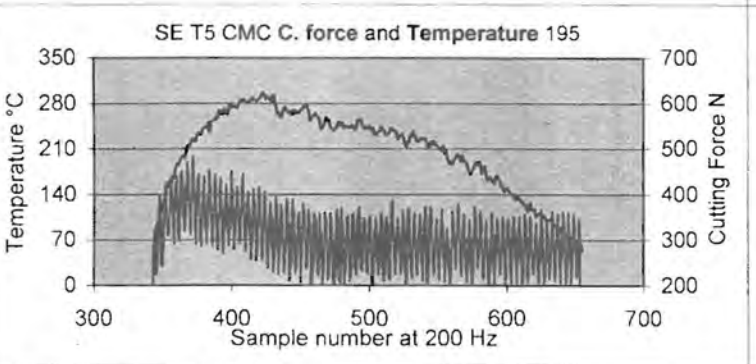
SE T5 CMC C. force and Temperature 195
Temperature °C
Cutting Force N
Sample number at 200 Hz

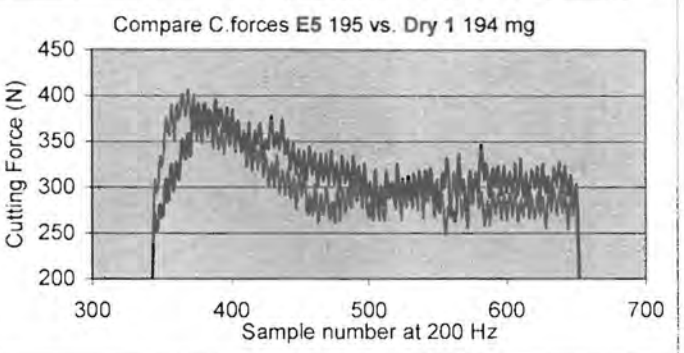
Compare C.forces E5 195 vs. Dry 1 194 mg
Cutting Force (N)
Sample number at 200 Hz

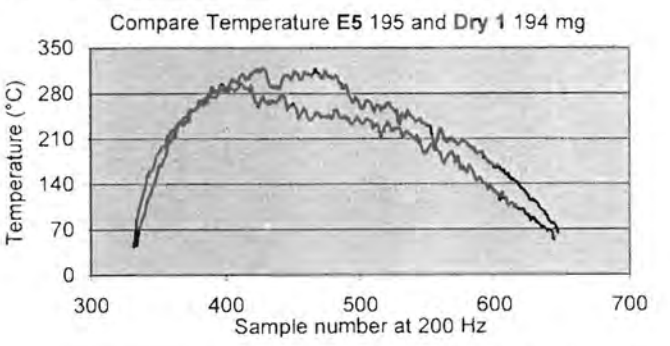
Compare Temperature E5 195 and Dry 1 194 mg
Temperature (°C)
Sample number at 200 Hz

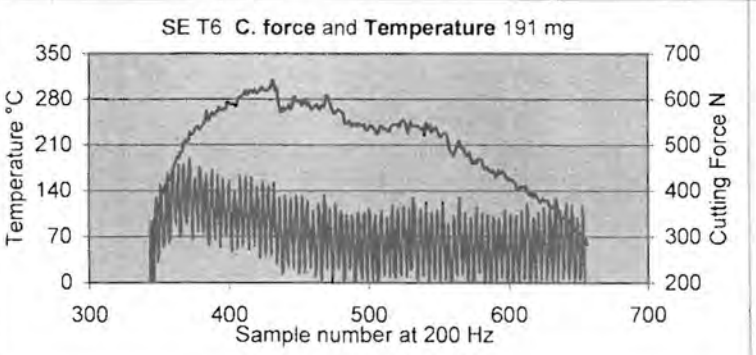
SE T6 C. force and Temperature 191 mg
Temperature °C
Cutting Force N
Sample number at 200 Hz

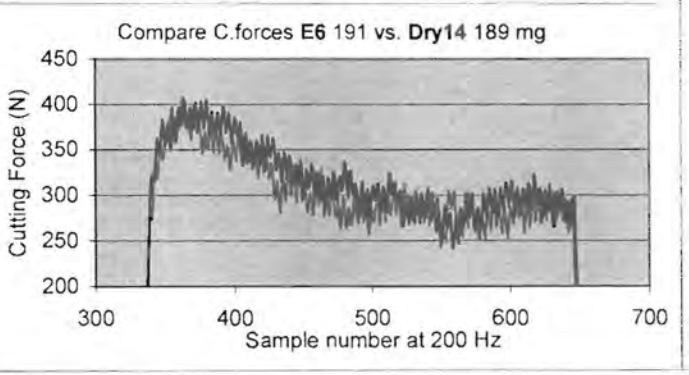
Compare C.forces E6 191 vs. Dry14 189 mg
Cutting Force (N)
Sample number at 200 Hz

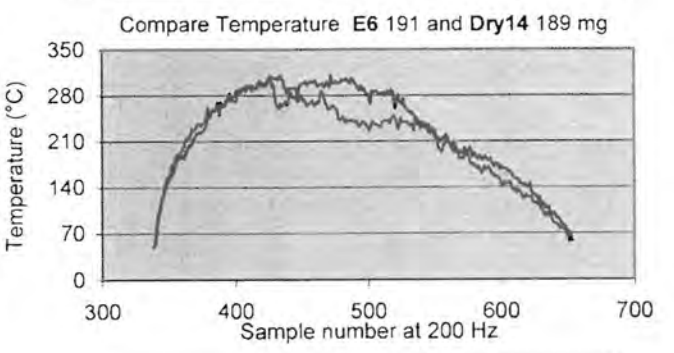
Compare Temperature E6 191 and Dry14 189 mg
Temperature (°C)
Sample number at 200 Hz

Cutting Force and Temperature: raw data	Cutting Force 5 point moving average : Sample and Dry	Cutting Temperature : Sample and Dry
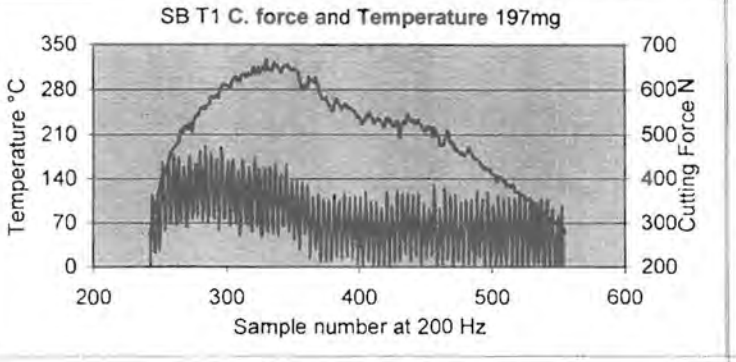	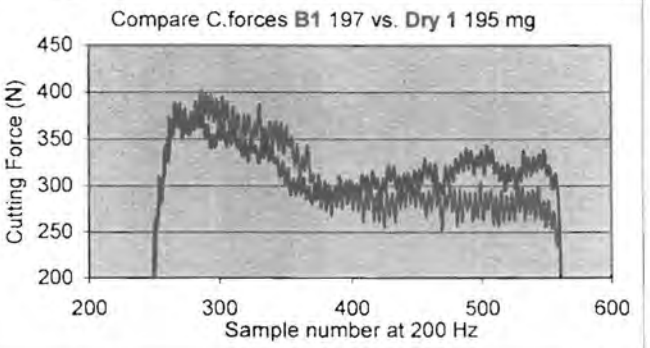	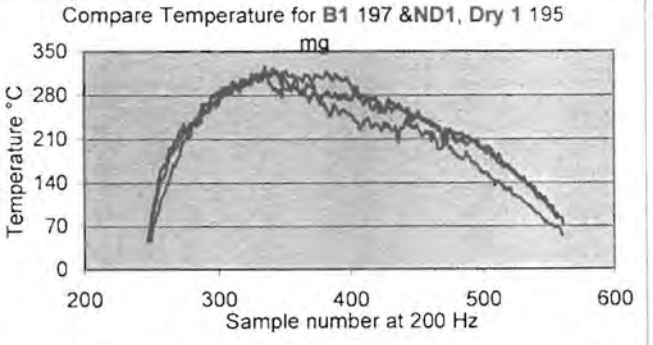
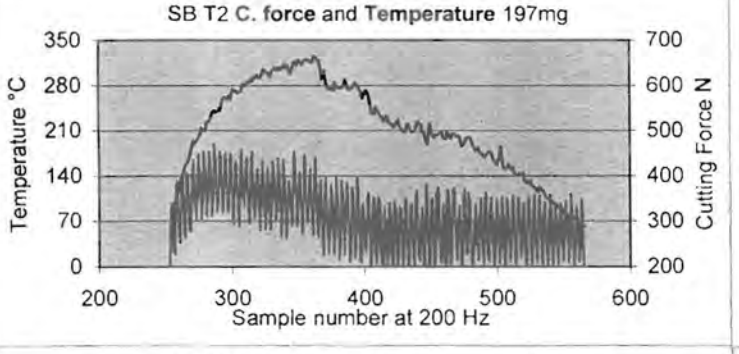	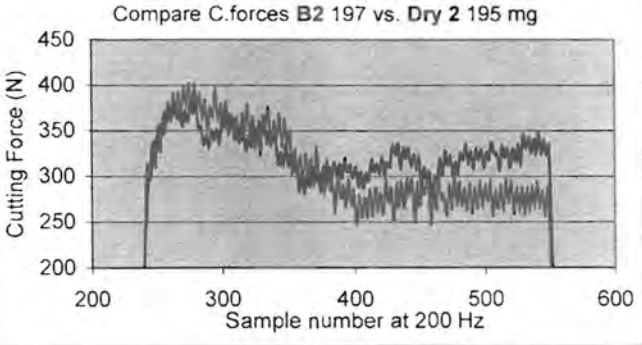	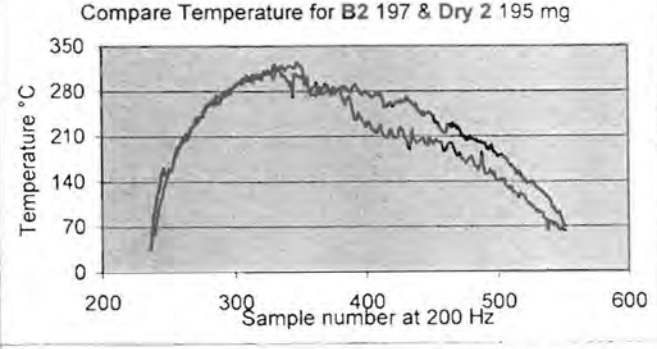
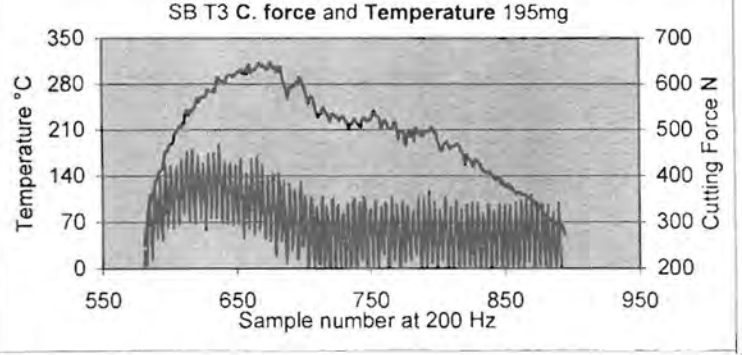	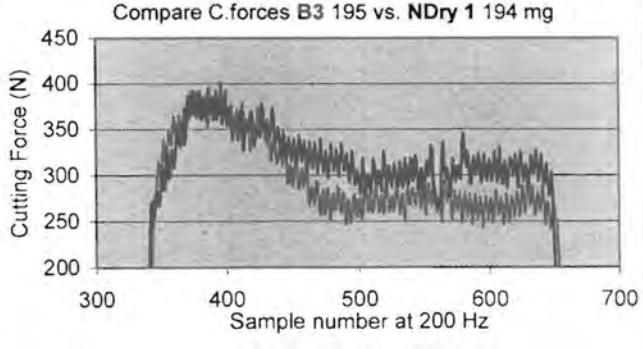	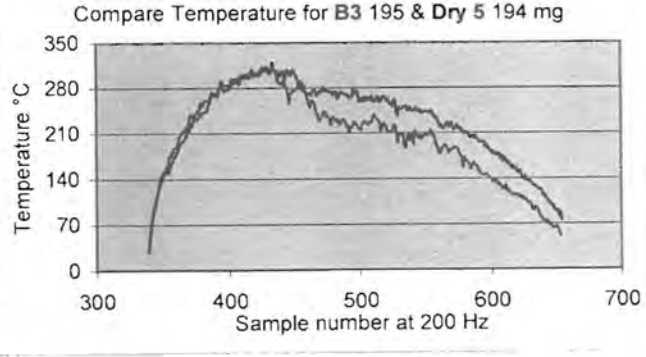

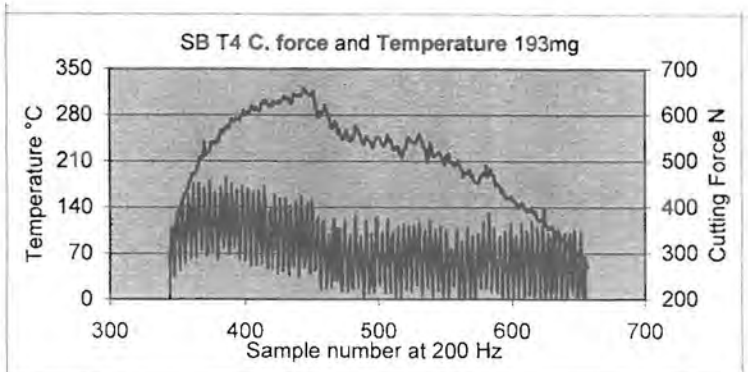
SB T4 C. force and Temperature 193mg
Temperature °C
Cutting Force N
Sample number at 200 Hz

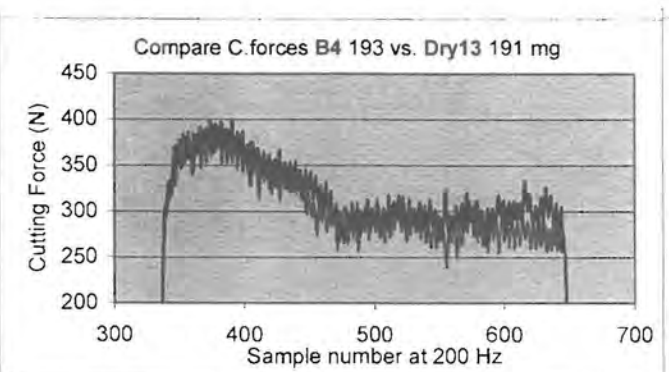
Compare C.forces B4 193 vs. Dry13 191 mg
Cutting Force (N)
Sample number at 200 Hz

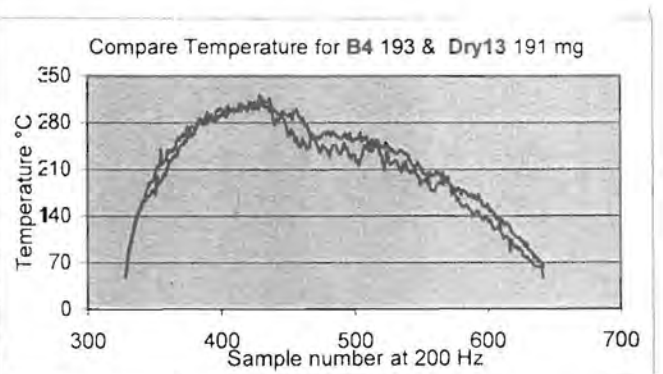
Compare Temperature for B4 193 & Dry13 191 mg
Temperature °C
Sample number at 200 Hz

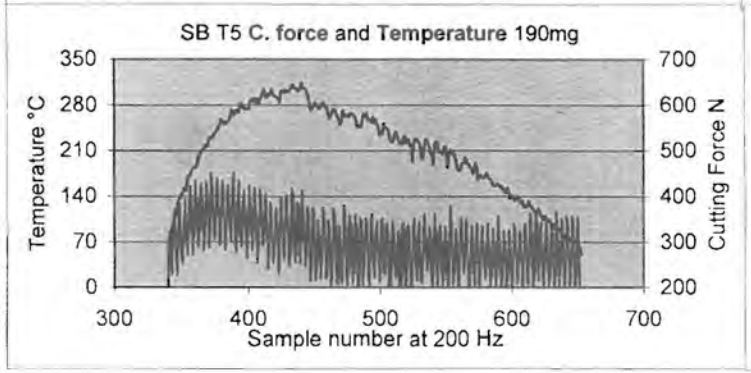
SB T5 C. force and Temperature 190mg
Temperature °C
Cutting Force N
Sample number at 200 Hz

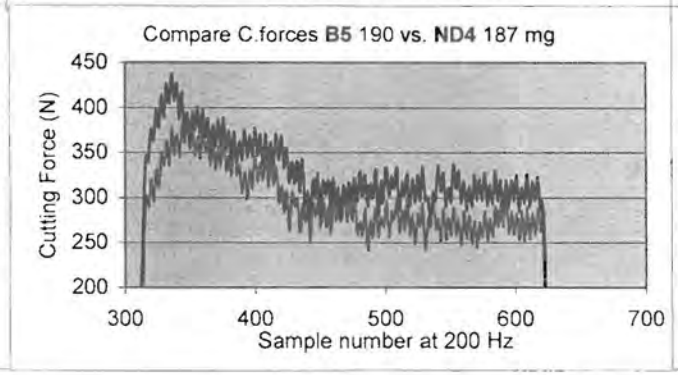
Compare C.forces B5 190 vs. ND4 187 mg
Cutting Force (N)
Sample number at 200 Hz

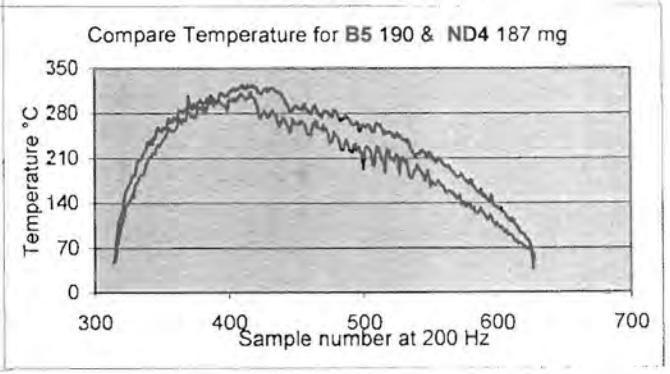
Compare Temperature for B5 190 & ND4 187 mg
Temperature °C
Sample number at 200 Hz

Appendix E:

The output code from the AD/DA card is binary. Direct memory access (D.M.A) is used to transfer data direct from the A/D-byte to memory. Sampling can be done in polled mode or in interrupt mode. For the former the PC is tied up until sampling is completed. For the latter the PC is configured to sample the selected channels independent of direct program control using hardware interrupts and timers. If this mode is used the PC is free for other uses. For the case that the PC exercises control it is tied up anyway because it must continuously output control signals and consequently all operations are performed in polled mode. All the background information for the development of the software for this may be found in the books by Tinker. (Tinker 1996 & 1990)

The binary data are converted to numeric format and the sampled temperature and cutting force data are continuously displayed on screen and dumped to file for later graphical presentation.

To be able to write the software for this case specific operation it is necessary that the EDR software developers kit for Eagle Technology boards be read. Chapter 2 states that EDR60.TPU from c:\EDR\TPAS must be copied to the units directory as EDR.TPU.EDR60 for Turbo Pascal 6.0. The uses EDR statement must then be included in the uses clause in the program for the programmer to have access to the pre-developed software functions, constants and procedures. Similar instructions follow for other programming languages. P3 of the developers kit manual should also be read when taking Eagle cards into use. The newer Eagle cards have different installation instructions than PC30 to PC30D. These are added from the control panel in windows at the applet for add new hardware.

Once this is done programming can start. Follow chapter 3 of the user manual and the EDR_InitBoard procedure description. In summary what is needed to take the board into use is the following: - Call these procedures with their relevant parameters.

1)EDR_AllocBoardHandle(bh); in 7.1 in the manual
2)EDR_InitBoard(bh,baseaddr); in 7.19 in the manual or
2)EDR_InitBoardType(bh,baseaddr,boardtype); 7.20
3)EDR_Set ADInConfig(bh,chan,range,adtype,gain); 7.25
4)EDR_SetDAOutConfig(bh,chan,range,gain); 7.30
5)EDR_GetBoardType(bh,boardtype);

If boardtype in this statement does not reflect your board type you must use the second procedure in 2) above. Consult also appendix A4 in the user manual.

For some cards it is necessary that the jumpers on the board be physically set to correspond to the configuration information specified in 3) and 4) above for the program to function correctly. The user manuals for the relevant cards must be consulted for these settings. When all of the above has been done then program communication between the

process hardware and the PC is open and the other procedures in the manual can be called whenever needed and programming can continue as required.

11. References:

1. Birmingham E., Henshall J.L., Hooper R.M., 1997, "The influence of cutting fluid composition on the wear of high speed steel tools in intermittent cutting", World Tribology Congress, Mechanical Engineering Publications limited P599

2. Boston, O.W. ASME Research Committee, (1952) "Manual on cutting of metals with single-point tools" Second edition published by ASME, P143-150

3. Brown, A. (2002) "Developments in process control monitoring" SA Mechanical Engineer *52* (10), P23-24

4. Considine, Douglas M., (Editor); (1974) Process Instruments & Controls Handbook; McGraw-Hill; 2nd Edition; (P2.23-2.34)

5. de Chiffre L. and Belluco W.,(2002) "Investigations of cutting fluid performance using different machining operations" Lubrication Engineering *58* (10), P22-29

6. du Plessis E. (2001) "The development of limited volume lubrication in metal working operations in South Africa" Seventh International Tribology Conference of the South African Institute of Tribology.

7. Follette, Daniel, (1980) "Machining Fundamentals : A basic approach to metal cutting" Society of manufacturing engineers. P46-55

8. Hill, R., (1950) "Plasticity", Oxford-Clarendon Press

9. Hoffmann Karl, (1989) "An introduction to measurements using strain gauges" Drach Druckerei, Alsbach, Federal Republic of Germany, Hottinger Baldwin Messtechnik GmbH

10. Hutchings I.M, (1992) "Tribology - Friction and Wear of Engineering materials" Edward Arnold a division of Hodder and Stoughton P116, 120-121

11. Kajdas C. (1996) "Tribology – Solving friction and Wear problems" Volume 1 tenth International Colloquium, Technische Akademie Esslingen., P40-45

12. Kelly J.F., and Cotterell M.G., (2002), "Minimal lubrication machining of aluminium alloys", Journal of Materials Processing Technology *120* (1-3), P 327-334 Mechanical and Manufacturing Engineering Department, Cork Institute of Technology, Bishopstown, Cork, Ireland

13. Le Grand R., (1971), "Manufacturing Engineers Manual" McGraw-Hill, (P254-255)

14. Liew W.Y.H., Hutching I.M., Williams J.A., (1997) "Friction and lubrication effects in the machining of aluminium alloys", World Tribology Congress, Mechanical Engineering Publications limited, P337

15. Montgomery, R.S. (1965), "The effect of alcohols and ethers on the wear behaviour of aluminium." Wear *8*, P466-473.

16. Mori S., (1995), "Tribochemical activity of nascent metal surfaces ", proceedings ITC, Yokohama , Satellite forum on Tribochemistry, Tokyo, October 28, 1995, P37-42.

17. Mortier R.M and Orszulik S.T., (1992) "Chemistry and Technology of Lubricants" Blackie Academic and Professional an imprint of Chapman and Hall P45, 217-219

18. Rank Taylor Hobson limited "Surtronic 3 User Manual" Rank Taylor Hobson P5-9

19. Rollason E.C., (1973) "Metallurgy for Engineers" Edward Arnold (P337-340)

20. Rowe, C.N. and Murphy, W.R., (1974), In: Proc. Tribology Workshop. Ling, F.F. (ed.) National Science Foundation, Washington D.C.

21. Tinker, D (1996) "EDR Software developers kit for Eagle Technology boards User manual" Eagle technology
(1990) "User Manual for PC30B/C/D" Eagle Technology

22. Trent E.M., (1977) "Metal Cutting" Butterworths

23. Van der Voort, George F., (1999), "Metallography, principles and practice." Mc Graw-Hill P196-198, 350-353

24. Van der Waal, G, (1985) "The relationship between chemical structure of ester base fluids and their influence on elastomer seals and wear characteristics" Journal of synthetic lubrication *1* (4) P281

25. Varadarajan A.S., Philip P.K. and Ramamoorthy B., (2001), "Investigations on hard turning with minimal cutting fluid application (HTMF) and its comparison with dry and wet turning", International Journal of Machine Tools and Manufacture *42* (2), January 2002, P 193-200, Manufacturing Engineering Section, Department of Mechanical Engineering, Indian Institute of Technology, Madras, Chennai, 600036, India

26. Vieira J.M., Machado A.R., and Ezugwu E.O., (2001) "Performance of cutting fluids during face milling of steels' Journal of Materials Processing Technology *116* (2-3), P 244-251

27. Xuegang M., Yangshan S., Feng X., Wenwen D. and Wu D., (2002) "Analysis of valence electron structure (VES) of intermetallic compounds containing Mg-Al-based alloys" Materials,Chemistry and Physics *78* (1) P88-93
Department of Material Science and Engineering, South E. University, Nanjing, China, 210096

28. Zorev N.N, Massey H.S.H.and Shaw M.C,. (1966) "Metal Cutting Mechanics " Pergamon Press London, P273

Web site references:

29. ARTX, (2002) Vortex tube coolers, http://www.artxltd.com, [2002, April 4]

30. Capgo, (2002) Software reference compensation, www.capgo.com, [2002, October 9]

31. Clark, J. (2002) Chemguide helping you to understand chemistry, http://www.chemguide.co.uk/atoms/bonding/metallic.html, [2002 October 29]

32. Nix, Roger (2002) An introduction to surface chemistry, http://www.chem.qmw.ac.uk/surfaces/scc, [2002 May 5]

33. Fox Valley Technical College (FVTC), (2000) Cutting fluid types and uses, http:\\its.foxvalleytech.com, [2002,April]